CHARACTERIZATION OF CMX-13 AND EVALUATION OF EFFICACY AND MECHANISMS OF ACTION IN AN ANIMAL MODEL OF AUTOIMMUNITY

BY

VINOD SATISCH RAMGOLAM

MSc (FREE UNIVERSITY, AMSTERDAM, THE NETHERLANDS)

A THESIS SUBMITTED FOR THE DEGREE OF

DOCTOR IN PHILOSOPHY

NATIONAL UNIVERSITY OF SINGAPORE

2005

THIS THESIS IS DEDICATED TO:

MY FATHER (IN MEMORIAL) FOR SECURING MY EDUCATION

MY MOTHER FOR BELIEVING IN MY FREEDOM

ACKNOWLEDGEMENTS

I wish to express my sincere gratitude and appreciation to my supervisors Professor Yap Hui Kim and Associate Professor Ang Siau Gek, from the Department Paediatrics and the Faculty of Chemistry, respectively, National University of Singapore for their invaluable advice and encouragement. The help of the collaborators in this project is highly appreciated. I am thankful to Associate Professor Lai Yee Hing; Associate Professor Loh Chiong Shiong for his kindness to let me work in botany lab; Associate Professor Koh Dow Rhoon, for his helpful advices on the MRL-*lpr/lpr* SLE mouse model; Associate Professor Fong Kok Yong for the SLE patient samples; Dr. Gilbert Chan for his help on the histological slides.

I wish also to record my thanks to the following for their technical advice: Md. Frances Lim, for her advice on HPLC; Mrs Ang, for her assistance in the Botany lab; Md Ho for her assistance in the ELISSA's; Melinda Leong (from Biomed Diagnostics) for her professionel help on FASCan.

My work would not be complete without the helpful advises from my colleagues in the Paediatrics lab: Danny Lai for helping me out with the histological staining and preparing the slides and creatinine analysis; Wai Cheung for his advice on quantitative real-time RT-PCR; Wee Song Yeo for doing his UROP project under my supervision; Sylvia Ang for her work in the botany lab; Seah

Ching Ching for helping out with administrative and lab work; Ai Wei Liang for donating blood generously and Shirley Kham for being a great friend in need.

TABLE OF CONTENTS

SUMMARY

Our research group's interest in the "Ming Decoction of 21 Tonics for Kidney" arose from treatment in a patient with lupus nephritis and chronic nephritic syndrome, in whom clinical remission started after ingestion of this Chinese herbal decoction (CM). Preliminary studies have demonstrated the immunosuppressive potency of both the crude decoction CM, as well as the active fraction CMX-13, a derivative of the herb *Rubia cordifolia*, on *in-vitro* T-lymphocyte proliferation, as well as B-cell secretion of immunoglobulins in both normal individuals as well as patients with SLE. In addition, we have shown the efficacy of CMX-13 on preventing acute rejection in a rat lung transplant model of hyperacute allograft rejection. This thesis utilizes the MRL-*lpr/lpr* murine model of lupus nephritis to study the mechanism of the immunosuppressive action of CMX-13 and its derivatives.

In the first part of this thesis, work was performed to characterize CMX-13, which is the fraction which contains the active component(s) of the herb *Rubia cordifolia,* following separation by liquid chromatography using spectroscopic and chemical methods. RP-HPLC revealed that CMX-13 contained a mixture of possibly 8 or more compounds. Two RP-HPLC fractions of CMX-13, namely CMX-13-1 and CMX-13-5 had 100% immunosuppressive properties. The RP-HPLC fraction CMX-13-5 contained fewer impurities than CMX-13-1 as illustrated by their respective RP-HPLC profiles. Therefore we attempted to elucidate the structure of CMX-13-5 by ^{1}H-NMR and LC-Mass spectrometry.

The LC chromatogram of CMX-13-5 showed a single peak, suggesting either a single molecule with a weight of 807.5 or two molecules with a weight of 270 and 537.5. ^{1}H-NMR spectrum of CMX-13-5 was shown to resemble the ^{1}H-NMR spectra of a bicyclic hexapeptide isolated by the group of Itokawa and co-workers [Itokawa et al., 1992; Itokawa et al., 1993]. Subsequent to our work, our collaborators were able to analyze the structure of the purified bioactive compound in CMX-13' (using material from the same source) and showed that the bioactive compound in CMX-13' was identical to a compound previously identified by Itokawa and co-workers, namely, RA-VII.

In the second part of the thesis examined the effect of CMX-13 on both cell cycle progression and the apoptotic events in peripheral blood mononuclear cells (PBMC) isolated from normal controls and patients with SLE, as well as Jurkat cells, a human T-cell line. In addition to its suppressive effect on PHA-stimulated PBMC proliferation, CMX-13 was also shown to significantly inhibit spontaneous Jurkat cell proliferation by >99% even at low concentrations of 1 μg/ml. The inhibitory effect of CMX-13 on Jurkat cell proliferation was not due to inhibition of cell-cycle progression, but rather by the induction of spontaneous apoptosis in cells in the G_0/G_1 phase. This effect of CMX-13 on apoptosis in Jurkat cells was confirmed by DNA fragmentation analysis and Annexin-V staining. Apoptosis was induced at a very early phase, as was demonstrated by the "sub-G1" or apoptotic peaks appearing in the cell-cycle

analysis. This mechanism of action was different from drugs such as cyclohexmide, which induces apoptosis related to a G_0/G_1 cell-cycle arrest.

In SLE, one of the hypothesis is that dysregulation of apoptosis might be responsible for the induction of anti-nuclear antibodies, pathognomonic of the disease. In some patients, decreased apoptosis in SLE appears to be associated with increased production of a soluble form of the Fas molecule that is capable of inhibiting apoptosis after a stimulus to proliferate [Cheng et al., 1994], whereas other studies reported accelerated apoptosis of lymphocytes in SLE patients [Emlen et al., 1992; Lorenz et al., 1998]. Similarly, in our SLE patients, the percentage of apoptotic cells was increased with increasing activity of the disease as measured by the SLICC score. Hence the immunosuppressive mechanism of CMX-13 could be partly related to its effect on apoptosis, especially in the context of suppression of SLE activity, where increased apoptosis has been demonstrated.

In the third part of this thesis, we examined the effect of CMX-13 on the development of lupus nephritis in the MRL-*lpr/lpr* mouse model of autoimmune disease. MRL-*lpr/lpr* mice spontaneously develop an autoimmune disorder with pathological features similar to human SLE, including vasculitis, generalized lymphadenopathy, arthritis and a severe immune complex glomerulonephritis, resulting in increased mortality, with the majority of mice dying of renal failure at 16-24 weeks of age. In our experiments, these clinical features, accompanied by elevation of serum anti-dsDNA antibody levels, were

seen in the untreated MRL-*lpr/lpr* mice and the control group treated with the solvent DMSO. The severity of the autoimmune disease increased with the age of the mice, with the majority of the untreated and DMSO control mice dying of renal failure at 16-24 weeks of age. Treatment of the MRL-*lpr/lpr* mice with CMX-13 and dexamethasone (DEX) resulted in delay by at least 4 weeks in the development of lymphadenopathy, which was also less severe than in the control groups. All of the mice developed anti-dsDNA antibodies from the age of 8 weeks, with the untreated and DMSO control mice having the highest level of rise in antibody concentrations by 16 weeks of age, whereas both the CMX-13 and DEX-treated groups had significantly lower anti-dsDNA antibody levels. CMX-13 was also able to improve survival of the MRL-*lpr/lpr* mice compared to the untreated or DMSO controls, where 48% of the mice treated with CMX-13 were still alive at 22 weeks of age, whereas only 4.5% of the untreated controls and 24% of the DMSO controls survived. Moreover, CMX-13 treatment of MRL-*lpr/lpr* mice with progressive lupus nephritis resulted in decrease in the degree of proteinuria and improvement in renal histological indices. Hence CMX-13 appeared to be effective in attenuating the clinical and histological disease activity in the MRL-*lpr/lpr* mouse model of SLE.

In the final part of the thesis, we examined the effect of CMX-13 on cytokine gene expression in PBMCs (in particular $CD4^+$ and $CD8^+$ T-cells), liver and glomeruli of the autoimmune MRL-*lpr/lpr* mouse. The mice were treated with either DMSO (solvent control), CMX-13 or DEX, from the age of 12 weeks, and real-time RT-PCR was used to examine IL-2, IL-6, IL-10 and IFN-γ mRNA

expression levels in PBMCs isolated at 16 weeks of age, and subsequently in tissues and lymphocyte subsets from each of the groups of MRL-*lpr/lpr* mice that were sacrificed at 23 weeks. Our studies showed that diseased MRL-*lpr/lpr* mice which did not receive any treatment had decreased $CD4^+$ and $CD8^+$ IL-2/IFN-γ mRNA ratio at the age of 23 weeks, as well as upregulation of $CD4^+$ IL-10 mRNA expression, similar to other reports in the literature. In addition, glomerular mRNA expression of IFN-γ, IL-6 and IL-10 were also increased. On the other hand, the CMX-13 treated group showed significantly higher $CD4^+$ and $CD8^+$ IL-2/IFN-γ mRNA ratio, and this was associated with improved clinical, serological and histopathological parameters, including survival. However, CMX-13 treatment did not improve the abnormality in glomerular IFN-γ, IL-6 and IL-10 gene expression.

In conclusion, one possible mechanism by which CMX-13 acts an immunosuppressive agent in the treatment of lupus nephritis in the autoimmune MRL-*lpr/lpr* mouse model is through the induction of apoptosis of autoreactive lymphocytes. Auto-aggressive $CD4^+CD8^-$ $\alpha\beta$T-cells have been postulated to be the driving force for autoreactive B-cells in SLE resulting in abnormalities in cytokine production, and suppression of these autoreactive lymphocytes could result in inhibition of autoantibody production, thus retarding the progression of lupus nephritis.

Further investigations into the apoptotic mechanisms are required to examine the transcription of apoptotic and cell-cycle genes, so that the exact molecular targets of CMX-13 or its purified molecule, RA-VII can be identified.

ABBREVIATIONS

Alb	Albumin
AR	Acute Rejection
Apaf1	Apoptotic protease activating factor
ARA	American Rheumatological Association
AZT	Azathioprine
BSA	Bovine Albumin Serum
C	serum Complement
CC	Cellcept
cDNA	Complementary DNA
CH	Cycloheximide
CH_2Cl_2	Dichloromethane
CFU-C	Colony Forming Units
CM	Chinese medicinal decoction
Con-A	Concavalin A
cpm	counts per minute
Cr	Creatinine
CsA	Cyclosporin A
DBP	Diastolic Blood Pressure
DEPC	Di-EthylPyroCarbonate
DEX	Dexamethasone
DMEM	Dulbecco's modification of Minimal Essential Medium
DMSO	DimethylSulfoxide

EX	Ethyle acetate extract of CM
E.coli	Escheria coli
EtOAc	Ethyle Acetate
FasL	Fas Ligand
FCS	Fetal Calf Serum
FCS	Forward Scatter
FITC	Fluorescein IsoThioCyanate
HBBS	Hanks Basal Salt Solution
HDCL	Hydroxychloroquine
Hex	n-Hexane
HLA-DR	Human Leucocyte antigen-DR
ICAM-1	Intercellular Adhesion Molecule-1
IFN-γ	Interferon gamma
IgG	immunoglobulin G
IL	Interleukin
LB	Luria-Bertani
LC-MS	Liquid Chromatography- Mass Spectrometry
lpr	lymphoproliferate
LPS	Lypopolysaccharide
MeOH	Methanol
MHC Class II	Major Histocompatilibility Complex Class II
MRL	Mixed lymphocyte reaction
MRL-*lpr/lpr*	MRL-mice mutated in the *Fas* gene

MRL-*wt*	MRL- wild type
mRNA	messenger RNA
NMR	Nuclear Magnetic Resonance
NZBxNZW	New Zealand black x New Zealand white
PBMC	Peripheral Blood Mononuclear Cells
PBS	Phosphate Basal Solution
PCR	Polymerase Chain Reaction
PHA	Phytohemaglutinin
PI	Propidium Iodide
PNL	Prednisolone
PS	Phosphadityl Serine
PWM	PokeWeed Mitogen
RC	*Rubia cordifolia*
RP-HPLC	Reverse Phase- High Performance Liquid Chromatography
RP-TLC	Reverse Phase-Thin Layer Chromatography
RT-PCR	Reverse Transcript PCR
SCC	Sideward Scatter
sFas	soluble Fas
SLE	Systemic Lupus Erythematosus
SLEDAI	SLE-Disease Activity Index
SLICC	Systemic Lupus International Collaborating Clinics
snRNP	small nuclear ribonucleoprotein
TAC	T-cell activation

TCM	Traditional Chinese Medicines
TCR	T-Cell Receptors
TNF	Tumor Necrosis Factor
TWHf	*Tripterium wilfordii* Hook F
TUP	Total Urinary Protein Excretion
WHO	World Health Organization

LIST OF TABLES

Chapter 5

Chapter 6

LIST OF FIGURES

Chapter 3

Chapter 4

Chapter 5

LIST OF APPENDICES

PUBLICATIONS AND CONFERENCE PAPERS

Publications and conference papers arising from work done for this thesis include:

Publications:

Yap HK, Zuo XJ, Toyoda M, Okada Y, Ang SG, Lai YH, Matloff JM, Marchevsky A, Ramgolam VS and Jordan SC. 1998. Immunosuppressive effect of the hydrophobic extract of a Chinese herb on rat lung allograft rejection. Transplant Proc. 30:980-1. Results reported in section 1.2.

Yap HK, Ang SG, Lai YH, Ramgolam V and Jordan SC. 1999. Improvement in lupus nephritis following treatment with a Chinese herbal preparation. Arch Pediatr Adolesc Med.153:850-2. Results reported in section 1.1.

Ramgolam V, Ang SG, Lai YH, Loh CS, and Yap HK. 2000.Traditional Chinese Medicines as Immunosuppressive Agents. Ann. Acad. Med. Singapore. 29:116. Results reported in section 1.1 and 1.2.

Conference Papers:

Ramgolam VS, Koh DR, Fong KY, Ang SG, Lai YH, Loh CS and Yap HK.2000. Decreased spontaneous apoptosis in lymphocytes patients with lupus erythematosus (SLE) is improved by a Chinese herbal medication (CMX-13). Submitted for presentation at the EMBO-FUNDACION BARCELO, Workshop for Immune Repertoire and Autoimmune Disease. Mallorca, Spain 22- 24 May 2000.

Results reported mainly in section 4.2.4.

Yeo WS, Ramgolam VS, Ang SG, Lai YH, Loh CS and Yap HK.

Apoptosis induced by CMX-13 in Jurkat cells.

Submitted for presentation at the Faculty of Medicine Annual Scientific Meeting, 30th June-1st July 2000

Results reported mainly in section 4.2.4.

Ramgolam VS, Koh DR, Fong KY, Ang SG, Lai YH, Loh CS and Yap HK. 2000.Effect of the hydrophobic extreact of a Chinese herb (CMX-13) on spontaneous apoptosis of lymphocytes from patients with systemic lupus erythematosus(SLE).

Submitted for presentation at the 34th Singapore-Malaysian Congress of Medicine, 3-6 August. Singapore.

Results reported in mainly section 4.2.4.

Ramgolam VS, Koh DR, Fong FK, Ang SG, Yee, Lai YH, Loh CS, Yap HK. 2000. Induction of Aopoptosis by a Chinese Herbal Extract (CMX-13) in Jurkat cells and lymphocytes of patients with Systemic Lupus Erythematosus. Submitted for presentation at the Seventh Asian Congress of Pediatric Nephrology, 4-6 November. Singapore.

Results reported in mainly section 4.2.4.

CHAPTER 1 INTRODUCTION

The first drugs used by human beings were plant extracts [Schultes, 1972]. Currently, 70% of the world population depends on remedies for diseases through the use of medicinal plants [Latiff, 1991]. About 80% of the population in developing countries depends entirely on higher plants as the main source of healing remedies, simply because of their availability [Farnsworth, 1990].

The plants employed in traditional medical practice have been included in traditional medicinal systems by trial and error, a development that took several centuries. The search for effective natural compounds for medicinal purposes is fraught with difficulties. Screening criteria and factors like time and money are crucial [Farnsworth, 1990]. The National Cancer Institute in the USA screened 32,000 plants at random over a period of 30 years, for their ability to inhibit tumors. Only 7% were found to be effective, however even these products could not be marketed because none of them were sufficient or consistent in their bioactivity [Farnsworth, 1990]. Approximately 119 pharmaceutical agents are currently derived from higher plants, of which 74% were discovered by chemists who were trying to identify the bioactive compound of therapeutic traditional medicines[1] [Farnsworth, 1990]. These Figures show that traditional medicine can serve as a great source for the development of new therapeutic agents.

[1] Traditional Medicine is according to the World Health Organization (WHO), a term to distinguish ancient and culture-bond health care practices which existed before the application of science to health matters in official modern scientific medicine or allopathy [Farnsworth, 1990].

1.1 TRADITIONAL CHINESE MEDICINE AS IMMUNOSUPPRESSIVE AGENTS

Traditional Chinese Medicine (TCM) are derivatives of natural products that have been used for centuries in China to treat a variety of human diseases, including immune-mediated diseases [Chen and Chen, 1989]. The development of immunosuppressive agents with high efficacy and minimal toxicities has been the focus of novel drug research. Current immunosuppressive drugs include corticosteroids, with their side-effect on growth in children, cataract formation, increased risk of unusual infections, hypertension and osteoporosis; alkylating agents such as cyclophosphamide, chlorambucil or azathioprine, with dose and time-dependent adverse effects on bone marrow, liver and the gonads, as well as a risk of malignancy [Donadio and Galssock, 1993] and more recently, Cyclosporin A (CsA) and tacrolimus with the potential for nephrotoxicity and neurotoxicity [Sewing et al, 1990; Bennett, 1995; Bennett et al., 1996; Tezcan et al, 1998]. Although TCM have been shown to be effective in various clinical studies, the mechanism of action has been less understood.

Systemic Lupus Erythematosus (SLE) is an autoimmune disease, which affects multiple organ systems. There have been several clinical studies on the use of TCM with and without conventional immunosuppressants for treatment of SLE [Ruan and Ye, 1994; Wang, 1989]. In one clinical trial whereby investigations were conducted upon the effect of a combination of TCM with steroids and

cyclophosphamide, the authors showed that this combination resulted in increased therapeutic efficacy in 41 active SLE patients, as compared to the control group of 35 patients treated only with steroids and cyclophosphamide [Ruan and Ye, 1994]. In another study an “anti-lupus pill” comprising of a decoction of 17 herbs was shown to improve the activity status of SLE patients, defined by an improvement in the skin manifestations, oral ulcers and arthritis, and a decrease in the anti-nuclear antibody titres [Wang, 1989]. Use of this “anti-lupus pill” in combination of steroids was effective in 92% of the 230 patients studied, and in another 76 patients treated with the “anti-lupus pill” alone, its efficacy was 85%.

The “thunder god” vine, *Tripterium wilfordii* Hook F (TWHf), has been extensively used in China for the treatment of SLE [Qin et al., 1981; Wang and Yuan, 1989] and rheumatoid arthritis [Yu, 1983; Li and Weir, 1990]. Ingestion of TWHf in conjunction with steroids has been associated with induction of remission in a patient with severe lupus nephritis [Kao et al., 1993]. Moreover its benefit has also been demonstrated in unblinded studies [Qin et al., 1981; Wang and Yuan 1989]. Another study using the Gentian macrophylla complex tablet together with prednisolone (PNL) in 62 patients with SLE was able to demonstrate a 86% remission rate as compared to 32% in the control group of 19 patients treated with PNL alone [Yuan and Feng, 1989]. This herbal complex appeared to improve erythema, arthritis, nephropathy and serological abnormalities such as serum complements.

Unfortunately, there are currently no reported well-controlled randomized clinical trials with TCM in the treatment of SLE. However, several experimental studies examining the effect of TCM on lymphocyte activation and function in SLE patients, as well as animal models of lupus nephritis have been described. Studies conducted on (New Zealand black x New Zealand white) F1 ([NZBxNZW] F1) mice with *Codonopsis pilosula* and *Cordyceps sinensis* was able to prolong the life span of these mice, which develop spontaneous SLE, as well as to inhibit anti-DNA antibody production. Yang and co-workers were able to extract H1-A a pure compound from *Cordyceps sinensis* and tested it on the MRL-*lpr/lpr* mice. They showed that H1-A prolonged life-span and normalized biochemical factors [Yang et al., 1999]. Refined extracts from the root xylem of TWHf have been shown to be effective in the treatment of lupus nephritis and arthritis in MRL-*lpr/lpr* mice [Zhang et al., 1992; Gu et al., 1992]. TWHf was able to decrease the amount proteinuria in this spontaneous lupus nephritis mouse model, as well as to improve survival. However no effect was demonstrated in the histopathology of lupus nephritis. Another herb, stragalin, was shown to inhibit deposition of intracellular adhesion molecule –1 (ICAM-1), immunoglubulins and C3 in the glomerular capillary walls of MRL-*lpr/lpr* mice [Chen et al., 1995].

The development of new immunosuppressive agents with a high therapeutic index for solid organ transplantation remains a priority. As an extension of their use in autoimmune diseases, TCM with immunosuppressive properties have been tested in animal models of organ transplantation.

Berbamine, an alkoloid from the plant, *Berberis juliane*, has been demonstrated to have anti-hypertensive, anti-arrthymic and immunosuppressive properties [Li et al., 1989]. Luo and colleagues [Luo et al., 1995] demonstrated that berbamine was able to inhibit the lymphoproliferate response to Concavalin A (Con-A) and Lypopolysaccharide (LPS), decrease the plaque-forming colonies to T-dependent antigens, as well as the $CD4^+/CD8^+$ ratio. Moreover, berbamine not only suppressed the mixed lymphocyte reaction (MLR) and delayed-type hypersensitivity reaction, but was also able to prevent rejection of skin grafts in mice [Luo et al., 1998].

TWHf has also been studied for its use in organ transplantation [Li et al., 1990]. Demethylzelasteral, a triterpenoid isolated from the root cortex of TWHf, was shown to inhibit the MLR in mice splenic cells [Tamaki et al., 1996]. Studies on heart allograft transplant in Lewis rats demonstrated that a combination of demethylzelasteral at 10 mg/kg/day with CsA A increased allograft survival to 15.0 ± 1.2 days, whereas single drug treatment with demethylzelasteral also improved survival to 17.4 ± 2.9 days. On the other hand, untreated control rats rejected their heart allograft after 6 days.

Although the Chinese philosophy of medical treatments is based on achieving a “perfect balance between the Yin and Yang”, in recent years, the use of TCM as immunosuppressive agents has been studied *in-vitro* and *in-vivo* in various experimental animal models of autoimmune diseases and allograft transplant.

Moreover, experimental studies based on active extracts of several different herbs commonly used as immunosuppressants, have identified a few extracts active in other cytokine-mediated diseases such as mesangial proliferative glomerulonephritis [Kuo et al., 1998]. There are very few well-designed randomized placebo-controlled clinical trials demonstrating their use in various diseases [Sheehan et al., 1992; Sheehan and Atherton, 1992]. In conclusion there is both laboratory and clinical evidence that the derivative of many of these herbs have significant beneficial immunosuppressive effects, however, concerns such as toxicity and dosage must be addressed [Harper, 1994]. This is especially true as the pot-pouri of chemicals produced by these plants are extremely variable, and may be affected by seasonal changes, agricultural conditions, to name a few. Hence exact dosing of the active components is difficult in the current TCM prescriptions.

1.2 BACKGROUND

Our research group's interest in the "Ming Decoction of 21 Tonics for Kidney" arose from treatment of a patient with lupus nephritis and chronic nephrotic syndrome, in whom clinical remission started after ingestion of this Chinese medicinal decoction (CM) [Yap et al, 1999]. This medicinal decoction included the following genera *Prubella, Lycium, Bletilla. Ligustrum, Dianthus, Myrrha, Eucommia, Rehmannia, Rosa, Rubia, Imperata, Curculigo, Panax, Astragalus, Codonopsis, Dioscorea, Nelumbo, Boswellia, Polygonum. Citrus*, and *Glycyyrrhiza*.

Case Report

A 16-year-old Chinese girl presented with features of SLE at the age of 7 years. Her initial manifestations were prolonged pyrexia for 1 month, arthralgia, and erythematosus rash over the malar region. She had oral ulcerations and hepatosplenomegaly. Her blood pressure was within normal limits at 120/80 mm Hg. Laboratory findings included hemoglobin of 120 g/L, white blood cell count of $5.6X10^9$/L. The erythrocyte sedimentation rate was 110 mm/hr: results of direct Coomb test, positive; serum total hemolytic complement (CH_{50}) level, 13 U (normal range 20-50 U); anti-nuclear antibody titer, 1:1280 (homogenous pattern); and anti-double stranded DNA antibody, greater than 15 mg/L (normal, <5 mg/L). Results of urinalysis did not reveal any microscopic hematuria, but proteinuria was present (1+). High-dose PNL therapy at 60 mg/day was started until the fever and anthralgia resolved. The PNL therapy was then slowly tapered to a maintenance dosage of 10 mg/day.

At the age of 12 years, she developed the nephrotic syndrome, with generalized edema, urinary total protein excretion of 1.7 g/day per $1.73m^2$, and low serum albumin level of 25 g/L.

Her renal function was normal. She refused a renal biopsy, as well as increase in her dose of PNL, or additional cytotoxic drugs such as azathioprine or cyclophosphamide. During the next 4 years, her nephrotic state worsened, with an increase in the urinary protein excretion to 13.4 g/day per 1.73m^2 and a decrease in serum albumin level to 11 g/L. Hypertension subsequently developed, with a blood pressure of 160/110 mm Hg and a rise in serum creatinine level to 132 μmol/L. She also had serological markers of active lupus, with an erythrocyte sedimentation rate of 108 mm/hr, C3 level of 58.5 mg/L (normal range, 83-177 mg/L), C4 level of 15 mg/L (normal range, 15-45 mg/L), and anti-double stranded DNA antibody level of greater than 15 mg/L. She again refused a renal biopsy and any increase in her immunosuppressive therapy. Instead, she took CM twice daily, together with PNL at the maintenance dose of 10 mg/day.

After 4 months of CM therapy, when the patient returned for follow-up (Figure 1.2.1), she was noted to be edema free, with blood pressure at 120/75 mm Hg (within normal limits). Her laboratory features continued to improve during the next few months with a urinary protein excretion of 1.3 g/d per 1.73 m^2, serum albumin level of 30 g/L, serum creatinine level of 61 μmol/L, erythrocyte sedimentation rate of 25 mm/hr, C3 level of 100 mg/L, ad C4 level of 24.7 mg/L (Figure 1.2.2). Her anti-double stranded DNA antibody level decreased to 11 mg/L. Subsequently her PNL dosage could be tapered to 5 mg/d, without any increase in the lupus activity. No adverse effects were noted with the use of CM.

The SLE patient had long-standing nephrotic syndrome with severe proteinuria of 13.4 g/day per 1.73 m^2. Although results of renal histological studies were not available, development of hypertension and a rising serum creatinine level accompanied with by low serum complement levels were harbingers of progressive lupus activity. The patient's clinical and serological features improved dramatically after starting on CM. At this time, the patient only

received 10 mg/day of maintenance PNL. As the PNL dose was not increased during this period, it could not account entirely for the significant improvement in the nephrotic state of the patient. Although it is conceivable that the lupus nephritis went into spontaneous remission, this was unlikely in view of the chronicity of the nephrotic syndrome before the ingestion of CM. CM may have a synergistic action with PNL, inducing clinical improvement of the nephrotic state and the lupus activity.

Figure 1.2.1 Treatment of a SLE patients with CM. Normalization of diastolic blood pressure (DBP), serum creatinine (Cr), albumin (Alb) and total urinary protein excretion (TUP) after treatment with CM and PNL.

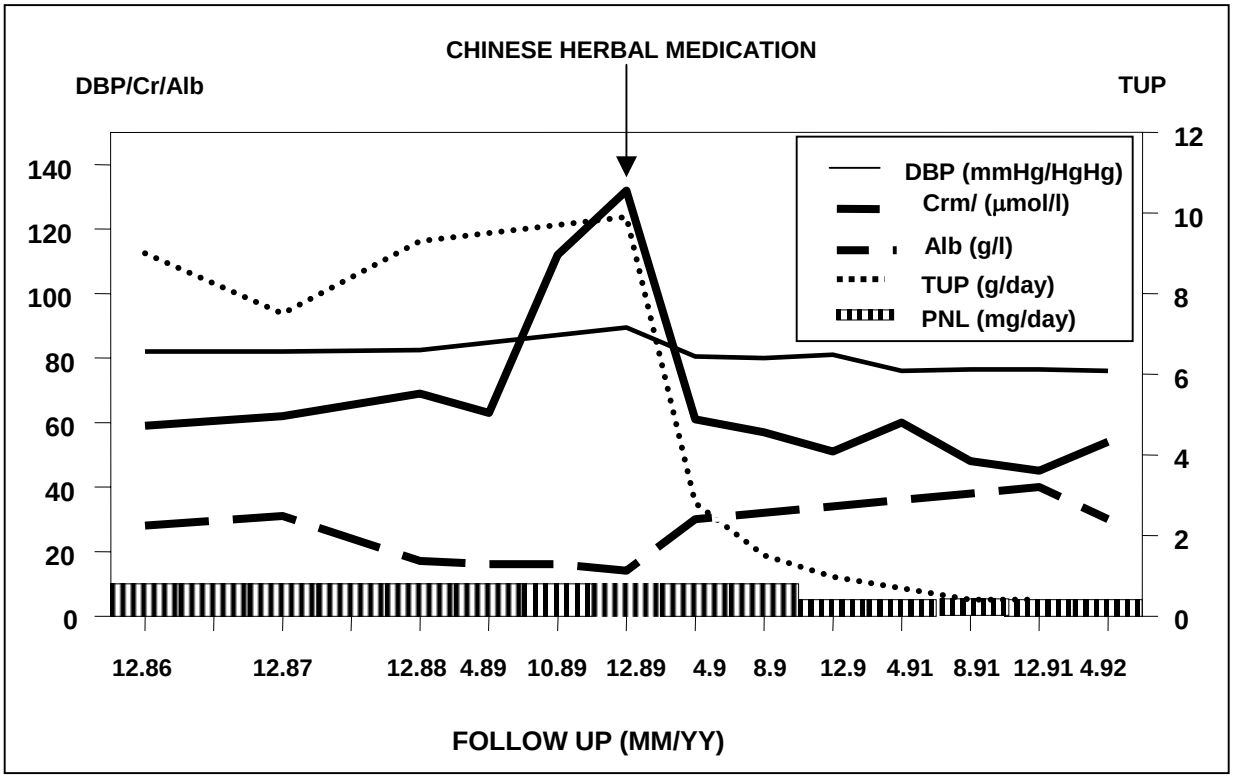

Figure 1.2.2 Effect of CM on serum complement (C) levels in a patient with lupus nephritis. PNL indicates prednisolone in milligrams per day. Complement levels are measured in milligrams per liter.

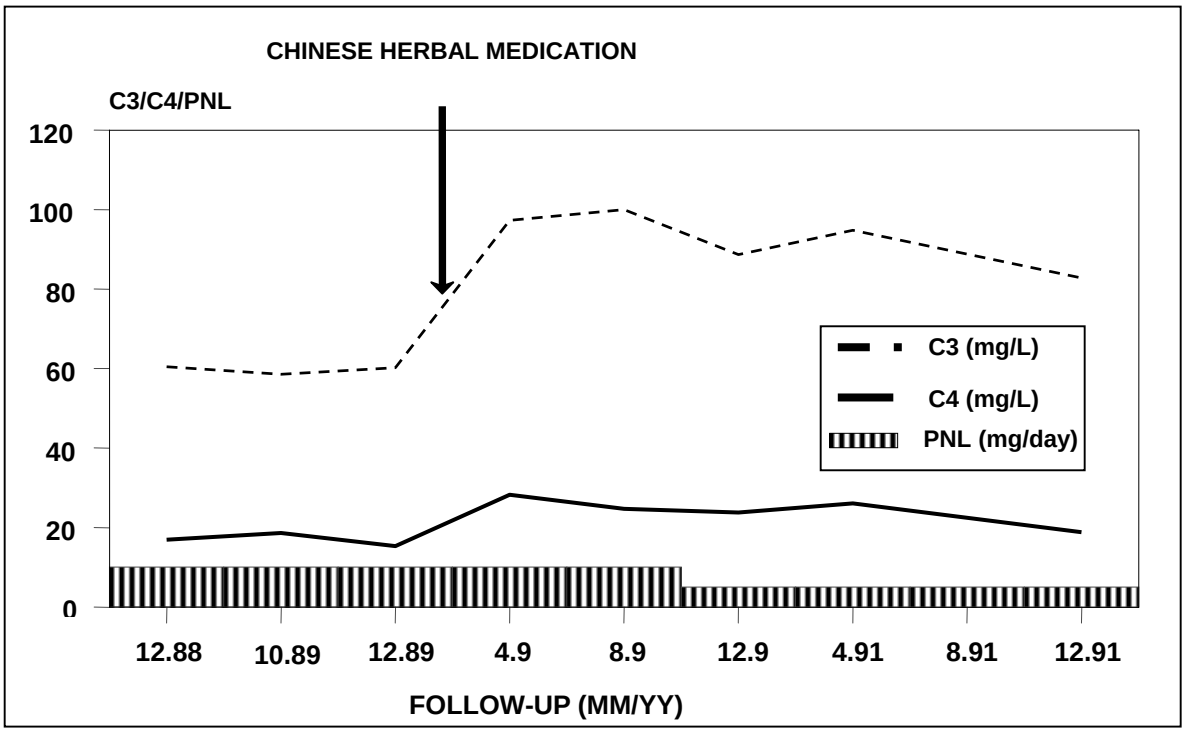

1.3 EFFECT OF CM ON BIOLOGICAL PROCESSES *in-vitro*

Preliminary studies done in our laboratory confirmed the *in-vitro* immunosuppressive activity of CM:

1. CM at a concentration of 440 μg/ml significantly inhibited normal lymphoproliferative response to phytohemaglutunin (PHA) in 5 normal subjects (C1, C2, C3, C4, C5), as measured by incorporation of ^{3}[H]-Thymidine in counts per minute (cpm) (Figure 1.3.1). Cell viability was greater than 90% as assessed by the trypan blue method.

Figure 1.3.1 Effect of CM on PHA-stimulated lymphoproliferation as measured by ^{3}[H]-Thymidine uptake

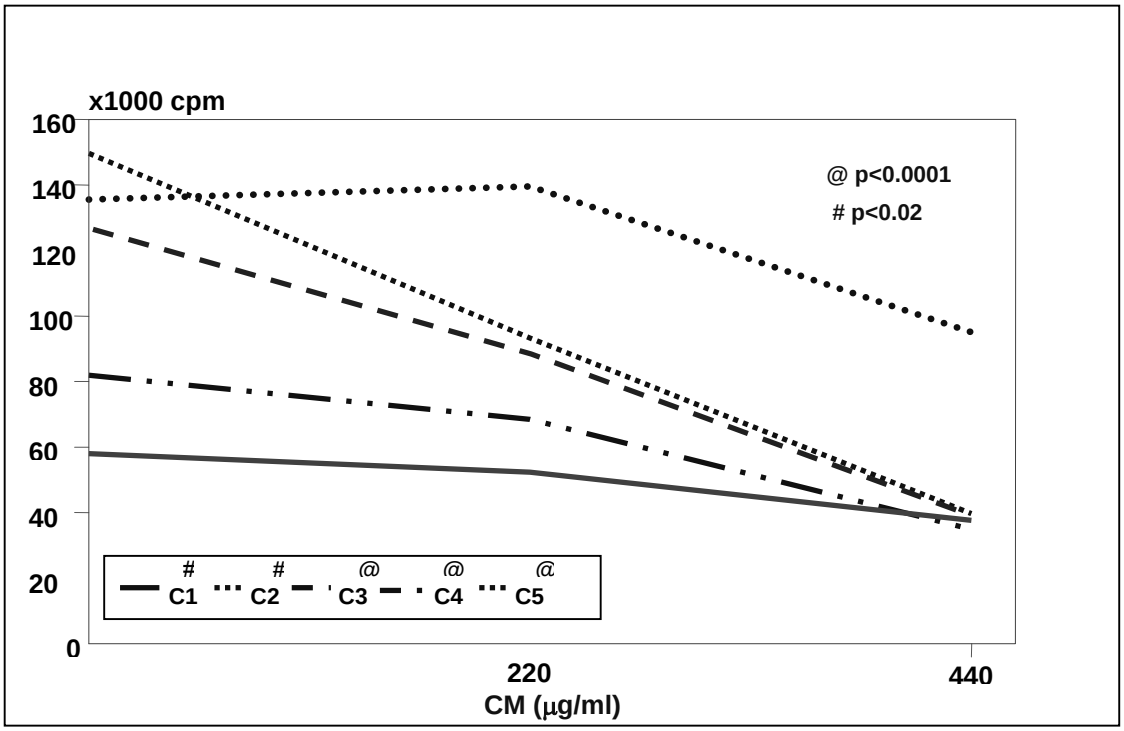

2. CM significantly inhibited the expression of CD25 and Human Leucocyte antigen-DR (HLA-DR) on CD3+ cells, markers of T-cell activation (Figure 1.3.2).

Figure 1.3.2 Effect of CM on T-cell activation markers CD25 (TAC) and HLA-DR (DR)

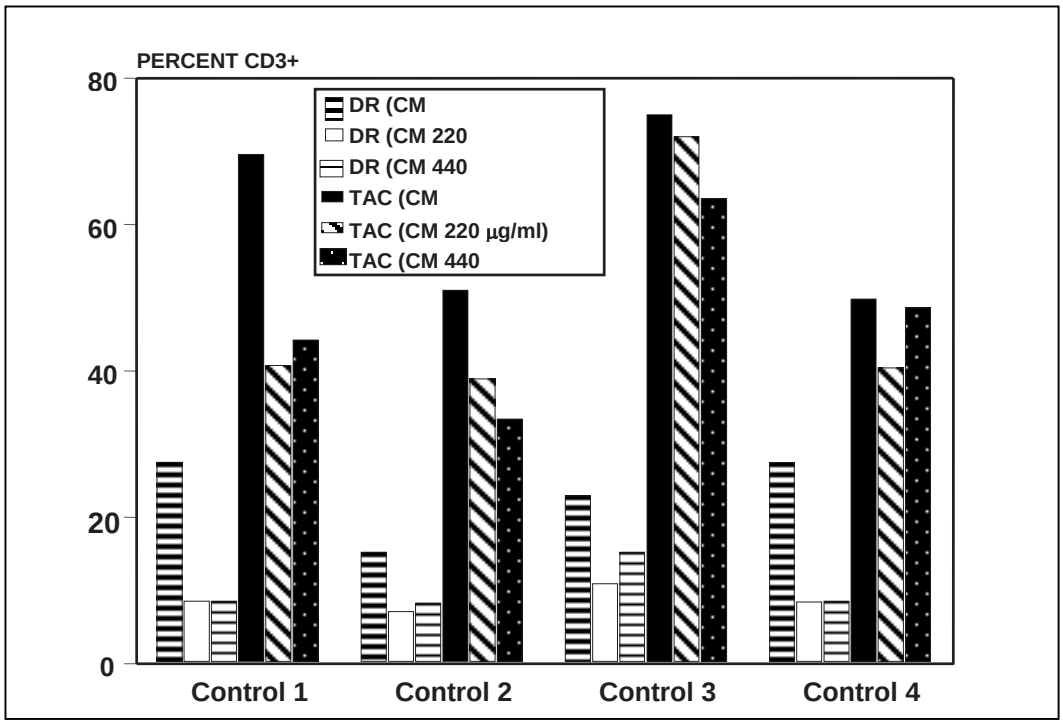

3. CM significantly inhibited the pokeweed mitogen (PWM)-stimulated lymphocyte production of immunoglobulins (Figure 1.3.3).

Figure 1.3.3 Effect of CM on PWM-stimulated Peripheral Blood Mononuclear Cells (PBMCs) immunoglobulin synthesis in normal individuals.

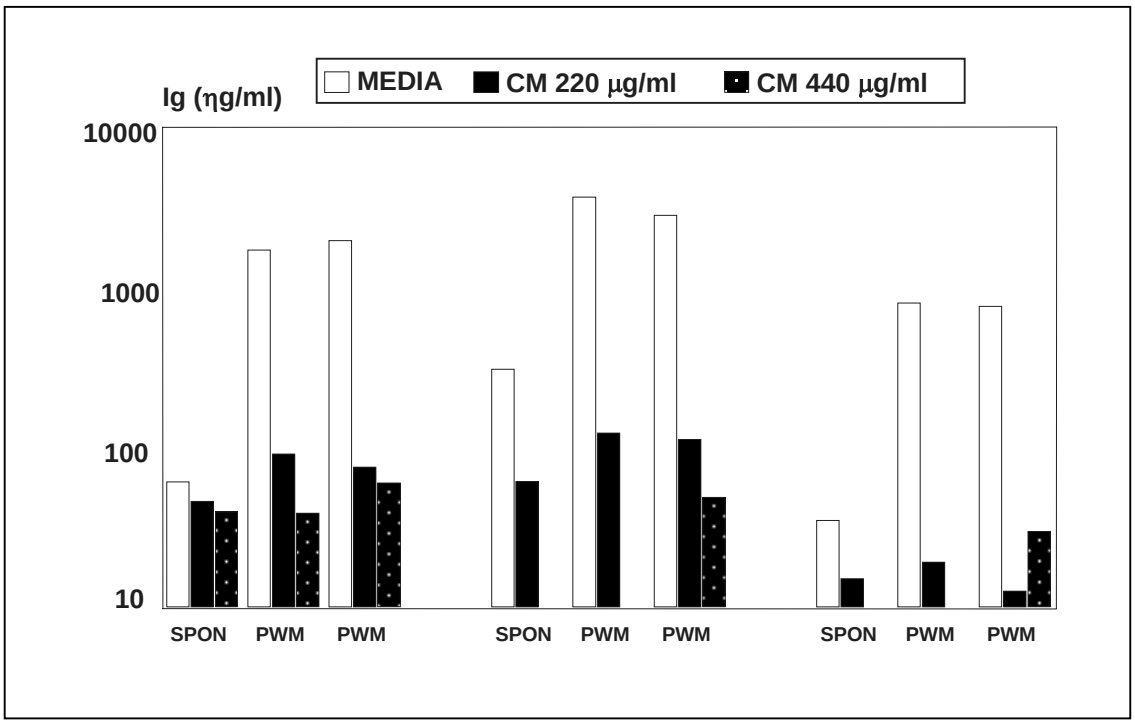

Additionally, our laboratory has examined the effect of the hydrophobic ethyl acetate extract (EX) of CM on PWM-stimulated immunoglobulin G (IgG) production by PBMCs from patients with active SLE. Previous *in-vitro* studies have shown that in patients with active SLE, spontaneous IgG production by PBMC was increased [Wigfall et al., 1988]. Our study confirmed that children with SLE had increased *in-vitro* spontaneous PBMC production of IgG (210±110 μg/ml) compared to normal controls (64±20 μg/ml) [Yap et al, 1999].

PBMCs from 10 SLE patients were subsequently cultured with the hydrophobic extract, EX. Significant suppression of IgG (96±52 ηg/ml) was observed in the group of the SLE patients when the PBMCs were cultured with CM ($p<0.005$) (Figure 1.3.4).

Figure 1.3.4 Effect of CM and its EX on PBMC IgG production in SLE patients.

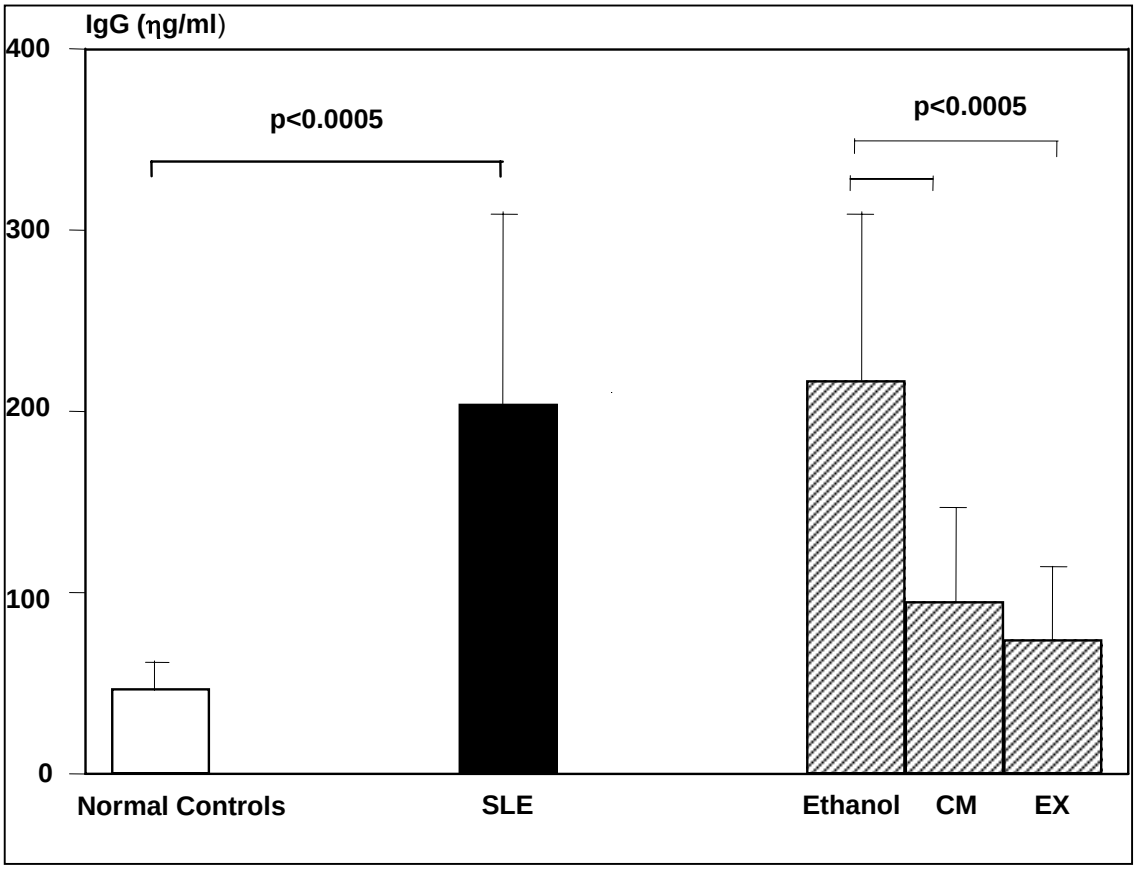

4. CM was also able to act in synergism with CsA to inhibit the lymphoproliferative response to both PHA and the anti-human CD3 T-cell antibody (OKT3) with a dose reduction index of 7.06 (Figure 1.3.5).

Figure 1.3.5 Drug interactions of CM with CsA and dexamethasone (DEX): Mean effect analysis

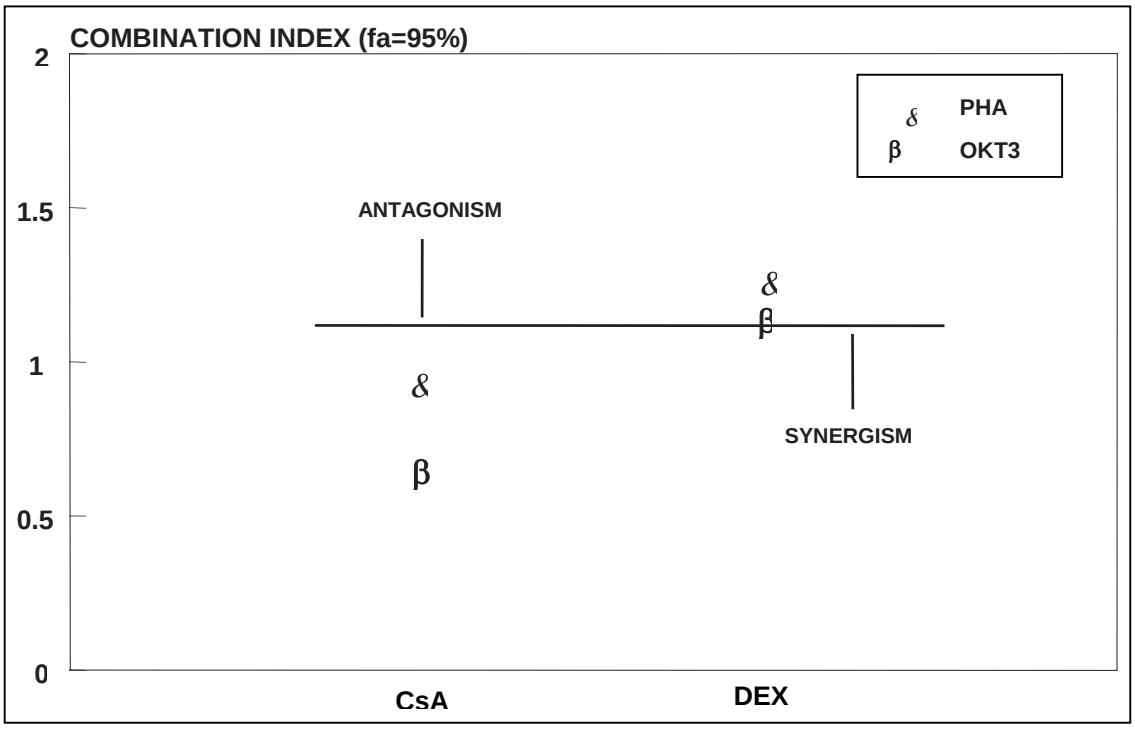

5. CM was able to inhibit both T-cell colony formation (Table 1.3.1) and bone marrow cultures (Table 1.3.2). Colony-forming units were significantly decreased in cultures when CM was added, indicating a mode of action at an early phase of cell proliferation, rather than on mature T-cells.

Table 1.3.1 Effect of CM on T-cell colony formation

	Plate 1#	**Plate 2#**	**Mean#**
Control	92	91	91.5
CM 220 μg/ml	49	65	57
CM 440 μg/ml	15	11	13

colonies/10^5 cells plated

Table 1.3.2 Effect of CM on bone marrow cultures (colony forming units or CFU-C)

	Control#	**CM# (220 μg/ml)**	**CM# (440 μg/ml)**
D7	234	53	3
D14	158	114	6

colonies/10^5 cells plated

1.4 PURIFICATION OF CMX-13 FROM CM

The “Ming Decoction of 21 Tonics for Kidney” crude CM preparation contained extracts from 21 Chinese herbs, which included the following genera *Prubella, Lycium, Bletilla. Ligustrum, Dianthus, Myrrha, Eucommia, Rehmannia, Rosa, Rubia, Imperata, Curculigo, Panax, Astragalus, Codonopsis, Dioscorea, Nelumbo, Boswellia, Polygonum. Citrus*, and *Glycyyrrhiza.* Identification of the bioactive components in this decoction (CM) was performed using a bioassay based on the ability of the components to suppress lymphoproliferation following stimulation with PHA, and measured by ^{3}[H]-Thymidine incorporation. Preliminary extraction processes involved first refluxing with methanol, followed by partitioning the methanol extract between ethyl acetate and water. The active components of CM in terms of immunosuppressive properties, were found in the organic layer (EX) (Figure 1.4.1). Further evaluation of various combinations of the herbs contained in CM showed that the extract of the herb *Rubia cordifolia (RC)* contained the most active components. Following ethyl acetate (EtOAc) extraction by the Soxhlet method, the EtOAc extract of *RC*, CMX, was again subjected to solvent extraction with n-Hexane (Hex) and 90% methanol (MeOH)/H_2O. The 90% MeOH/H_2O fraction was mixed with dichloromethane (CH_2Cl_2) and made up to 50%MeOH/H_2O. The CH_2Cl_2 fraction was found to have the highest immunosuppressive activity, and was subsequently subjected to purification by flash column chromatography. Fourteen fractions were obtained, of which fraction 13 was the most active and was labelled CMX-13. CMX-13 was shown

to be at least 1000 times more potent in terms of inhibition of PHA-stimulated lymphocyte proliferation, as compared to the original medicinal decoction CM.

Figure 1.4.1 Comparison of the inhibitory effect of the various extracts of CM on lymphoproliferation following PHA stimulation.

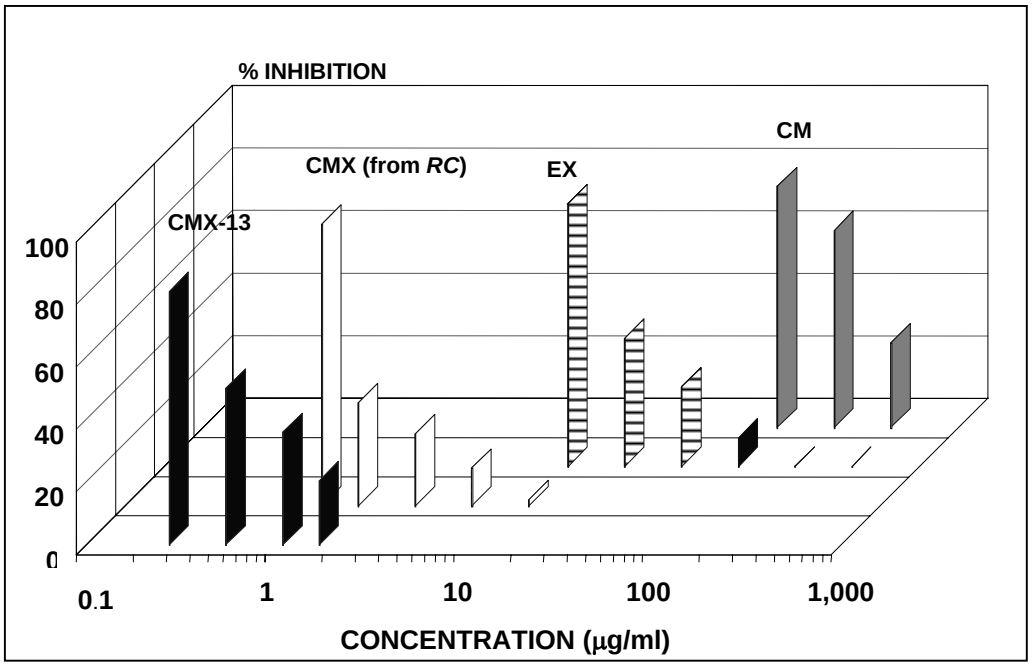

1.5 PRELIMINARY STUDIES OF CMX-13 ON A RAT LUNG ALLOGRAFT MODEL OF ACUTE REJECTION

A pilot study was performed to test the efficacy of CMX-13 in the Brown-Norway→Lewis rat lung transplant model. This is a model of aggressive and rapid allograft rejection with all grafts completely destroyed by day 6 post-transplant. In this model, acute rejection (AR) was graded using a pathologic intensity score (stages I to IV), based on perivascular and peribronchial mononuclear cell infiltrates, oedema, vasculitis, necrosis, and intra-alveolar haemorrhage [Kondo et al, 1991]. CMX-13 given at 5 mg/day IV to 5 rats daily for 3 days, resulted in a significant inhibition of the acute rejection response, with treated animals showing no necrosis, oedema, intra-alveolar haemorrhage or vasculitis (Figure 1.5.1). This effect was similar to that seen with a single high dose CsA given at 25 mg/kg (Yap et al, 1998; Zuo et al, 2000).

Figure 1.5.1 The effect of CMX-13 and CsA on acute rejection in the Brown Norway→Lewis rat lung transplant model. The stages of AR was graded by a pathologic intensity score (stages I to IV), based on perivascular andperibronchial mononuclear cell infiltrates, oedema, vasculitis, necrosis, and intra-alveolar haemorrhage. The rats treated with 5mg/kg CMX-13 had similar pathological intensity scores to those treated with 25 mg/kg CsA.

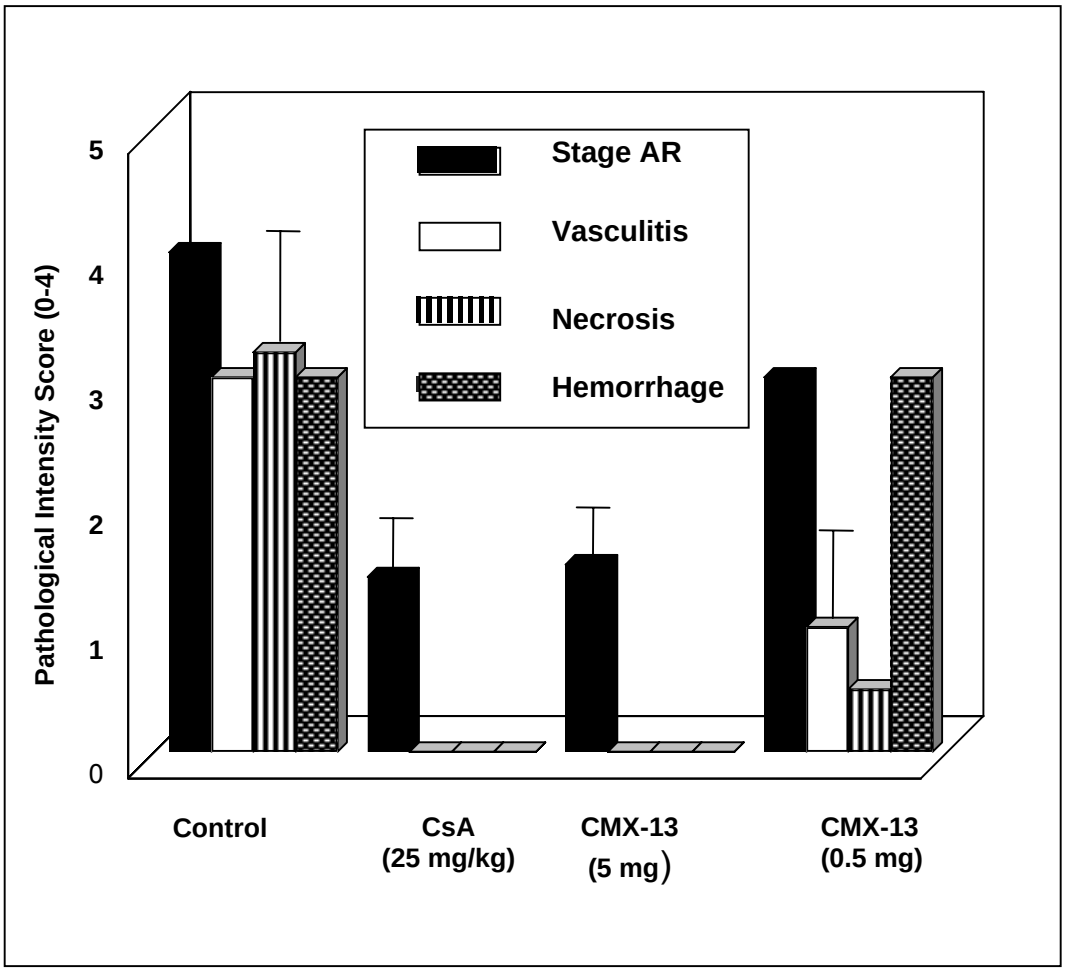

The effect of CMX-13 on Con-A stimulated proliferation of isolated spleen cells from the Lewis rat showed that CMX-13 at 0.25 μg/ml and 1 μg/ml was able to suppress cell proliferation in a dose-dependent manner, similar to the effect of CsA at similar concentrations (Figure 1.5.2).

Figure 1.5.2 Comparison of CMX-13 with CsA on rat splenic cell proliferation following Con-A stimulation.

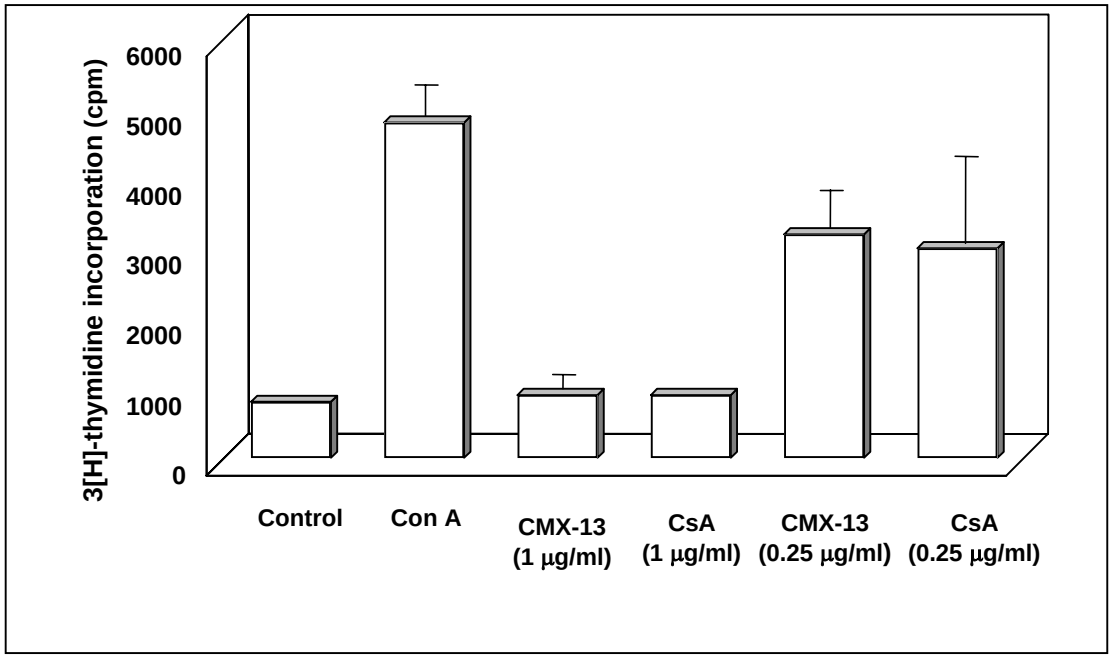

The effect of CMX-13 on the Th1 cytokines, interleukin (IL)-2 and interferon (IFN)-γ gene expression in Con-A stimulated rat spleen cells has also been examined. Rat splenic cells were stimulated with 5.0 μg/ml Con-A and cultured either with or without CMX-13 or CsA. CsA showed significant inhibition of IL-2 messenger RNA (mRNA) expression at 6, 24 and 40 hours following Con-A stimulation. CsA also significantly inhibited IFN-γ mRNA expression at 6 hours following Con-A stimulation. In contrast, CMX-13 did not have any significant effect on both IL-2 and IFN-γ mRNA expression at all the time points tested [Zuo et al, 2000]. These findings suggested that the immunosuppressive effects of CMX-13 were possibly post-transcriptional and antiproliferative.

1.6 SLE: CLINICAL SYNDROME

SLE is considered to be the prototypic systemic autoimmune disease, in which autoantibodies have the potential to damage diverse organs. The immunopathogenesis of SLE is complicated, involving genetic susceptibility elements, poorly defined cellular immune mechanisms, and mostly unknown triggering agents. SLE predominantly affects women at any age (~ 90%), but women at childbearing age are primarily affected [Gaffney et al.,1998; Kotzin, 1996]. The female to male ratio is maximum (>8:1) for patients between 15-50 years and the ratio decreases to 2:1 for disease that develops during childhood or after menopause. A role for estrogens contributing to the development of SLE and androgens protecting against disease development have thus been postulated [Kotzin, 1996]. The overall prevalence of SLE (~1 in 2000) is about the same as multiple sclerosis and about 5-to 10-fold less than type 1 diabetes mellitus and rheumatoid arthritis [Lindqvist and Alarcon-Riquelme, 1999]. SLE is more prevalent in certain ethnic groups when compared to Caucasians [Kotzin, 1996].

The clinical presentation and progression of disease are extremely varied [Vyse and Kotzin, 1998; Kotzin, 1996]. Individual patients exhibit striking variability in their clinical symptoms and laboratory findings. For example, some patients go into spontaneous remission, while others present predominantly with skin rashes and joint pains requiring little medication, and yet others develop severe and progressive organ involvement such as lupus nephritis,

requiring therapy with high doses of steroids and cytotoxic drugs such as cyclophosphamide. Due to the variability in clinical presentation and clinical course, criteria for the classification of SLE have been established to facilitate the uniform reporting of SLE cases in epidemiological and research studies (Table 1.6.1) [Tan et al., 1982].

The modified American Rheumatological Association (ARA) classification is based on 11 criteria. For the purpose of identifying patients in clinical studies, a person is diagnosed to have SLE if any 4 or more of the 11 criteria are present, serially or simultaneously, during any interval of observation [Tan et al., 1982].

Table 1.6.1 The 1982 revised ARA criteria for classification of SLE [Tan et al.,1982]

Criterion	Definition
1 Malar Rash	Fixed erythema, flat or raised, over the malar eminences, tending to spare the nasolabial folds
2 Discoid lesions	Erythematous raised patches with adherent keratotic scaling and follicar plugging
3 Photosensitivity	Skin rash as a result of unusual reaction to sunlight, documented by patient history or physician observation
4 Oral ulcers	Oral or nasopharyngeal ulceration, usually painless, observed by a physician
5 Arthritis	Nonerosive arthritis involving 2 or more peripheral joints, characterized by tenderness, swelling, or effusion
6 Serositis	a) pleuritis (a convincing history of pleuritic pain or rub or evidence of pleural effusion) b) pericarditis (documented by electrocardiogram, or evidence of pericardial effusion)
7 Nephropathy	a) persistent proteinuria> 0.5 g/day or >3+ if quantitation not performed b) cellular casts (may be red cell, hemoglobin, granular, tubular, or mixed) c) otherwise unexplained elevation of serum creatinine >75 μmol/L
8 Neurological Involvement	a) Seizures in the absence of offending drugs or known metabolic derangements, e.g., uremia, ketoacidosis, or electrolyte imbalance b) Psychosis in the absence of offending drugs or known metabolic derangements, e.g., uremia, ketoacidosis, or electrolyte imbalance
9 Hematological Disorder	a) Hemolyitc anemia with reticulocytosis b) Leukopenia:< 4000/μl total on two or more occasions or c) Lymphopenia: < 1500/μl on two or more occasions or d)Thrombocytopenia < 100,000/mm^3 in the absence of offending drugs
10 Immunological Disorders	a) Positive LE cell preparation or b) Anti-DNA:antibody to native DNA in abnormal titer c) Anti-Sm: presence of antibody to SM nuclear antigen d) False-positive serological test for syphilis known to be positive for at least 6 months and confirmed by TPI or FTA-ABS
11 Antinuclear Antibody	An abnormal titer of ANA by immunofluorescence or an equivalent assay at any point in time and in the absence of drugs known to be associated with “drug—induced lupus” syndrome.

1.7 PATHOGENESIS OF SLE

SLE is an immune-mediated disorder characterized by autoantibody formation. The major hallmark of this disease is the elevated serum levels of antibodies to nuclear constituents (i.e., anti-nuclear antibodies), the principal targets include protein-nucleic acid complexes, notably chromatin, the U1 and Sm small nuclear ribonucleoprotein (snRNP) particles, and the Ro/SSA and La/SSB RNP complexes [Tan, 1989; Kotzin and O' Dell, 1995]. In contrast to other autoimmune diseases, T-cells do not appear to play a direct role in tissue damage in SLE, but are indirectly involved in the production of IgG autoantibody production. The mechanism by which many autoantibodies mediate SLE pathology remains unclear. IgG autoantibodies to double-stranded DNA appear to play a prominent role in the genesis of lupus nephritis [Lindqvist and Alarcon-Riquelme, 1999; Vyse and Kotzin, 1998]. Deposition of immune complexes containing these antibodies does not appear to mediate renal damage. The proposed mechanisms for lupus nephritis include *in-situ* immune complex formation following binding of DNA to the glomerulus, and cross-reactive anti-DNA antibodies to non-DNA glomerular structures [Bernstein et al., 1995]. Immune complexes may also be responsible for other disease manifestations such as arthritis, rashes, serositis, and vasculitis, whereas a separate group of autoantibodies that are directed to cell surface determinants may cause problems such as hemolytic anemia, thrombocytopenia, and central nervous system damage [Vyse and Kotzin.,

1998]. Thus, the development of disease in SLE appears to involve the development of both autoreactive T-cells and B-cells.

Evidence from several studies strongly supports the hypothesis that pathogenic IgG autoantibody production in SLE is selective for only certain self-antigens, and that autoreactive B-cells are driven by self-antigens. In SLE and lupus mice, studies have shown that a subset of anti-DNA antibody-producing B-cells are clonally expanded [Radic et al., 1993]. Experiments with transgenic mice encoding self-reactive antibodies have demonstrated that B-cell development involves a process of tolerance that deletes or functionally inactivates autoreactive cells. Hence SLE could be considered a disease syndrome involving loss of self-tolerance [Steinberg, 1994]. Tolerance to self could involve intrathymic deletion, peripheral deletion, and peripheral tolerization without deletion. A loss of any of these processes could result in disease.

Genes encoding for the major histocompatilibility complex (MHC) Class II antigens seem to play a pivotal role in the development of SLE [Vyse and Kotzin, 1998; Lindqvist and Alarcon-Riquelme, 1999; Drake et al., 1995]. MHC Class II proteins bind to T cell receptor (TCR) of the $CD4^{+}CD8^{-}$ $\alpha\beta$-T-cells in the thymus thus preparing them for positive selection [Nikolic-Zugic et al., 1991; Rothenberg, 1990; Sha et al., 1988]. Autoreactive T-cells that escape negative selection have a low affinity for the MHC Class II proteins, and populate the periphery [Guerder and Flavell, 1996]. Studies have shown that these genes

may be involved in the development of auto-aggressive $CD4^+CD8^-$ $\alpha\beta$ T-cells and lupus nephritis [Jevnikar et al., 1994]. The role of the auto-aggressive $CD4^+CD8^-$ $\alpha\beta$ T-cells is further demonstrated in SLE murine lupus models where they are found to be related to autoantibody production [Peng et al., 1996, Peng et al., 1998; Seery et al., 1999; Koh et al., 1995]. Moreover, the central role of these cells in murine lupus is further supported by the demonstration that the elimination or down-regulation of these cells result in significant disease amelioration [Jevnikar et al, 1994; Steinberg et al, 1978; Yamamoto et al, 1990; Koh et al, 1995].

$CD4^+$ T-cell dependence of autoantibody production has been demonstrated in studies where blocking of T-cell activation or T- and B-cell interactions prevented autoantibody production and the development of murine lupus [Finck et al., 1994a; Mohan et al., 1993; Mohan and Datta, 1995]. Additionally, treatment with anti-CD4 antibodies ameliorated IgG autoantibody production and disease [Kotzin, 1996]. The $CD4^+$ T-cells play an important role in Kotzin's hypothesis for immunopathogenic events that contributes to the development of SLE. According to this hypothesis auto-aggressive $CD4^+CD8^-$ $\alpha\beta$T-cells are generated through genetic susceptibility and environmental triggers. They act as a driving force for autoreactive B-cells, which become hyperreactive and produce autoantibodies. The hypothetical model for the development of SLE is depicted in Figure 1.7.1.

Figure 1.7.1 Hypothetical model for immunopathogenic events in the development of SLE [Kotzin, 1996].

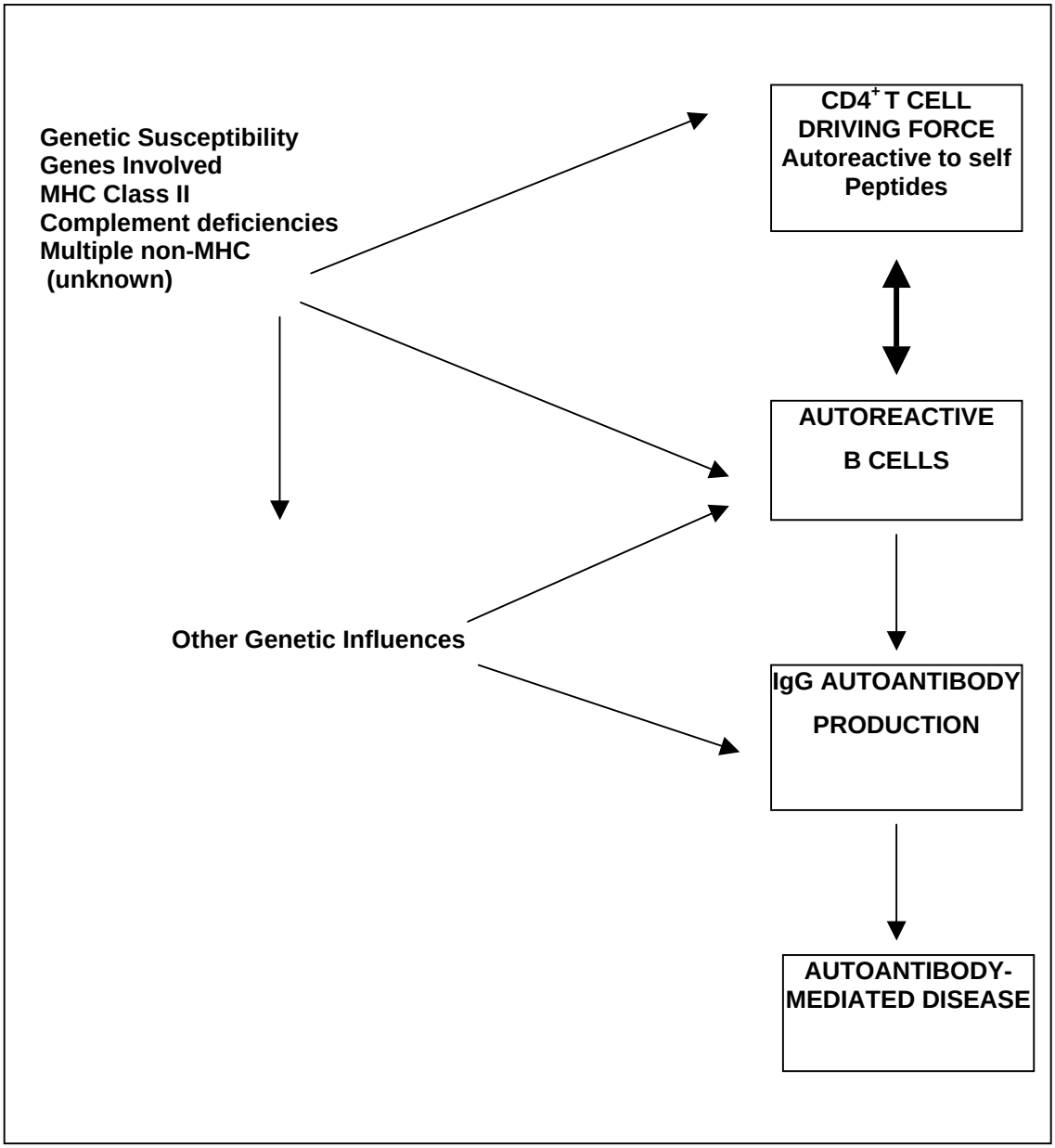

1.8 MRL-*lpr/lpr* AUTOIMMUNE MOUSE MODEL

MRL-*lpr/lpr* mice represent an excellent model to study the pathogenesis of lupus nephritis [Theofilopoulos and Dixon, 1985]. These mice spontaneously develop a generalized autoimmune disease, including vasculitis, generalized lymphadenopathy, arthritis and a severe immune complex glomerulonephritis, dying of renal failure between 5 to 8 months of age [Andrews et al, 1978]. These mice also produce autoantibodies such as anti-double-stranded DNA antibodies and anti-IgG (rheumatoid factor). Moreover, MRL-*lpr/lpr* mice display proinflammatory alterations in the intrarenal cytokine network [Boswell et al, 1988a; Boswell et al, 1988b; Fan et al, 1997]. Alterations in the cytokine network are characteristic of many immune-mediated disorders. Cytokines produced by Th1 type lymphocytes, such as Tumor necrosis factor (TNF)-α and IFN-γ, may play a major role in the pathogenesis of autoimmune diseases.

The role of MHC Class II proteins in the genesis of SLE has also been demonstrated in gene knockout models of murine lupus. The development of SLE was inhibited in lupus-susceptible mice in which the genes encoding for the MHC Class II proteins were deleted [Ibnou-Zekri et al., 1997]. MRL-*lpr/lpr* mice which were rendered MHC Class II-deficient, did not exhibit any autoantibody production [Anderson et al., 1993]. Moreover, these mice had a reduced level of total serum immunoglobulin, implying defective polyclonal regulation of B cells by T-cells [Anderson et al., 1997].

Apoptosis genes are another set of candidate genes, which are involved in the development of SLE. Mutations in the lymphoproliferative (*lpr)* Fas gene and in the *gld* or Fas ligand (FasL) gene result in the development of an autoimmune illness resembling SLE in mice. The *Fas* and *FasL* genes are involved in programmed cell death through apoptosis [van Houten and Budd, 1994]. Complete development of SLE in the MRL-*lpr/lpr* mouse is dependent on the presence of homozygous mutations of the *Fas* and the *FasL* gene. The exact mechanism by which these mutations result in disease in MRL-*lpr/pr* mouse model is unknown. A hypothesis which is widely accepted is that self-reactive T- and B-cells are generated when they fail to undergo apoptosis. Studies have shown that Fas (CD95) is not essential in intrathymic tolerance during T-cell development, and that peripheral T-cell tolerance mechanisms are affected by the *lpr* mutation [Singer and Abbas, 1994; Herron et al., 1993]. Defective transcription of the apoptosis gene encoding Fas causes massive lymphoproliferation of double-negative ($CD4^-CD8^-$) T-cells [Watanabe et al., 1992; Adachi et al., 1993]. These $CD4^-CD8^-$ T-cells are a rich source of proinflammatory cytokines including TNF-α and IFN-γ [Murray et al., 1990; Murray and Martens, 1990].

Only two mutations in the *Fas* gene [Rieux-Laucat et al., 1995; Fisher et al., 1995] and the *FasL* gene [Wu et al., 1994] have been reported in humans, these were patients with autoimmune lymphoproliferative syndrome. However no mutations in the *Fas* or *FasL* genes have been found in SLE patients.

Hence there may be other genes or pathways related to apoptosis which may be involved in the generation of autoreactive lymphocytes. In the sera of SLE patients high expression levels of a soluble form of the Fas (sFas) molecule have been identified. Studies have shown that sFas inhibits apoptosis in lymphocytes [Cheng et al., 1996] and may consequently lead to the development of autoimmunity [Mountz et al., 1994].

1.9 SCOPE OF THE THESIS

Preliminary studies have demonstrated the immunosuppressive potency of both the crude decoction CM, as well as the active fraction CMX-13 on *in-vitro* T-lymphocyte proliferation, as well as B-cell secretion of immunoglobulins in both normal individuals as well as patients with SLE. In addition, we have shown the efficacy of CMX-13 on preventing acute rejection in a rat lung transplant model of hyperacute allograft rejection. This thesis utilizes the MRL-*lpr/lpr* murine model of lupus nephritis to study the mechanism of the immunosuppressive action of CMX-13 and its derivatives.

Objective 1:

To characterize CMX-13, which is the fraction which contains the active component(s) of the herb *RC.* following separation by liquid chromatography) using spectroscopic and chemical methods.

Objective 2:

To explore the molecular mechanisms of action of CMX-13 *in-vitro.*

The molecular basis for the immunosuppressive effects of CMX-13 remains to be elucidated. We have previously shown that CMX-13 was able to suppress mitogen-stimulated lymphoproliferative responses and immunoglobulin production, as well as inhibit T-cell colony formation. In our earlier studies on the possible mechanisms of action, CMX-13 did not show any inhibitory effects

on IL-2 and IFN-γ mRNA expression, suggesting that its mechanism of action is different from that of CsA [Zuo et al., 2000]. As there is strong evidence that dysregulation of apoptosis in the immune regulatory cells could have a role in the genesis of SLE, this part of the thesis will examine the effect of CMX-13 on:

(1) Cell cycle progression in PBMC isolated from normal controls and patients with SLE, as well as Jurkat cells, a human T-cell line

(2) Apoptotic events.

Objective 3:

To study the effect of CMX-13 in a mouse model of generalized autoimmune disease, which resembles human SLE (MLR-*lpr/lpr* mice).

The MRL-*lpr/lpr* mouse strain has a mutation in the *fas* gene, which leads to the development of SLE in these mice. Significant similarities exist with the human form of SLE and the MRL-*lpr/lpr* mouse model. Studies have shown that $CD4^+$ T-cells are responsible for the development of SLE in these mice. Our earlier studies have shown that CMX-13 had immunosuppressive effects on stimulated lymphocytes, therefore the aims of this section of the thesis are to study the effect of CMX-13 on the following parameters in the MRL-*lpr/lpr* mouse strain:

1. Development of clinical disease, as assessed by degree of lymphadenopathy, articular swelling and proteinuria, including survival analysis

2. Development of autoantibodies, namely, anti-double stranded DNA antibodies and anti-IgG (rheumatoid factor)
3. Histolopathological evidence of glomerulonephritis
4. Dysregulation of cytokines, especially IL-2, IFN-γ, IL-6 and IL-10, important in the genesis of the disease.

CHAPTER 2 MATERIALS AND METHODS

2.1 BIOASSAY GUIDED ISOLATION AND PURIFICATION OF BIOACTIVE COMPOUNDS

2.1.1 Soxhlet Extraction

The roots of *RC.* used in this experiment were purchased from local Chinese Traditional Medicine shops in Singapore. The crude roots were grounded (45 grams each time) and extracted with 500 ml EtOAc using a Soxhlet apparatus for 5-8 hours. The EtOAc extract was then lypholized under reduced pressure and tested for its immunosuppressive properties.

2.1.2 Solvent Partition

The bioactive EtOAc extract was dissolved in MeOH followed by addition of water to MeOH a ratio of 9:1. The 90% MeOH aqueous solution was partitioned three times with Hex in a separation funnel. The organic phase (Hex) was collected and evaporated, which produced the Hex extract. Water was added to the 90% MeOH aqueous extract phase until the MeOH:H_2O ratio was 1:1. The 50% MeOH/H_2O solution was then partitioned three times with CH_2Cl_2.

2.1.3 Isolation of CMX-13 from EtOAc extract by Flash Column Chromatography and Reverse Phase-Thin Layer Chromatography

Approximately 4.2 g of CH_2Cl_2 extract was subjected to flash chromatography (column diameter 8 cm, 60A silica gel (Kieselgel 60 with a mesh range 230-400 ASTM from Merck) 25 cm high, 100% Hex wet packed. The CH_2Cl_2 extract was eluted with Hex, followed by a Hex-EtAOc solvent system, and subsequently by an EtOAc-MeOH solvent system. Sixteen fractions were isolated by Reverse Phase-Thin Layer Chromatography (RP-TLC). RP-TLC on Flash Column Fractions. RP-TLC was carried out on silica gel pre-coated glass plates (Merck, Kieselgel $60F_{254}$, 250 μm layer thickness). Solvent system: 90% EtOAc/MeOH. The R_f value defined as the distance moved by the spot relative to that moved by the solvent front. Two samples that have similar compounds will have an identical R_f value. The solvent systems for the Flash Column Chromatography are summarized in Table 2.1.3.1.

Table 2.1.3.1 Mobile phase for Flash Column Chromatography

Step	Solvent	Volume in ml
1	100% Hex	250
2	80% Hex/20% EtOAc	300
3	60% Hex/40% EtOAc	300
4	50% Hex/50% EtOAc	300
5	40% Hex/60% EtOAc	300
6	20% Hex/80% EtOAc	300
7	0% Hex/100% EtOAc	300
8	100% EtOAc	300
9	80% EtOAc/ 20%MeOH	300
10	60 % EtOAc/ 40%MeOH	300
11	50 % EtOAc/ 50%MeOH	300
12	20 % EtOAc/ 80%MeOH	300
13	100% MeOH	400

2.1.4 Purification of CMX-13 fractions by Reverse Phase- High Performance Liquid Chromatography (RP-HPLC)

RP-HPLC conditions were optimized and were as follows, Column: Nova-pack C18 Column, pore size 4 μm, 3.9 x 300 mm from WATERS; Mobile phase 100% water/acetonitrile: water/100% acetonitrile in a gradient program; flow rate: 0.6 ml/min; detection: Ultra Violet 254 nm or PDA detection varying from 200-600 nm; performed on a Waters 600E system; software: Millenium from Waters; injection volume of 50 μl at a concentration of 5.0 mg/ml dissolved in 50% MeOH/Acetonitrile. The complete RP-HPLC program is shown in Table: 2.1.4.1.

Table 2.1.4.1 RP-HPLC conditions for CMX-13. Stationary Phase: C18 Reverse phase column; Mobile Phase: 0% Acetonitrile 100% Water to 100% Acetonitrile 0% Water.

Time (min)	Flow (ml/min)	% Acetonitrile	% Water
0	0.6	0	100
15	0.6	50	50
25	0.6	65	35
40	0.6	100	0
65	0.6	0	100

2.1.5 Nuclear Magnetic Resonance (NMR)

The proton spectra were recorded on a Bruker Spectrometer (AM 500) and processed on a Bruker data station. CMX-13-5 purified from RP-HPLC was dissolved in 0.5 ml deuteriated MeOH in a 5 mm tube.

2.1.6 Liquid Chromatography- Mass Spectrometry (LC-MS)

Mass spectral analysis was conducted on a Finnigan Thermo-Quest LCQ triple quadrupole mass spectrometer using FAB mode of ionization while scanning in alternating positive full-scan mode. Mass spectrometer was coupled to a Hewlett-Packard 1090A HPLC and chromatographic analyses were conducted by reversed-phase on a Nova-pack C18 Column, pore size 4 μm, 3.9 x 300 mm from WATERS with UV detection at 254 nm. Solvents for elution consisted of 100% water/acetonitrile to water/100% acetonitrile in a gradient program at a flow rate of 0.6ml/min.

2.1.7 Bioassay Based On Inhibition of Cellular Proliferation

PBMCs were isolated from Heparinized blood using standard Ficoll-Hypaque (Amersham Pharmacia Biotech AB, Uppsala Sweden) density-gradient centrifugation at 2000 rpm for 30 minutes. The mononuclear cell interface was collected and washed twice in RPMI 1640. The Jurkat cells and PBMCs were

maintained in complete media RPMI 1640 (Gibco, Life Technologies, Grand Island NY, USA), supplemented with 10% fetal calf serum (FCS) (Gibco, Life Technologies, Grand Island NY, USA), 100 U/ml penicillin, 100 μg/ml streptomycin (Gibco, Life Technologies, Grand Island NY, USA) and 1 mM of L-glutamine (Sigma Chemicals, USA).

Jurkat cells or PBMCs were cultured in flat-bottomed microtitre plates (200 μl/well) in triplicates at a concentration of $1x10^6$ cells/ml in RPMI 1640, supplemented with 10% FCS, 100 U/ml penicillin, 100 μg/ml streptomycin and 1 mM of L-glutamine. The PBMCs were stimulated with 0.75 μg/ml PHA for cell proliferation. The Jurkat cells and PHA-stimulated PBMCs were incubated for 24 hours and 72 hours respectively with or without treatment, after which the cells were pulsed with ^{3}[H]-Thymidine (New England Nuclear, Boston, MA) at 2 μCi/well. The cells were harvested after 16 hours, following which the incorporated radioactivity was measured in a liquid scintillation counter (Beckman Instruments, CA, USA). Cells treated with 0.004% Dimethylsulfoxide (DMSO), the solvent for CMX-13, served as the DMSO control.

Inhibition of cell proliferation was calculated as follows:

Percent Inhibition = [1-(cpm of treated cells)/(cpm of untreated cells)]*100

Cell viability was assessed by the Trypan Blue exclusion method, and only those experiments where the cell viability was >90% were included in the results.

2.2 STUDIES ON CELL CYCLE PROGRESSION AND APOPTOSIS

2.2.1 Patients and Controls

The study population consisted of 20 patients who fulfilled the modified ARA criteria for SLE [Tan et al, 1982]. The patients were recruited from the Departments of Medicine and Pediatrics outpatient clinics at the National University Hospital. The normal controls for the study included 20 healthy age-sex matched individuals.

SLE disease activity in the patients was defined using 2 different scoring systems: University of Toronto SLE-Disease Activity Index (SLEDAI) [Tan et al, 1982; Arnett et al., 1988; Bombardier et al., 1992; Hochberg, 1997] and the Systemic Lupus International Collaborating Clinics (SLICC) Damage Index [Stoll et al.,1996; Gladman et al.,1997]. The SLEDAI measures disease activity in the various organs, whereas the SLICC Damage index measures accumulated organ damage that has occurred since the onset of SLE, resulting from the disease process, and include descriptors in the different organ systems. The SLEDAI (Appendix 4.2) and SLICC Damage Index (Appendix 4.3) were able to discriminate single disease activity states among subjects better than other scoring systems. Each patient was scored according to the clinical descriptor(s) present at the time of blood sampling, and the total score for each Index was then

computed as a measured of disease activity. The scoring systems for the SLEDAI and SLICC methods are shown in Table 2.2.1.1 and Table 2.2.1.2, respectively. Informed consent was obtained prior to blood sampling.

Table 2.2.1.1 (I): SLICC scoring system

ITEM	Score
Ocular	
Any cataract	0 1
Retinal change OR Optic atrophy	0 1
Neuropshychiatric	
Cognitive impairment	
OR Major psychosis	0 1
Seizures requiring therapy for 6 months	0 1
Cerebral vascular accident ever (score 2 if > 1), resection not for malignancy	0 1 2
Cranial or peripheral neuropathy (excluding optic)	0 1
Transverse myelitis	
Renal	
Estimated or measured GFR < 50%	0 1
Proteinuria 24 h, ≥ 3.5 g	0 1
OR	
End-stage renal disease (regardless of dialysis or transplantation)	3
Pulmonary	
Pulmonary hypertension (right ventricular prominence, or loud P2)	0 1
Pulmonary fibrosis (physical and X-ray)	
Shrinking lung (X-ray)	0 1
Pleural fibrosis	0 1
Pulmonary infarction (X-ray) OR resection not for malignancy	0 1
	0 1
Cardiovascular	
Angina OR coronary artery bypass	0 1
Myocardial infarction ever (Score 2 if > 1)	0 1 2
Cardiomyopathy (ventricular dysfunction)	1 1
Valvular disease (diastolic murmur, or a systolic murmur >3/6)	0 1
Pericarditis x 6 months or pericardiectomy	0 1
Peripheral Vascular	
Claudication x 6 months	0 1
Minor tissue loss (pulp space)	0 1
Significant tissue loss ever (eg. loss of digit or limb, resction) (Score 2 if > 1)	0 1 2
Venous trombosis with swelling, ulceration, OR venous stasis	0 1

Table 2.2.1.1(II): SLICC scoring system

ITEM	Score
Gastrointestinal	
Infarction or resection of bowel (bowel duodenum) , spleen, liver or gall bladder ever (Score 2 if > 1)	0 1 2
Mesenteric insufficiency	0 1
Chronic peritonitis	0 1
Stricture OR upper gastrointestinal tract surgery	0 1
Pancreatic insufficiency requiring enzyme replacement or with pseudocyst	0 1
Musculoskeletal	
Atrophy or weakness	0 1
Deforming of erosive arthritis (including reducible defomrmities, excluding avascular necrosis)	0 1
Osteoporosis with fracture or vertebral collapse (excluding avascular necrosis)	0 1
Avascular necrosis (Score 2 if >1)	0 1
Osteomyelitis	0 1
Ruptured tendons	0 1
Skin	
Alopecia	0 1
Extensive scarring or panniculum other than scalp and pulp space	0 1
Premature Gonadal Failure	0 1
Diabetes (regardless of treatment)	0 1
Malignancy (exclude dysplasia)	0 1 2

Table 2.2.1.2 (l): SLEDAI scoring system

Weight	Descriptor	Definition
8	Seizure	Recent onset. Exclude metabolic, infectious, or drug causes
8	Psychosis	Altered ability to function in normal activity due to severe disturbance in the perception of reality. Include hallucinations, incoherence marked loose associations, impoverished thought content,marked illogical thinking, nizarre disorganized, or catatonic behavior. Exclude uremia and drug causes
8	Organic brain syndrome	Altered mental function with impaired orientation, memor,orother intellectual function, with rapid onset and fluctuating clinical features. Include clouding of consciousness with reduced capacity to focus, and inability to sustain attention to environment, plus at least 2 of the following: perceptual disturbance, incoherent speech, insomnia or daytime metabolic, infectious, or drug causes.
8	Visual disturbance	Retinal changes of SLE. Include cytoid bodies, retinal hemorrhages, serous exudates or hemorrhages in the choroids, or optic neuritis. Exclude metabolic, infectious, or drug causes.
8	Cranial nerve disorder	New onset of sensory or motor neuropathy involving cranial nerves
8	Lupus headache	Severe, persistent headache: may be migrainous, but must be nonresponsive to narcotic analgesia
8	CVA	New onset of cerebrovascular accident (s). Exclude arteriosclerosis.
8	Vasculitis	Ulceration, gangrene, tender finger nodules, periungual infarction, splinter hemorrhages, or biopsy or angiogram proof of vasculitis
4	Arthritis	More than 2 joints with pain and signs of inflammation (i.e. tenderness, swelling or effusion)
4	Myositis	Proximal muscle aching/weakness, associated with elevated creatine phosphokinase/aldolase or electromygram changes or a biopsy showing mysitis.
4	Urinary casts	Heme-granular or ed blood cell casts
4	Hematuria	> 5 red blood cell/high power field. Exclude stone, infection, or other cause.

Table 2.2.1.2 (II): SLEDAI scoring system

Weight	Descriptor	Definition
4	Proteinuria	> 0.5 gm.24 hours. New onset or recent increase of more than 0.5 mg/24 hours
4	Pyuria	> 5 white blood cells. Exclude infection.
4	New rash	New onset or recurrence of inflammatory type rash
2	Alopecia	New onset or recurrence of abnormal, patchy or diffuse loss of hair.
2	Mucosal ulcers	New onset or recurrence of oral or nasal ulcerations.
2	Pleurisy	Pleuritic chest pain with pleural rub or effusion, or pleural thickening.
2	Pericarditis	Pericardila pain with at least 1 of the following: rub, effusion, or electrocardiogram or echocardiogram confirmation.
2	Low complement	Decrease in CH50, C3, or C4 below the low limit of normal for testing laboratory.
2	Increased DNA binding	> 25% binding by Farr assay or above normal range for testing laboratory.
1	Fever	>38^{o}C. Exclude infectious cause.
1	Trombocytopenia	<100.000 platelets/mm^{3}
1	Leukopenia	< 3.000 white blood cells/ mm^{3}. Exclude drug causes.

2.2.2 DEX dose response on PBMCs

A dose response was conducted based on the earlier data published by Seki at el., 1998, in which they used PNL. Briefly, PBMCs were isolated from Heparinized blood using standard Ficoll-Hypaque (Amersham Pharmacia Biotech AB, Uppsala Sweden) density-gradient centrifugation at 2000 rpm for 30 minutes. The mononuclear cell interface was collected and washed twice in RPMI 1640. PBMCs were maintained in complete media RPMI 1640 (Gibco, Life Technologies, Grand Island NY, USA), supplemented with 10% fetal calf serum

(FCS) (Gibco, Life Technologies, Grand Island NY, USA), 100 U/ml penicillin, 100 μg/ml streptomycin (Gibco, Life Technologies, Grand Island NY, USA) and 1 mM of L-glutamine (Sigma Chemicals, USA). DEX was diluted at a concentration of 1000 μg/ml, 500 μg/ml, 100 μg/ml, 5 μg/ml, 1 μg/ml 0.5 μg/ml in culture media. Cycloheximide (CH), a protein synthesis inhibitor and apoptosis inducer, was used to treat cells as a positive control for apoptosis [Terui et al, 1995; Gong et al, 1993]. PBMCs were also treated with DMSO, the vehicle for CMX-13 at a concentration of 0.008%. The cells were incubated for 24 hrs at a concentration of $1x10^6$ cells/ml in 5 ml polypropylene round-bottomed tubes in a final volume of 1.0 ml (Falcon, Becton and Dickinson and Company, Franklin Lakes, NJ). Apoptosis was analyzed by Annexin V- Fluorescein-isothiocyanate (FITC) /PI Staining as described in section 2.2.5.

2.2.3 Cell-Cycle Progression Analysis

The effect of CMX-13 on cell-cycle progression was studied in Jurkat cells, as well as PBMCs stimulated with PHA. CMX-13 dissolved in DMSO was tested in varying concentrations of 1, 2, 4, and 8 μg/ml, with DMSO 0.004% as the negative control. For the Jurkat cell cultures, 1.4 mg/ml CH was used to treat cells as a positive control for apoptosis [Terui et al, 1995; Gong et al, 1993], while for PBMCs, 2.0 μg/ml CsA (Sandoz, Switzerland) was the positive control. The cells were incubated for 24 hrs at a concentration of $1x10^6$ cells/ml in 5 ml polypropylene round-bottomed tubes in a final volume of 1.0 ml (Falcon, Becton

and Dickinson and Company, Franklin Lakes, NJ). The cells were harvested by centrifugation for 5 minutes at 1500 rpm and washed with 1.0 ml phosphate buffered solution (PBS).Cells with an 1N content are considered to be in the G_0/G_1 phase, those with 2N in the G_2/M-phase and those with greater than 1N and less than 2N in the S-phase. In an untreated normal cell population, most of the cells will be in the G_0/G_1 phase, followed by the S-phase, and finally in the G_2/M-phase [Bedner et al., 1999].

During apoptosis, chromatin fragmentation occurs and is considered as a hallmark of this process. The nuclei of apoptotic cells take up less PI than the nuclei of normal cells, resulting in a decreased fluorescence signal from the apoptotic nuclei. As a consequence, apoptotic cells can be identified by PI staining. The apoptotic cell population will be observed in the “sub-G1” or the hypodiploid area. Nuclei are scored as apoptotic if they demonstrated a decrease in PI fluorescence relative to the nuclei of healthy non-apoptotic cells [Caricchio and Cohen, 1999].

Cell-cycle analysis was conducted by staining DNA with Propidium Iodide (PI) [Nicoletti et al., 1991; Bedner et al., 1999]. Cell-cycle analysis was performed using the CycleTEST™ PLUS DNA Reagent Kit (Becton and Dickinson Immunocytometry Systems, San Jose, CA, USA) [Nicoletti et al., 1991; Bedner et al., 1999]. Briefly, $5x10^5$ cells were trypsinised using a solution containing trypsin and spermine for 10 minutes, treated with RNAse and a trypsin inhibitor for

another 10 minutes, and subsequently incubated, on ice, with PI for 30 minutes. Samples were then analyzed for total DNA content per cell by flow cytometry (FACScan, Becton Dickinson, Mountain View, CA). Cell death by necrosis results in a large decrease in forward scatter (FSC) and sideward scatter (SSC) [Nicoletti et al., 1991]. Dead cells and debris were excluded from analysis by selective gating for healthy cell populations [Caricchio et al., 1998]. In each experiment 10,000 events were analyzed. The coefficient of variation of the peaks of the control G_0/G_1 and G_2/M phases were less than 3%. Differential expression of the cell-cycle phases was calculated with the ModFit LT Software, (Cell Cycle Analysis Software from Verity Software House, Becton Dickinson). The majority of cells in a resting population will be in the G_0/G_1 phase, upon stimulation cells will proliferate and will be distributed over the G_0/G_1, S-phase, and the G_2/M-phase [Bedner et al., 1999].

2.2.4 Low Molecular DNA Isolation

The DNA ladder that forms during apoptosis results from the activation of an endogenous endonuclease that is seen in conjunction with the various structural changes described in apoptotic cells [Schwartz et al., 1993]. Briefly, 3 x 1.10^6 of cells (either PBMC's or Jurkat cells) were fixed in 10 ml of 70% ethanol on ice for 4 hours. Cells were centrifuged at 1000 *g* for 5 minutes, and the cell pellet was resuspended in 40 μl of phosphate-citric acid buffer (0.2 M disodium hydrogen phosphate and 0.1 M citric acid), and incubated for 30 minutes at room

temperature. Following centrifugation at 1500 *g* for 5 minutes, the supernatant was concentrated in a SpeedVac concentrator (Savant Instruments, Inc., Farmingdale, NY, USA) and treated with 3 μl (1 mg/ml) RNAse for 30 minutes at 37°C. Subsequently, 3 μl proteinase K (1 mg/ml) was added and incubated for another 30 minutes at 37°C. DNA in 12 μl loading buffer was then subjected to electrophoresis on a 0.8% agarose gel at 2 V/cm for 16-20 hours, and the bands were visualized following staining with 5 μg/ml ethidium bromide.

PBMCs from SLE patients and controls were cultured with 0.004% DMSO, 4 μg/ml CMX-13 and 1.4 mg/ml CH. CMX-13 at 4 μg/ml was chosen because this concentration was previously demonstrated to cause maximal inhibition of PHA-stimulated lymphocyte proliferation with good cell viability. Jurkat cells were treated in a similarly as the PBMC, but were harvested at different time-points (0, 4, 6, 8 hrs).

2.2.5 Annexin V- FITC /PI Staining of Apoptotic Cells

Plasma membrane phospholipids are asymmetrically distributed between the inner and outer membrane. The outer membrane bilayer predominantly contains the neutral phospholipids sphingomyelin and phosphaditylcholine, while anionic phospholipids, such as phosphaditylserine (PS), are restricted to the inner monolayer. During early apoptosis a breakdown occurs of this asymmetry, and PS undergoes translocation to the outer membrane of the plasma membrane

[Bedner et al., 1999; Vermes et al., 1995], and becomes exposed on the outer membrane. The PS exposure upon apoptosis is illustrated in Figure 2.2.4.1. PS exposure functions as specific recognition by macrophages and for phagocytosis of apoptotic cells [Fadok et al., 1992; Cohen et al., 1993; Savill et al., 1993; van Engeland et al., 1998].

The anticoagulant Annexin-V binds with high affinity to PS, and when conjugated to the fluorochrome, FITC, it can be used in flow cytometry analysis to identify apoptotic cells. When cells are stained with a combination of PI and Annexin-V conjugated with FITC (Annexin-V-FITC), four different cell populations can be distinguished. Viable cells are Annexin-V-FITC negative and PI negative, early apoptotic cells are Annexin-V-FITC positive and PI-negative, while late apoptotic cells are Annexin-V FITC positive and PI positive. Necrotic cells will also be Annexin-V FITC positive and PI positive, but these can be excluded through gating for the viable cells by FSC and SSC. [Nicoletti et al., 1991; Bedner et al., 1999].

PS exposure on the cell surface membrane was measured using the Annexin V-FITC Kit1 (PharMingen, CA, USA) [Carricchio et al., 1999]. Briefly, cells were resuspended at a concentration of $1x10^6$ cells/ml after centrifugation for 5 minutes at 1500 rpm. One hundred μl ($1x10^5$ cells) were double-stained with 5 μl of Annexin V-FITC and 2 μl of PI, incubated in the dark at room temperature for 15-30 minutes. Flow cytometric analysis was performed on the FACScan, using the

CellQuest Software (Becton Dickinson, Mountain View, CA) with windows gated on Annexin V-FITC as well as PI positive cells, to include 10,000 events. Dead cells and debris were excluded from analysis by selective gating based on FCS and SSC [Lorenz et al., 1997; Emlen et al., 1994]. Data were displayed on a logarithmic scale of increasing fluorescence intensity and each histogram plot was generated from at least 10^4 events per sample in all experiments. PBMC from controls and SLE patients were treated with 0.004% DMSO (vehicle control), with 4 μg/ml CMX-13, or 0.5 mg/ml DEX [Seki et al, 1998], and with 1.4 mg/ml CH for the duration of 24 hrs. Jurkat cells were treated for 8 and 24 hrs also with 0.004% DMSO, 4 μg/ml of CMX-13, and with 1.4 mg/ml CH (positive control).

Figure 2.2.5.1 PS exposure on apoptotic cells. During apoptosis, PS which is located in the inner side on the cell membrane becomes exposed on the outer membrane, allowing binding of Annexin V-FITC conjugate.

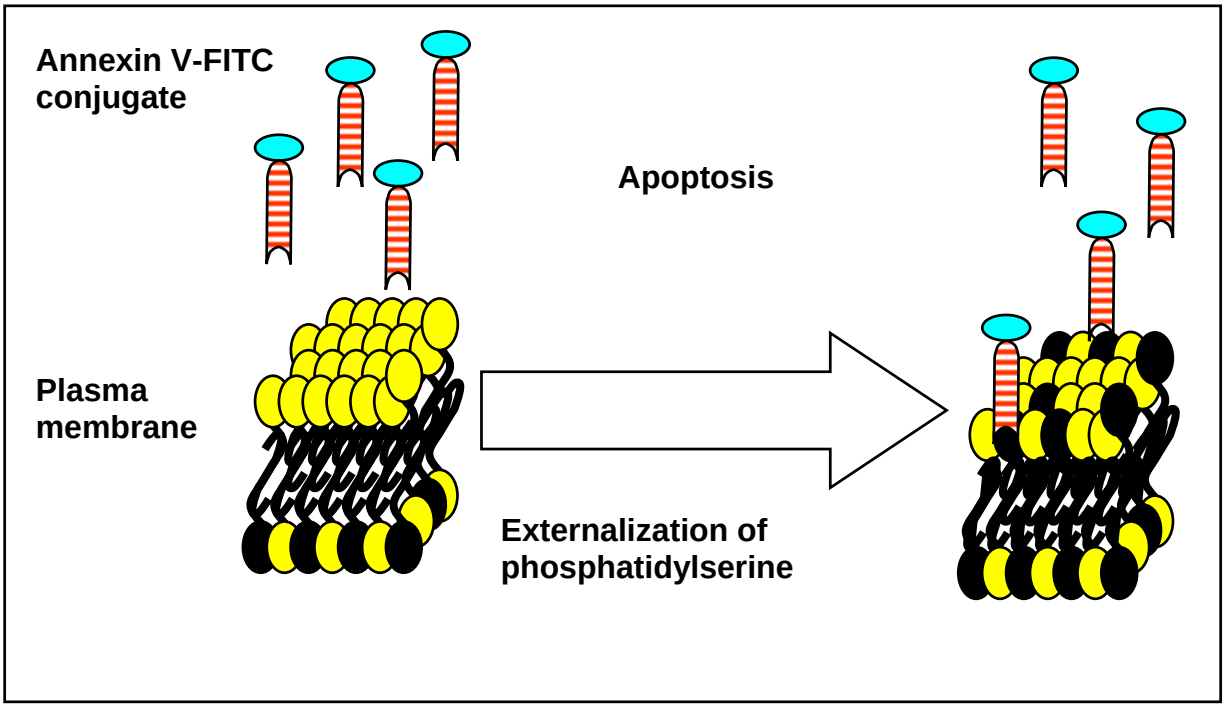

2.3 CLINICAL AND HISTOLOGICAL STUDIES ON MRL-*lpr/lpr* MICE

2.3.1 Breeding Conditions and Examination for Clinical Disease

Fifty-two, 8 week-old female MRL-*lpr/lpr* mice were purchased from the Jackson Laboratory (Bar Harbor, ME), stock number 000482. Mice were bred under normal conditions (room temperature 23.0±2.0^{o}C, ±60% relative humidity, and a 12-hours light/dark cycle) in the facilities of the Animal Holding Unit of the National University of Singapore. Mice had free access to pelleted laboratory chow and acidified tap water. Mice were observed for signs of autoimmune manifestations, namely hair loss, foot-pad swelling, and lymphadenopathy, and their survival was charted over a period of 22 weeks. Mouse found to be moribund were euthanized by inhalation of chloroform. Each animal was subjected to necropsy, and samples of liver, kidney, and spleen were collected and snap-frozen at -70ºC for RNA isolation, as well as prepared for histological examination.

2.3.2 Treatment Groups

The mice were separated into four groups of 13 mice each. The four groups were treated as follows: mice injected with 100 μl PBS were considered as the Untreated animals; the second group was treated with 16% v/v DMSO, which

served as the vehicle for CMX-13; the third group was treated with 25.0 mg/kg/day CMX-13: and the fourth group was given 1.0 μg/kg/day DEX. 16% v/v DMSO was prepared by dissolving 250 μl DMSO in 1250 μl PBS. CMX-13 was prepared by dissolving 7.5 mg into 250 μl DMSO followed by resuspension in 1250 μl PBS. DEX was dissolved directly in PBS to a concentration of 1.0 μg/kg/day. The mice were treated from the age of 12 weeks to 22 weeks, on alternate days by intra-peritoneal injection after filter sterilization (0.20 μm syringe filter (Sartorius, Germany) of the diluents. At the age of 23 weeks, all the mice that were still alive were sacrificed. Tissue was collected for histological analysis and RNA was isolated for quantitative real-time polymerase chain reaction (PCR) of cytokine mRNA transcripts.

2.3.3 Urine Collection and Proteinuira Measurement

Every single mouse was placed in a clean cage for the collection of urine. They were left for approximately 30-60 minutes or until they urinated. Urine was collected at 8, 12, 16, 20 and 22 weeks. The urine samples were analyzed by colorimetric reaction with urine reagent strips (TECO Diagnostics, URS-2P) and were graded semi-quantitatively as follows:

0 = Negative

1 = Trace

2 = 0-30 mg/dl (+)

3 = 30-100 mg/dl (++)

4 = 100- 300 mg/dl (+++)

5 = > 300 mg/dl (++++)

2.3.4 Sera collection from Mice

Blood was drawn by retro-orbital puncture [Peng et al.; 1996] with a 3mM Pasteur pipette at the age of 8, 12, and 16 weeks for sera collection. Approximately 200 μl blood was drawn each time, 50 μl was left on the bench top for 30 minutes to clot. Sera were obtained after centrifugation for 10 minutes at 10,000 rpm.

.2.3.5 Serological Analysis

Serum samples were obtained from mice at the age of 8, 12 and 16 weeks for anti-double stranded DNA (anti-dsDNA) antibody analysis. Serum levels of IgG-specific anti-dsDNA antibody were measured using an enzyme immunoassay (ELISA). Briefly, 96-well plates (Corning, ELISA plate) were coated with 100 μl/well of 10 μg/ml bovine serum albumin (BSA). After overnight incubation at 4°C, plates were washed with PBS-Tween 0.05%. Subsequently, 100 μl/well of 2.5 μg/ml calf thymus DNA in 0.1 mmol/l phosphate was added. After another overnight incubation, the plates washed three times with PBS-Tween 0.05%, and 200 μl/well of 1.0 mg/ml gelatin was added for blocking. The plates were incubated for 2 hours at 37°C, washed with PBS-Tween 0.05% three times. Serum samples were diluted 1/500 in

PBS, and 100 μl was added to each well. After 1 hour of incubation at room temperature, plates were washed, and 100 μl/well affinity-purified goat-anti-mouse IgG (H+L)-horse-radish peroxidase diluted 1:2000 in PBS was added to each well. After incubation for 1 hour at 37°C, plates were washed and 100 μl/well of substrate solution containing o-phenylenediamine (0.4 mg/ml) and 0.001% hydrogen-peroxide was added. Following 30 minutes of incubation in the dark at room temperature, 50 μl of 10% sodium dodecyl sulfate was added to stop the reaction. Absorbance was determined at 405nm. All samples were assayed in triplicates on the same day.

Serum creatinine was measured by the alkaline picrate method. A standard curve was created using the Sigma creatinine Standards Cat # 925-11. Briefly, 50 μl serum was mixed with 50 μl H_2O, 50 μl Na. Tungstate (5%) and 50 μl sulphuric acid and left on room temp for 10 minutes. The samples were spun for 10 minutes at 3000 rpm. The 100 μl supernatant was collected and mixed with 20 μl saturated picric acid and 30 μl 1N Sodium hydroxide and left for 20 minutes for color development. The plate was analyzed in a plate reader at 490 nm.

2.3.6 Preparation of Kidney Slides and Histological Grading of Lupus Nephritis Examination

The surviving mice in all the groups were sacrificed at 23 weeks for histological examination. Mice, which became moribund at the age of 23 weeks were sacrificed. Briefly, the mice were euthanized by chloroform inhalation.

Kidneys specimens from moribund mice were fixed in 10% neutral buffered formalin with phosphate buffer (pH 7.4) for 24 hrs for histological evaluation. The samples were dehydrated with an automated processing machine (Leica) as follows:

1) 70% Ethanol for 1 hour
2) 95% Ethanol for 1 hour
3) 3 x 100% Ethanol for 2 hours
4) 2 x Xylene for 2 hours

The samples were subsequently embedded in paraffin as follows:

1) Wax for 1 hour
2) 2x Wax for 2 hours

Each sample was then cut into 4 μm sections using a microtone (Reichert-Jung). The sections were dried for 5 minutes, followed by heating on a 80°C hotplate for 10 minutes.Periodic Acid-Schiff (PAS) stain [Bancroft et al, 1990] was prepared as follows:

1) PAS consisted of 1.0 gram periodic acid, 200 ml of distilled water.

2) Schiff Reagent was prepared by dissolving 1.0 gram of basic fuchsin in 200 ml of boiling distilled water. The solution was cooled to 50°C, and 2.0 gram of potassium metabisuphite was added and mixed. After cooling to room temperature, 2.0 ml of concentrated hydrochloric acid and 2.0 gram of activated charcoal were added. The solution was left overnight in the dark at room temperature. The solution was then filtered through a number 1 Whatman paper and stored until use in a dark container at 4°C.

The sections were deparaffinized, treated for 5 minutes with periodic acid and washed several times with distilled water. The sections were then covered with Schiff's solution for 15 minutes and washed in running water. The nuclei were stained with Harris haematoxylin, washed in water and rinsed in absolute alcohol. The sections were subsequently cleansed in xylene.

The kidney sections were graded using a score based on the activity of lupus nephritis. All the mice developed diffuse proliferative lupus nephritis which was similar to human Class IV lupus nephritis as defined by the WHO [Peutz-Kootstra et al, 2001; Appel and Valeri, 1994]. The slides were evaluated by two "blinded" observers who were not aware of the experimental groupings. Histological grading was based on a continuous grading system from 0 to 3+, where 2+ and 3+ were considered severe disease, while 0 and 1+ were considered to be mild disease. The histological features that were graded included:

1. glomerular cell proliferation
2. leucocyte exudation
3. karyorrhexis and fibrinoid necrosis
4. cellular crescents
5. hyaline deposits
6. interstitial inflammation.

A minimum of 20 glomeruli/slide were assessed and scored. In calculating the activity index, fibrinoid necrosis and cellular crescents were weighted by a factor of 2. The activity index for lupus nephritis was defined as the sum of individual scores [Austin et al, 1984], and the maximum activity index was 24 points. As some mice died before 23 weeks, an overall histological index for each kidney was obtained by a score/age ratio to compensate for the effect of age on the progression of disease.

2.4 CYTOKINE GENE EXPRESSION STUDIES IN THE MRL *lpr/lpr* MICE

2.4.1 Isolation of Murine Splenic $CD4^+$ and $CD8^+$ T-Cells

The spleens were excised using and ruptured in a petri-dish containing 5 ml HBSS. Debris of the tissue was separated using a 70.0 μm cell strainer (Becton and Dickinson, USA). Lymphocytes were isolated using the Ficoll-Hypaque centrifugation method. The isolated cells were washed and the supernatant was removed completely. The cells were resuspended in 90 μl of buffer (PBS + 2mM EDTA + 0.5% BSA) per 10^7 cells and incubated with 10 μl of MACS CD4 (L3T4) Microbeads (Miltenyi Biotech, Germany) per 10^7 total cells, for 15 minutes at 6 -12°C. The cells were then washed with 10-20x labeling volume of PBS supplemented with 2 mM EDTA and 0.5% BSA (Sigma) (PBS/BSA/EDTA) and centrifuged at a speed of 300 x g for 10 minutes. The cell pellet was resuspended in 0.5 ml PBS/BSA/EDTA per 10^8 total cells. The LS^+ Magnetic Separation columns with positive selection (Miltenyi Biotec, cat no. 130-042-401) were attached to the magnetic separator. The column was prepared by washing with 5 ml PBS/BSA/EDTA. The cell suspension was applied onto the column. The column was then washed with 3x 3 ml of PBS/BSA/EDTA. The effluent was collected as the negative fraction. The column was removed from the separator and placed under a new collection tube and finally 5 ml of PBS/BSA/EDTA was applied to the reservoir of the LS^+ column and the cells were flushed out. The cells were then

harvested by centrifugation at 1500 rpm for 5 minutes. The supernatant was discarded and the pellet was resuspended in 1 ml of TRIZol (Gibco BRL) for RNA isolation.

CD4-FITC conjugated antibody and CD8-FITC conjugated antibody were used to stain the isolated cells to assess the uniformity of each cell preparation. Approximately 0.2 x 10^6 cells/ml were stained with 1 μl of $CD4^+/CD8^+$ antibody (Becton and Dickinson, USA) for 20 minutes in 100 μl staining buffer, composed of 100 ml RPMI1600, 2.5% FCS, and 50 μl of 20% sodium azide. The cells were washed with PBS and spun down for 10 min at 1400 rpm at 4°C. The cells were resuspended and stained with 5 μl of goat antibody and 100 μl of staining buffer and incubated for 20 min at room temperature. The samples were analyzed by flow cytometry as shown in Figure 2.4.1.1.

Figure 2.4.1.1 Flow-cytometric analysis of $CD4^+$ and $CD8^+$ T-cells isolated from spleen.

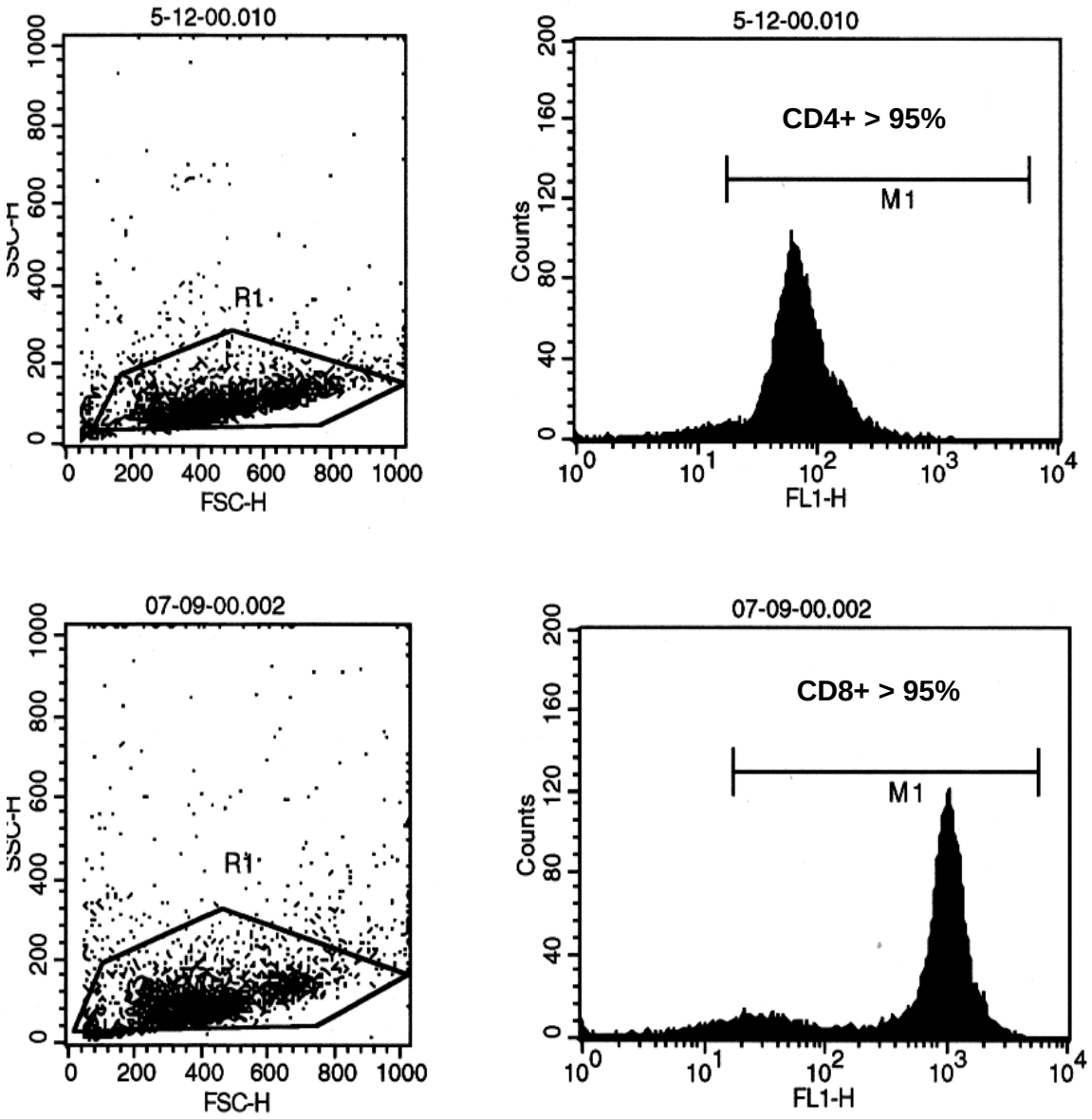

2.4.2 Isolation of Glomeruli from Cortex of Mouse Kidneys using the Graded Sieving Technique

The kidneys were excised using an aseptic technique and transferred to Dulbecco's modification of Minimal Essential Medium (DMEM), the capsules were removed, and the cortices were dissected from each kidney [Kreisberg, et al 1978]. Glomeruli were isolated from the renal cortex as described by Kreisberg with some modifications [Kreisberg, et al 1978]. The cortex were sliced into small pieces with a blade and pressed with a spatula through a stainless steel screen of 60-mesh (pore size, 250; W.S. Tyler, Inc., Mentor, Ohio). The minced cortices were collected on a petri-dish placed underneath the stainless steel screen by washing with DMEM. The filtrate was then passed through a 100 μm nylon cell strainer and again through a 70 μm cell strainer (Becton and Dickinson, USA). The glomeruli remained on the 70 μm nylon cell strainer, due to their size. Tubular debris and small fragments were removed by washing. The 70 μm nylon strainers were then placed upside down onto a 50 ml culture tube and the isolated glomeruli were collected in the culture tube by washing with 10 ml of DMEM. Single isolated glomeruli are shown in Figure 2.4.2.1. The glomeruli were incubated at a concentration of 0.5 glomeruli/ml for 30 minutes with 1 mg/ml collagenase (Gibco BRL) at 37°C [Boswell, et al 1988]. The glomeruli were then harvested by centrifugation at 600 rpm for 10 minutes. The supernatant was discarded and the pellet was resuspended in 1 ml of TRIZol (Gibco BRL), followed by RNA isolation.

Figure 2.4.2.1 Isolated glomeruli

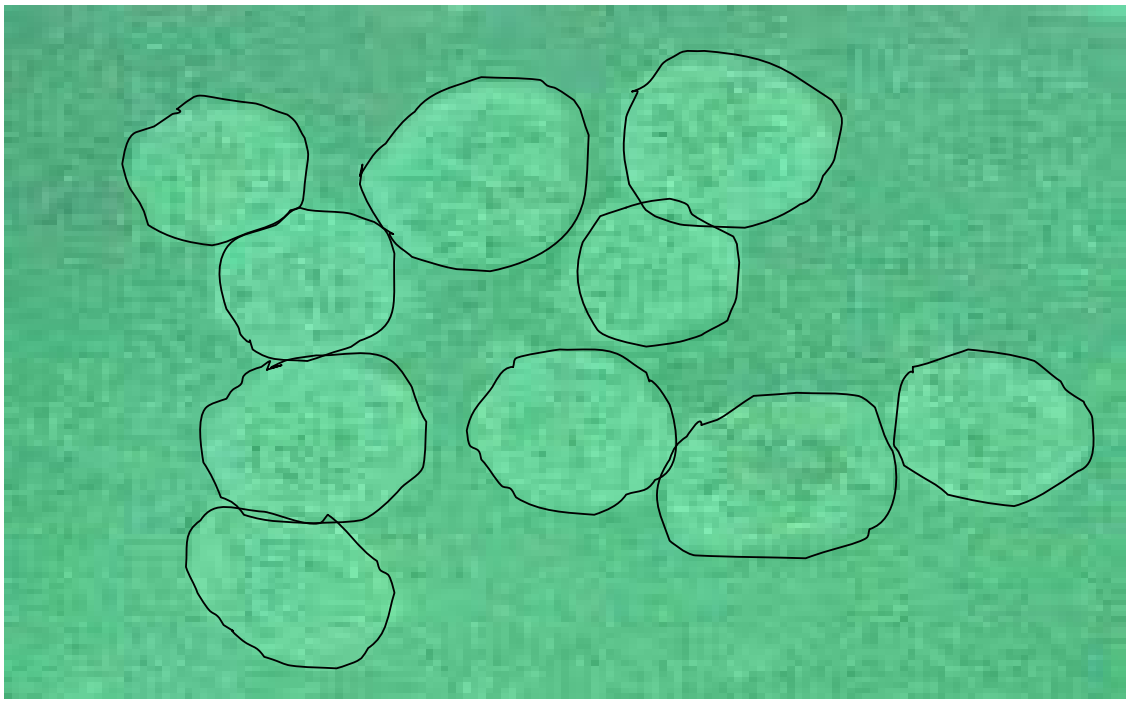

2.4.3 RNA isolation and complementary DNA (cDNA) preparation

Total cellular RNA from organs was isolated using TRIZol reagent (Gibco BRL), which is a modification of the standard guanidinium-phenol-chloroform extraction method [Lemay et al, 1996]. Briefly, $1x10^6$ cells/ml were treated with 1 ml of TRIZol and subjected to repetitive pipetting. The samples were incubated for 5 minutes at room temperature. Two hundred μl of chloroform per ml of TRIZol was added and then shaken vigorously for 15 seconds. The samples were incubated for 2-3 minutes at room temperature and then spun at 12000 rpm for 15 minutes at 4°C. The colorless phase was obtained and placed into di-ethylpyrocarbonate (DEPC)-treated 1.5 ml microcentrifuge tubes. Five hundred μl of 100% isopropanol was added and incubated for 10 minutes at room temperature, followed by centrifugation at 12000 rpm for 10 minutes at 4°C. The supernatant was removed and the pellet was washed with 1.0 ml of 75% ethanol, and mixed by vortex. The samples were then centrifuged at 9500 rpm for 5 minutes at 4°C. The supernatant was removed and air-dried briefly for 5-10 minutes. The RNA pellet obtained was dissolved in 35 μl DEPC-H_2O.

The RNA was subsequently diluted 20x (5 μl RNA+ 95 μl DEPC-H_2O) and the concentration measured by spectrophotometry using the Ultrospec 2000 UV/visible spectrophotometer (Pharmacia Biotech) at a wavelength of 260nm in a 10mm pathlength cell. The RNA concentration was calculated as follows:

$[RNA]/(ng/\mu l) = 40 \times A_{260} \times DF$

Total RNA (ηg) = [RNA] x Vol. of Sample.

DF = Dilution factor.

Reverse transcription (RT) reactions were carried out in a Hybaid Touchdown PCR thermocycler for 1 hour at 37°C followed by 5 minutes at 95°C in 0.6 ml thin walled MicroAmp reaction tubes using M-MLV Reverse Transcriptase (Promega, USA). Each reaction contained 200 ηg of total RNA in a volume of 20 μl containing 1x M-MLV RT reaction buffer, 1 U RNasin Ribonuclease Inhibitor, 2.5 μM $OligoT_{20}$, 0.5 mM dNTP, 20 U M-MLV Reverse Transcriptase. The reagents and conditions are summarized in Table 2.4.3.1.

Table 2.4.3.1 Reagents and Enzymes Used in the preparation of cDNA

Reagents	**Stock**	**Final**	**Volume used for 1 reaction (μl)**
Reaction Buffer	5 x	1 x	4
DNTP	25 mM	0.5 mM	0.4
$OligoT_{20}$	100 μM	2.5 μM	0.5
Rnasin	40 U/μl	1 U/μl	0.5
Reverse Transcriptase	250 U/μl	20 U	0.08
H_2O			9.5
Total RNA		200 ng	5.0
Total Volume			20.0

2.4.4 Reverse Transcript PCR (RT-PCR)

Optimization of the PCR for each cytokine was performed using freshly prepared cDNA following reverse transcription. The primers for the PCR reactions are listed in Table 2.4.4.1. The PCR reaction was set up as follows: 10x PCR reaction, 2.5mM $MgCl_2$, 25 mM dNTP, 10 μM primer pairs, 0.5 U of Taq polymerase, and buffer with 4μl of cDNA making a final volume of 20.0 μl. The reagents are listed in Table 2.4.4.2 (Promega cat. no. M1665). The PCR reactions were run on a HyBaid Touchdown PCR thermocycler using the conditions as shown in Table 2.4.4.3.

Table 2.4.4.1 Mouse cytokine primers [Murray et al., 1990].

Gene (Accession no.)	Primers	Tm (°C)	Product (bp)
Cyclophilin-α (X52803)	Sense: ATTATTCCAGGATTCATGTGCCAG Antisense:TGAAGGGGAATGAGGAAAATATGG	56	476
IL-2 (K02292)	Sense: TGATGGACCTACAGGAGCTCCTGA Antisense: CTGCGGCATGTTCTGGATTTGACTC	56	168
IL-6 (J03783)	Sense: TGGAGTCACAGAAGGAGTGGC TAAG Antisense:TCTGACCACAGTGAGGAATGTCCA C	56	155
IL-10 (NM010548)	Sense: AGACTTTCTTTAAACAAAGGA Antisense: ATCGATGACAGCGCCTCAG	56	231
IFN-γ (K00083)	Sense: AGCGGCTGACTGAACTCAGATTGTAG Antisense: GTCACAGTTTTCAGCTGTATAGGG	56	244

Table 2.4.4.2 PCR reagents

Master mix	Volume for 1 reaction
ddH_2O	7.7 μl
10x PCR reaction buffer	2.0 μl
$MgCl_2$, 25mM	2.0 μl
DNTP, 25mM	0.2 μl
Forward primer, 10μM	2.0 μl
Reverse primer, 10μM	2.0 μl
Taq polymerase, 5U/μl	0.1 μl
CDNA	4.0 μl
Total	16 μl

Table 2.4.4.3 PCR amplification conditions

Steps	Temperature (°C)	Time	No. of cycles
Denaturation	95	30 sec	40
Annealing	54	30 sec	
Extension	72	45 sec	
Final extension	72	10 min	1
Cooling	4	Hold	1

2.5 PREPARATION OF STANDARDS FOR QUANTITATIVE REAL-TIME PCR

2.5.1 Cloning of Cytokine cDNA into Plasmids for External Standard Curves Designated for Quantitative Real-time- PCR

The amplified PCR products were cloned into a plasmid vector using the TOPO TA cloning kit (Invitrogen, USA). The plasmid vector was supplied in linearized form with a single 3'-thymidine (T) overhang for TA cloning. It is important that Taq polymerase was used in the above PCR reaction because it has a nontemplate-dependent terminal transferase activity that adds a single deoxyadenosine (A) to the 3'ends of PCR products. This allows PCR products to insert into the cloning vector efficiently by the principle of TA cloning. The reagents employed in the cloning reactions are listed in Table 2.5.1.1.

The reagents were mixed gently and incubated for 15 minutes at room temperature. Two μl of the cloning reaction mixture were mixed with a vial of *Escheria coli (E.coli)* cells, incubated at room temperature for 15 minutes, and subsequently subjected to heat shock treatment at 42°C for 30 seconds. The heat shock- treated cells were mixed with 250.0 μl of LB medium and left in a shaker for 1 hour at 37°C. After incubation, 50μl of the incubation mixture were spread onto each of the 2 Luria-Bertani (LB) plates containing X-Galactoside) and 50 μg/ml ampicillin. The LB plates were then incubated at 37°C overnight.

Positive clones were identified by the principle of blue/white screening. Transformed *E.coli* are ampicillin-resistant because the plasmid vector carries the ampicillin-resistant gene. Therefore*, E.coli* that are not transformed will not survive. The plasmid vector also carries a *LacZα* gene, and the protein translated by this gene is able to turn X-gal blue. This function will be lost if the PCR products were successfully cloned into the vector. Ten white colonies were chosen from each cloning experiment. The colonies were cultured in a 50.0 ml culture tube containing 10ml of LB medium with 50.0 μg/ml of ampicillin (Gibco, BRL). The culture tubes were incubated in a shaker at 37°C overnight.

Table 2.5.1.1 Cloning Reagents

Reagent	Volume
Fresh PCR product	4.0 μl
Salt solution	1.0 μl
TOPO vector	1.0 μl
Final Volume	6.0 μl

Extraction and purification of plasmid DNA were carried out using the QIAprep Spin Miniprep kit, cat. no. 27104 (Qiagen, USA). The QIAprep miniprep procedure is based on alkaline lysis of bacterial cells followed by adsorption of DNA onto silica in the presence of high salt. The procedure consists of three basic steps: preparation and clearing of the bacterial lysate, adsorption of DNA onto the QIAprep membrane, and washing and elution of plasmid DNA. The last 2 steps were performed on a spin column.

The concentration of plasmid DNA was measured by spectrophotometry using the Ultrospec 2000 UV/visible spectrophotometer (Pharmacia Biotech). DNA concentration was measured by its absorbance at OD_{260nm} since a solution of DNA with an optical density of 1.0 (1.0 absorbance unit) has a concentration of 50 μg/ml respectively, in a 10 mm pathlength cell. The constructs were analyzed for insertion by restriction digestion [Blaschke et al, 2000] with *EcoRI.* An *EcoRI* restriction site is present at the cloning site of the plasmid. The plasmid DNA was treated with 5 μl of *EcoRI* (10.0 U/μl, Gibco BRL), 2 μl of reaction buffer (10x), and 5 μl of plasmid DNA in a final volume of 20 μl for 2 hours at 37°C. In Figure 2.5.1.1 the *EcoRI* digestion of shown of the inserts in the plasmid.

Figure 2.5.1.1 *EcoRI* restriction digestion of inserts from plasmid. *EcoRI* restriction digestion profile of the clones containing the cytokine cDNA inserts: 100 bp DNA ladder was used as a size marker; cyclophilin-α (476 bp); IL-2 (165 bp); IL-6 (155 bp); IL-10 (231 bp); IFN-γ (244 bp).

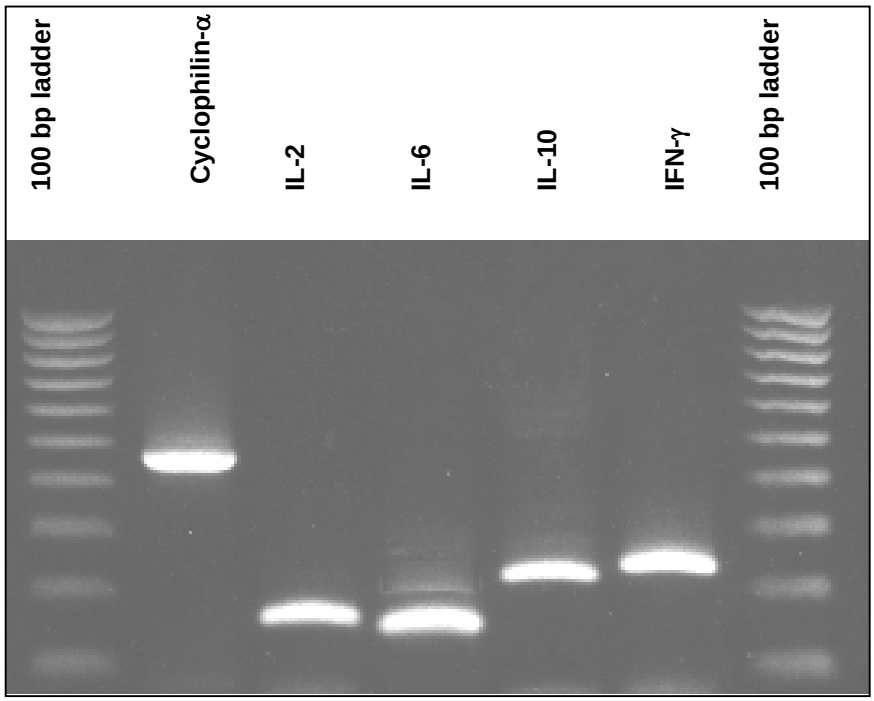

2.5.2 Calculation of Plasmid DNA Copy Number and Dilution of Standards

To determine the absolute copy number of the target transcript, cloned plasmid DNA for each cytokine studied was used to generate a standard curve. The plasmid DNA was prepared as described above. The concentration of the plasmid DNA was determined based upon the OD_{260}. The copy number of plasmid DNA template was calculated according to the molecular weight of the plasmid (662×10^6 kb^{-1} average value) and Avogrado's number (1 mol = 6.022×10^{23} molecules), using the formula:

$$\frac{6.022 \times 10^{23}}{\text{(plasmid size + size of insert) x (molecular weight of plasmid)}} = \frac{\text{copies per } \mu\text{g of plasmid}}{\text{concentration of plasmid DNA}}$$

The cloned plasmid DNA were serially diluted from 10^{-7} to 10^{-3} in order to generate the standard curve.

2.5.3 Quantification of Cytokine mRNA transcripts by Real-time PCR

The primers employed for the generation of cytokine cDNA constructs could not be used for the quantitative real-time PCR, as they resulted in the formation of primer dimers. New primers within the cloned inserts were designed. All

primers (OPERON), except those for cyclophilin-α, were re-designed using the software program from the website: http://www.path.cam.ac.uk/cgi-bin/primer3.cgi. Primers for Cyclophilin- α (Gibco BRL) were designed using the OLIGO primer design program. The primers are listed in Table 2.5.3.1.

Table 2.5.3.1 Primers for Real-Time RT-PCR

Gene	Primers	Tm (°C)	Product (in bp)
Cyclophilin-α	Sense: ATTATTCCAGGATTCATGTGCCAG Antisense:TGAAGGGGAATGAGGAAAATATGG	20	476
IL-2	Sense: AACCTGAAACTCCCCAGGATG Antisense: CGCAGAGGTCCAAGTTCATC	5	104
IL-6	Sense: GGAGTCACAGAAGGAGTGGC Antisense: ATAACGCACTAGGTTTGCCG	5	111
IL-10	Sense: CCAAGCCTTATCGGAAATGA Antisense: GGTCTTCAGCTTCTCACCCA	5	115
IFN-γ	Sense: CATTCAGAGCTGCAGTGACC Antisense: CACATTCGAGTGCTGTCTGG	4	100

Freshly prepared reverse-transcribed total RNA from cells or tissues were subjected to real-time PCR analysis. Reactions were conducted using Roche LightCycler DNA Master SYBR Green Kit 1 (Roche Molecular Biochemicals, Mannheim, Germany) for the detection of PCR products. Real-time PCR was carried out on the LightCycler (Roche Molecular Biochemicals, Mannheim, Germany). Briefly, the PCR was set up using 5 μl PCR master mix (Light Cycler DNA Master SYBR Green Kit 1) supplemented with 3.0 mM $MgCl_2$ and

custom synthesized primers (Operon). In order to reduce primer dimer formation, the amount of each primer was reduced to 0.25 μM [Dumoulin et al., 2000].

Optimization was done employing a new set of primers (Table 2.5.3.1), which were different from the ones used for cloning. This optimization was required to circumvent primer dimer formation, which interferes with the quantification of the absolute copy numbers. When these new sets of primers were employed, no primer dimers were present from analysis of the melting curve. The PCR reagents are listed in Table 2.5.3.2.

Table 2.5.3.2 Real-Time PCR reaction mixture using Roche LightCycler DNA Master Kit 1.

Master mix	Volume (1x)
ddH_2O	2.9 μl
$MgCl_2$ (25mM)	0.6 μl
SYBR Green I	0.5 μl
Forward primer (10μM)	0.25 μl
Reverse primer (10μM)	0.25 μl
CDNA	0.5 μl
Total	5.0 μl

The duration of the amplification reaction was calculated based on the product size: Product size (bp)/25 = seconds for amplification. The annealing temperature was optimized for each cytokine insert. Real-time PCR was performed in glass capillaries with an initial denaturation step of 30 seconds at

95°C, followed by 40 cycles of denaturation for 10 seconds at 95°C, annealled for 5 seconds at the following temperatures: Cyclophilin-α 60°C; IL-2 64°C; IFN-γ 62°C; IL-6 62°C; IL-10 62°C, and extension for (product length (bp)/25) seconds at 72°C. At the end of each cycle, the fluorescence emitted by the SYBR Green was measured. After completion of the cycling process, samples were subjected to a temperature ramp (from above 5°C annealing temperature to 95°C at 2°C/second) with continuous fluorescence detection for melting curve analysis. For each PCR product a single narrow peak was obtained by melting curve analysis at the specific melting temperature and only a single band of the predicted size was observed by gel electrophoresis [Blaschke et al., 2000].

Quantification in real-time RT-PCR is based on the threshold cycle of detectable cDNA molecules. For each sample, a determination is made of the cycle number at which the fluorescence related to the amount of double-stranded DNA is significantly elevated above background fluorescence. By using external standard curves, a calibration curve can be generated and samples can be quantified according to their threshold cycle [Heid et al., 1996.

Quantification data was analysed using the LightCycler analysis software. Background fluorescence was removed by setting a noise band. The log-linear portion of the standard's amplification curve was identified and the crossing point was the intersection of the best-fit line through the log-linear region and

the noise band. The standard curve is the plot of the crossing point versus the log of the copy numbers. The acquired standard curves, amplification plots and melting curves are shown for mouse cyclophilin-α, IL-2, IFN-γ, IL-6, and IL-10 are shown in Figures 2.5.3.1, 2.5.3.2, 2.5.3.3, 2.5.3.4, and 2.5.3.5 respectively.

Figure 2.5.3.1 Quantification of Mouse Cyclophilin-α mRNA transcripts by quantitative real-time PCR. The quantification was based on a standard curve which was obtained by analyzing the amplification of a 476 bp mouse Cyclophilin-α sequence cloned in a plasmid, in the range from 10^7 - 10^3 copies. Panel A shows the standard curve; panel B shows the amplification plots of the cloned sequence; panel C shows the the melting curves, which signifies product specificity.

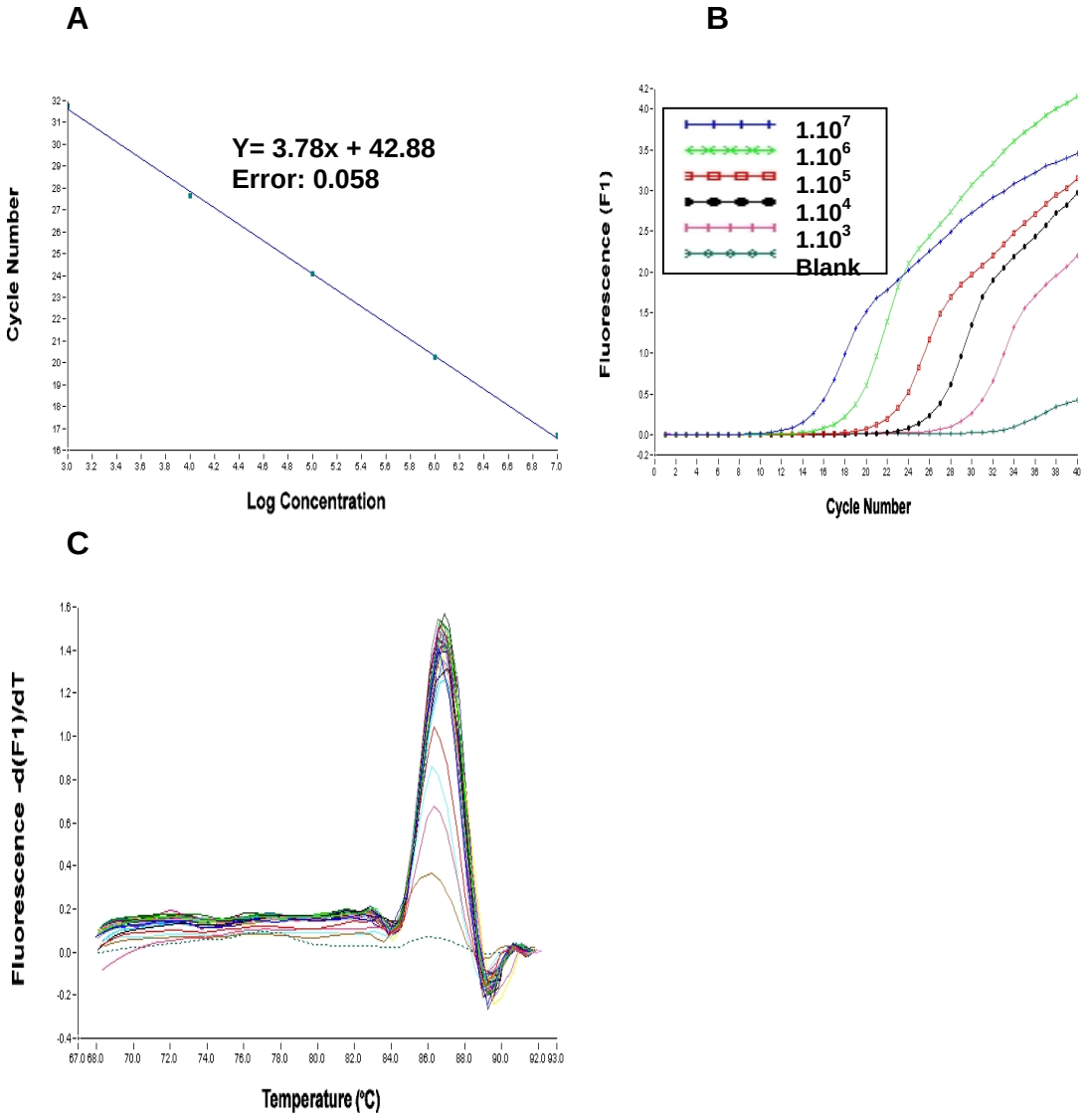

Figure2.5.3.2 Quantification of IL-2 mRNA transcripts by quantitative real-time PCR. The quantification was based on a standard curve which was obtained by analyzing the amplification of a 168bp mouse IL-2 sequence cloned in a plasmid, in the range from 10^7 - 10^3 copies. Panel A shows the standardcurve; panel B shows the amplification plots of the cloned sequence; panel C shows the the melting curves, which signifies product specificity.

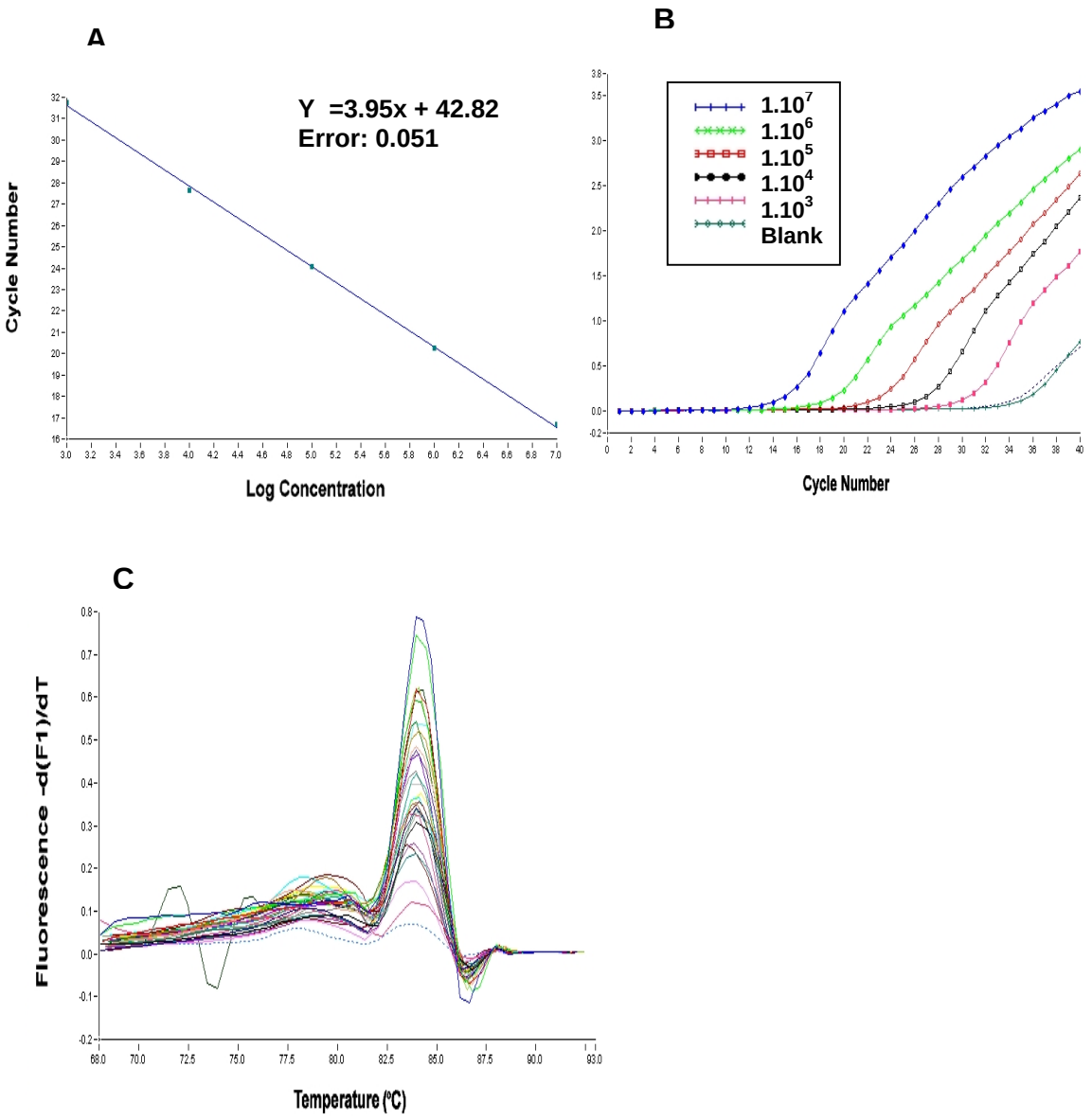

Figure 2.5.3.3 Quantification of IFN-γ mRNA transcripts by quantitative real-time PCR. The quantification was based on a standard curve which was obtained by analyzing the amplification of a 155bp mouse IFN-γ sequence cloned in a plasmid, in the range from 10^6 – 10^2 copies. Panel A shows the standard curve; panel B shows the amplification plots of the cloned sequence; panel C shows the the melting curves, which signifies product specificity.

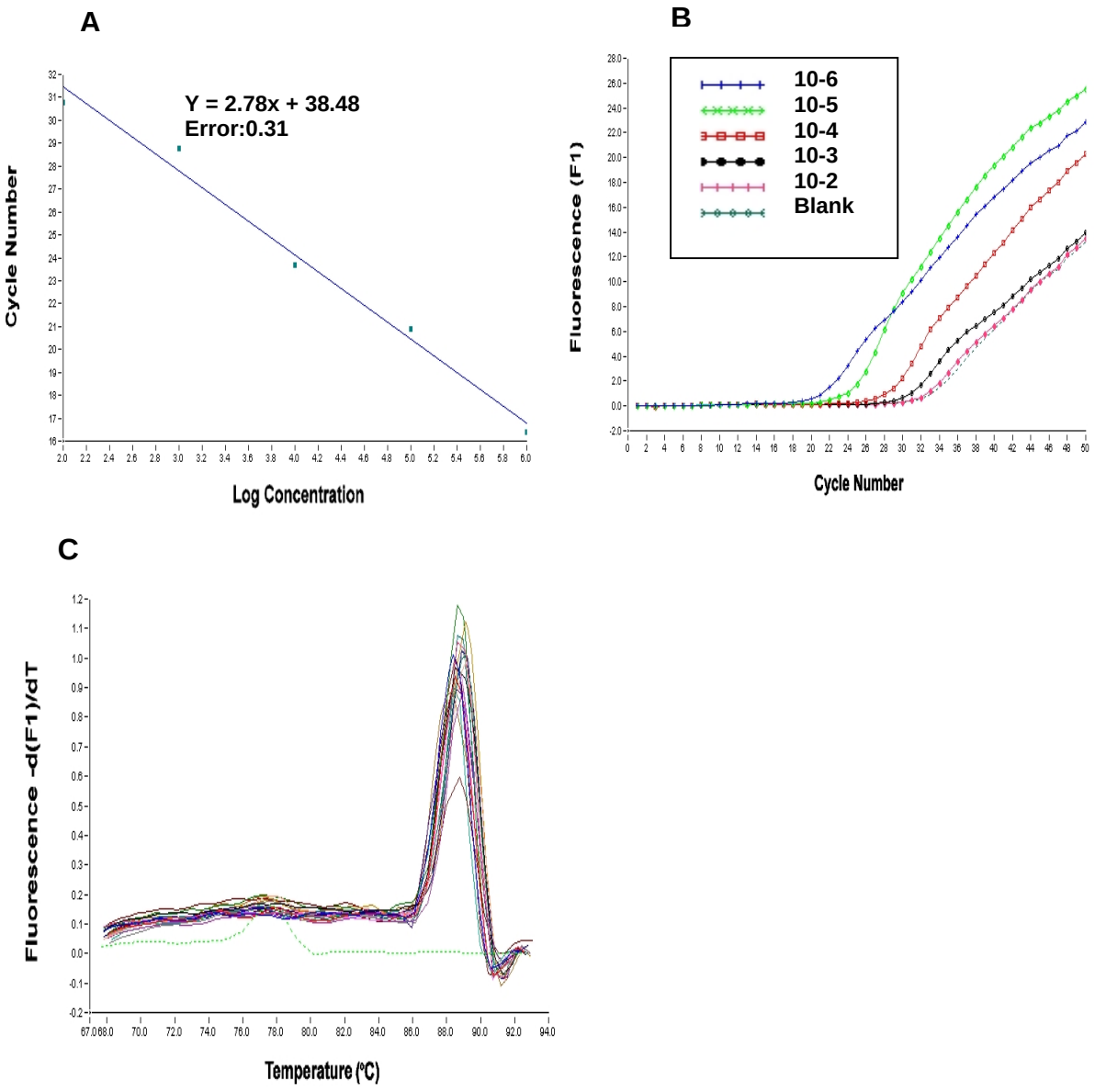

Figure 2.5.3.4 Quantification of IL-6 mRNA transcripts by quantitative real-time PCR. The quantification was based on a standard curve which was obtained by analyzing the amplification of a 155bp mouse IL-6 sequence cloned in aplasmid, in the range from 10^7 – 10^3 copies. Panel A shows the standard curve;panel B shows the amplification plots of the cloned sequence; panel C shows the the melting curves, which signifies product specificity.

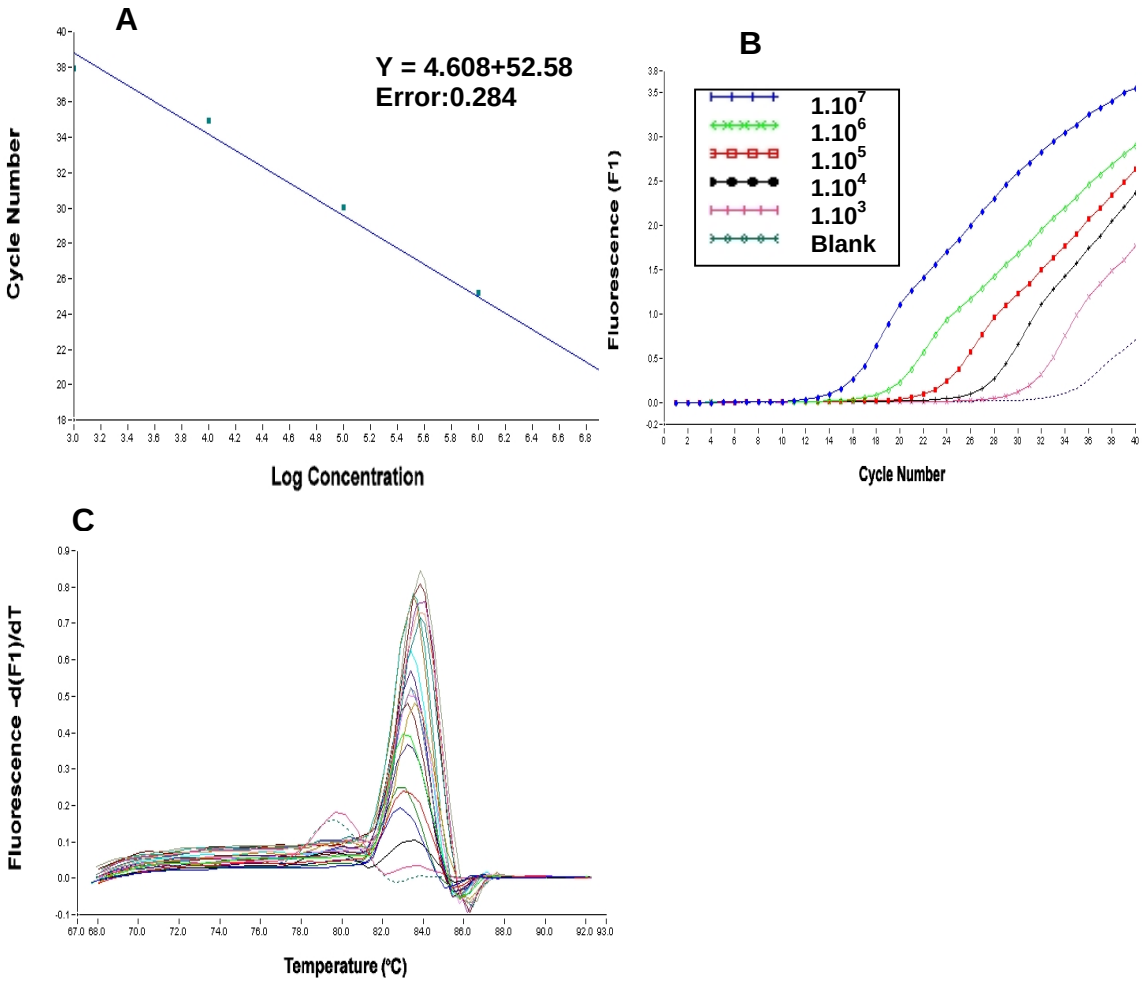

Figure 2.5.3.5 Quantification of IL-10 mRNA transcripts by quantitative real-time PCR. The quantification was based on a standard curve which was obtained by analyzing the amplification of a 231bp mouse IL-10 sequence cloned in a plasmid, in the range from 10^6 – 10^2 copies. Panel A shows the standard curve; panel B shows the amplification plots of the cloned sequence; panel C shows the the melting curves, which signifies product specificity.

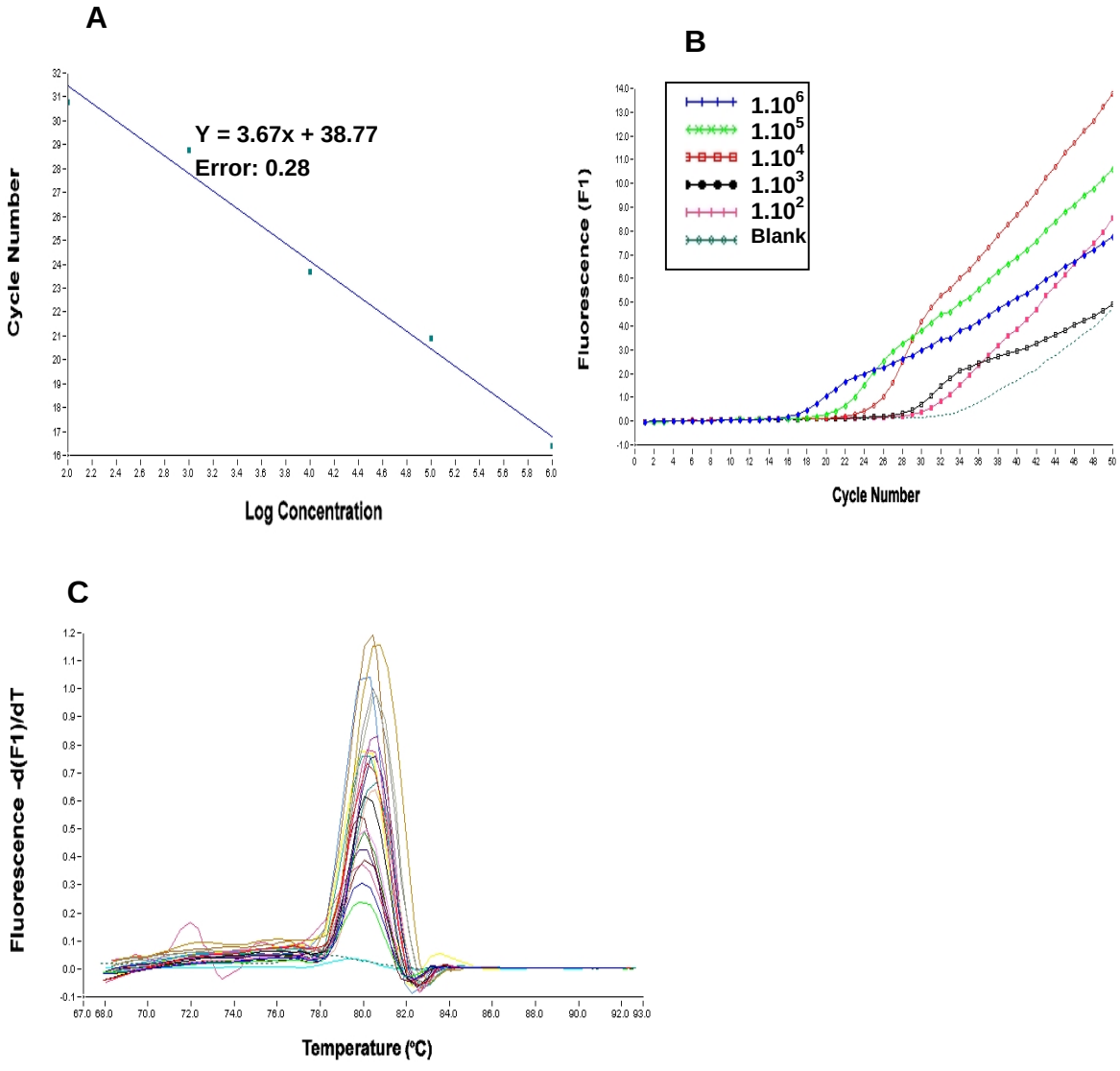

2.5.4 Quantification of cDNA by real-time PCR

Gene expression levels of IL-2, IFN-γ, IL-6, and IL-10 were determined by real-time PCR using the Roche LightCycler. Samples (determined in duplicate) were quantified using the LightCycler analysis software, version 3.39. A standard curve was generated for each gene targeted as described above. The mRNA expression level was quantified based on the external standard curve. cDNA samples from the MRL-*lpr/lpr* mice were analyzed, and compared with those obtained from MRL-*wt* mice as the normal control. The housekeeping gene, cyclophilin, was used as the common denominator for calculation of a cytokine index.

2.5.5 Statistical Analysis

Statistical analysis was performed using SPSS for Windows (version 11.5, SPSS Andover, Mass., USA). The differences between CMX-13 treated experimental groups and untreated or DMSO controls were compared using the Mann-Whitney rank sum test for non-parametric variables. Paired data were compared using the Wilcoxon signed-rank test. Spearman's correlation coefficient was used to determine the significance of correlations between non-parametric variables. In addition, the effect of CMX-13, compared to the untreated and DMSO controls, on the survival of MRL-*lpr/lpr* mice was performed using the Kaplan-Meier analysis, with death before the age of 22

weeks as the outcome parameter. A p-value of less than 0.05 was considered significant.

CHAPTER 3 ISOLATION AND STRUCTURE ELUCIDATION OF BIOACTIVE COMPOUNDS FROM *RC*

3.1 INTRODUCTION

Natural products are a major source for new medicines. However there are various obstacles up to the commercialization process of natural products as modern medicines. Firstly the isolation and purification process from the crude herb can be laborious, time-consuming and unreliable. Secondly the production of natural products in plants is subjected to many factors like seasonal changes, and soil composition [Itokawa et al, 1984] consequently leading to inconsistent bioactivity of plant extracts. This inconsistency may cause problems regarding toxicity in the case of strong bioactivity or insufficient dosage administration when the extract has poor bioactivity. For adequate production and commercialization as a reliable product, standardization of the production method is essential. Chemical synthesis of plant derived bioactive products is a viable alternative. This method creates the possibility to control and produce medicines with consistent bioactivity.

Chemical synthesis of a molecule requires the knowledge of the molecular structure. Therefore structure elucidation of the bioactive molecule in medicinal extract is necessary. However, in the application of traditional medicines a part of the plant is used or a combination of several different parts of plants is used, resulting in a mixture of many unknown compounds. In many cases only one

compound in the whole plant extract is responsible for the therapeutic effect and acts as the principle bioactive compound for the whole herbal mixture. It is often unknown in these herbal mixtures as to the actual herb, which has the actual bioactive effect. All the herbs have to be tested separately in order to identify the sole bioactive herb before isolation of the active compound can commence. Here we developed a bioassay-guided fractionation method for the isolation of bioactive plant extracts with immunosuppressive properties. We employed a bioassay based on the proliferation of PBMCs when stimulated with PHA. An active plant extract when incubated with PHA-stimulated PBMCs will result in suppression of PBMC proliferation, i.e., immunosuppression. During the bioassay-guided fractionation the plant extracts were tested for their immunosuppressive properties after each step of isolation and purification.

We have shown in our previous work that the roots of *RC* contain compounds that have immunosuppressive properties [Yap et al, 1999]. The bioassay-guided fractionation procedure depicted in Figure 3.1.1 has been developed based on results from our previous studies. By employing this bioassay we were able to purify bioactive fractions from extracts of herbal medicines. The extracts with significant immunosuppressive properties are underlined and the follow up process indicated with a bold arrow.

In the initial step, the herb was grounded and extracted with EtOAc, followed by solvent partition with MeOH, water, Hex and CH_2Cl_2. The CH_2Cl_2 extract was

found to have immunosuppressive properties and was subjected to flash column chromatography. Reverse phase thin-layer chromatography (RP-TLC) was employed to distinguish the fractions that were obtained by flash column chromatography based on the R_f values. Fourteen flash column chromatography fractions were obtained of which fraction 13 (CMX-13) had significant immunosuppressive properties.

In this work we report our approach to further purify the bioactive compound in CMX-13 employing a bioassay-guided fractionation strategy using RP-HPLC. CMX-13 produced 8 fractions of which CMX-13-5 had significant bioactivity. The bioactive RP-HPLC fraction CMX-13-5 was subjected to preliminary structure elucidation studies by nuclear magnetic resonance and liquid chromatography (LC)-mass spectrometry experiments.

In order to obtain sufficient amounts of CMX-13 for *in-vitro* and *in-vivo* experiments new batches of *RC* roots were purchased and subjected to bioassay-guided fractionation employing the methods established earlier. From these subsequent batches we isolated fraction CMX-13', (Figure 3.1.2) also a flash column chromatography fraction as CMX-13. CMX-13 was used as a reference material in the isolation process of CMX-13'. CMX-13' showed to be a more potent immunosuppressant than CMX-13. Further comparison analysis of CMX-13' showed that it is a less complex mixture of compounds than CMX-13. Both flash column fractions had similar chromatographic profiles when subjected to RP-HPLC and RP-TLC. This led us to conclude that CMX-13' and

CMX-13 are flash column fractions with similar properties, with the difference that CMX-13' is a less complex mixture of compounds.

Figure 3.1.1 Strategy employed for the isolation of the bioactive compound CMX-13 from *RC*. After each step of purification the compound was subjected to an immunosuppressive bioassay.

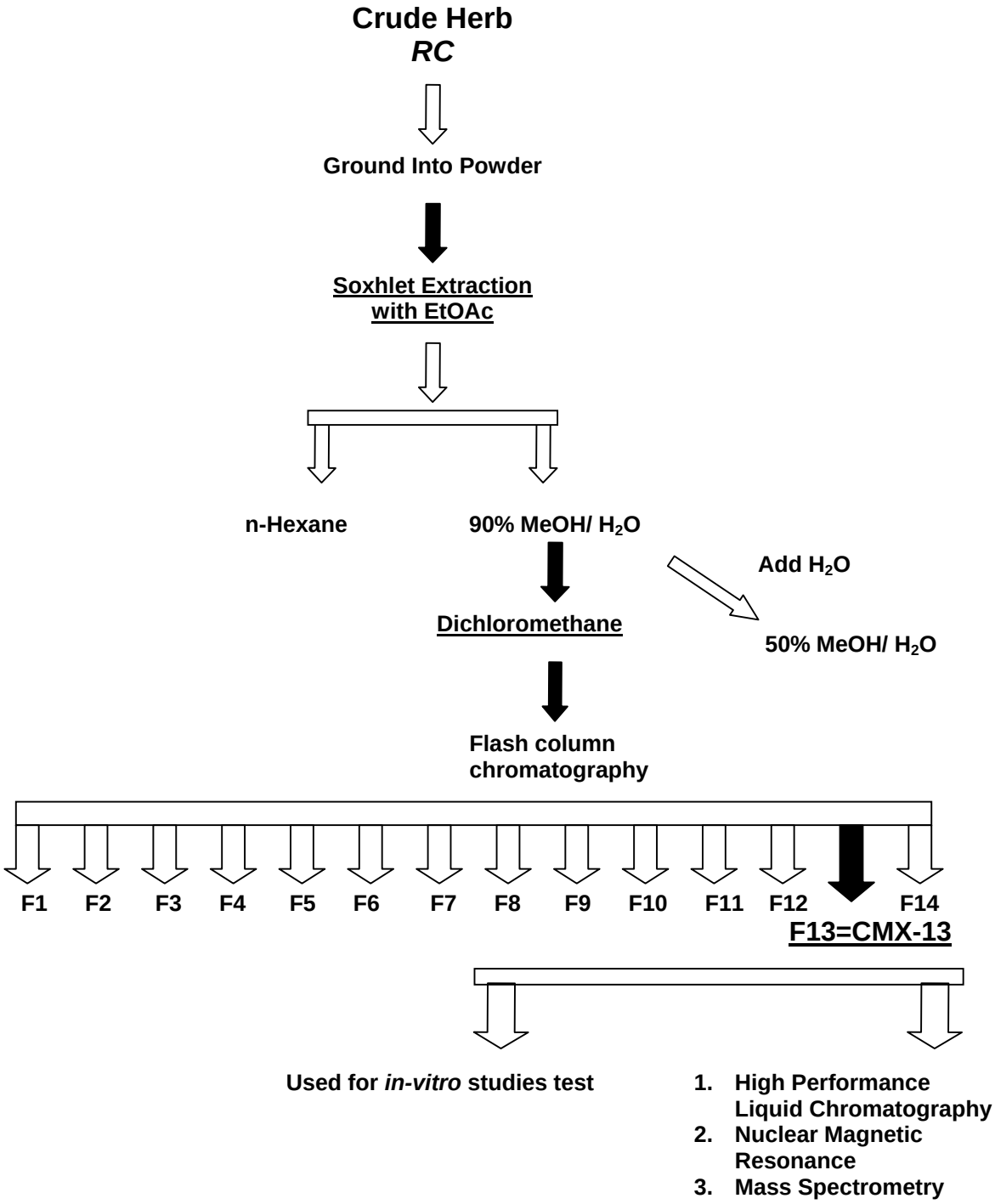

Figure 3.1.2 Strategy employed for the isolation of the bioactive compound CMX-13' from *RC*. The same bioassay-guided fractionation strategy employed for CMX13 was used to isolate CMX-13'. Flash column chromato-graphy of the CH_2Cl_2 fraction produced 16 compounds of which fraction 7 showed was bioactive. Chemical analysis of CMX-13' and CMX13 revealed that these two compounds have similar chromatographic properties.

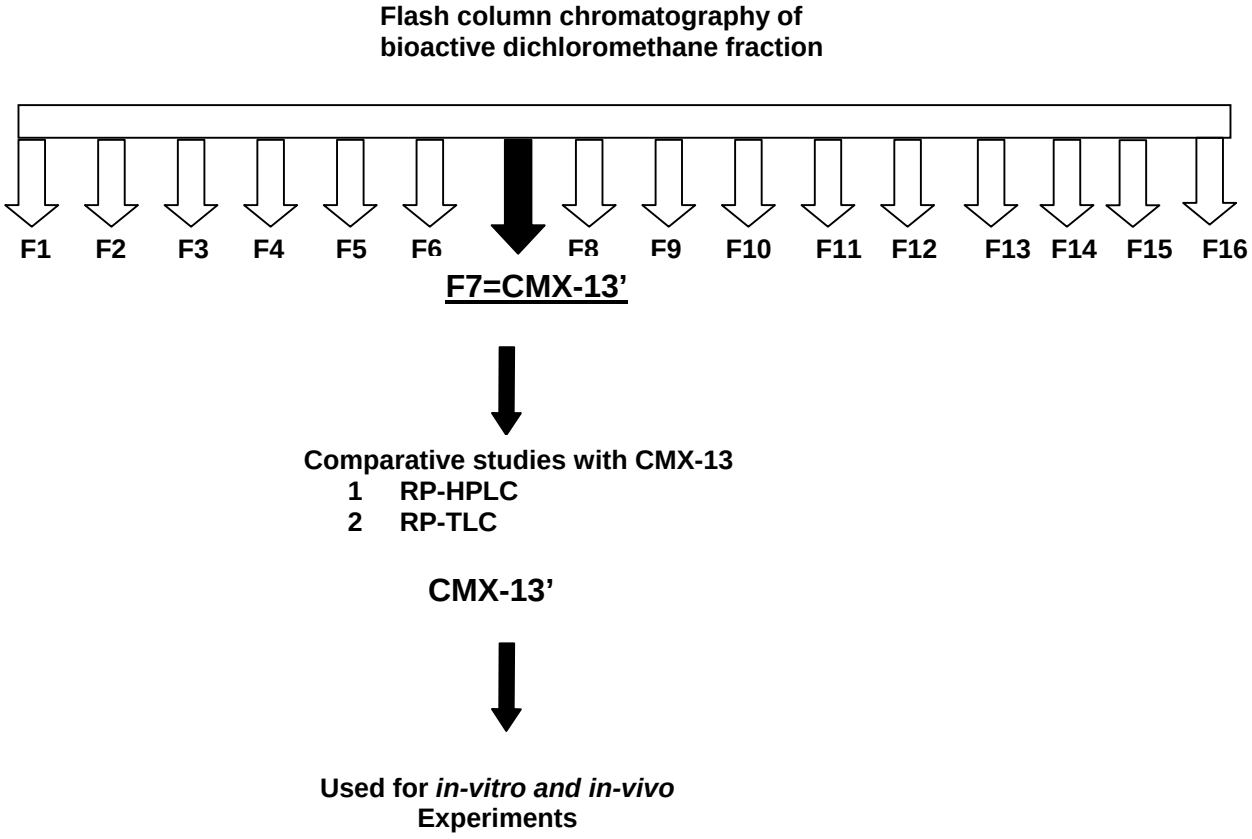

3.2 RESULTS

3.2.1 Isolation and Immunosuppressive Bioassay of Commercial Crude Herb

PHA stimulates proliferation of PBMCs or the lymphoproliferative response (LPR). In the course of cell proliferation DNA is synthesized. When proliferating cells are cultured in the presence of ^{3}[H]-Thymidine, incorporation of ^{3}[H]-Thymidine into DNA occurs. Therefore, cell proliferation can be measured by the amount of incorporated ^{3}[H]-Thymidine into the newly synthesized DNA.

The immunosuppressive properties of the herbal roots of *RC* were tested on PBMCs stimulated with PHA (PHA+PBMCs). All experiments were conducted in triplicates. In the experimental set up, PHA+PBMCs were cultured with no additional treatment (negative control), with DMSO (DMSO-control), or with the plant extract. DMSO served as a vehicle for the extracts and therefore was used as the solvent control. The degree of immunosuppression was calculated as follows: Percent immunosuppression = [1-(cpm of treated cells)/(cpm of untreated cells)]*100

New batches of *RC* roots were purchased, processed and subjected to extraction with EtOAc, as described in section 2.1.1 of Materials and Methods.

The EtOAc extracts (EtOAc EXT) were tested for their immunosuppressive properties on PHA+PBMCs. Figure 3.2.1.1 shows the results of the immunosuppressive bioassay on PHA+PBMCs derived from 3 individuals on 3 different occasions.

The DMSO-treated PHA+PBMCs showed slight suppression (4.5±4.8%) when compared to the untreated PHA+PBMCs, but this was not statistically significant. EtoAC EXT showed a dose-response effect on suppression of LPR, with 4 μg/ml EtOAC EXT resulting in 67.6±2.7% immunosuppression ($p<0.05$), while 1.0 μg/ml EtOAc EXT resulting in only 46.3±17.7% suppression of the LPR (p=ns) (Table 3.2.1.1 and Figure 3.2.1.1). Hence only the EtOAc EXT of *RC* which had an immunosuppressive effect of 60% or above at a concentration of 4 μg/ml were considered suitable for further bioassay-guided fractionation**.**

Table 3.2.1.1 Immunosupression of PHA+PBMCs by EtOAc EXT

PHA+PBMC treatment	PHA+PBMC Proliferation in cpm x 10^3	Immunosuppression (%)	p value
Unt. PHA+PBMC	93.6±14.3	0	
DMSO	89.4±17.9	4.5±4.8	NS
1 μg/ml EtOAc EXT	53.2±38.7	46.3±17.7	NS
2 μg/ml EtOAc EXT	32.6±2.3	64.8±1.9	< 0.05
4 μg/ml EtOAc EXT	29.8±0.7	67.6±2.7	< 0.05

Figure 3.2.1.1 Grounded roots of *RC* was extracted with EtOAc by Soxhlet extraction. The PHA+PBMCs were treated with 1, 2 and 4 μg/ml of EtOAc EXT. 4 μg/ml of EtOAc EXT resulted in 67.6±2.7% immunosuppression.

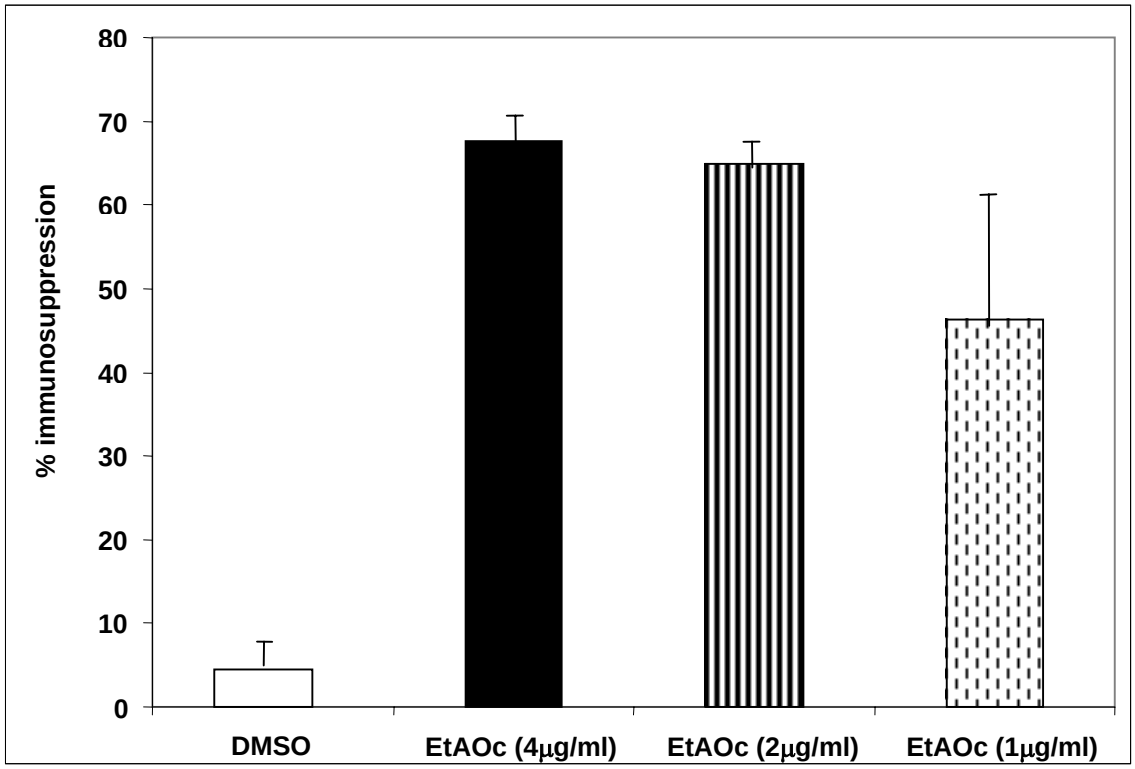

3.2.2 Immunosuppressive Effect of the Extracts Obtained Through Solvent Partition

The EtOAc EXT with immunosuppressive properties was subjected to solvent partition with 50% MeOH/H_2O, Hex and CH_2Cl_2 as described in section 2.1.2 of Materials and Methods. After partition, the 3 solvent extracts were lyophilized and tested at a concentration of 4 μg/ml for their immunosuppressive properties. Figure 3.2.2.1 shows the results of the immunosuppressive bioassay conducted on PHA+PBMCs from 3 individuals on different occasions.

The DMSO-treated PHA+PBMCs showed slight suppression (5.7±4.7%) when compared to the untreated PHA+PBMCs, but this was not statistically significant. The PHA+PBMCs treated with the CH_2Cl_2 extract (CH_2Cl_2 EXT) showed significant immunosuppression (71.6±0.8%, $p<0.05$) (Table 3.2.2.1 and Figure 3.2.2.1). The Hex extract (Hex EXT) and the 50% MeOH/H_2O extract (50% MeOH/H_2O EXT) did not have any immunosuppressive effect on the PHA+PBMCs. The CH_2Cl_2 EXT was re-tested in 3 further individuals to confirm the immunosuppressive effect on PHA+PBMCs. A similar degree of immunosuppression was obtained (72.9±12.9%, $p<0.05$). The CH_2Cl_2 EXT was then subjected to flash column chromatography for further purification.

Table 3.2.2.1 Suppression of PHA+PBMCs by Solvent Extracts.

PHA+PBMC Treatment	PBMC Proliferation in cpm x10^3	Immunosuppression in %	p value
Unt.PHA+PBMC	114.2±3.3	0	
DMSO	107.8±7.0	5.7± 4.7	NS
50% MeOH /H_2O EXT	99.7±5.0	12.5 ± 9.1	NS
Hex EXT	114.5±1.9	-0.4 ± 2.8	NS
CH_2Cl_2 EXT	32.2±0.8	71.6 ± 0.8	<0.05

Figure 3.2.2.1 Immunosuppressive effect of solvent extracts on PHA+PBMCs. The CH_2Cl_2 extract was shown to significantly suppress the LPR of the PHA+PBMCs (71.6 ± 0.8% p<0.05). No effect was seen with DMSO, Hex EXT, and 50% Meth/H_2O EXT treatment.

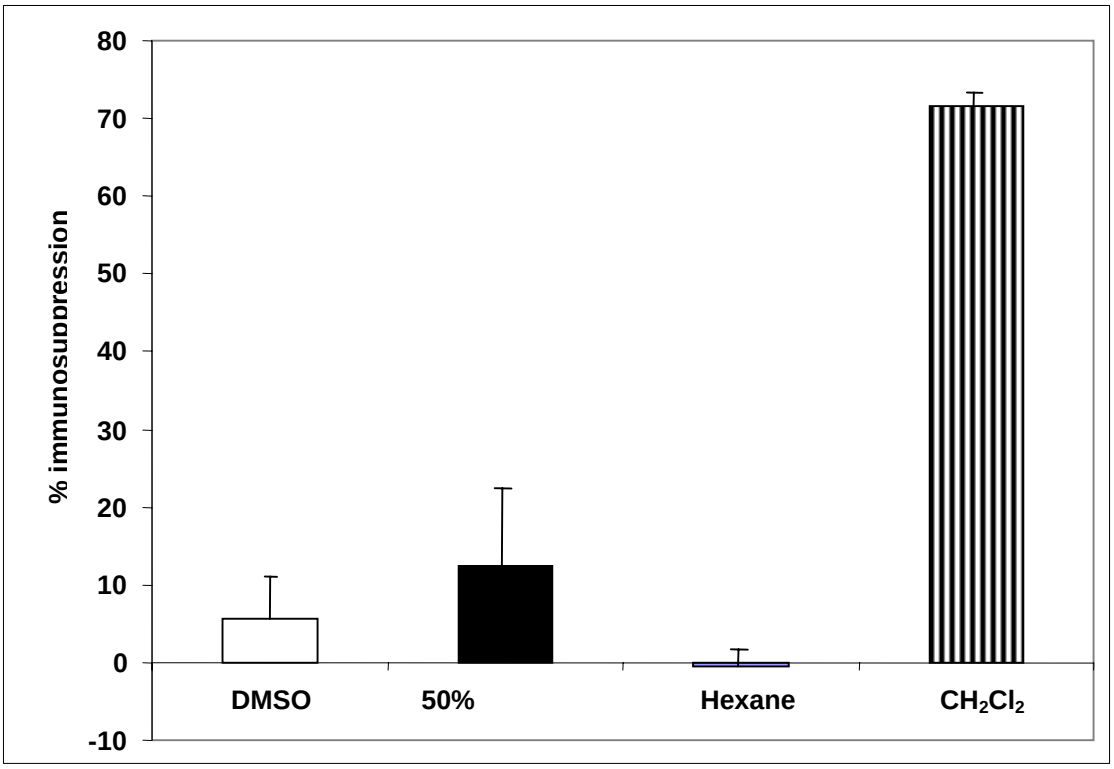

3.2.3 Immunosuppressive Effect of the Fractions Obtained Through Flash Column Chromatography

The CH_2Cl_2 EXT was subjected to flash column chromatography as described in Section 2.1.3 (Materials and Methods). The flash column chromatography fractions were distinguished from each other based on the retention times (R_f) when analyzed by thin layer chromatography. Sixteen flash column chromatography fractions were obtained and all these fractions were tested on

PHA+PBMCs from one blood donor. As testing of all 16 fractions involved a large amount of blood, this experiment was conducted only once but in a triplicate experimental set up. The immunosuppression experiments were conducted using concentrations of 4 μg/ml for each fraction. The results are shown in Figure 3.2.3.1. Fraction 7 (CMX-13') had the highest (75%) immunosuppressive effect on PHA+PBMCs.

Figure 3.2.3.1 Imunosuppressive properties of flash column chromatography fractions. Sixteen fractions were tested at a concentration of 4 μg/ml for their immunosuppressive properties. Fraction 7 (F7), showed 75% suppression of the lymphoproliferative response, and was named CMX-13'.

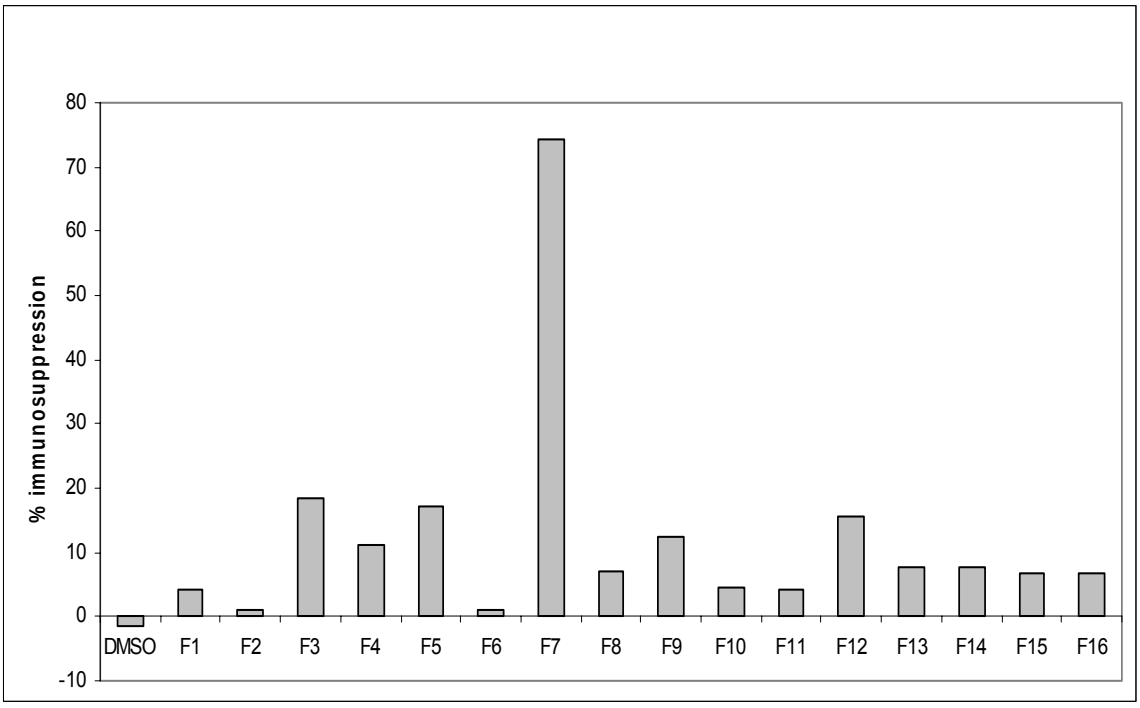

To determine the potency of CMX-13' as compared to the original CMX-13, the effect of both compounds at a concentration of 4 μg/ml were tested

simultaneously on PBMCs from 3 individual donors in triplicates (Figure 3.2.3.2). The immunosuppressive effects of CMX-13 and CMX-13' on PHA+PBMCs were 70.9±14.5% and 91.6±7.1% respectively, that is, CMX-13' was at least 20% more potent than CMX-13 at this concentration. Approximately 600mg of CMX-13' was hence obtained and used for further *in-vivo* and *in-vitro* studies.

Figure 3.2.3.2 Comparative bioassay of flash column chromatography fractions CMX-13 and CMX-13'. CMX-13 and CMX-13' were tested for their immunosuppressive properties at a concentration of 4 μg/ml. CMX-13 had an inhibitory activity of 70.9±14.5% and CMX-13' 91.6±7.1% on PHA-stimulated PBMC proliferation.

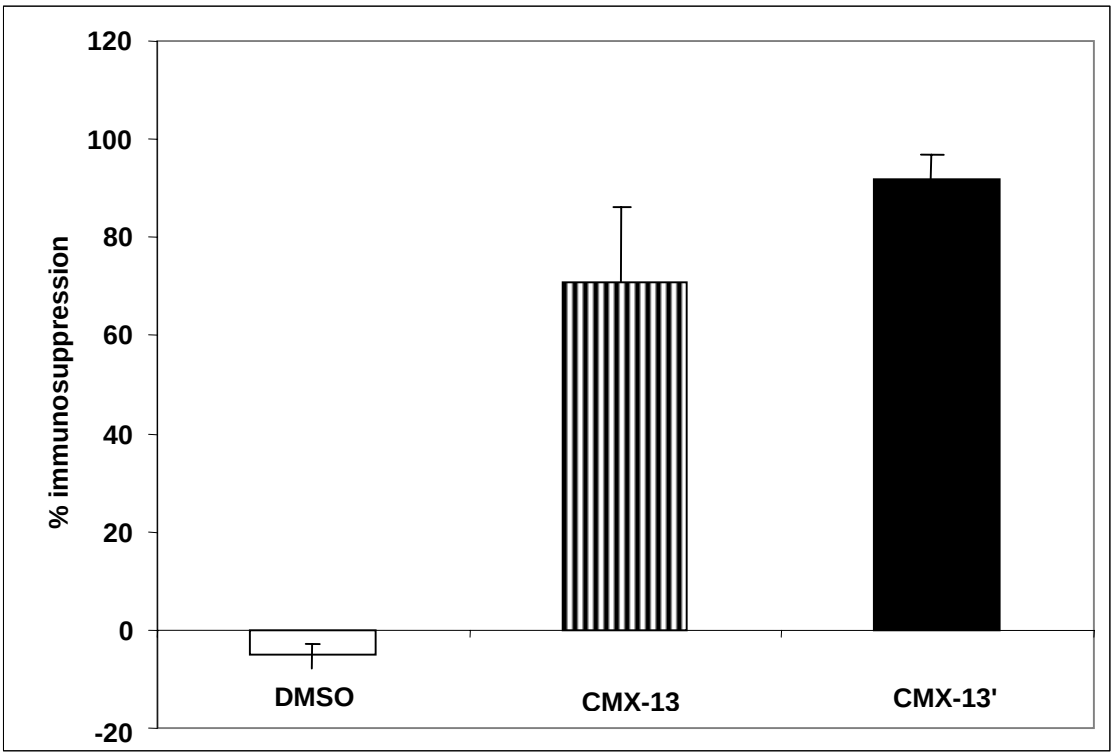

Figure 3.2.3.3 shows a summary of the increase in immunosuppressive activity of the extracts after each step of purification. The immunosuppressive activity of the extracts ranged from 66.0% for the EtOAc extract of the crude herb to 92.2 % after further purification by flash column chromatography. Only 600 mg (0.4% from the original mass) was obtained with 92.2% immunosuppressive bioactivity. The weights of the active extracts and the corresponding immunosuppressive potencies (% inhibition of LPR) are shown in Table 3.2.3.1.

Figure 3.2.3.3 Immunosuppressive bioactivity in bioassay-guided fractionation of CMX-13'. The extracts were tested at a concentration of 4 μg/ml. The immunosuppressive effect increased after each step of purification.

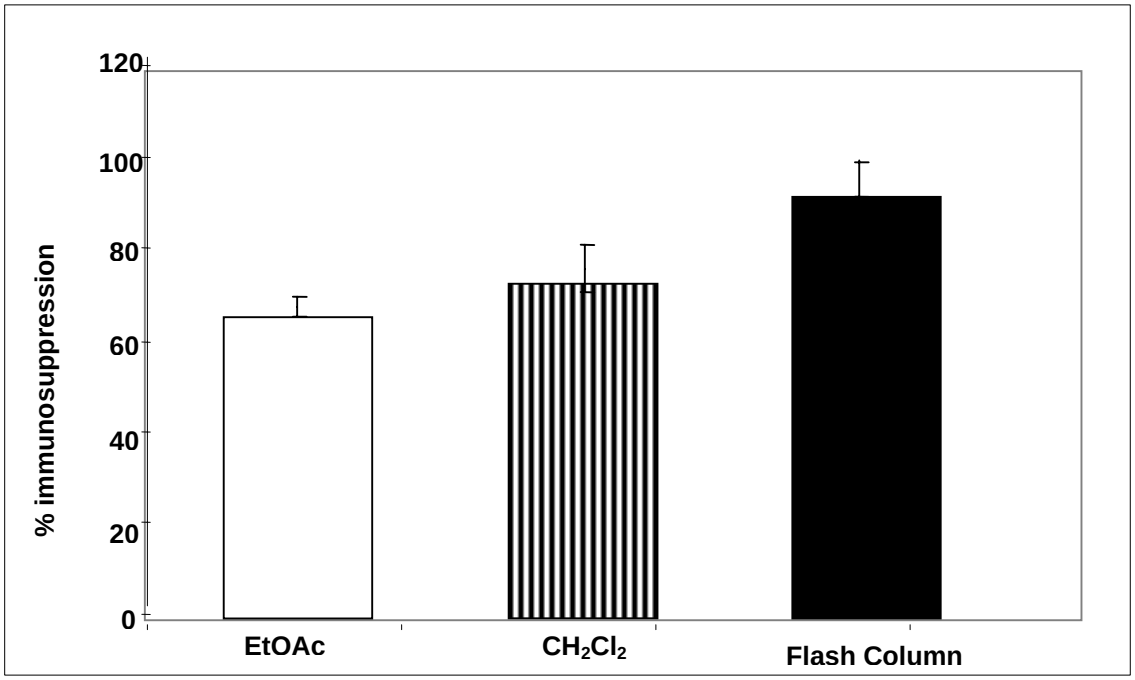

Table 3.2.3.1 Bioassay-guided fractionation of CMX-13'. The yield obtained from the roots after flash column chromatography was only 600 mg, which accounted for 0.4% from the total weight.

	Weight in grams	% weight of crude herb	Immunosuppression (%)
Crude Herb	150		
EtOAc	15	10	66.0±5.5
CH_2Cl_2	4.2	2.8	72.9±12.9
Flash column chromatography fraction 7 (CMX-13')	0.6	0.4	92.2±11.6

3.2.4 RP-HPLC and RP-TLC of CMX-13'

Two chemical experiments were conducted in order to confirm if the flash column fraction CMX-13' and CMX-13 contained similar compounds. RP-HPLC and RP-TLC were employed in these comparative studies.

RP-HPLC was conducted with a Nova-pack C18 Column of 4 μm pore size. Water and acetonitrile were used as the mobile phase with a flow rate of 0.6 ml/min. CMX-13' and CMX-13 were dissolved in 50% MeOH/Acetonitrile at a concentration of 5 mg/ml. The injection volume was set to 50 μl. The RP-HPLC chromatogram of CMX-13' is shown in Figure 3.2.4.1. CMX-13' was subjected to RP-HPLC for comparison studies with CMX-13. The compounds in CMX-13' had a retention time from 25-40 minutes. CMX-13 had compounds with similar

retention times. The similarities of CMX-13 and CMX13' were confirmed by the retention time of their RP-HPLC profiles.

Figure 3.2.4.1 RP-HPLC Chromatogram of CMX-13'. Conditions; Novapack C18 Column of 4μm pore size, Gradient: Water-Acetonitrile (100-0% to 0 -100%); Flow rate: 0.6 ml/min.

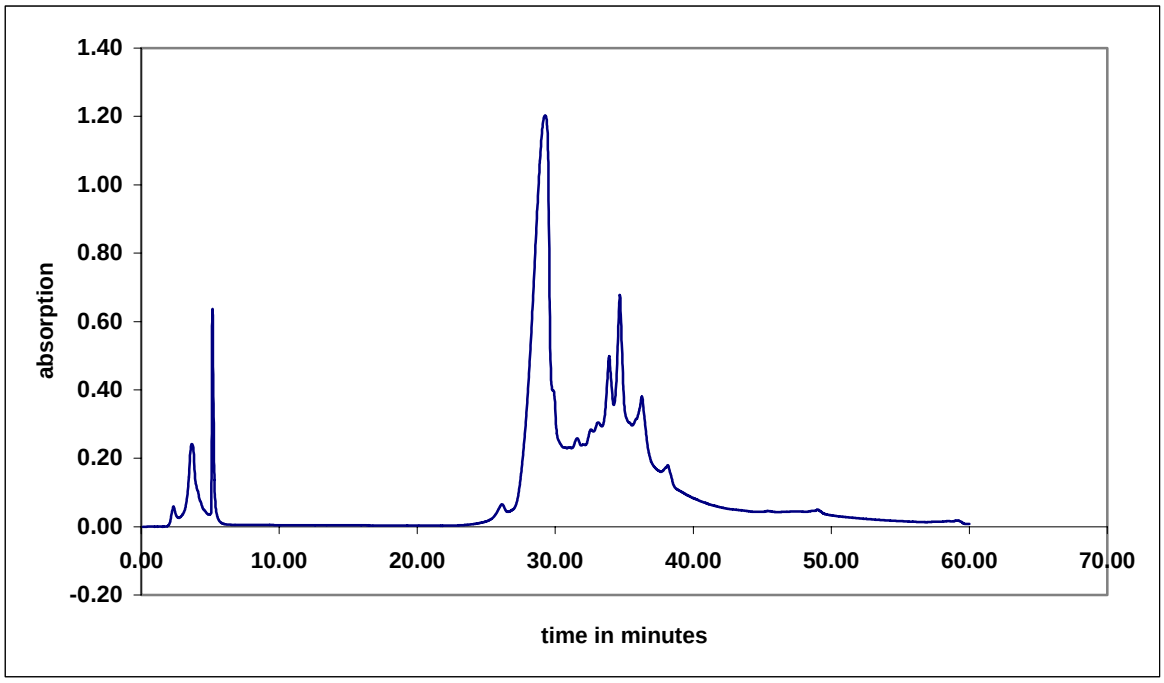

3.2.5 Immunosuppressive Bioassay of RP-HPLC Fractions Derived From CMX-13

CMX-13 was subjected to RP-HPLC in order to isolate and purify the bioactive compounds for structure elucidation. The RP-HPLC conditions for CMX-13 were optimized with water and acetonitrile as the mobile phase at a flow rate of 0.6 ml/min. CMX-13 was dissolved in 50% MeOH/Acetonitrile at a concentration of 5.0 mg/ml and injected at a volume of 50 μl on a gradient run which lasted 70 minutes.

The RP-HPLC eluents were collected based on the retention time in 8 fractions (CMX-13-1 to CMX-13-8). The retention of the fractions times are summarized in Table 3.2.5.1 and were collected automatically with a fraction collector. These fractions were named in order of appearance and are shown in the HPLC Chromatogram in Figure 3.2.5.1. The retention times of the compounds are listed in Table 3.2.5.1. Twenty RP-HPLC runs of CMX-13 using a solution of 5.0 mg/ml were conducted and the products were collected and freeze-dried. The products of the 20 runs were used in the immunosuppressive bioassay.

Each collected fraction was re-analyzed by RP-HPLC. The RP-HPLC Chromatograms of the eight fractions obtained from CMX-13 (CMX-13-1 to CMX-13-8) are depicted in Figures 3.2.5.3-10. The re-injected fractions

generally reproduced the original retention time and CMX-13-1 was consistently present in all fractions (in small amounts) for some reason.

The CMX-13 RP-HPLC fractions were tested for their immunosuppressive activity on PHA+PBMCs. This experiment was conducted in triplicates in one experimental set up, due to limited availability of the material. The immunosuppressive activity of the CMX-13 fractions is shown in Figure 3.2.5.2. CMX-13-1, CMX-13-4, CMX-13-5 and CMX-13-8 had significant immunosuppressive activity as shown in Table 3.2.5.2. The RP-HPLC fractions CMX-13-1 and CMX-13-5 showed nearly 100% immunosuppression when compared to the DMSO-treated PHA+PBMCs.

The RP-HPLC chromatograms of CMX-13-4 and CMX-13-8 are shown In Figures 3.2.5.6 and 3.2.5.10. These CMX-13 fractions contained peaks with shoulders, which are indicative of the presence of more than one compound.

The RP-HPLC chromatogram of CMX-13-1 is shown in Figure 3.2.5.3. CMX-13-1 consisted of at least 3 different components, which was shown by the appearance of two peaks in the 1-5 minutes region and one peak in the 25-27 minutes region. These 3 peaks implied that CMX-13-1 was a less pure fraction. The RP-HPLC chromatogram of CMX-13-5 had two peaks one more predominant than the other as shown in Figure 3.2.5.7. This implied that the

fraction CMX-13-5 was much purer than CMX-13-1. Therefore CMX-13-5 was selected for further structure elucidation experiments.

CMX-13-5 was subjected to preliminary structure elucidation by NMR and LC-Mass Spectrometry experiments. The CMX-13-5 fraction was subjected for a second time to RP-HPLC to remove impurities before conducting NMR experiments. However some impurities remained in the 1-5 minute region. This persistent impurity could be due to the susceptibility to biodegradation.

Figure 3.2.5.1 RP-HPLC Chromatogram of CMX-13. Conditions; Nova-pack C18 Column with 4μm in pore size, Gradient: Water-Acetonitrile (100-0% to 0-100%); Flow rate:0.6 ml/min.

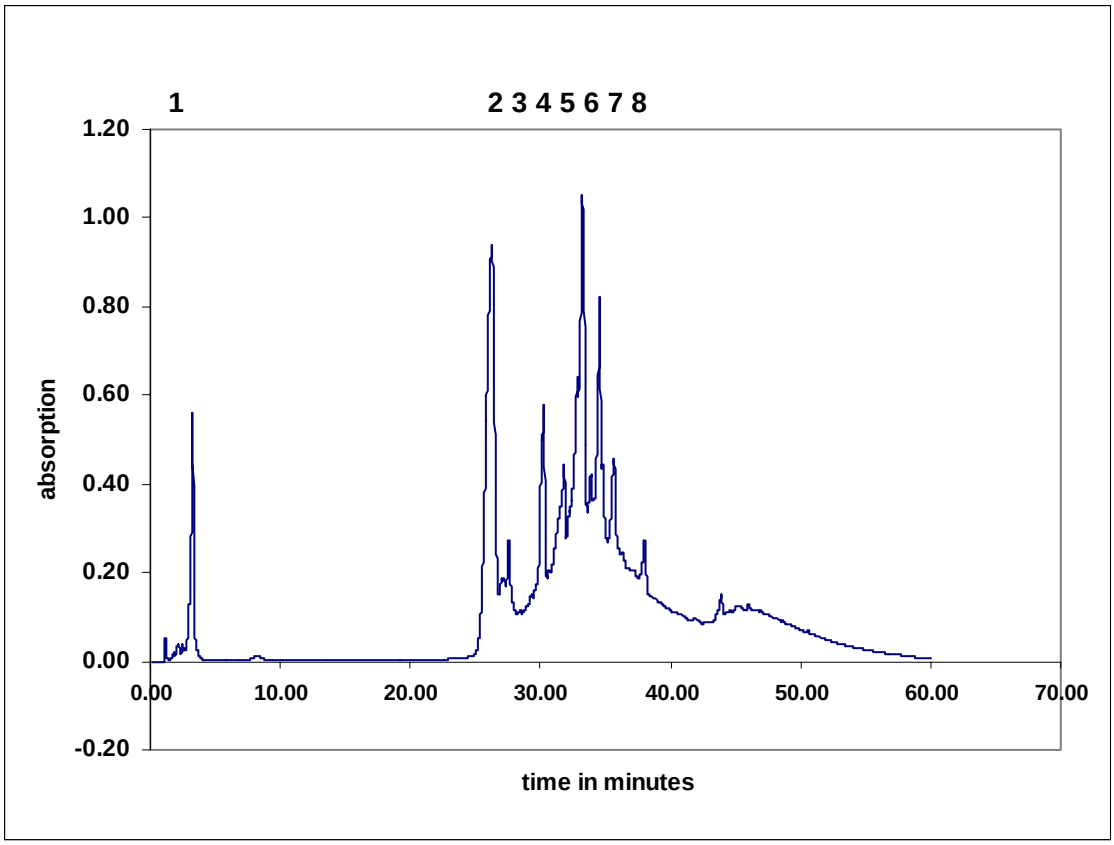

Table 3.2.5.1 Retention times of RP-HPLC isolates from CMX-13.

CMX-13 Fractions from RP-HPLC	Retention time in minutes
1	1.0 - 5.0
2	25.0 – 27.0
3	27.0 – 29.0
4	29.0 – 31.0
5	31.0 – 33.0
6	33.0 – 35.0
7	36.0- 37.0
8	37.0 - 39.0

Figure 3.2.5.2 Immunosuppression of PHA+PBMCs by subfractions of CMX-13 after RP-HPLC. PHA+PBMCs were treated with 4 μg/ml of each fraction. Significant immunosuppression with the subfractions, CMX-13-1 and CMX-13-5 was obtained.

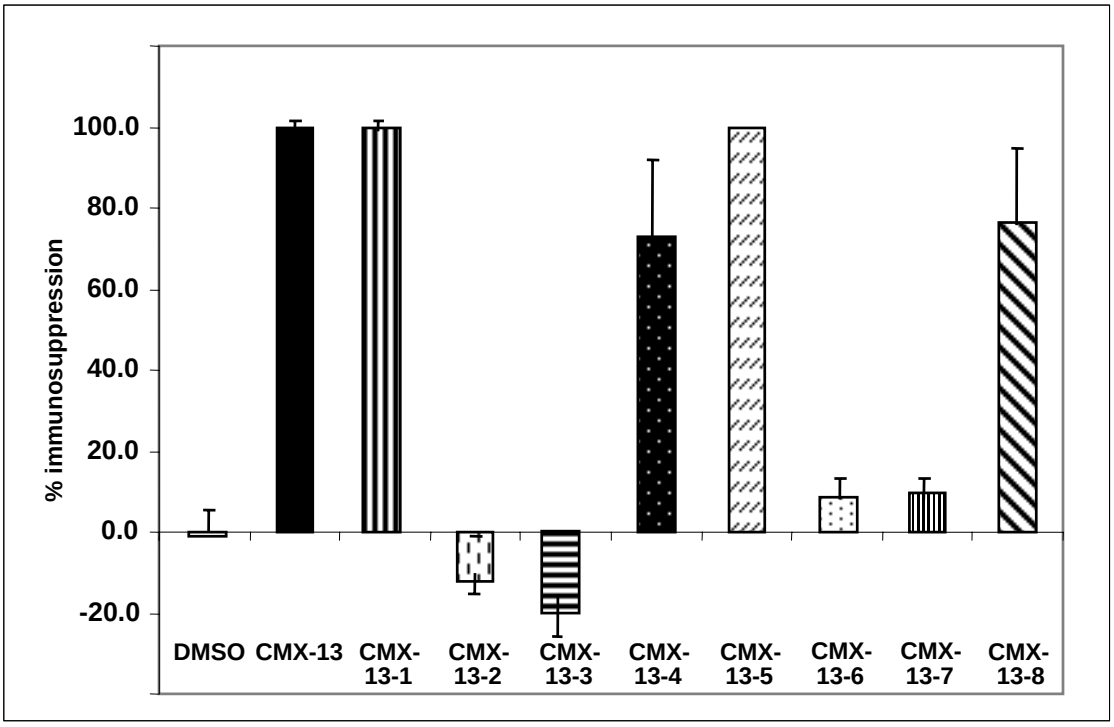

Table 3.2.5.2 Immunosuppression of PHA+PBMC by CMX-13 fractions isolated by RP-HPLC.

PHA+PBMC treatment	PBMC Proliferation (cpm x 10^3)	Suppression (%)	p value
Unt PHA+PBMC	76.2±8.2	0	
DMSO	75.3±3.5	-1.1± 11.2	NS
CMX-13	9.3±7.6	99.8±0.2	0.05
CMX-13-1	0.018±0.9	100.0±0.0	0.05
CMX-13-2	84.1±5.1	-12.0±19.3	NS
CMX-13-3	88.2±6.5	-20.0±20.4	NS
CMX-13-4	24.4±21.4	72.8±23.2	NS
CMX-13-5	0.021±0.0	100.0±0.0	0.05
CMX-13-6	67.6±2.2	8.6±12.4	NS
CMX-13-7	67.3±3.6	9.4± 12.4	0.275
CMX-13-8	21.2±19.9	76.7±21.7	0.05

Figure 3.2.5.3 RP-HPLC Chromatogram of CMX-13-1. Retention time 1.0-5.0 minutes.

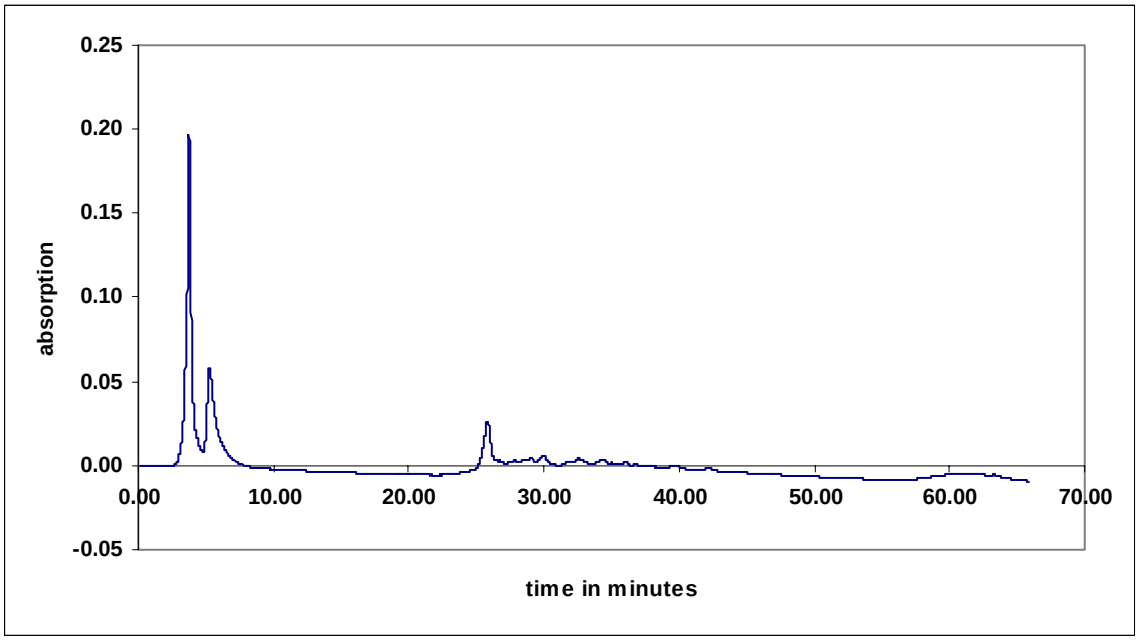

Figure 3.2.5.4 HPLC Chromatogram of CMX-13-2. Retention time 25-27 minutes.

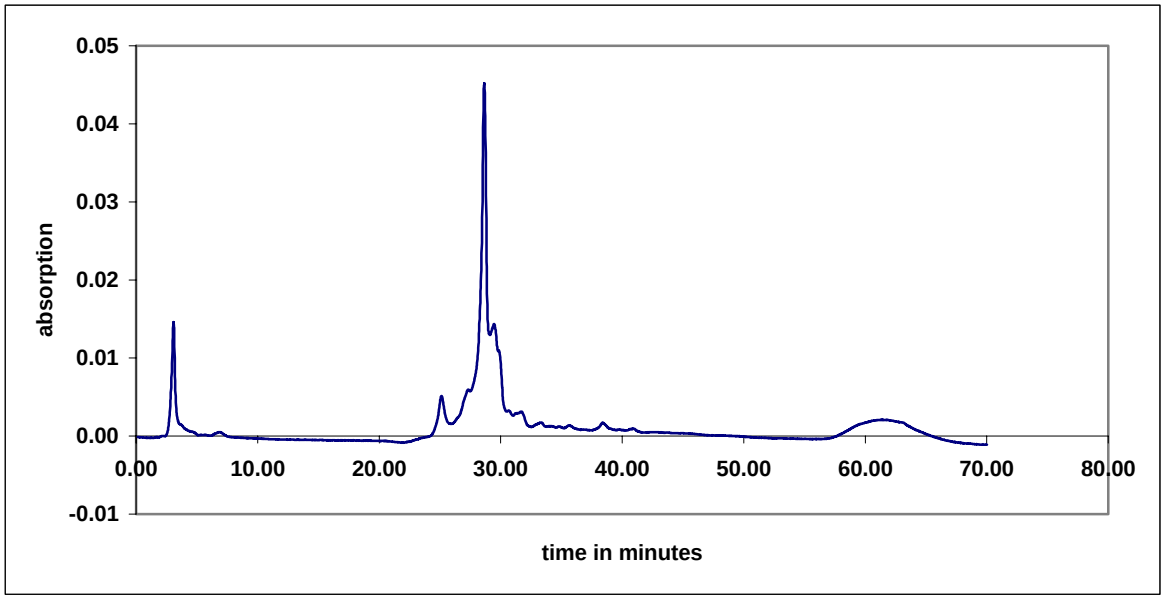

Figure 3.2.5.5 HPLC Chromatogram of CMX-13-3: retention time 27.0-29.0 minutes.

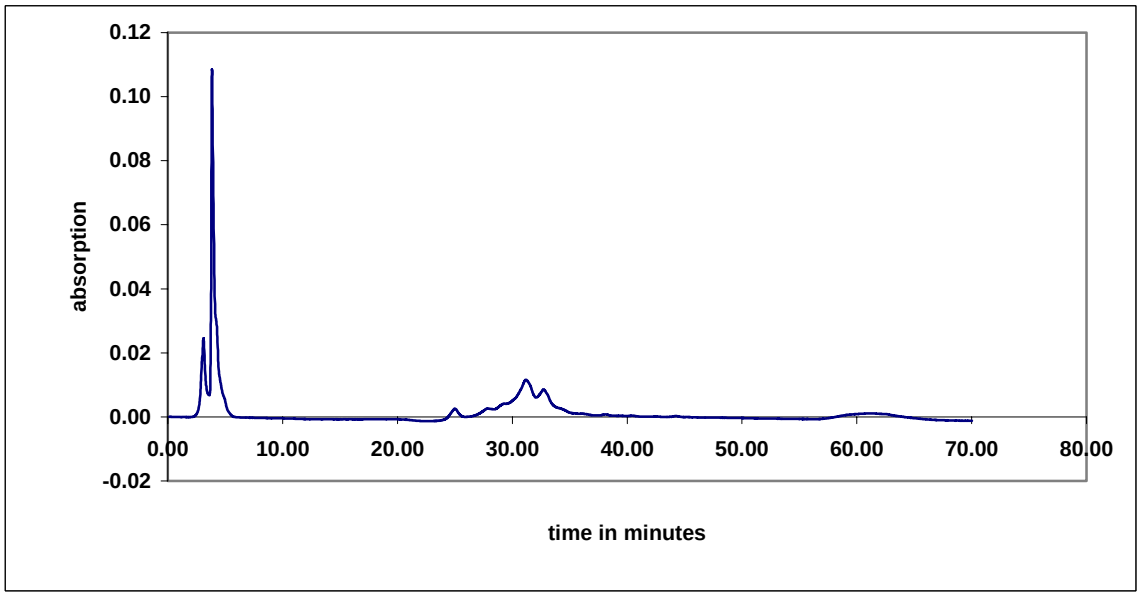

Figure 3.2.5.6 HPLC Chromatogram of CMX-13-4. Retention time 29-31 minutes.

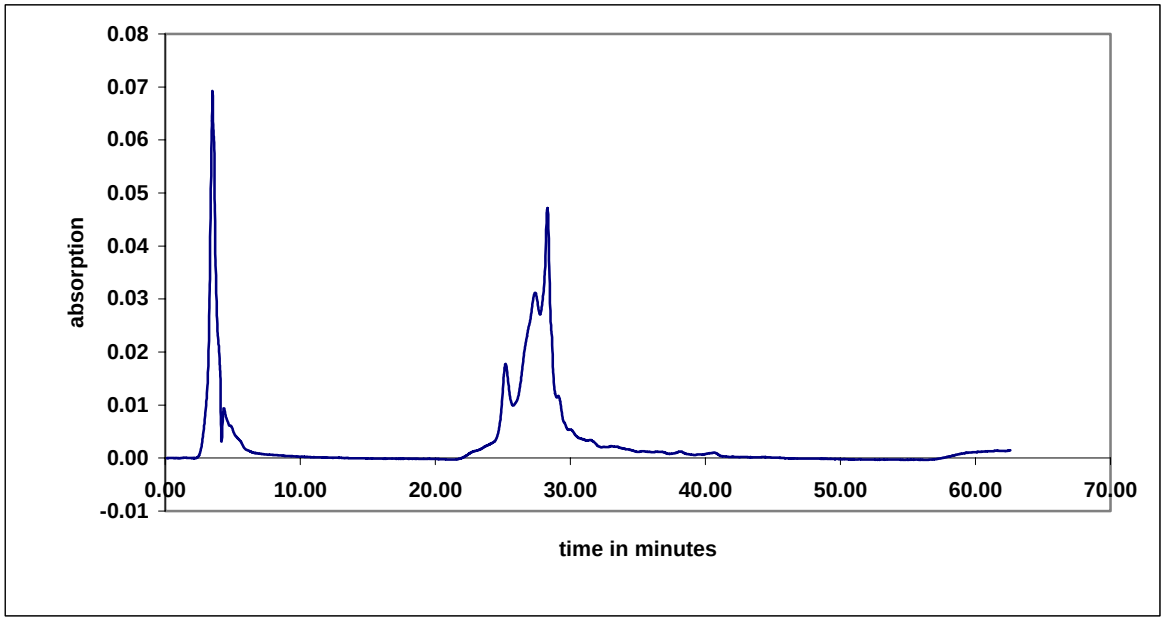

Figure 3.2.5.7 HPLC Chromatogram of CMX-13-5. Retention time 31-33 minutes.

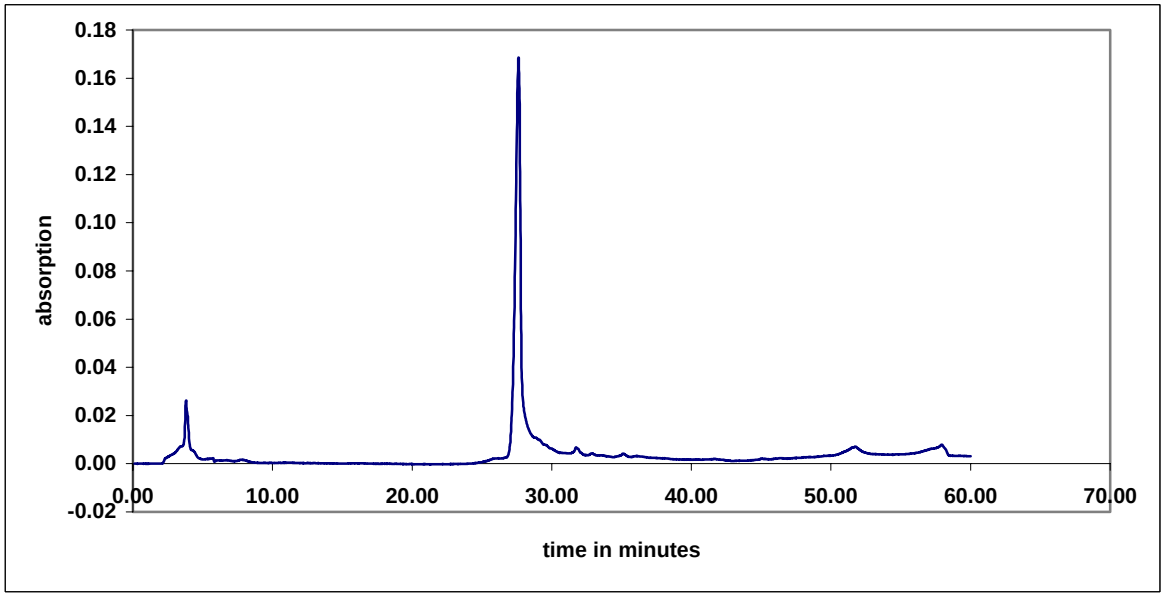

Figure 3.2.5.8 HPLC Chromatogram of CMX-13-6. Retention time 33- 35 minutes.

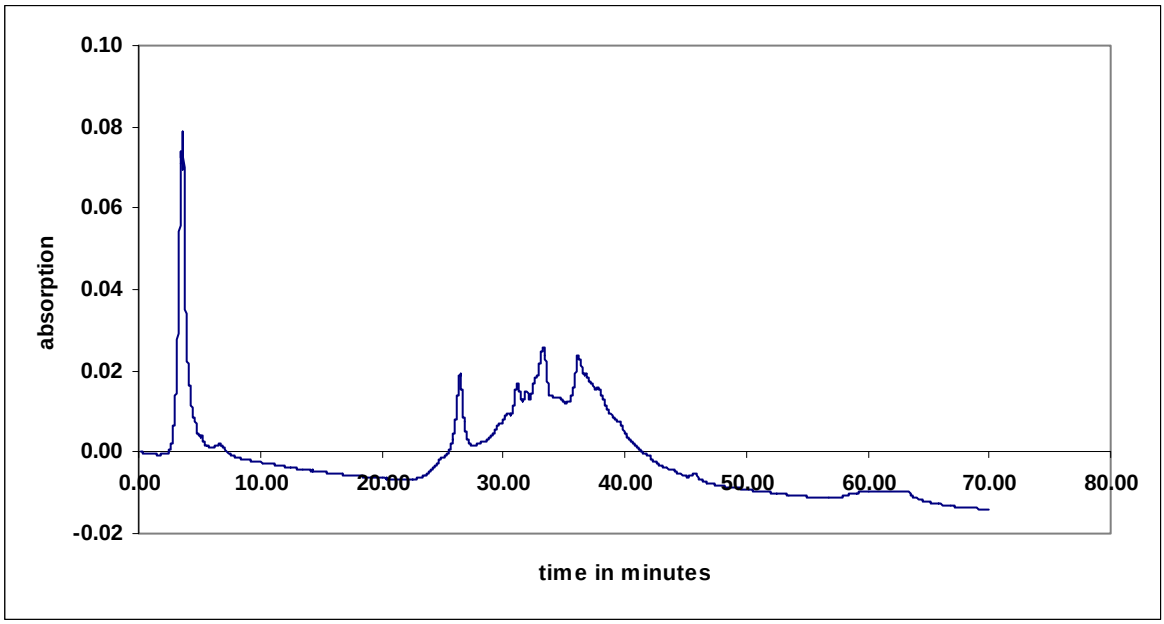

Figure 3.2.5.9 HPLC Chromatogram of CMX-13-7. Retention time 35.0-36.0 minutes.

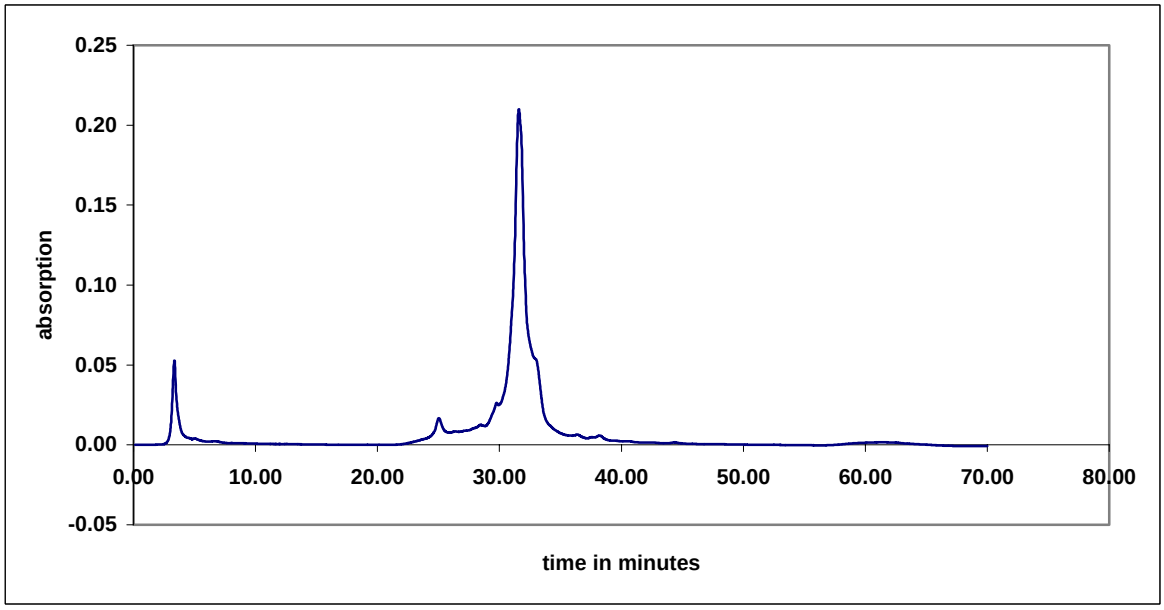

Figure 3.2.5.10 HPLC Chromatogram of CMX-13-8. Retention time 36.0-39.0 minutes.

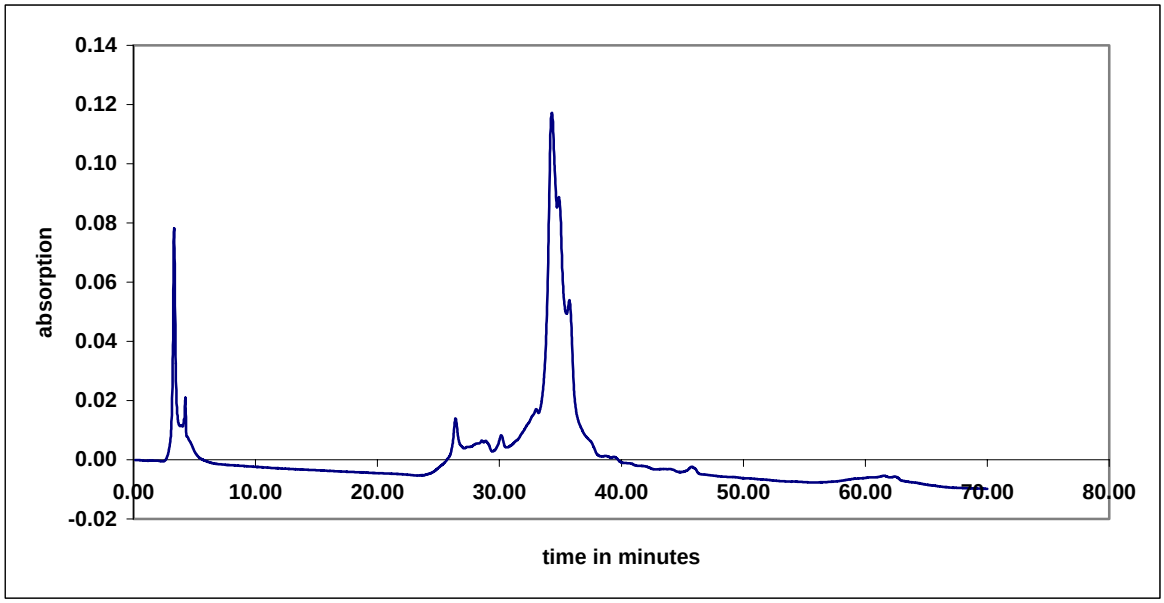

3.2.6 Reverse Phase Thin Layer Chromatography (RP-TLC)

The 3 bioactive fractions CMX-13', CMX-13 and CMX-13-5 were subjected to RP-TLC. The solvent system used was 90% EtOAc/ MeOH. CMX-13' produced one spot at R_f of 0.40, CMX-13 6 spots, and CMX-13-5 3 spots. The 3 samples produced a common spot at R_f = 0.40. The results are listed in Table 3.2.6.1. The single spot produced by CMX-13' by RP-TLC shows that this fraction is the least complex mixture of compounds.

Table 3.2.6.1 RP-TLC of CMX-13, CMX-13-5 and CMX-13'. Solvent system: 90% EtOAc/ MeOH

RP-TLC Fraction	R_f CMX-13	R_f CMX-13-5	R_f CMX-13'
1	0.72	0.72	
2	0.64	0.64	
3	0.6		
4	0.55		
5	0.40	0.40	0.40
6	0.32		

3.2.7 NMR Studies of CMX-13-5

The ^{1}H-NMR spectrum for CMX-13-5 and is shown in Figure 3.2.7.1. CMX-13-5 from all the fractionated collections was dissolved in deuteriated MeOH. Impurities remained in the CMX-13-5, and this made data analysis difficult. However, the total amount of material was not sufficient for complete spectral analysis. The spectrum (Figure 3.2.7.1) bore some resemblance to that of a reported peptide RA-VII (Figure 3.3.1).

Figure 3.2.7.1 NMR spectrum of CMX-13-5. (A) 500-MHz ^{1}H-NMR Spectrum of CMX-13-5 in deuteriated MeOH.

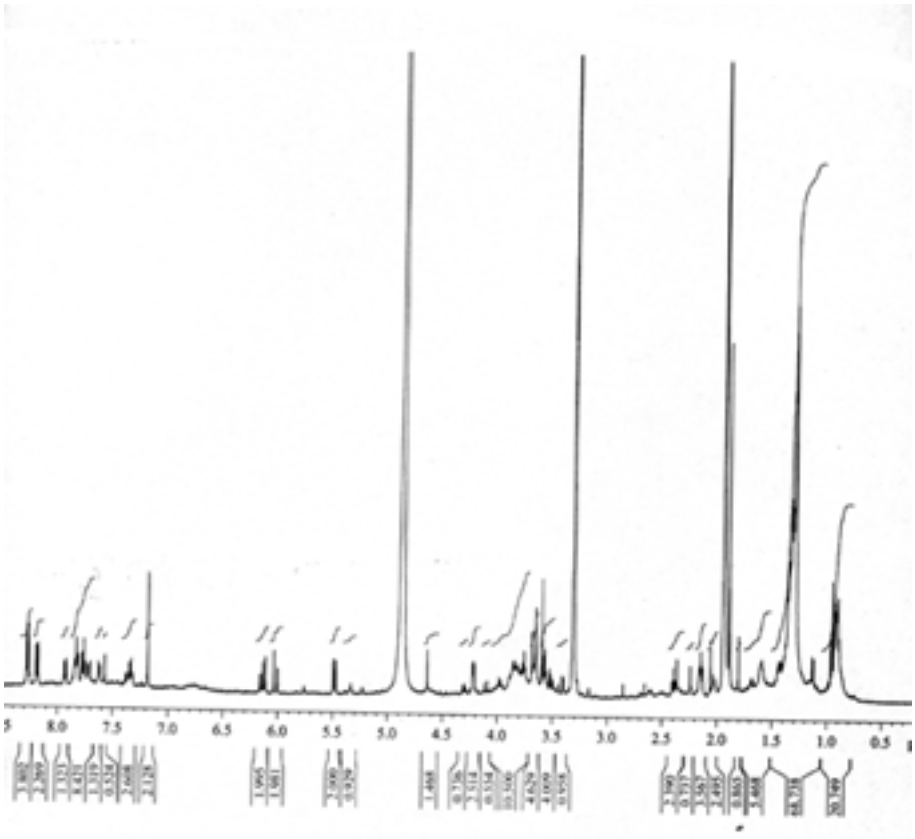

3.2.8 LC-Mass Spectrometry on CMX-13-5

LC-Mass Spectrometry (LC-MS) was performed on CMX-13-5 samples, employing similar RP-HPLC settings as was used to purify CMX-13-5 from CMX-13. Very low concentrations of CMX-13-5 were used for the analyses. The LC chromatogram of CMX-13-5 is shown in Figure 3.2.8.1A. A single peak appeared at 27.07 minutes, which was close to the retention time of CMX-13-5. The molecules were ionized by Fast Atom Bombardment. The LC-MS analysis in Figure 3.2.8.1B shows *m/z* values of 270.2, 537.5 and 1003.5.

Figure 3.2.8.1 LC-Mass Spectrum of CMX-13-5: (A) RP-HPLC \chromatogram; (B) LC-Mass spectrum. The LC-Mass spectrum suggested either a single molecule with a weight of 807.5 or two molecules with a weight of 270 and 537.5.

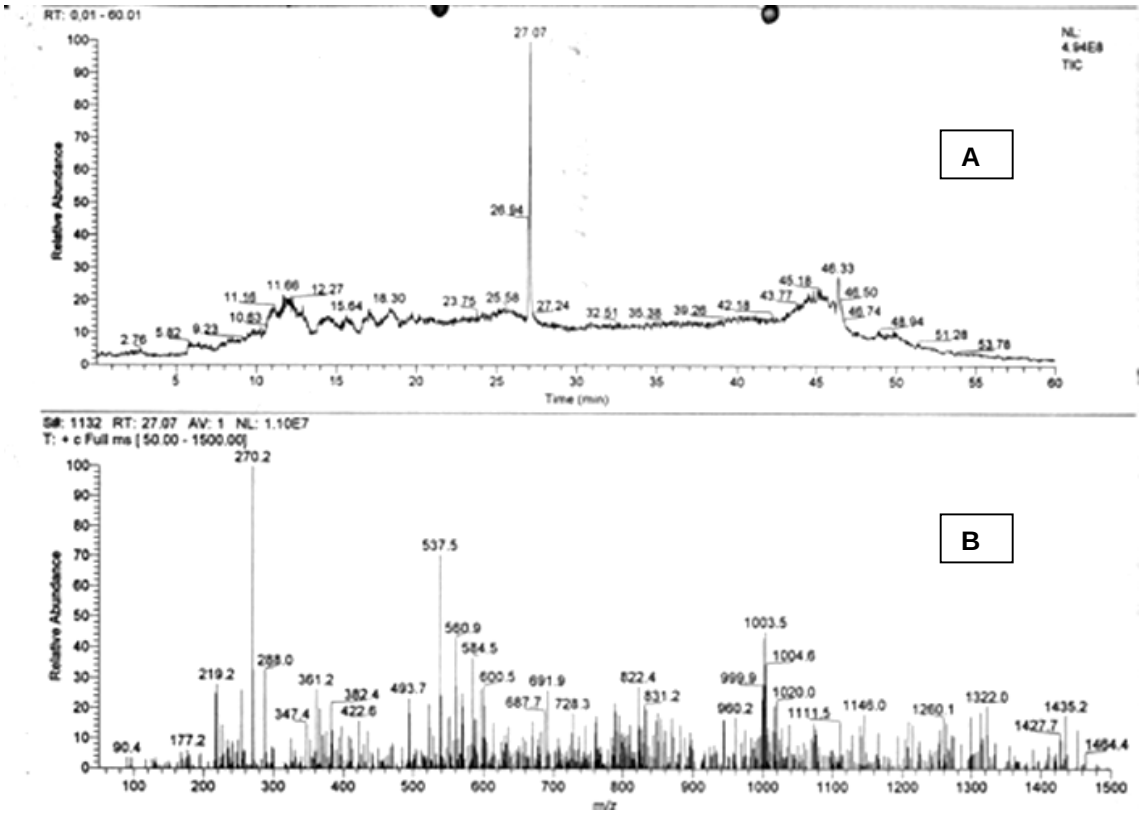

3.3 DISCUSSION

The extraction and purification of bioactive compounds from herbal medicines is laborious and time consuming. In some cases, such as the herb under investigation, *RC*, the bioactivity of the compounds is influenced by factors such as soil composition and seasonal changes. Chemical synthesis allows the production of molecules with consistency, facilitating the production process of bioactive compounds. By employing chemical synthesis the whole process of purification and the problem of inconsistent behaviour of herbal preparations can be eliminated. Hence this chapter focused on the characterization of the molecular structure of the active compound(s) extracted from *RC*.

In our previous work we have shown that CMX-13, a plant-derived compound from the roots of *RC*, has significant immunosuppressive properties. In the first phase of the work in this chapter, we attempted to identify the bioactive molecule(s) in CMX-13, and to elucidate the structure(s) of the molecule(s). In the second phase, we isolated sufficient amounts of CMX-13' following the same procedure as for the isolation of CMX-13 for the *in-vitro* and *in-vivo* experiments in subsequent chapters, and showed that CMX-13' comprised an active component similar to that of CMX-13.

The persistent difficulty in our work was in obtaining sufficient amounts of *RC* with significant bioactivity from one single source. We found that batches of roots possessed immense variability in immunosuppressive properties, ranging from

little or no immunosuppressive properties to 30-40% immunosuppression at most. The group of Itokawa and co-workers have previously shown that plants produced different amounts of compounds depending on factors such as season and soil composition [Itokawa et al.,1984]. It was difficult to trace down the geographical sources as well as the season the roots of *RC* was harvested. As several batches of *RC* were tested and shown to have no immunosuppressive bioactivity, one reason could be that these batches were not harvested at the right season when synthesis of compounds with immunosuppressive activity in the plant was occurring. Another second possibility is that the particular batch of herb was grown on a soil composition that did not lead to production of the relevant compound in the herb. In some cases the batches of *RC* were a mixture of several other different subspecies [Itokawa et al, 1984]. These factors made it very difficult to find batches of *RC* with sufficient immunosuppressive bioactivity.

New batches of *RC* roots were subjected to similar bioassay-guided fractionation as employed for the isolation of CMX-13. CMX-13' was isolated and purified from these new batches, and was shown to have similar immunosuppressive properties as CMX-13. CMX-13 and CMX-13' were both subjected to RP-HPLC and RP-TLC. The RP-HPLC analysis showed that CMX-13 and CMX-13' contained compounds that have similar retention times. The compounds in the RP-HPLC chromatograms of CMX-13' and CMX-13 appeared in the time interval of 25-40 minutes, see Figure 3.2.4.1 and Figure 3.2.5.1. The retention time of the fraction CMX-13-5 was between 31–33 minutes, which was well within the 25-40 minutes range, as shown in Figure 3.2.5.7. RP-TLC studies of CMX-13, CMX-13-

5 and CMX-13' showed the presence of one spot with the same R_f value (0.4). We concluded from the RP-HPLC, RP-TLC and the immunosuppressive bioassays that CMX-13' and CMX-13 consisted of at least one common compound. These results led us to conclude that CMX-13' and CMX-13 comprised similar active compounds. Hence CMX-13' was subsequently utilized for *in-vitro* and *in-vivo* experiments.

RP-HPLC revealed that CMX-13 contained a mixture of possibly 8 or more compounds. These compounds were isolated (some impurely) and tested for their immunosuppressive properties. Each experiment was conducted in triplicates. Two RP-HPLC fractions of CMX-13, named CMX-13-1 and CMX-13-5 had 100% immunosuppressive properties, as shown in Figure 3.2.5.2. Our results showed that these CMX-13-1 and CMX-13-5 were at least as potent as CMX-13 and CMX-13'. A point to note here was that there was some variability in the PHA-stimulated lymphoproliferative response of PBMCs from different donors, and this probably accounted for the variability in their response to the suppressive effects of CMX-13 as seen in the different experiments. One of the factors which influenced the variability in lymphoproliferative response was the age of the healthy blood donors, as older donors had poorer response to PHA-stimulation. Hence, only those donors who were within the age group of 18-30 years were utilized as the lymphoproliferative response was more consistent.

RP-HPLC fraction CMX-13-5 contained fewer impurities than CMX-13-1 as shown in the RP-HPLC profiles of CMX-13-1 and CMX-13-5 in Figure 3.2.5.2 and 3.2.5.7

respectively. Therefore we attempted to elucidate the structure of CMX-13-5 by ^{1}H-NMR and LC-Mass spectrometry. The ^{1}H-NMR spectrum of CMX-13-5 was shown to resemble the ^{1}H-NMR spectra of a bicyclic hexapeptide isolated by the group of Itokawa and co-workers [Itokawa et al., 1992; Itokawa et al., 1993]. CMX-13-5 produced 3 spots on RP-TLC analysis, signifying the presence of impurities. This has hindered the structure elucidation experiment. Subsequent to our work, our collaborators were able to analyze the structure of the purified bioactive compound in CMX-13' (using material from the same source) and showed that the bioactive compound in CMX-13' was identical to a compound previously identified by Itokawa and co-workers, namely, RA-VII (Figure 3.3.1).

We isolated approximately 600mg of CMX-13' from *RC* employing the same bioassay-guided fractionation procedure for the isolation of CMX-13 (i.e. CMX-13 and CMX-13' were both flash column chromatography fractions). However, CMX-13' showed an immunosuppressive activity of 91.7$\pm$7.1%, which was higher than the immunosuppressive effect of CMX-13, (at 70.9$\pm$14.5%). Chemical experiments revealed that CMX-13' was a less complex mixture than CMX-13 (Figures 3.2.4.1. and 3.2.5.1). The presence of fewer impurities may be the reason for the apparent higher activity of CMX-13' as these would have a direct effect on the concentration of the bioactive compounds. This observed difference in purity was also illustrated by RP-TLC analysis. In the RP-TLC analysis, 6 spots appeared in the CMX-13 sample while CMX-13' produced only 1 spot at R_f=0.4. The spot at R_f=0.4 was seen in both the CMX-13 and CMX-13' samples.

Elucidation of the complete molecular structure of the bioactive compound CMX-13-5 was difficult, mainly because of the complexity of the molecule, persistent impurities and the presence of analogs. We have shown that CMX-13-5 was a bicyclic hexapeptide, and our collaborators have shown that this was identical to RA-VII as previously identified by Itokawa and co-workers (Figure 3.3.1).

Figure 3.3.1 Structure of RA-VII as described by Itokawa and co-workers (Itokawa et al, 1993).

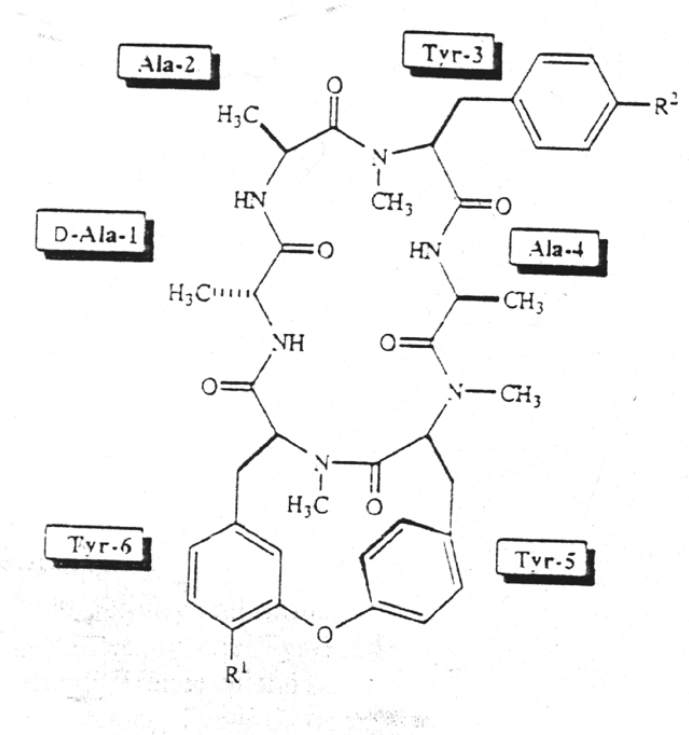

CHAPTER 4 EFFECT OF CMX-13 ON CELL-CYCLE EVENTS AND APOPTOSIS

4.1 INTRODUCTION

Two distinct mechanisms that direct cell death are known: programmed cell death (PCD) and necrosis. The major differences between PCD and necrosis are in the morphological changes, the mechanism and the stimuli that trigger these processes [Searle et al., 1982; Arends et al., 1990; Wyllie, 1986; Wyllie, 1993; Wyllie et al., 1980]. PCD occurs via the apoptotic or paraptotic mechanisms. Apoptosis or physiological cell death [Kerr et al., 1972] is only one of the mechanisms leading to PCD, though it is often equated with PCD. [Schwartz et al., 1993; Sperandio et al., 2000].

Cellular necrosis is a passive process which occurs when cells sustain severe and sudden injury and is referred to as accidental cell death [Searle et al., 1982; Cohen, 1993]. In contrast, apoptosis is an intrinsically programmed active process involving the *de novo* synthesis of proteins. Morphologically, necrosis involves dissolution of DNA (karyolysis), vacuolization and eventual rupture of the plasma membrane resulting in cell lysis, and subsequent induction of the inflammatory process. Apoptosis, on the other hand, involves nuclear fragmentation via the activation of endonucleases secondary to an increase in intracellular calcium, without vacuolization of cytoplasm and formation of apoptotic bodies and hence absence of release of cellular organelles, or elicitation of an inflammatory

process. The distinct morphological changes that occur during necrosis and apoptosis are as illustrated in Figure 4.1.1.

Figure 4.1.1. Morphological changes during apoptosis and necrosis. Shrinkage, blebbing, fragmentation and the formation of apoptotic bodies are significant characteristics of apoptosis. During necrosis, the cell swells followed by breaking down of the cell membrane.

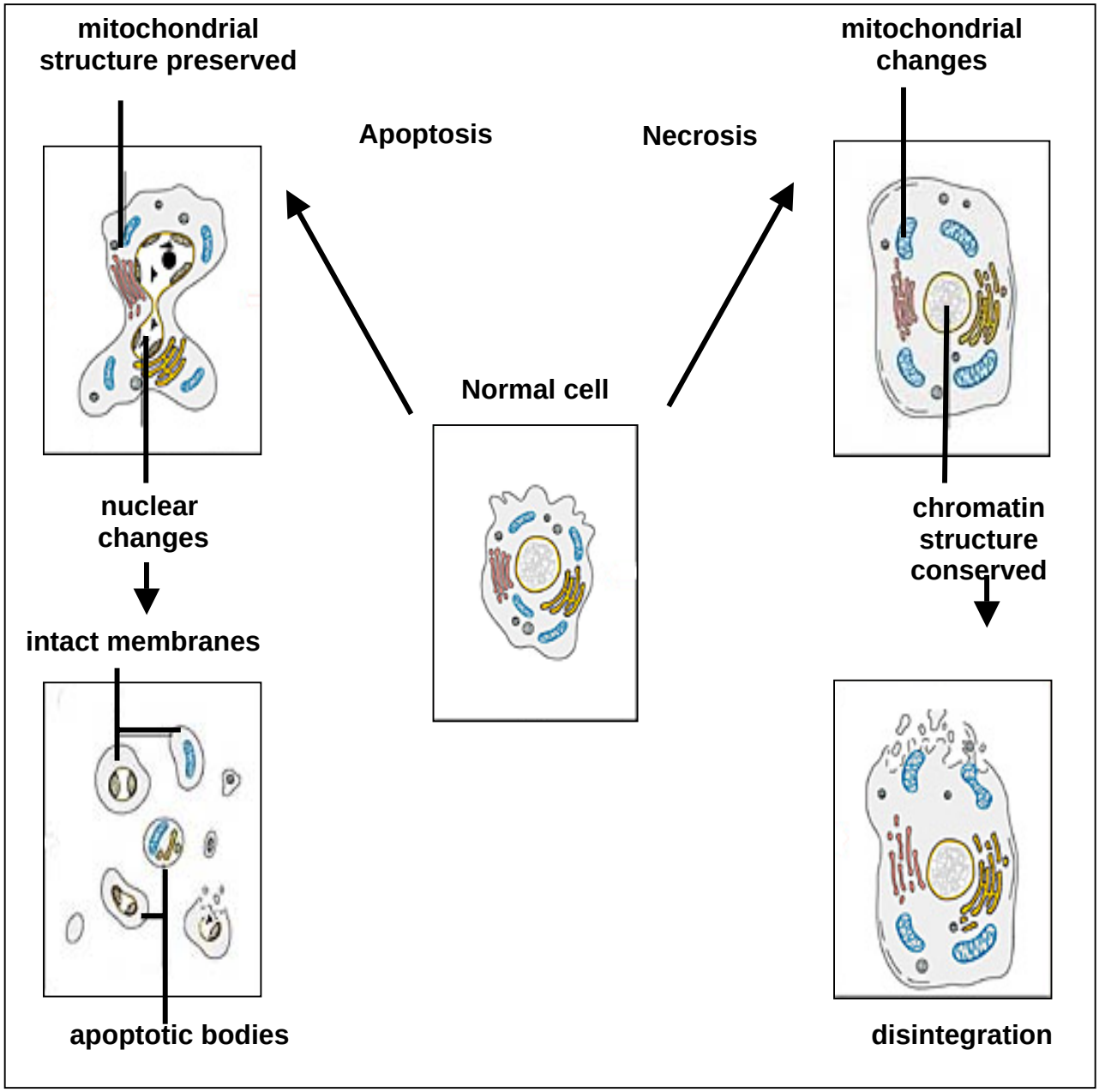

The molecular mechanism of apoptosis is complex, involving different pathways, which overlap. The distinct pathways are tissue-specific and dependent on the stimulus. Several ligand interactions, hormone stimulation, growth deprivation and many other triggers lead to apoptosis [Planey et al., 2000]. Despite the various pathways by which apoptosis is stimulated, a common molecular mechanism is activated. Upon activation of apoptosis a general process occurs in the following sequence:

1) Receptor activation
2) Cytochrome c/Apaf-1 complex formation on the mitochondria [Planey et al., 2000; Yoshida et al., 1998].
3) Decreasing mitochondrial potential is the point of no return for the cell undergoing apoptosis [Bedner et al., 1999].
4) Activation of cysteine proteases that cleave cellular substrates at specific aspartate residues, termed caspases [Alnemri et al., 1996], leading to cleavage of apoptosis-related proteins [Los et al., 1999]. Major differences are found in different cell types and tissues in the pathway of caspase activation [Salvesen et al., 1997].
5) PS exposure due to "flipping" from the inner side of the cell membrane to the outer side [Fadok et al., 1992; Savill et al., 1993].
6) Morphological changes like blebbing of the cell membrane, cytoplasmic compaction, shrinkage of total cellular volume [Bedner et al.,1999].
7) DNA fragmentation and condensation, one of the major hallmarks of apoptosis, is the last process in the apoptotic cells before the

membrane starts to bleb and the vesicles are digested by macrophages [Cohen 1992; Cohen et al 1993].

Apoptosis is important in the development and functions of many biological systems**,** including regulated cell death in the developing embryo [Searle et al., 1982], deletion of autoreactive T-cells clones in the thymus [Shi et al., 1989; Mustelin and Altman, 1993] and senescence of neutrophil polymorphs [Savill et al., 1993]. Additionally, apoptosis of neutrophil polymorphs occur as a response to treatment with physiologically-regulated hormones like glucocorticoids [Wyllie and Morris, 1982; Wyllie et al., 1986; Ashwell et al., 2000; Planey et al., 2000] or as a cellular response to non-physiological stimuli [Raff, 1992].

Apoptosis is pivotal in tissue homeostasis and serves often as a counterbalance to cell proliferation [Los et al., 1999; Piacentini et al., 1993;van Parijs et al., 1998]. Genes involved in apoptosis and cell proliferation are closely linked, as illustrated by the relationship between proto-oncogenes, oncosuppressor genes and caspases [Mountz et al., 1994; Los et al., 2001]. The oncosuppressor gene *p53,* which enhances apoptosis [Talal, 1994; Colombel et al.,1992], operates at different points along the pathway leading to apoptosis [Mountz et al., 1994]. One role of the oncosuppressor gene *p53,* may be to initiate apoptosis by causing cell-cycle arrest at the G_1/S phase in cells expressing *c-myc* [Wyllie, 1993; Yu et al., 1997; Lane, 1992]. The myc protein, derived from the *c-myc* gene, can act as a bivalent regulator, determining either cell proliferation or apoptosis, depending on whether the cell-cycle is supported by growth factors or whether it is limited by

growth factor deprivation or treatment with other agents leading to cell-cycle blockade [Evan et al., 1992]. *In-vivo, c-myc* expression has been proposed to be associated with a "high turnover" state where both cell proliferation and apoptosis co-exist [Wyllie, 1993]. Other oncogenes, such as *bcl-2*, inhibit apoptosis, converting this "high turnover" state into rapid population expansion [Terui et al., 1995; Reed et al., 1992; Mazel et al., 1996]. Recently, caspases have been found to be involved not only in the process of apoptosis itself, but also in the control of cell cycle progession [Los et al., 2001].

In the immune system, apoptosis occurs during the development of lymphocytes and is also important in the regulation of normal immune responses [van Parijs et al., 1998]. Immature T-cells that recognize autoantigens are removed in the thymus via two main selective processes, namely negative selection and positive selection. Negative selection is an apoptotic process responsible for the elimination of $CD4^{-}CD8^{-}$ cells in the mouse thymus [Nikolic-Zugic, 1991; Pircher et al., 1989; Shi et al., 1989; Mustelin et al., 1993]. Positive selection of T-cells involve the selection of immature T-cells which interact with the MHC expressed in the thymus, and only those T-cells which attach to this ligand are selected, and survive [Sha et al., 1988]. T-cells that escape negative selection populate the periphery. The failure of these T-cells to undergo negative selection and consequently apoptosis, may be related to the low affinity for the MHC complex [Guerder et al., 1996]. In both humans and animal models of autoimmunity, defective apoptotic mechanisms in the immune system may have a role in the genesis of disease [Mountz et al., 1994; Emlen et al., 1994]. The oncogenes *p53,*

bcl-2 [Reap et al., 1995] and *c-myc* have all been found to be abnormally expressed in animal models of autoimmunity [Mountz et al., 1994].

Mutations in the Fas cell surface (death) receptor, the FasL [Watanabe et al., 1992; Reap et al., 1995] and the anti-apoptotic *bcl-2* genes [Kroemer, 1997], have been linked to the development of lupus-like systemic autoimmune disease in mice and some humans. In lymphocytes, Fas, FasL [Sakata, et al 1998a] and bcl-2 molecules regulate two distinct apoptotic pathways [van Parijs et el, 1998; Strasser, 1995]. Fas/APO-1 (CD95) is a cell surface molecule belonging to the TNF superfamily and induces apoptosis in several cell lines [Sakata, et al 1998b], including lymphocytes [Strasser et al., 1991]. FasL is a type II transmembrane protein predominantly expressed on activated CD8 and CD4 Th1 T-cell subsets. In normal situations, autoreactive T-cells are eliminated in the germinal centers of secondary lymphoid organs via the Fas-FasL apoptotic pathway, resulting in immune tolerance [Nagata and Suda, 1995; Singer et al., 1994; van Parijs et al., 1998]. Defects in either *Fas* or *FasL* result in acceleration of murine lupus-like diseases. In humans two mutations in the *Fas* gene [Fisher et al., 1995; Rieux-Laucat et al., 1995; Rathmell et al., 1995] and the *FasL* gene [Wu et al., 1996;Vaishnaw et al., 1999a; Vaishnaw et al., 1999b] have been found in patients with autoimmune lymphoproliferative syndrome, however mutations in *Fas* or *FasL* have not been found in all patients with SLE, neither has there been any consistent finding of a defect in the expression or function of the receptor in most patients [Mysler et al., 1994].

One of the current hypotheses for the occurrence of SLE in humans is based on the finding of high levels of sFas in the serum of SLE patients [Rose et al., 1997; van der Linden et al., 2001; Sato et al., 2000]. sFas is a variant of the receptor molecule which lacks the transmembrane segment. Binding of sFas to FasL blocks the interaction of FasL with the Fas antigen, inhibiting apoptosis of auto-reactive lymphocytes [Cheng et al., 1994; Cheng et al., 1996; Papo et al., 1998]. The surviving $CD4^+$ lymphocyte subset becomes the driving force for stimulation of B-cell hyperreactivity. These B cells produce IgG autoantibody, leading to autoantibody-mediated responses [Kotzin, 1996; Suda and Nagata, 1997]. The proposed molecular mechanism is depicted in Figure 4.1.2.

However, this hypothesis is still controversial, as not all studies were able to demonstrate the relationship between inhibition of the Fas-FasL pathway and apoptosis in patients with SLE [Nozawa et al., 1997; Suda and Nagata, 1997]. In fact, several studies have shown that the Fas-FasL pathway of apoptosis was not defective in the lymphocytes of SLE patients [McNally et al., 1997; Carrichio et al., 1999]. On the contrary, accelerated *in-vitro* apoptosis of SLE lymphocytes have been described [Emlen et al., 1994; Lorenz et al., 1997; Perniok et al., 1998; Courtney et al., 1998].

Figure 4.1.2. Blockade of the Fas apoptosis pathway by sFas results in SLE. In normal healthy individuals, apoptosis is triggered by binding of FasL to Fas antigen. In SLE, the Fas apoptosis pathway is inhibited following binding of sFas to FasL, preventing the interaction between Fas and FasL.

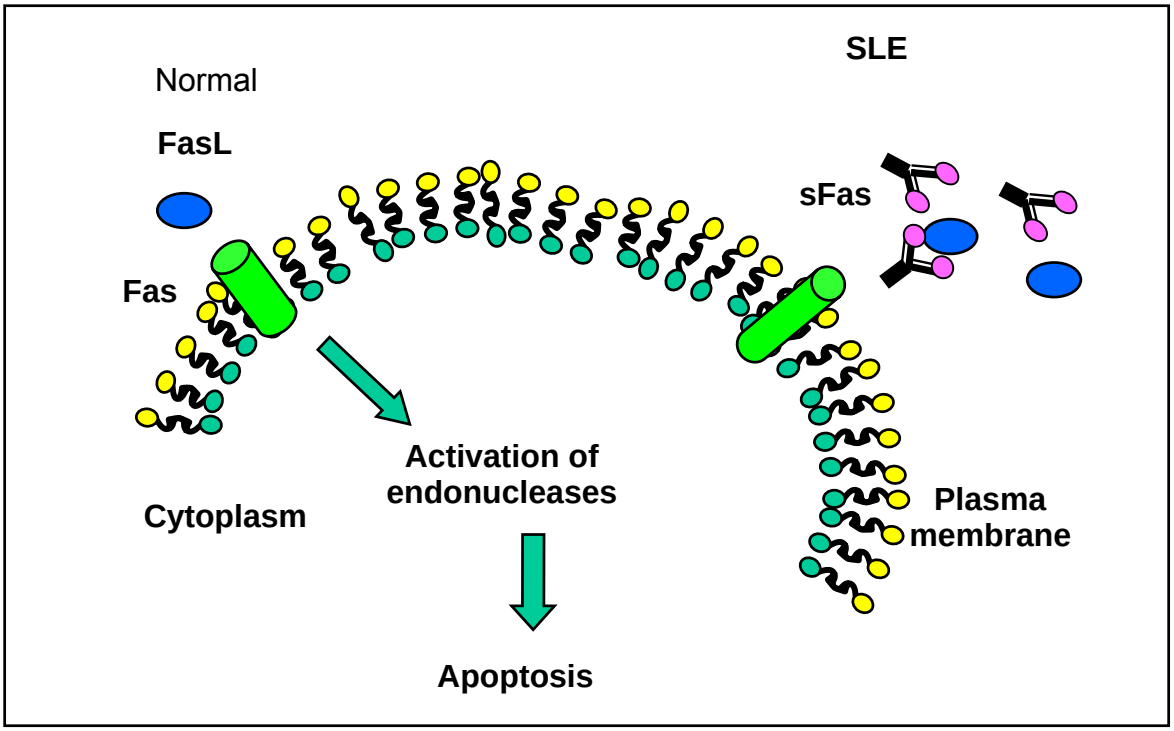

However, there has not been consistent evidence of upregulation of apoptotic genes in PBMCs of SLE patients. On the other hand, increase in the expression of the anti-apoptotic *bcl-2* gene has been demonstrated in autoimmune murine models [Strasser et al., 1991]. Additionally, increase in lymphocyte Fas and intracellular bcl-2 expression, as well as serum sFas have been observed in SLE patients [Graninger et al., 2000; Mehrian et al., 1998; Aringer et al., 1994; Lorenz et al., 1997], suggesting that there is a block in the apoptotic mechanism in the PBMCs of SLE patients. In fact, current therapy for SLE patients includes the use of immunosuppressive drugs that induce apoptosis [Amano et al., 2000; Dooley et al., 1998; Steinberg, 1994], demonstrating that restoration of the apoptotic

mechanism in the PBMCs of SLE patients may be effective as a form of therapy [Sakata et al., 1998a; Seki et al., 1998].

We have previously shown that CMX-13 was able to suppress PHA-stimulated lymphoproliferative responses and immunoglobulin production, inhibit the expression of T-cell activation markers CD25 and HLA-DR [Yap et al., 1993], as well as inhibit T-cell colony formation [Yap et al., 1998; Yap et al., 1999]. In our earlier studies on the possible mechanisms of action, CMX-13 did not show any inhibitory effects on IL-2 and IFN-γ mRNA expression, suggesting that its mechanism of action is different from that of cyclosporine [Zuo et al., 2000]. As there is strong evidence that dysregulation of apoptosis in the immune regulatory cells could have a role in the genesis of SLE, this chapter examined the effect of CMX-13 on:

1) Cell proliferation in Jurkat cells, a human leukaemic $CD4^+CD8^-$ T-cell line;
2) Cell cycle progression in Jurkat cells, and PBMCs isolated from 20 SLE patients and age/sex-matched normal healthy controls;
3) Apoptotic events in both Jurkat cells, and PBMCs derived from SLE patients and normal controls, using Annexin-V and DNA fragmentation assays.

4.2 RESULTS

4.2.1 Inhibition of Jurkat Cell Proliferation by CMX-13

Jurkat cells are derived from a human leukaemic $CD4^+CD8^-$ T-cell line, and exhibit spontaneous cell proliferation without the need for mitogenic stimulation. Jurkat cells were cultured with and without 0.004% v/v DMSO, the solvent for CMX-13, as the negative control. CMX-13 was added in concentrations of 1, 2, 4 and 8 μg/ml to determine the effect on cell proliferation. Cell proliferation was measured by [^{3}H]-thymidine incorporation [Morsaki et al., 1992; Morsaki et al**.,** 1994; Covas et al., 1996]. Cell viability, as measured by trypan blue exclusion, was greater than 90% in all experiments.

The effect of serial dilutions of CMX-13 on Jurkat cell proliferation is illustrated in Table 4.2.1.1. CMX-13 was found to significantly inhibit Jurkat cell proliferation (99.5 to 99.9%) in all the dilutions tested (1, 2, 4, 8 μg/ml). The solvent, DMSO, did not have any effect on Jurkat cell proliferation. As cell viability remained greater than 90% for all CMX concentrations, the concentration of 4 μg/ml was selected to perform the subsequent experiments on Jurkat cell proliferation, cell-cycle progression and apoptosis.

Table 4.2.1.1 Effect of serial dilutions of CMX-13 on Jurkat cell proliferation (triplicate experiments).

Treatment	Cell Proliferation (cpm)	% Inhibition of Cell Proliferation	% Cell Viability
Jurkat cells in R10	131227 ± 5674		>90
DMSO	128396 ± 2864	2.2 ± 0.0	>90
8 μg/ml CMX-13	67 ± 11	99.9 ± 0.0	>90
4 μg/ml CMX-13	811 ± 7	99.9 ± 0.0	>90
2 μg/ml CMX-13	156 ± 84	99.9 ± 0.0	>90
1 μg/ml CMX-13	598 ± 187	99.5 ± 0.1	>90

4.2.2 Effect of CMX-13 on Cell-Cycle Progression in Jurkat cells and PBMCs

The effect of CMX-13 on cell-cycle progression was studied in Jurkat cells and PBMCs isolated from both normal controls and SLE patients using flow cytometric analysis of the nuclear DNA contents following PI staining. Jurkat cells were treated with 0.004% DMSO (solvent for CMX-13 as the negative control), 4 μg/ml CMX-13 and CH a known apoptosis-inducer [Davidoff et al., 1992; Gong et al., 1993; Dhein et al., 1995] for 24 hrs in cell culture medium and analyzed by flow cytometry for DNA content following PI staining. Jurkat cells treated with DMSO had a normal cell-cycle pattern, with the following distribution pattern: 57.0±5.5% in G_0/G_1 and 34.0±6.7% in the S phase. Cells treated with CMX-13 and CH had a markedly increased population in the "sub-G_1" area, a distinct hypo-diploid cell population consisting of apoptotic cells. The cell population in the G_0/G_1 phase decreased when treated with CMX-13 (35.7±5.39%) or CH (31.6±16.9%), as compared to the Jurkat cells cultured in DMSO (57.0.±5.5%) ($p<0.001$). An increase of cells in the "sub-G_1" or apoptotic phase were evident in cells treated with CMX (33.7±4.3%) and CH (54.6±17.9%) as compared to the DMSO-treated cells (7.4±9.0%) ($p<0.02$) (Figure 4.2.2.1). Unlike the CH-treated cells where the increase in the apoptotic fraction was associated with cell cycle arrest in the G_0/G_1 phase, CMX-13 did not result in an inhibition of cell-cycle progression (Table 4.2.2.1).

Figure 4.2.2.1 Representative DNA distribution histograms of Jurkat cells incubated with DMSO, CMX-13 and CH for 24 hrs. The cells incubated with DMSO had a normal cell-cycle pattern with very few apoptotic cells, whereas following treatment with CMX-13 or CH, a "sub-G1" peak consisting of apoptotic cells, became visible.

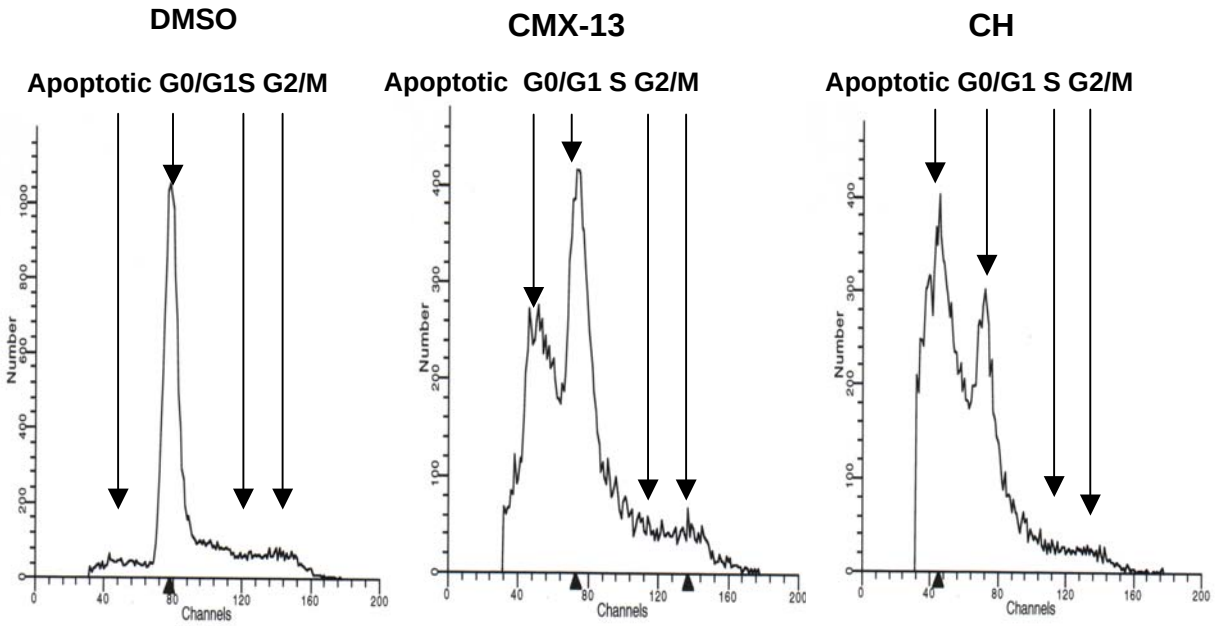

Table 4.2.2.1 Jurkat cells incubated with DMSO, CMX-13 and CH in different phase of the cell-cycle. CMX-13 and CH induced apoptosis in Jurkat cells after 24 hours incubation.

Treatment	Apoptosis (Sub-G_1) (%)	G_0/G_1 (%)	S (%)	G_2/M (%)
DMSO (0.004%)	7.4 ± 9.0	57.0 ± 5.5	34.0 ± 6.7	1.4 ± 1.9
CMX-13 (4 μg/ml)	33.7± 4.3*	35.9 ± 5.9#	27.7 ± 8.0	2.4 ± 2.4
CH (1.4 mg/ml)	54.6 ± 17.9*	31.6 ± 16.9#	12.8 ± 10.5	0.8 ± 1.5

*Comparing to DMSO-treated cells (negative control), p<0.02
#Comparing to DMSO-treated cells (negative control), p<0.001

The effect of CMX-13 on PBMCs stimulated with 0.5 μg/ml PHA was studied after culture for 72 hours in the following conditions: PHA control, control with DMSO 0.004% (solvent for CMX-13), CMX-13 at dilutions of 4.0 μg/ml and 2.0 μg/ml and CsA 2 μg/ml and 0.078 μg/ml. A negative control consisting of unstimulated PBMCs was also included. The cells were subsequently stained with PI for analysis by flow cytometry, and the percentages of cells at the G_0/G_1, G_2/M and S phases were determined. Nearly all (99.8%±0.30) of the unstimulated PBMCs remained in the G_0/G_1 phase (Figure 4.2.2.2). Table 4.2.2.2 shows the effect of CMX-13 and CsA on the percentages of cells (mean±SD) in the different phases of the cell-cycle. The apoptotic populations in these cell cultures were low.

PHA stimulation of PBMC (DMSO control) resulted in an 18.4% decrease in the percentage of cells in the G_0/G_1 phase, with a shift to the G_2/M and S phases (Figure 4.2.2.2). Addition of CMX-13 in both concentrations resulted in a complete inhibition of cell-cycle progression, similar to CsA at 2 μg/ml (Figure 4.2.2.3). Hence these results suggest that the immunosuppressive effect of CMX-13 could be related to negative regulation of cell-cycle progression.

Table 4.2.2.2 Effect of CMX-13 on PHA-stimulated PBMCs. Data expressed as percentage of cells in each cell cycle phase.

Cell Culture	G_0/G_1 (%)	G_2/M (%)	S (%)
PBMC	98.9 ± 0.3	0.5 ± 0.04	0.6 ± 0.3
PBMC+PHA+ DMSO	80.5 ± 11.0*	3.5 ± 2.5*	16.0 ± 8.9*
PBMC+PHA+ CMX-13 (4.0 μg/ml)	99.5 ± 0.1*	0.3 ± 0.2*	0.2 ± 0.03*
PBMC+PHA+ CMX-13 (2.0 μg/ml)	99.2 ± 0.20*	0.6 ± 0.2*	0.2 ± 0.07*
PBMC+PHA+ CsA (2.0 μg/ml)	96.0 ± 1.5*	0.8 ± 0.4*	3.2 ± 1.4*
PBMC+PHA+ CsA (0.078 μg/ml)	86.9 ± 8.8	2.8 ± 2.3	10.3 ± 6.5

*p<0.05 compared to PBMC+PHA+ DMSO.

Figure 4.2.2.2. DNA distribution histograms of cell-cycle progression in unstimulated and PHA-stimulated PBMCs. Most of the unstimulated PBMCs remained in the G_0/G_1 phase, whereas PHA-stimulated PBMCs had a typical cell-cyle progression pattern.

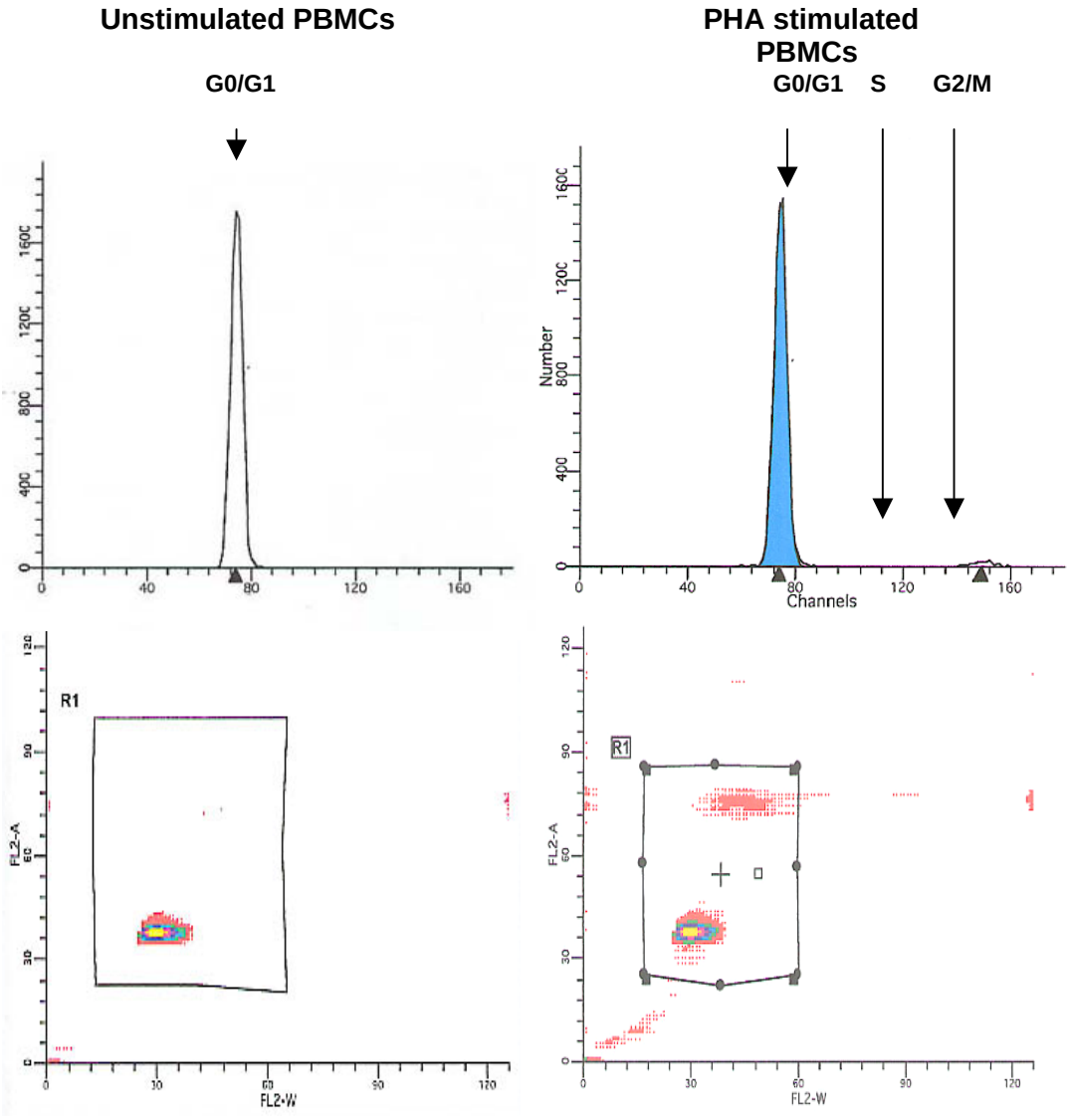

Figure 4.2.2.3. DNA distribution histograms of cell-cycle progression in PHA-stimulated PBMCs with CMX-13 and CsA. Complete inhibition of cell-cycle progression occurred following CMX-13 and CsA treatment.

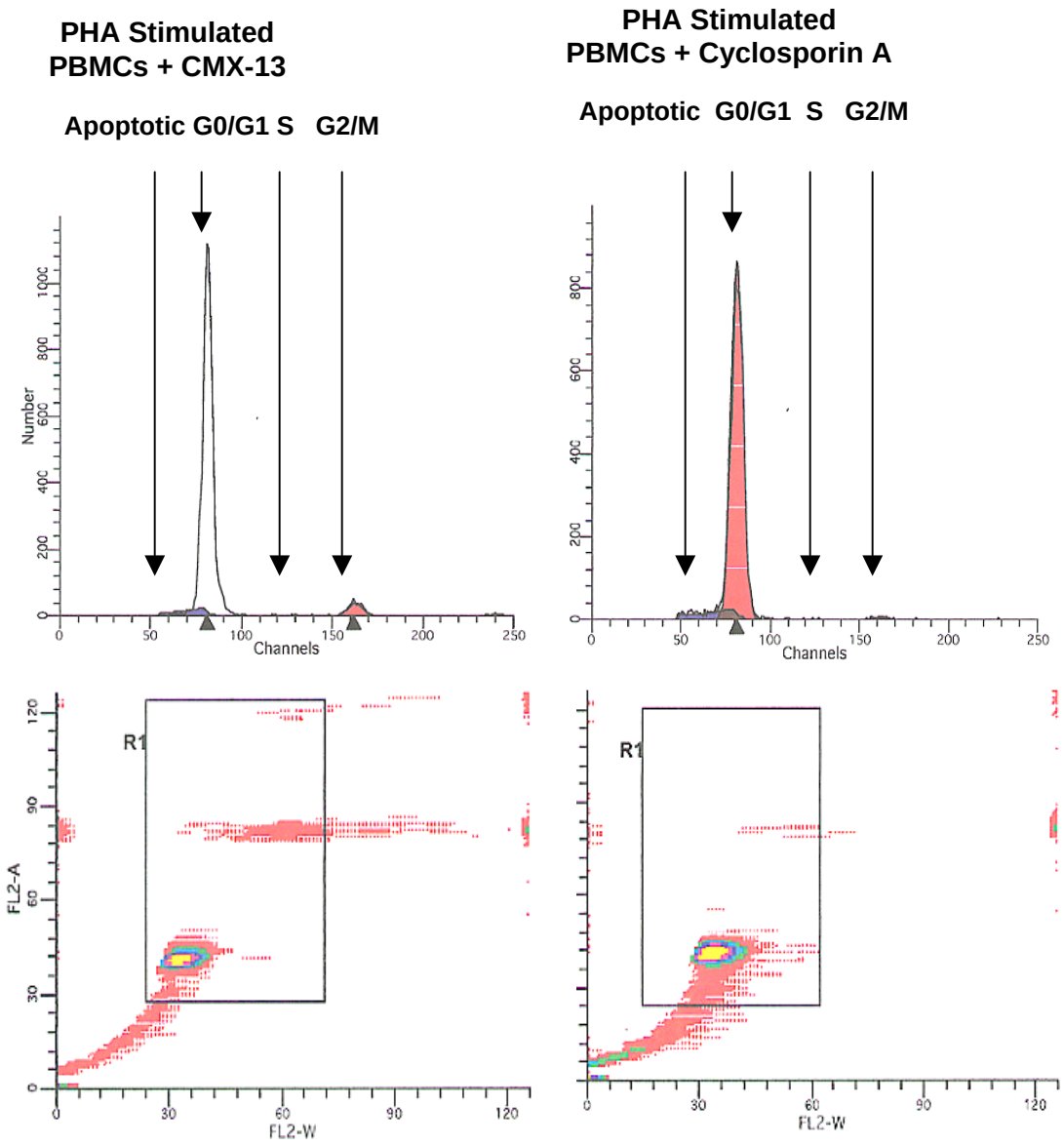

4.2.3 Effect of CMX-13 on DNA Fragmentation in Jurkat cells and PBMCs

The major biochemical hallmark of apoptotic cell death is the cleavage of chromosomal DNA at inter-nucleosomal sites into fragments or multiples of about 180 bp by endonucleases [Arends et al., 1990; Cohen 1993; Bedner et al., 1999]. This phenomenon causes the hypodiplod peak in the DNA histograms of the cell-cycle progression analysis. Another method of studying DNA fragmentation is by extracting the fragmented DNA and subjecting it to gel electrophoresis.

Jurkat cells were treated with 0.004% DMSO, 4 μg/ml CMX-13 and 1.4 mg/ml CH for 4, 6, and 8 hours. DNA fragmented bands appeared after 4 hours of treatment with CMX-13 and CH. This phenomenon was not observed in the DMSO cells at all the time points studied as shown in Figure 4.2.3.1**.** The appearance of the DNA ladder indicated that CMX-13 induces apoptosis as early as 4 hours.

Similarly PBMCs from 3 healthy individuals were incubated for 24 hrs with 0.004% DMSO, 4 μg/ml CMX-13 and 1.4 mg/ml CH. DNA fragmented bands appeared after treatment with CMX-13 and CH as shown in Figure 4.2.3.2. This phenomenon was not observed in the DMSO-treated cells. Hence CMX-13 also induced apoptosis in PBMCs.

Figure 4.2.3.1. DNA fragmentation of Jurkat cells after incubation with CH and CMX-13 for 0, 4, 6 and 8 hours. Fragments in the treated cells occurred after 4 hours incubation.

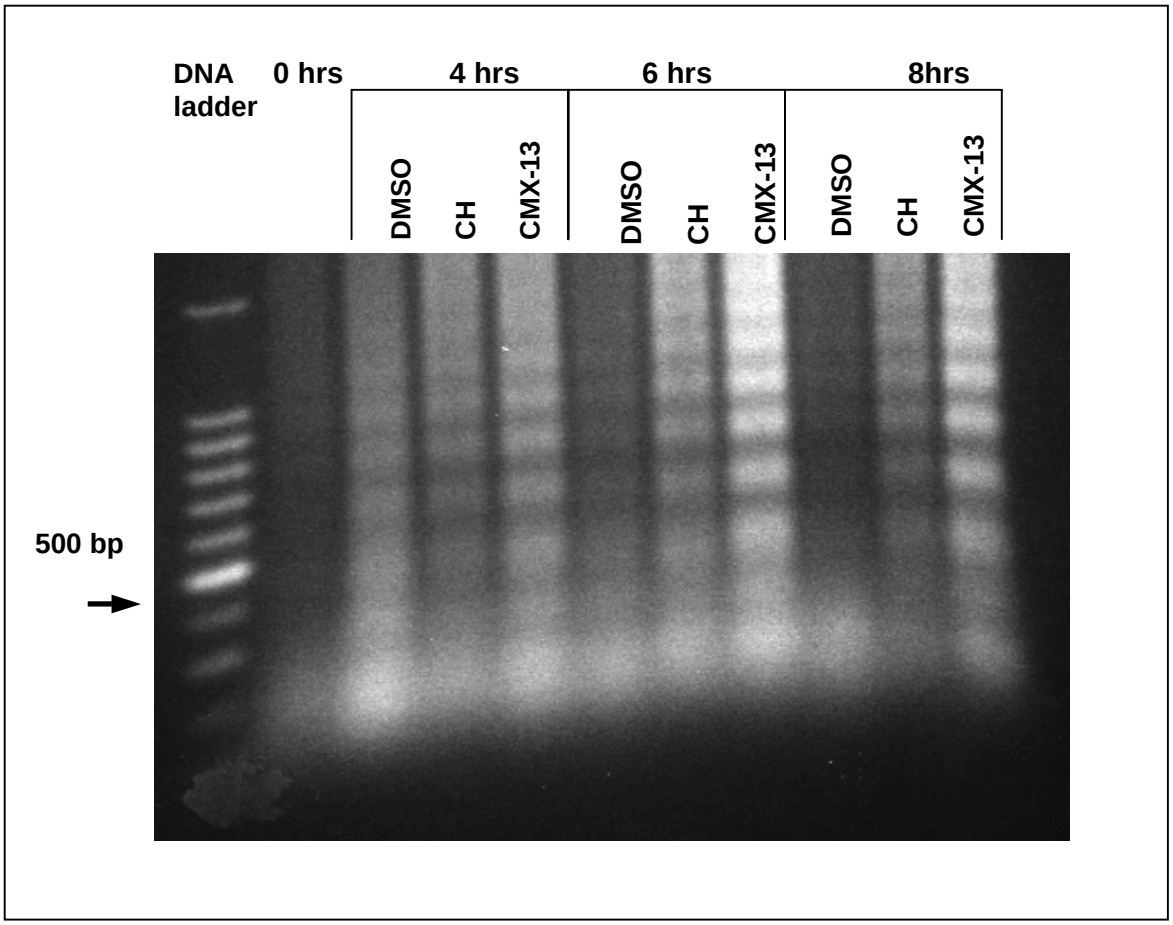

Figure 4.2.3.2. DNA fragmentation of PBMCs after incubation with CH and CMX-13 for 24 hours. DNA fragmentation was observed after CMX-13 and CH treatment.

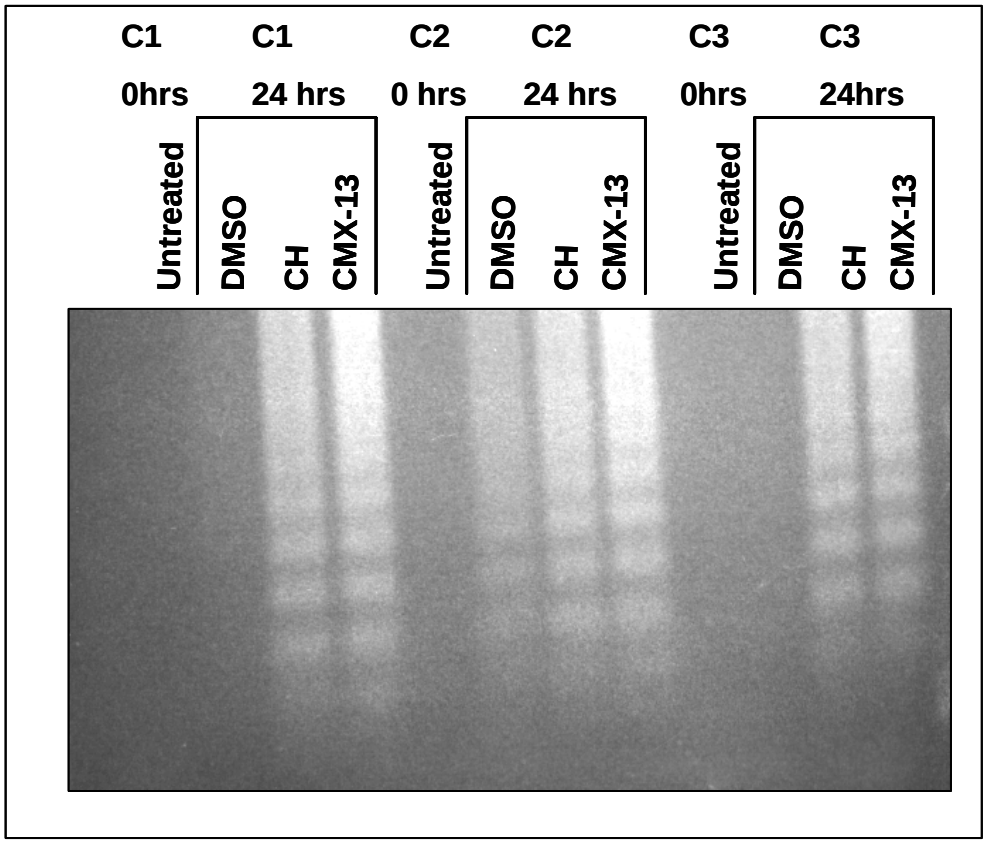

4.2.4 Effect of CMX-13 on PS Exposure in Jurkat cells

Jurkat cells were treated with 0.004% DMSO, 4 μg/ml CMX-13 and 1.4 mg/ml CH for 8 and 24 hours and stained with Annexin-V FITC and PI. Figure 4.2.4.1 shows the results of the flow cytometric analysis of Jurkat cells following Annexin V-FITC and PI staining in a representative experiment. The cells were gated (R1 and R2) as shown in the upper panel. In the lower panel, the lower left quadrant shows the viable cells (mainly R1), which were FITC negative/ PI negative. The lower right quadrant represents the early apoptotic cells (FITC positive/PI negative, R1 and R2). The upper right quadrant represents the late apoptotic cells (FITC positive and PI positive, mainly R2). The percentage of total apoptotic cells was given by the formula:

$$\frac{\text{Cells in the Lower Right Quadrant + Upper Right Quadrant}}{\text{Total Gated Cells in R1 and R2}}$$

Figure 4.2.4.1. Apoptosis of Jurkat Cells induced by CH and CMX-13 after 24-hour culture (representative experiment). Flow cytometric analysis of Jurkat cells following Annexin V-FITC and PI staining. The upper panels show the dot plots of the gated cells (R1 and R2) where the cell debris and necrotic cells were excluded based on FSC and SSC. An increase of apoptotic cells occurred following treatment with CH (96.0%) and CMX-3 (89.3%), as compared DMSO (40.0%).

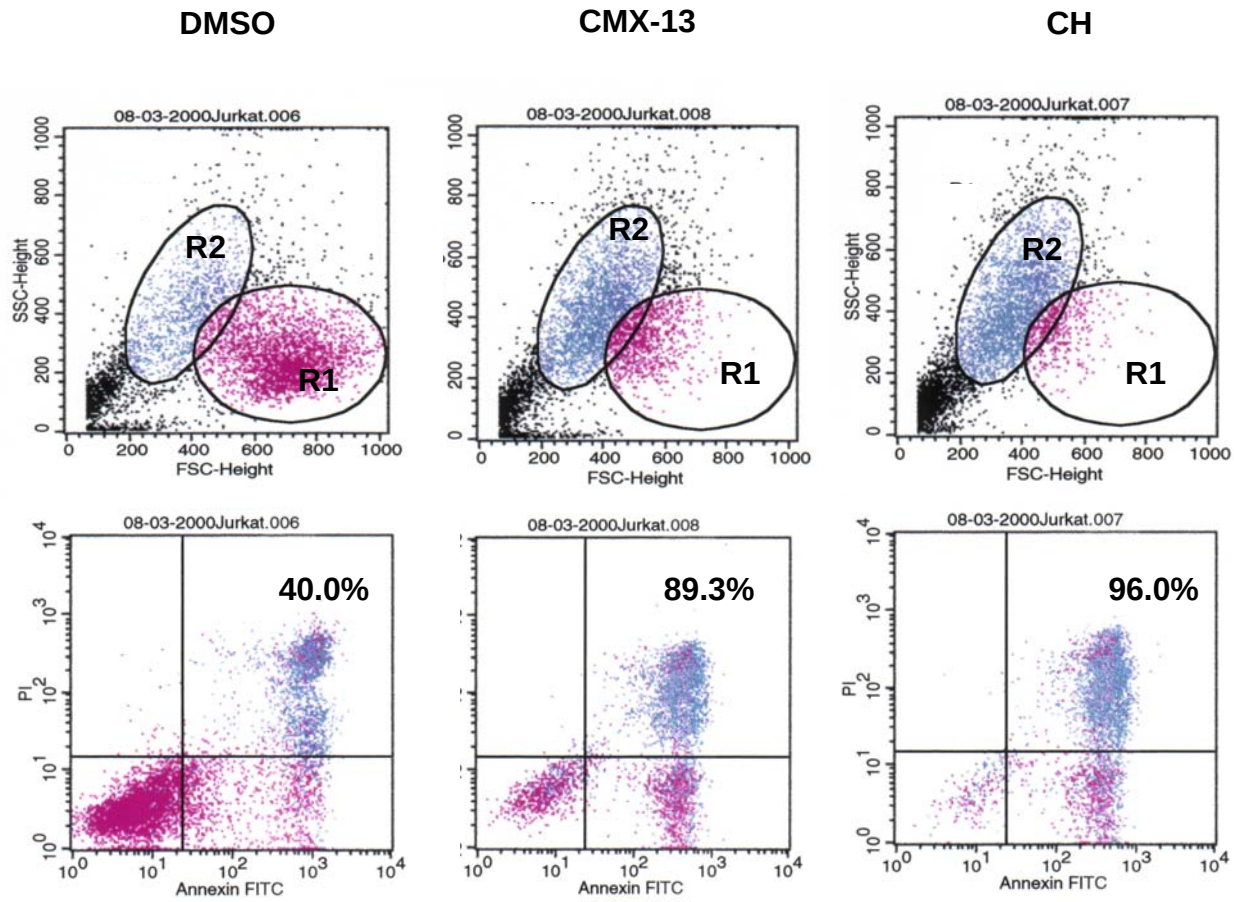

Figure 4.2.4.2 shows the increase in the percentage of apoptotic population after 8 and 24 hours of treatment. After 8 hours of incubation with 0.004% DMSO, the spontaneous apoptotic cell population was 21.3±2.9%, whereas treatment with 1.4 mg/ml CH resulted in a significant shift of the apoptotic population to 68.0±0.0% ($p<0.04$). A similar population shift was caused by CMX-13 treatment with increase of the apoptotic population to 53.0±9.5% ($p<0.05$). The apoptotic population increased significantly when treated for 24 hours: DMSO-treated cells 40.1±2.1%; CMX-13-treated cells 89.3±1.2% ($p<0.005$); CH-treated cells 96.0±0.0% ($p<0.04$).

Figure 4.2.4.2 Percentage of apoptotic cells after 8 and 24-hour cultures, as determined by Annexin V-FITC and PI-staining of Jurkat cells following incubation with 4 μg/ml CMX-13 and 1.4 mg/ml CH. Significant increase of apoptotic cells after 8 and 24 hours incubation with CMX-13 and CH compared to DMSO ($p<0.05$).

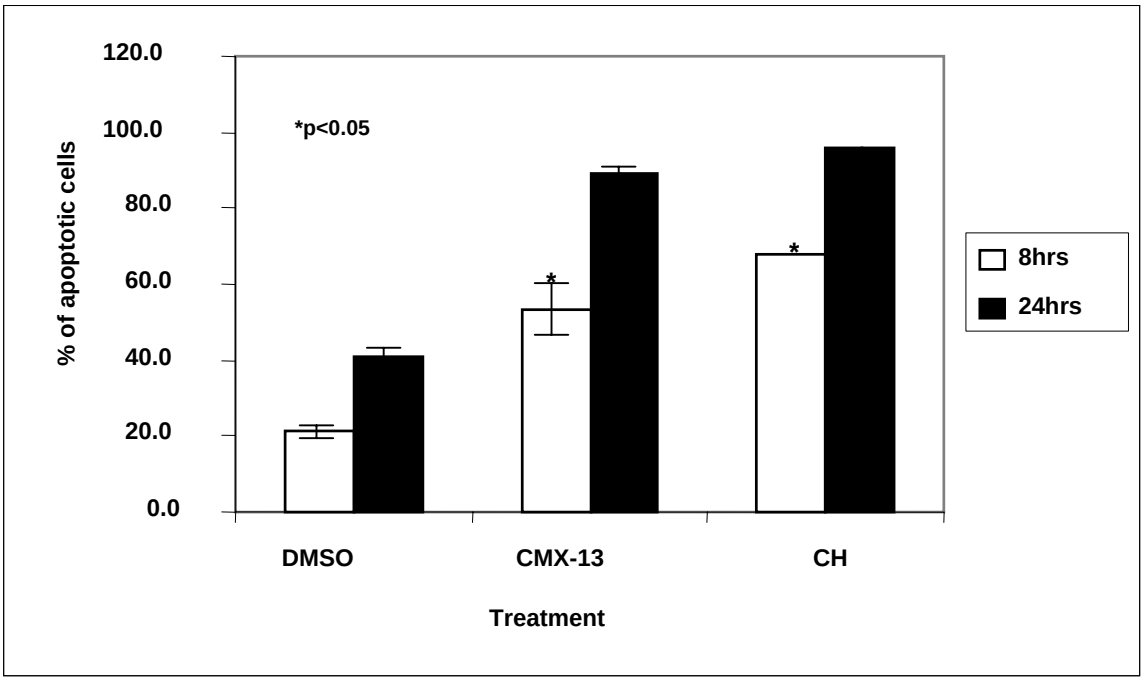

4.2.5 Apoptosis induced by CMX-13 in PBMC of SLE patients.

PBMCs were obtained from 20 SLE patients who fulfilled the criteria for SLE as defined by the American College of Rheumatology [Tan et al., 1982]. Disease activity in these patients were scored using two clinical scoring systems, SLE-Disease Activity Index (SLEDAI) [Bombardier et al, 1992] and Systemic Lupus International Collaborating Clinics (SLICC) [Gladman et al, 1996]. In this group of 20 patients, 8 (40%) had SLEDAI scores of > 2 and 5 (25%) had SLICC scores of > 2. The individualized scores are listed in Appendices 4.1 and the SLICC and SLEDAI score in Appendix 4.2 and 4.3, respectively.

As all of the SLE patients were on prednisolone as maintenance treatment, a dose-response experiment was conducted to examine the apoptotic effect of DEX on PBMCs in culture. Freshly isolated PBMCs from 3 normal controls were incubated with DEX at different concentrations (1000 μg/ml, 500 μg/ml, 100 μg/ml, 5 μg/ml, 1.0 μg/ml, 0.5 μg/ml) for 24 hours, following which the percent apoptotic cells were measured by Annexin-V/PI staining. The results are summarized in Table 4.2.5.1.

Table 4.2.5.1 Apoptosis induced by DEX in PBMCs derived from healthy controls.

Treatment	Experiment 1	Experiment 2	Experiment 3	Mean ± SD	p value
Untreated	13.82	12.8	17.8	14.81±2.6	.011
CH	53.4	70.33	66.28	63.33±8.8	.172
1000 μg/ml DEX	14.9	24.16	23.79	17.8±5.0	.376
500 μg/ml DEX	11.95	17.67	22.18	16.08±3.89	.054
100 μg/ml DEX	20.59	15.89	25.52	17.7±4.72	.097
5 μg/ml DEX	20.1	14.69	21.26	16.7±3.5	.165
1 μg/ml DEX	14.0	15.21	19.37	15.5±2.55	.170
0.5 μg/ml DEX	14.08	17.22	23.46	16.5±3.9	.889
0.004% DMSO	9.6	10.21	22.33	14.4±7.8	.501

The percent of apoptotic cells was increased in DEX-treated PBMCs at a concentration of 1000 μg/ml (17.8±5.0%). Although this was higher than Untreated PBMCs cultured in media (14.8±2.6%) or DMSO-treated cells (solvent control) (14.4±7.8), however this did not reach statistical significance. There was also no difference in percent apoptotic cells induced with the varying concentrations of DEX. The dose-response curve is shown in Figure 4.2.5.1. On the other hand, the positive control, CH, at a concentration of 1.4 mg/ml induced apoptosis significantly (63.3±8.8%) when compared to the Untreated and DMSO-treated PBMCs ($p<0.02$).

Figure 4.2.5.1 Effect of DEX on apoptosis in PBMCs. PBMC from 3 healthy individuals were treated with 1000 μg/ml, 500 μg/ml, 100 μg/ml, 5 μg/ml, 1 μg/ml, 0.5 μg/ml. CH at a concentration of 1.4 mg/ml was used as a positive control. DMSO at at concentration of 0.004% was used a vehicle control for CMX-13.

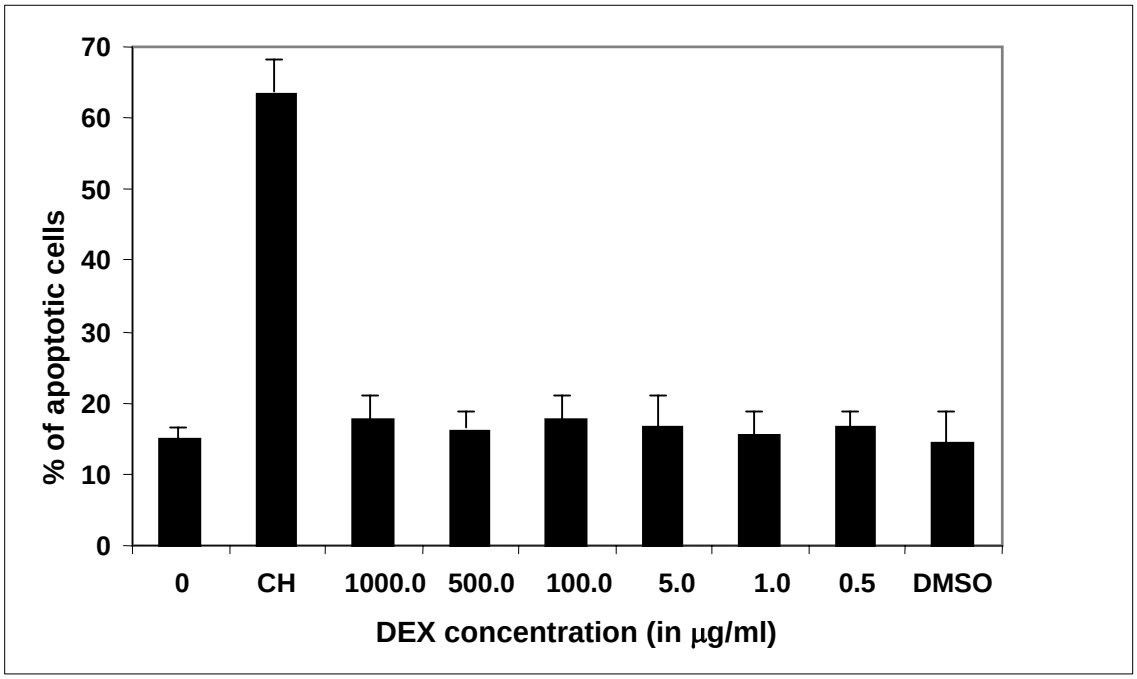

In separate experiments to compare the effect of CMX-13 on PBMCs from normal controls and SLE patients, PBMCs from the SLE patients were treated with 0.004% DMSO, 4 μg/ml CMX-13 and 1.4 mg/ml CH for 24 hours and analyzed for apoptosis using flow cytometric analysis following Annexin-v FITC/PI staining. PBMCs were also obtained from normal healthy age/sex-matched controls, and treated with 0.004% DMSO, 4 μg/ml CMX-13, 1.4 mg/ml CH, 0.5 mg/ml DEX [Seki et al., 1998; Potter et al., 1999] and a combination of: 0.5 mg/ml DEX and 4 μg/ml CMX-13. The DEX treatment in the control groups was included in order to take into consideration any possible effects corticosteroids may have on apoptosis, as all the patients with SLE were on PNL.

Figure 4.2.5.2 shows representative flow cytometric histograms of PBMCs from a normal control. In the lower panel, the percentage of cells in the early and late apoptotic stages is shown. A significant increase of the total apoptotic population occurred when the cells were treated with CH (72.1±12.3%) or CMX-13 (51.1±14.1%) compared to the DMSO-treated cells (37.3±20.5%) ($p<0.05$). The DEX-treated cells (38.2±16.7%) did not exhibit an increase of the apoptotic population compared to the DMSO group (37.3±20.5%). The combination of 4 μg/ml CMX-13 and 0.5mg/ml DEX did increase the apoptotic population slightly (44.3±16.0%), but was not statistically significant.

Figure 4.2.5.2 Representative flow cytometric histograms of PBMCs from a normal control. Percent spontaneous apoptotic cell population incubated with DMSO was 37%. Increase of the apoptotic population was observed following treatment with CMX-13 (51%) and CH (72%) for 24 hours as shown in the lower panel.

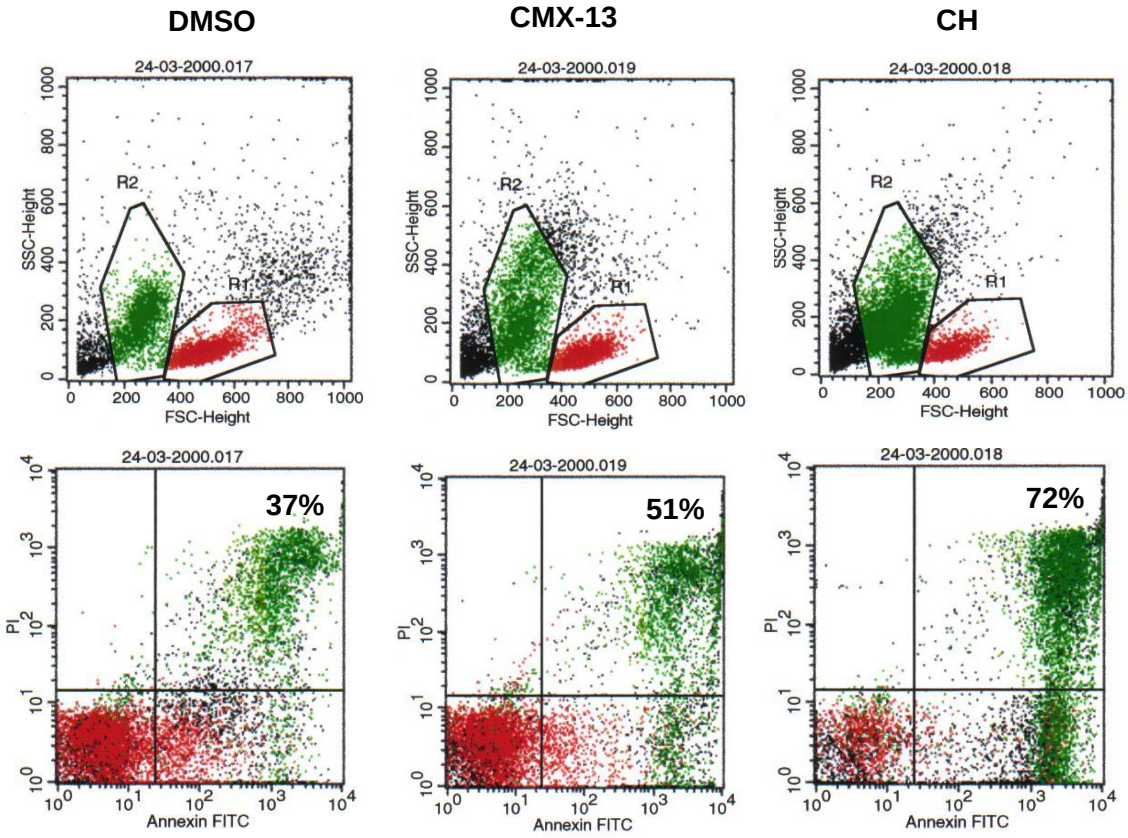

Figure 4.2.5.3 shows the representative flow cytometric histograms of the PBMCs from a SLE patient. In the cells incubated with DMSO, the spontaneous apoptotic population was 31.8±15.0%, whereas following incubation with CH and CMX-13, the apoptotic population increased to 63.2±21.0% and 44.3±15.7% respectively ($p<0.05$).

Figure 4.2.5.3 Representative flow cytometric histograms of PBMCs from a SLE patient. Percent spontaneous apoptotic cell population incubated with DMSO was 32%. Increase of the apoptotic population was observed following treatment with CMX-13 (44%) and CH (63%) for 24 hours as shown in the lower panel.

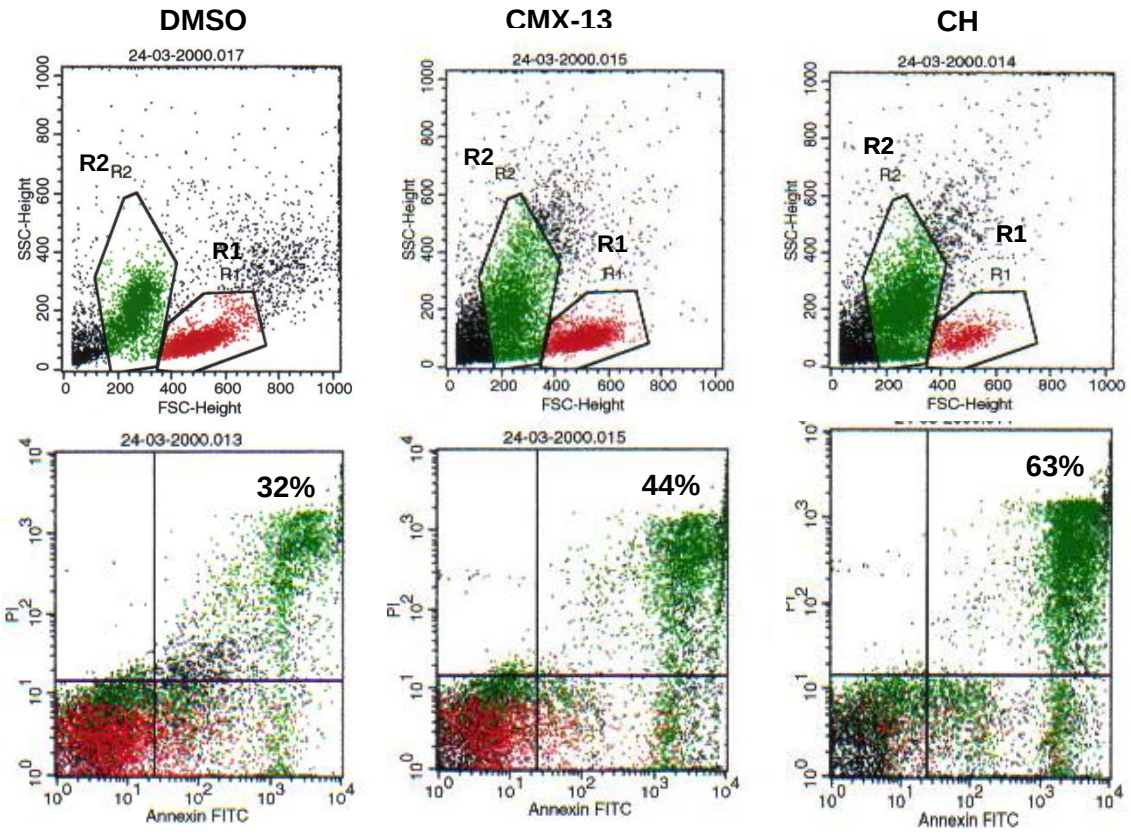

The mean percentages of apoptotic cells following incubation with CMX-13 or CH comparing with DMSO, the solvent control, are summarized in Table 4.2.5.2

Table 4.2.5.2 Percentage of apoptotic PBMCs in 20 SLE patients and age/sex-matched healthy controls after treatment with CMX-13. Values are expressed as mean±SD. *p<0.05 compared to DMSO, the solvent control.

PBMC treatment	Control (n=20)	SLE (n=20)
DMSO	37.3±20.5	31.8±15.0
CMX-13	51.1±14.1*	44.3±15.7*
CH	72.1±12.3*	63.2±21.0*
DEX	38.2±16.7	
DEX+CMX-13	44.3±16.0	

Paired analysis of the effect of CM on apoptosis in both normal controls and SLE patients is depicted in Figure 4.2.5.4. There was a significant increase in the percentage of apoptotic cells in both the SLE and control PBMCs following treatment with CMX-13 ($p<0.001$). This was in coordance with our DEX dose response experiment.

Figure 4.2.5.4 Effect of CMX-13 on apoptosis in PBMCs from SLE patients and age-sex matched healthy controls. Paired analysis showed a significant increase in apoptotic cells following 24-hour incubation with CMX-13 in both SLE and controls.

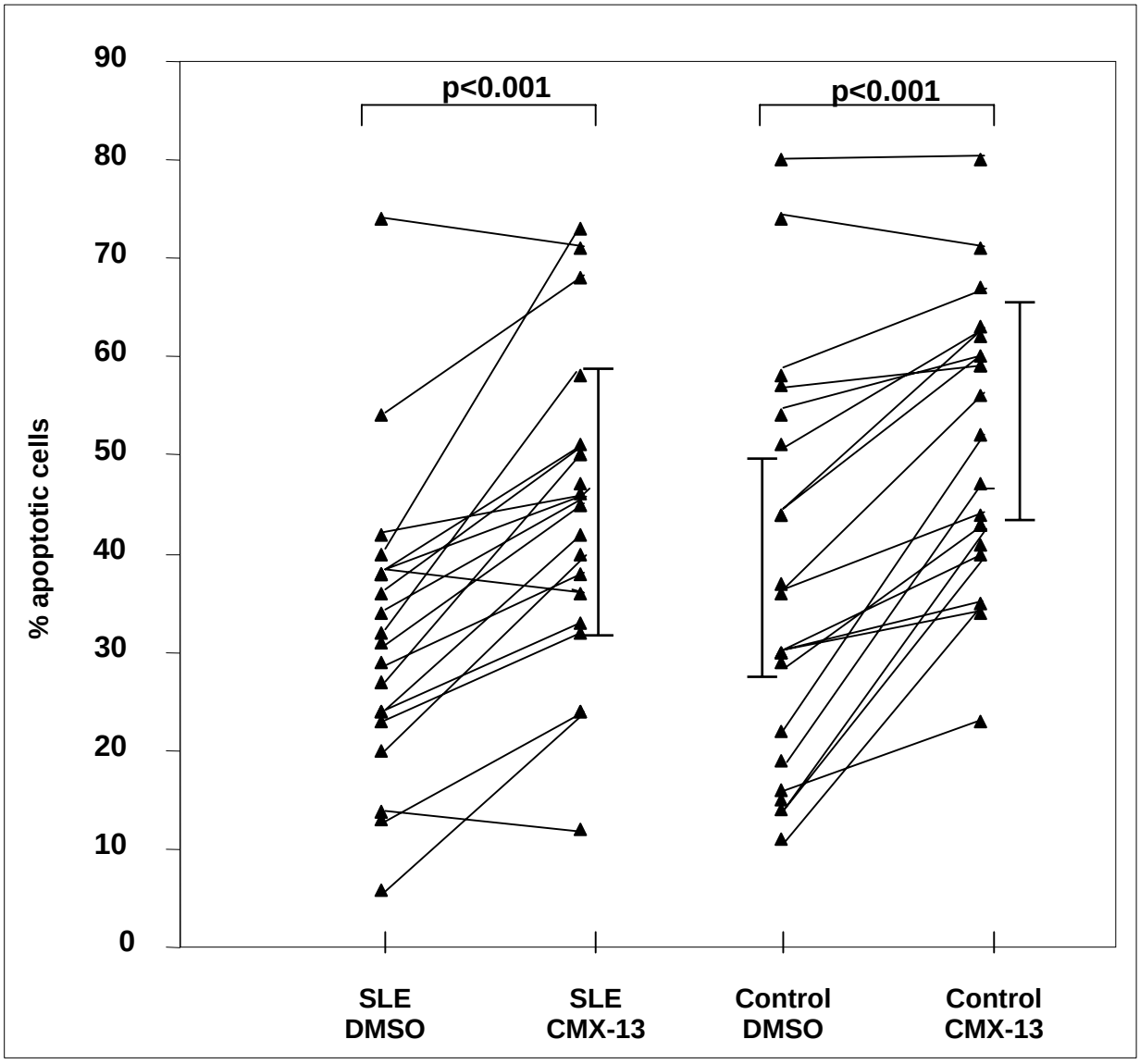

Table 4.2.5.3 outlines the SLEDAI and SLICC scores of the individual patients, and the percentages of apoptotic cells present before and after incubation with CMX-13. In Table 4.2.5.4 the SLEDAI/SLICC scores are tabulated with the medication the patients were on, the activity of the disease, the status of the kidney. With increasing SLE activity as determined by the SLICC score, an increase in the percentage of spontaneous apoptotic PBMCs was seen, although this did not reach statistical significance (r=0.40, p=0.08) (Figure 4.2.5.5).

Table 4.2.5.3 Total SLICC/SLEDAI scores of SLE patients and the percentage of apoptotic PBMCs before and after incubation with CMX-13.

Patient No.	SLEDAI	SLICC	Percent apoptotic PBMCs before CMX-13 treatment	Percent apoptotic PBMCs after CMX-13 treatment
1	0	1	13.8	12.0
2	6	0	23.0	33.0
3	0	1	31.0	45.0
4	0	3	24.0	42.0
5	4	0	34.0	46.0
6	1	1	36.0	51.0
7	0	2	29.0	38.0
8	16	4	38.0	36.0
9	0	0	74.0	71.0
10	2	2	38.0	45.0
11	4	2	27.0	50.0
12	20	3	42.0	47.0
13	0	3	54.0	68.0
14	18	2	40.0	73.0
15	0	1	5.7	24.0
16	0	0	20.0	40.0
17	2	1	35.0	32.0
18	12	1	32.0	58.0
19	0	2	13.0	24.0
20	10	4	38.0	50.0

Table 4.2.5.4 Details of Patients. Disease Activity, Anti-DNA levels, Kidney disease from individual patients, Proteinuria levels and Medication during the time of assessment. (Prednisolone = PNL; Azathioprine = AZT; Cellcept = CC; Cyclosporine A = CsA; Hydroxychloroquine = HDCL)

Patient	SLEDAI	SLICC	SLE activity (Active/ Remission)	Anti-DNA levels *	Status of Kidney disease/ Proteinuiria	Current Drug Treatment
1	0	1	Active			PNL 3 mg om
2	6	0	Remission			PNL 12 mg om AZT 50 mg om
3	0	1	Active	> 100		
4	0	3	Active	> 100		CC 500 mg bd CSA 100 mg bd PNL 5 mg om
5	4	0	Remission		Renal transplant	
6	1	1	Active		Nephritis Class IV (c) Proteinuria 2.12 g	
7	0	2	Active			AZT 50 mg om HDCL 200 mg om
8	14	4	Active			PNL 10 mg om HDCL 200 mg om
9	0	0	Remission	31		PNL 10 mg om HDCL 200 mg om
10	2	2	Active	32		AZT (day 1,3,5,7) 50 mg om AZT (day2,4,6)25 mg om
11	4	2	Active			
12	20	3	Active	>100	Nephritis Class IV (c) Proteinuria 11.06 g	PNL 13 mg om HDCL 200 mg om
13	0	3	Active		Proteinuria 0.19 g	HDCL 200 mg om PNL 50 mg om
14	18	2	Active	72	Chronic renal failure Proteinuria 3.97 g	PNL 3 mg om
15	0	1	Active		Proteinuria 120 mg	
16	0	0	Remission			AZT 50 mg om PNL 30mg om
17	2	1	Active	>100	Proteinuria 3.84 g	PNL 15 mg om
18	12	1	Active	41		
19	0	2	Active			
20	10	4	Active			

Figure 4.2.5.5 Correlation between SLICC score and baseline percent apoptotic PBMCs in SLE patients.

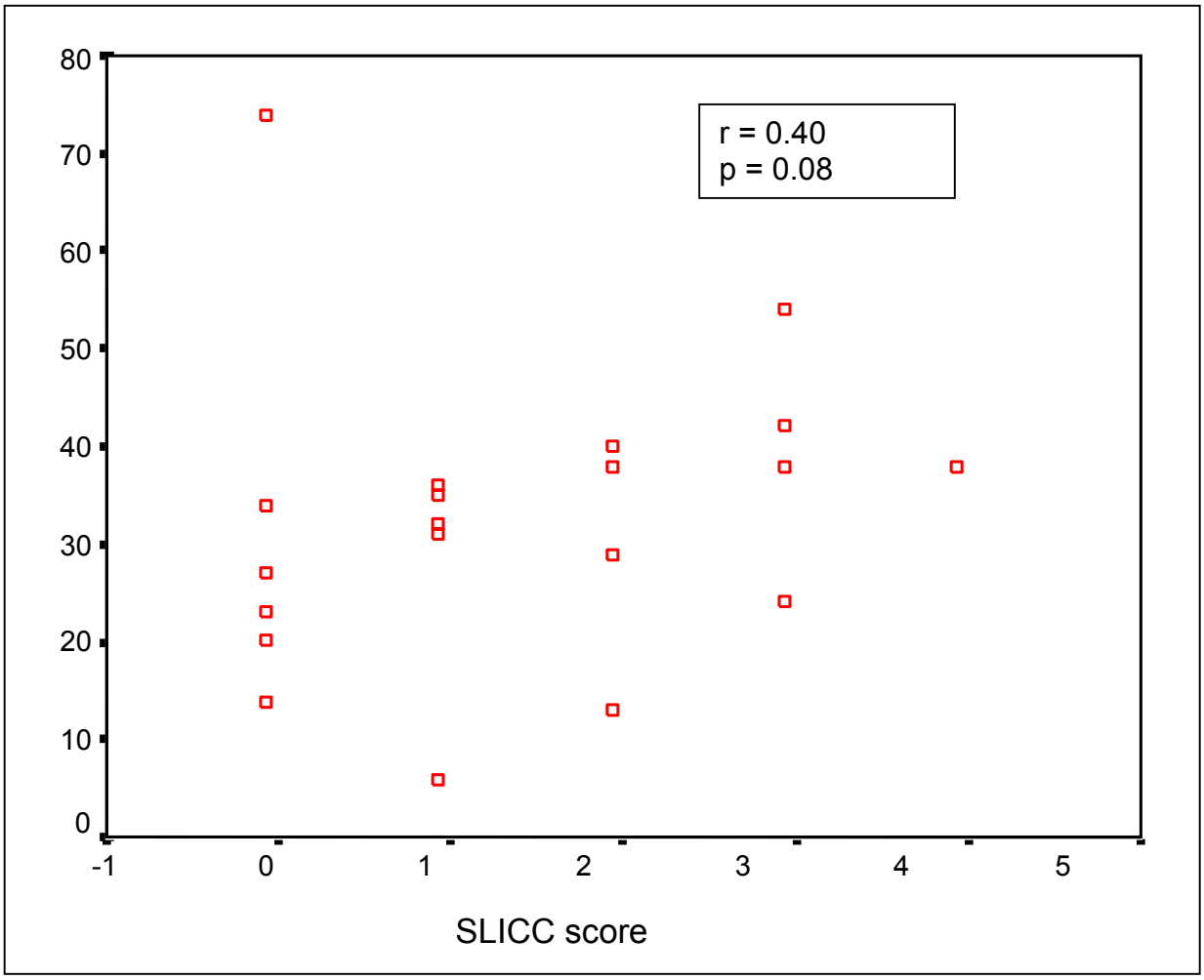

4.3 DISCUSSION

We have previously shown that the hydrophobic extract, CMX-13, of a Chinese herbal decoction used in the treatment of patients with SLE, inhibited lymphocyte proliferation following PHA stimulation. In this chapter, we have shown that this phenomenon was also demonstrated in Jurkat cells, which is a CD4+CD8- T-cell line. CMX-13 significantly inhibited spontaneous Jurkat cell proliferation by >99% in all the concentrations tested (1-8 μg/ml).

In order to further elucidate the immunosuppressive action of CMX-13 on Jurkat cells, we examined its effect on cell-cycle progression as well as the induction of apoptosis, and compared this to CH, a known protein synthesis inhibitor. Apoptosis is intimately linked to cell stimulation and proliferation [Van Parijs et al., 1998], and is initiated by ligand-receptor interactions that are highly regulated. It can also result from the removal of growth factors that are necessary for sustaining cell proliferation. In Jurkat cell cultures, the percentage of spontaneous apoptotic cells is low, as the cells are proliferating actively. CMX-13 was able to inhibit Jurkat cell proliferation, not by inhibiting cell-cycle progression, but by inducing spontaneous apoptosis in cells in the G_0/G_1 phase. This effect of CMX-13 on apoptosis in Jurkat cells was confirmed by DNA fragmentation analysis and Annexin-V staining. Apoptosis was induced at a very early phase, as was demonstrated by the “sub-G1” or

apoptotic peaks appearing in the cell-cycle analysis. This mechanism of action was different from drugs such as CH, which induces apoptosis related to a G_0/G_1 cell-cycle arrest.

There is a close linkage between the genes that determine cell proliferation on the one hand, and apoptosis on the other [Evan et al., 1992]. For example, *c-myc* can act as a bivalent regulator and is able to induce either cell proliferation or apoptosis [Mountz et al., 1994]. In addition, both extra- and intra-cellular stimuli can induce apoptosis by triggering a group of intracellular cysteine proteases known as caspases [Thornberry et al., 1998]. Caspases are also thought to be involved in cell-cycle progression [Los et al., 2001] and cellular stress-related apoptosis [Planey et al., 2000]. Two distinct pathways of apoptosis have been described that induce the activation of caspases and other pro-apoptotic activities. One of the pathways leading to apoptosis is activation of caspase 8 upon binding of a death ligand on the cell membrane [Hakem et al., 1998]. The second pathway is related to cellular stress, whereby mitochondria release cytochrome *c* which binds to Apaf-1 [Zheng et al., 1999; Cecconi, 1999]. This complex activates caspase-9, which subsequently activates downstream caspases [Yoshida et al., 1998]. Therefore further studies are required to determine if induction of apoptosis by CMX-13 is related to the caspase-8 or caspase-9 pathway.

Defective apoptosis has been suggested to be an important mechanism in the pathogenesis of various autoimmune diseases [Mountz et al., 1994; Carrichio

et al., 1999; Papo et al., 1998]. Apoptosis is important for the immune system to regulate cell growth and terminate immune responses in order to ensure that overall the rate of division is balanced by cell death [Lorenz et al., 2001]. In SLE, one of the hypothesis is that dysregulation of apoptosis might be responsible for the induction of anti-nuclear antibodies, pathognomonic of the disease. In some patients, decreased apoptosis in SLE appears to be associated with increased production sFas molecule that is capable of inhibiting apoptosis after a stimulus to proliferate [Cheng et al., 1994], whereas other studies reported accelerated apoptosis of lymphocytes in SLE patients [Emlen et al., 1992; Lorenz et al., 1997]. This increased rate of apoptosis was not affected by treatment with corticosteroids [Emlen et al., 1992]. Similarly, in our SLE patients, the percentage of apoptotic cells was increased with increasing activity of the disease as measured by the SLICC score (Figure 4.2.5.5). Although all of the patients were on corticosteroid treatment, this should not have affected the apoptotic rate, as addition of DEX to control PBMCs did not induce apoptosis (Table 4.2.5.2).

A high threshold for DNA damage-induced apoptosis might also explain the presence of DNA mutations in T cells from SLE patients [Gmelig-Myeling et al., 1992], where such mutations could lead to T cell death and increased release of non-degraded DNA by necrosis instead of apoptosis, contributing to the production of anti-DNA antibodies seen in this disease. Apoptosis-induced nucleosomes constitute a unique reservoir of potentially immunogenic nuclear autoantigens. In SLE, it has been postulated that there is defective

macrophage clearance of early apoptotic cells. Hence binding of nuclear autoantigens to follicular dendritic cells in lymph nodes may provide a signal for autoreactive B cells, overriding the control mechanism of B-cell tolerance [Baumann et al., 2002].

We have shown that CMX-13 was able to induce apoptosis in Jurkat cells, but to a lesser extent than CH, a known apoptosis inducer. In addition, its effect on cell-cycle progression was less. Similarly, its apoptotic effect on PHA-stimulated PBMC was less than that of CH, although it completely inhibited cell-cycle progression. Hence the immunosuppressive mechanism of CMX-13 could be partly related to its effect on apoptosis. However further studies are required to elucidate other possible mechanisms of its immunosuppressive action, especially in the context of suppression of SLE activity, where increased apoptosis has been demonstrated.

CHAPTER 5 EFFECT OF CMX-13 ON THE MRL-*lpr/lpr* SLE MOUSE MODEL

5.1 INTRODUCTION

MRL-*lpr/lpr* mice spontaneously develop an autoimmune disorder with similar pathological features to human SLE. The symptoms are characterized by lupus nephritis, the production of anti-double stranded DNA (dsDNA) and anti-IgG or rheumatoid factor-specific autoantibodies, proteinuria, skin lesions at the back and the ear, and distorted cytokine levels [Andrews et al., 1978; Steinberg et al., 1978; Jonsson et al., 1987; Bigazzi and Rose, 1996; Theofilopoulos ,1993]. The severity of the autoimmune disease increases with the age of the mice, with the majority dying of renal failure at 16-24 weeks of age. A main characteristic of the MRL-*lpr/lpr* mouse is massive lymphadenopathy, an exclusive feature found in mouse SLE but not in human SLE, and is caused by a defective Fas molecule.

The MRL-*lpr/lpr* SLE mouse model has a recessive gene defect [Cohen and Eisenberg, 1991] in the apoptotic *Fas* gene or the lymphoproliferative (*lpr*) gene located on chromosome 19 [Watanabe et al., 1992; Watson et al., 1992]. This mutation is caused by an insertion of a retrotransoposon element, *Et*n, in the intron between exon 2 and exon 3 [Adachi et al., 1993; Wu et al., 1993; Chu et al., 1993]. The *lpr* mutation leads to loss of functional *Fas* mRNA expression, consequently leading to non-production of the Fas protein (CD95) [Adachi et

al.,1993]. The dysfunctional *Fas* mRNA expression in the MRL-*lpr/lpr* mice is depicted in Figure 5.1.1. Insertion of a full-length murine *Fas* cDNA has been shown to correct the dysfunctional Fas mRNA expression resulting in elimination of disease manifestations [Wu et al., 1994]. A second murine SLE model, the MRL-*lpr/lpr*^{gld} mouse has been described, consisting of a point mutation on the *Fas* ligand, with similar disease manifestations.

Figure 5.1.1 Dysfunctional *Fas* gene expression in the MRL-*lpr/lpr* mouse. Insertion of the transposable element, *Etn*, in the *fas* gene located on mouse chromosome 19 leads to dysfunctional Fas mRNA expression.

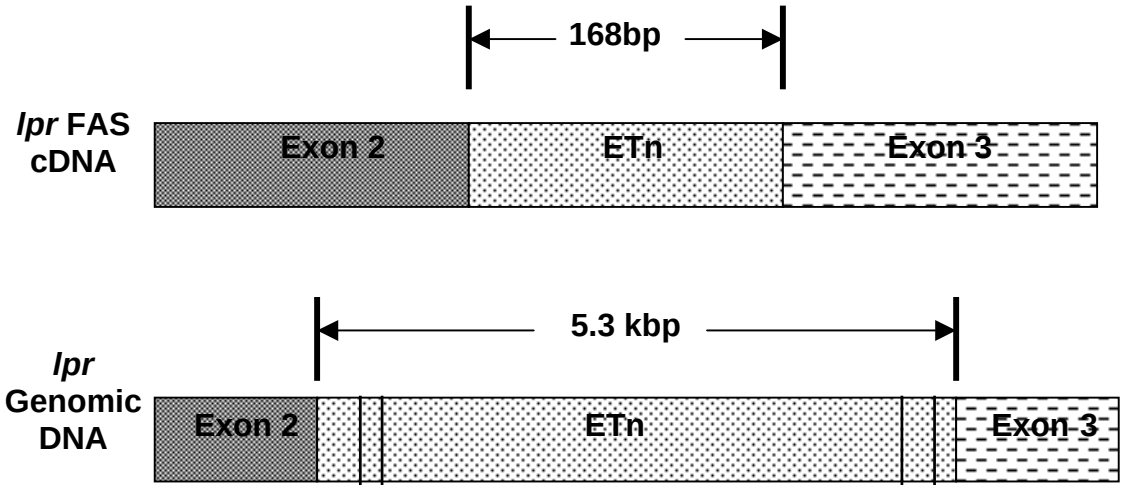

The development of autoreactive T-cells in the MRL-*lpr/lpr* SLE mouse model was thought to be a consequence of T cells escaping negative selection secondary to defective apoptosis caused by the deficient Fas molecule (CD95). However, recent studies have shown that negative selection of T- and B-cells is intact in the MRL-*lpr/lpr* mice [Rathmell and Goodnow, 1994]. The defective Fas molecule in the MRL-*lpr/lpr* SLE mouse model leads to defective cell death

of peripheral αβ T cells [Singer and Abbas, 1994; Renno et al., 1996], consequently resulting in expansion of double negative TCRαβCD3$^+$CD4$^-$CD8$^-$ B220$^+$ T-cells [Morse et al., 1982]. The presence of TCRαβCD3$^+$CD4$^-$CD8$^-$ B220$^+$ T-cells has been identified in the lymph nodes of the MRL-*lpr/lpr* mice leading to lymphadenopathy at the age of 13-14 weeks [Theofilopoulos et al., 1979; Lewis et al., 1981; Morse et al., 1982; Wofsy et al., 1984; Murray et al, 1990]. The contribution of these cells to the development of SLE has been investigated, but no direct link to the pathogenesis of other symptoms of SLE has been demonstrated except lymphadenopathy in the MRL-*lpr/lpr* mice [Singer and Abbas, 1994]. Nevertheless, these cells are a distinctive consequence of the *lpr* mutation.

The TCRαβCD3$^+$CD4$^-$CD8$^-$B220$^+$ T-cells have unique characteristics, for example, they do not proliferate *in-vivo* [Sobel et al., 1995] or *in-vitro* [Budd et al., 1985], and they also fail to respond to IL-2 and other agents that activate T-cells [Wofsy et al., 1981; Altman et al., 1981]. The origin of the CD4$^-$CD8$^-$ B220$^+$ T-cells has been thought to be the *lpr* CD4+ T-cells. Following the injection of CD4+ T-cells from B6 *lpr* mice into nude mice, the presence of TCRαβCD3$^+$CD4$^-$CD8$^-$B220$^+$ T-cells was observed [Santoro et al., 1987; Laouar and Ezine, 1994]. Hence the *lpr* CD4+ T-cells could play an important role in the development of SLE in the MRL-*lpr/lpr* mouse. There is also evidence suggesting that these cells are resistant to apoptosis [Bossu et al., 1993].

These TCR$\alpha\beta$CD3$^+$CD4$^-$CD8$^-$B220 T-cells are a rich source of proinflammatory cytokines including TNF-α and IFN-γ [Murray and Martens, 1990]. Moreover, MRL-*lpr/lpr* mice also display proinflammatory alterations in the intrarenal cytokine network [Boswell et al., 1988a; Boswell et al., 1988b; Fan et al., 1997]. Alterations in the cytokine network are characteristic of many immune-mediated disorders, and the pro-inflammatory cytokines such as TNF-α and IFN-γ, may play a major role in the pathogenesis of autoimmune diseases.

In our previous studies using the Brown Norway$\rightarrow$Lewis (BN$\rightarrow$LEW) rat lung transplant model, we showed that 25 mg/kg/day of CMX-13 was effective in suppressing acute allograft rejection. CMX-13 was able to prevent vasculitis, necrosis and hemorrhage, which are features of an aggressive rejection process [Yap et al, 1998; Zuo et al, 2000]. In these studies, CMX-13 did not inhibit IL-2 and IFN-γ mRNA expression, suggesting that its mechanism of action was different from that of CsA. We also showed, in our *in-vitro* studies discussed in Chapter 4 that CMX-13 successfully induced apoptosis in Jurkat cells and PBMCs of SLE patients and age-sex matched normal controls. In the MRL-*lpr/lpr* SLE mouse model, the Fas apoptosis pathway is non-functional [Rose et al., 1997; van der Linden et al., 2001; Sato et al., 2000]. Current immunosuppressive agents that are used in the treatment of SLE have been shown to act in part via the induction of apoptosis [Amano et al., 2000; Dooley and Falk, 1998; Steinberg, 1994].

In this chapter, we studied the effects of CMX-13 on:

1. Progression of autoimmune disease in the MRL-*lpr/lpr* lupus mouse model, in terms of skin lesions, joint involvement and lymphadenopathy
2. Development of anti-DNA antibodies
3. Development of lupus nephritis as measured clinically by the onset and degree of proteinuria and histological scoring of severity of the nephritis
4. Survival of the MRL-lpr/lpr mouse.

5.2 RESULTS

5.2.1 Clinical Observation on the MRL-*lpr/lpr* Mice

MRL-*lpr/lpr* mice typically develop skin lesions on the back, neck and ears by the age of 20-24 weeks [Reininger et al., 1990; Chan et al., 2001]. To determine if CMX-13 had any effect on the development of clinical disease, the mice were treated with either DMSO (solvent control), CMX-13 or DEX as described in chapter 2.3.2, from the age of 12 weeks, and were observed for development of skin vasculitic lesions, articular hind pad swelling and lymphadenopathy. The mice were examined for the development of skin lesions at 22 weeks. The DMSO control group had visible vasculitic skin lesions on the ear (Figure 5.2.1.1) and back (Figure 5.2.1.2). Surprisingly, the untreated control group did not demonstrate any skin lesions. Both the CMX-13 and DEX-treated mice also did not develop these features.

Figure 5.2.1.1 Vasculitic skin lesions in the ear in MRL-*lpr/lpr* mice in the DMSO-control group at age 22 weeks. No skin lesions were seen in the untreated controls, CMX-13 and DEX-treated mice.

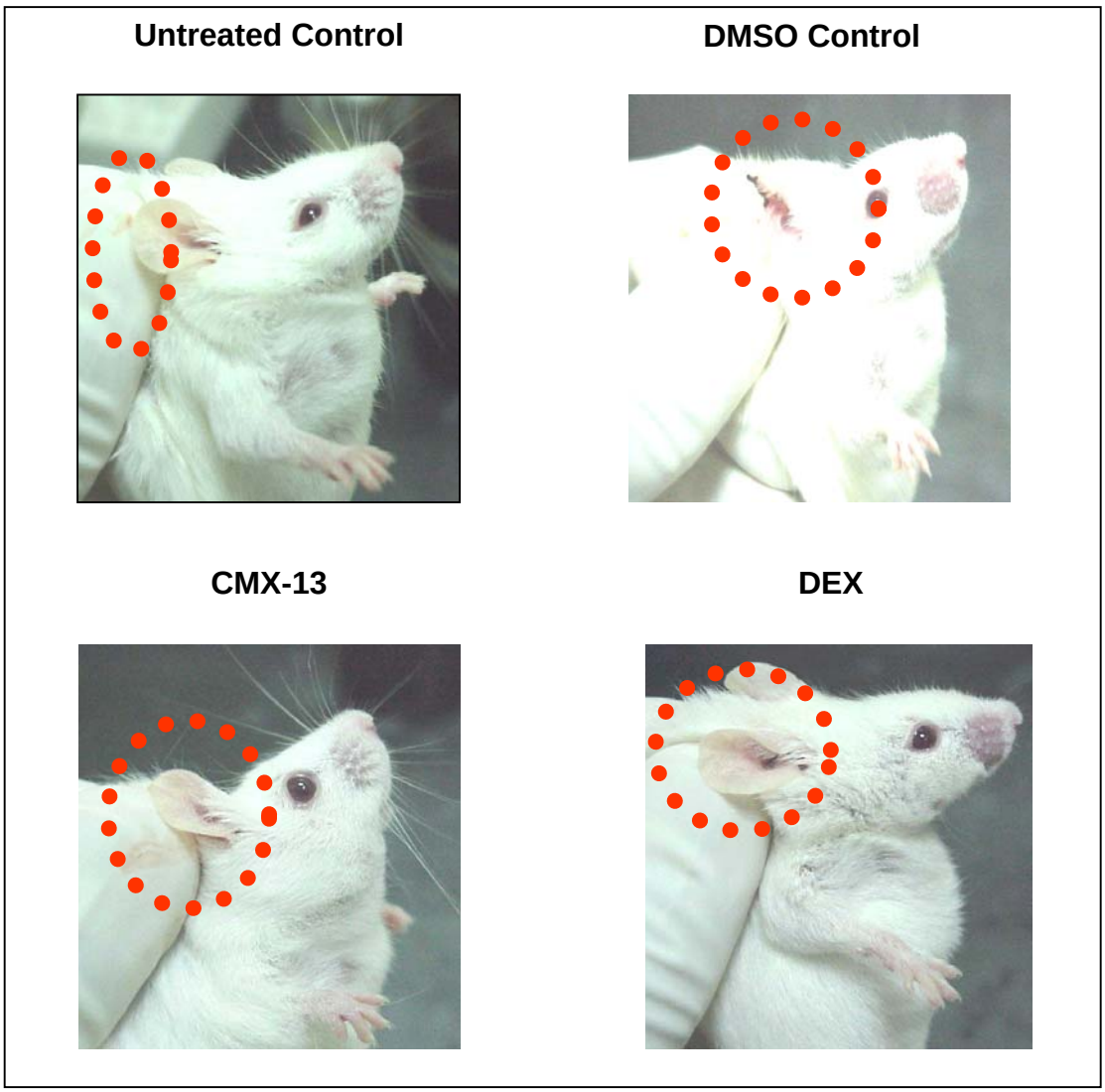

Figure 5.2.1.2 Vasculitic skin lesions on the back of DMSO control mice at age of 22 weeks. No skin lesions were seen in the untreated controls, CMX-13 and DEX-treated mice.

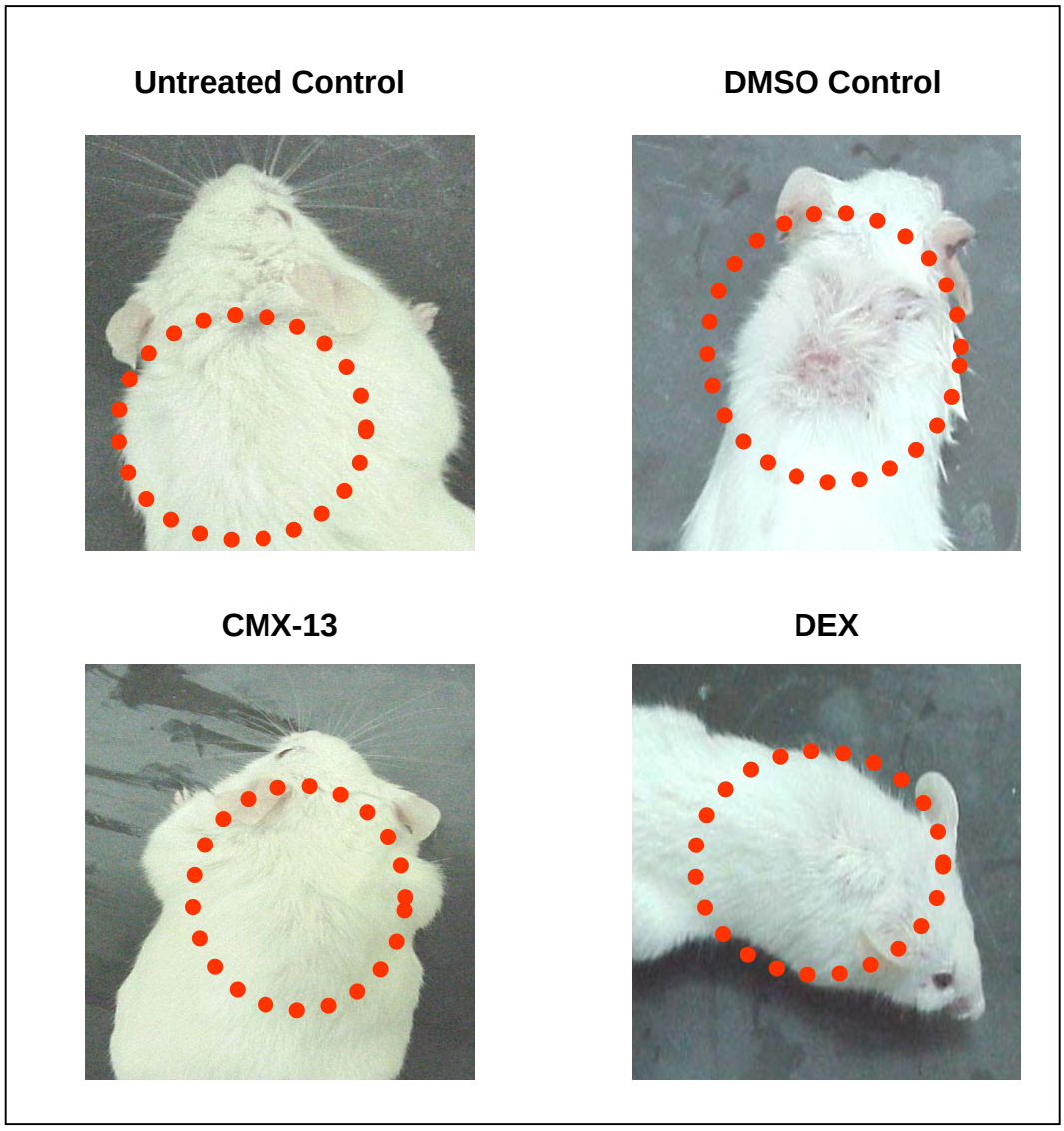

Similarly, articular swelling of the hind footpads was only observed in the DMSO-control mice but not in the untreated controls, CMX-13-treated and DEX-treated groups. These features are shown in Figure 5.2.1.3.

Figure 5.2.1.3 Severe articular swelling of the hind footpads seen only in the DMSO-control mice at age 22 weeks.

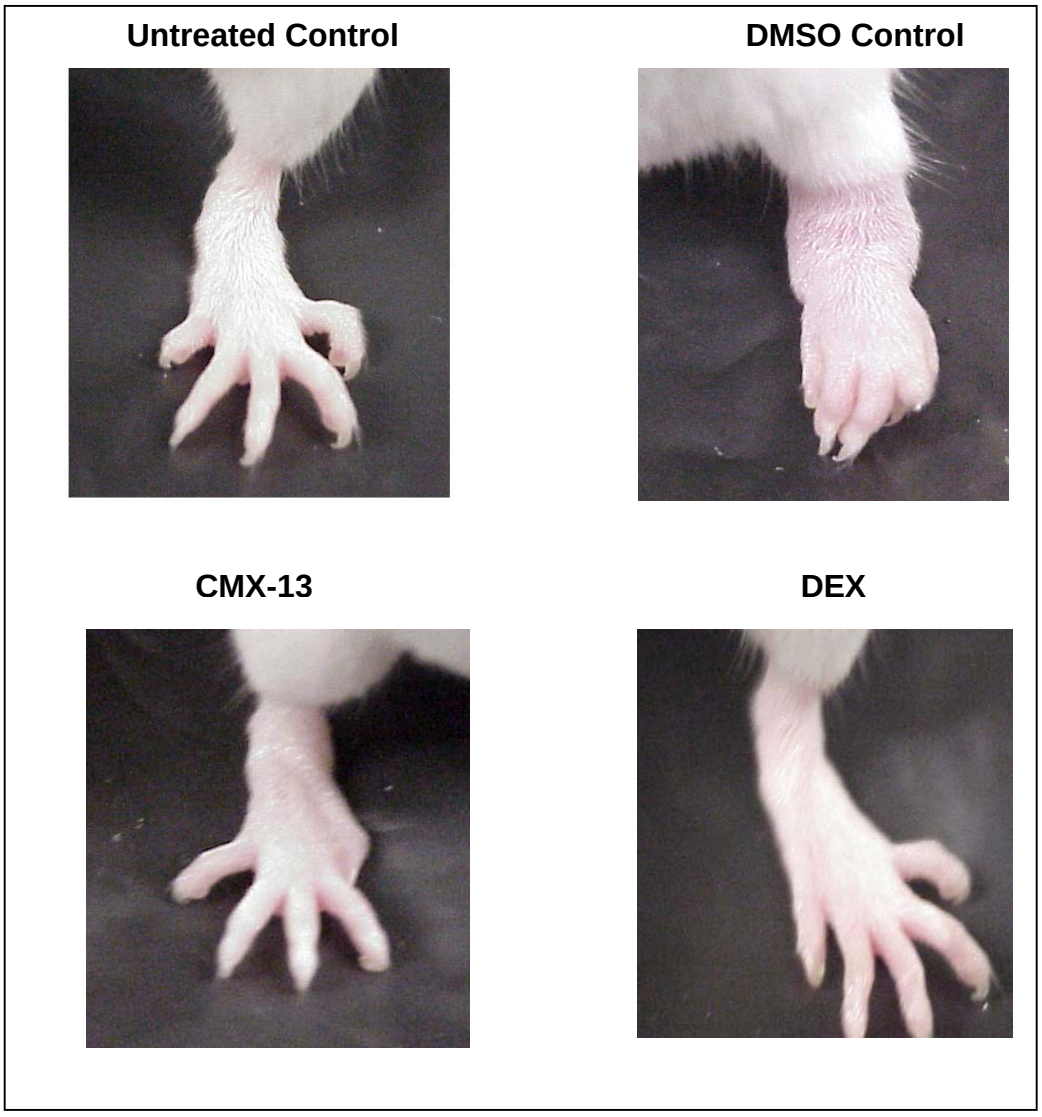

MRL-*lpr/lpr* mice generally develop lymphadenopathy and splenomegaly as a consequence of accumulation of the double negative T cells that down-regulate their co-receptor, primarily CD8, and up-regulate B220 with a cell phenotype that is TCR$\alpha\beta$CD3$^+$CD4$^-$CD8$^-$B220$^+$ compared to conventional CD3$^+$CD4$^+$B220$^-$ or CD3$^+$CD8$^+$B220$^-$ cells. Thus, we next assessed the effect of CMX-13 treatment on the development of lymphadenopathy in these mice. Lymphadenopathy started to become visible from the age of 12-13 weeks in the untreated and DMSO control groups (Figure 5.2.1.4). The CMX-13 and DEX treatment groups did not develop lymphadenopathy until at least 18 weeks. The severity of lymphadenopathy increased with age.

Figure 5.2.1.4 Lymphadenopathy visible at age 12 weeks only in the untreated and DMSO control groups.

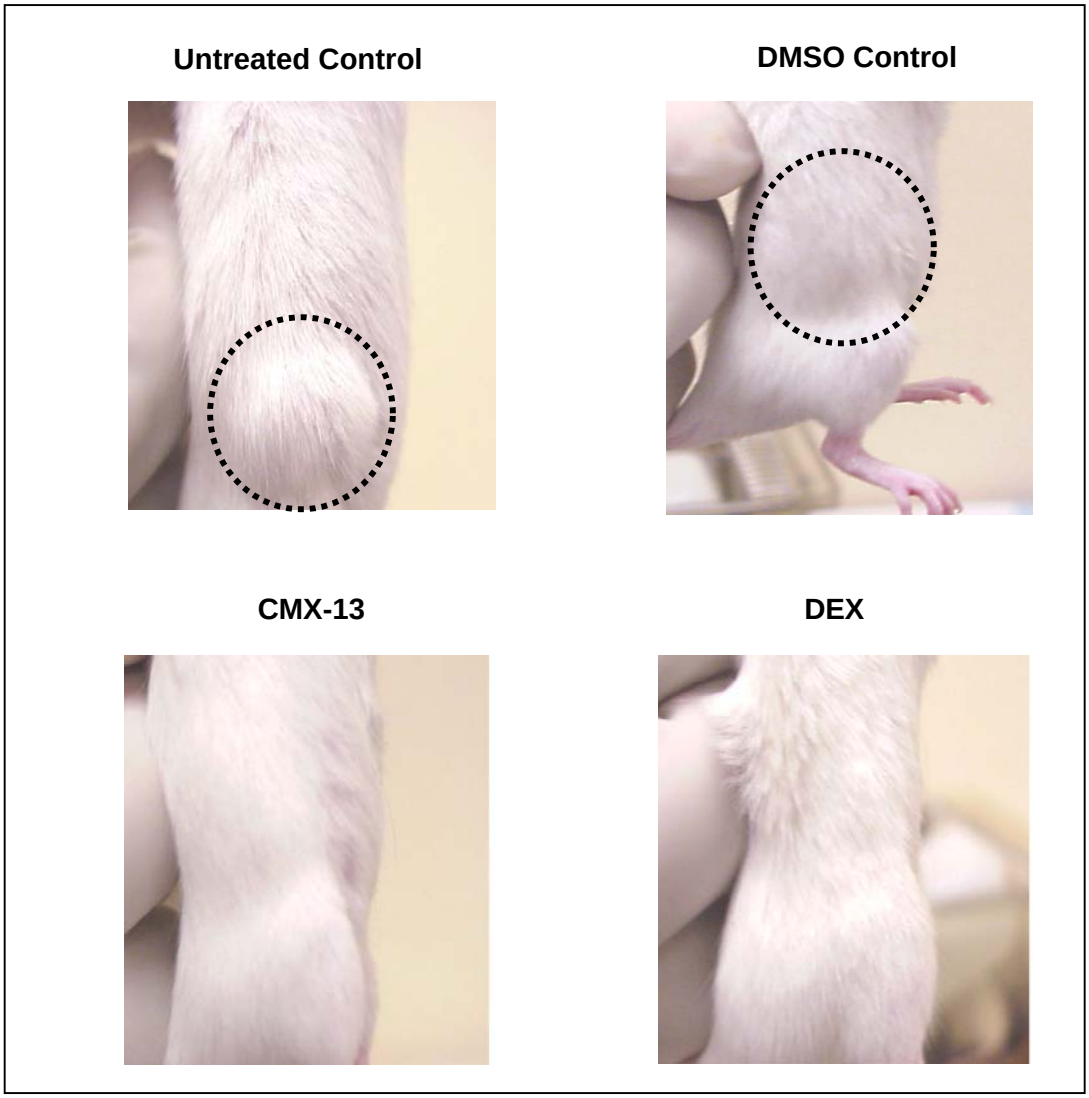

5.2.2 Effect of CMX-13 on Proteinuria

Proteinuria starts to occur by the age of 8–12 weeks in the MRL-*lpr/lpr* mice due to development of lupus nephritis [Eilat and Naparstek, 1999; Appel and Valeri, 1994]. This is associated with increased levels of IL-6 in the urine, possibly related to the glomerular inflammation [Iwano et al., 1993]. In this study, the development of proteinuria in the untreated controls, DMSO controls, CMX-13-treated and DEX-treated mice was monitored every 4 weeks from the age of 8 weeks up to the age of 22 weeks (Appendix 5.1). Urinary protein concentration was graded semi-quantitatively by a proteinuria score raging from 0 to 5 scale (0 = Negative; 1 = Trace; 2 = 0-30 mg/dl (+); 3 = 30-100 mg/dl (++); 4 = 100- 300 mg/dl (+++); 5 = > 300 mg/dl (++++)) [Ishida et al., 1994; Yamamoto et al., 1990; Mihara et al., 1997; Aihira M, et al., 1997], using urine reagent strips as described in section 2.3.3.

After 4 weeks of treatment at the age of 16 weeks, a reduction of proteinuria in the CMX-13-treated and DEX-treated mice was observed. Compared to the untreated and DMSO-treated mice, CMX-13-treated mice ($p<0.005$ and $p<0.04$ respectively) and DEX-treated mice ($p<0.001$ and $p<0.006$ respectively) had a significantly lower level of proteinuria (Figure 5.2.2.1).

Figure 5.2.2.1 Effect of CMX-13 on proteinuria score in MRL-*lpr/lpr* autoimmune mice compared to untreated controls, DMSO controls and DEX-treated mice at the age of 16 weeks (after 4 weeks of treatment).

Proteinuria Score

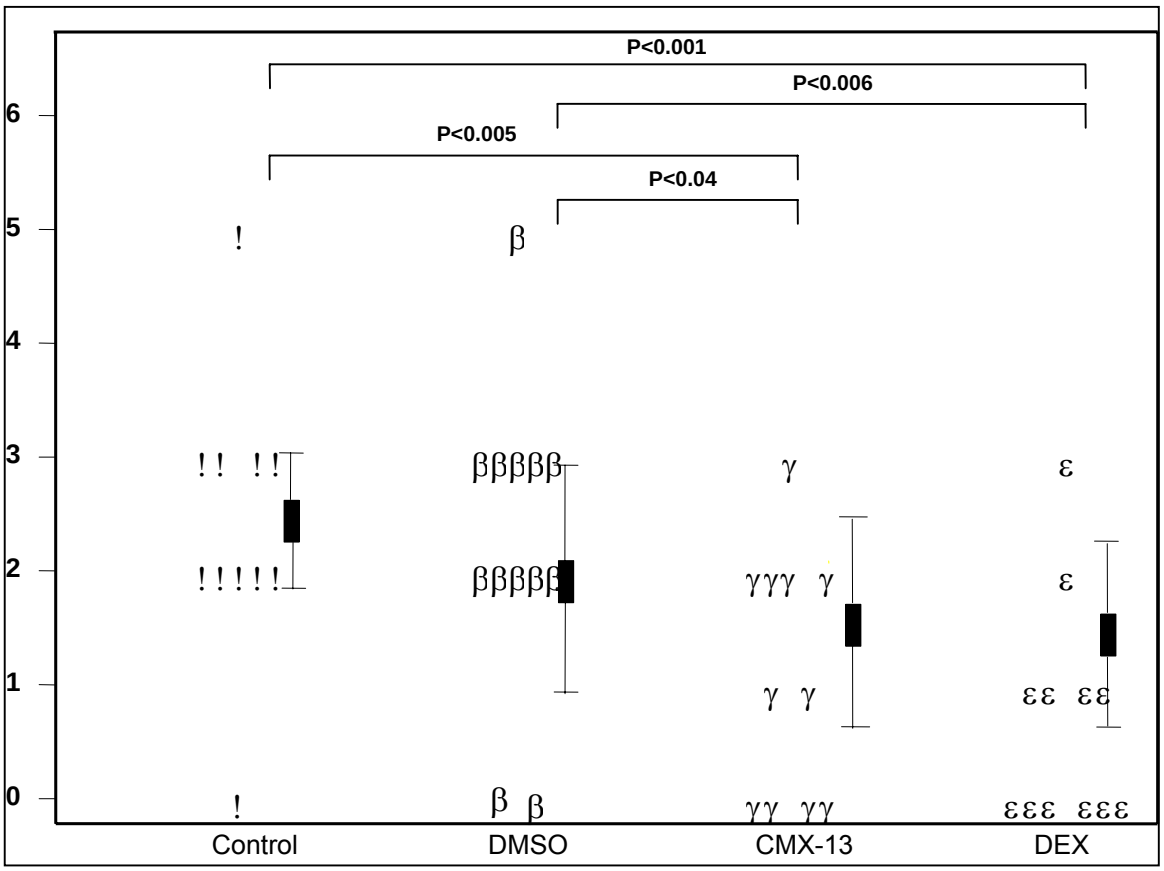

Over the 10 weeks of treatment up to the age of 22 weeks, there was an increase in the proteinuria score in all the groups (Figure 5.2.2.2). However, there was no significant difference in the proteinuria scores between the groups at 22 weeks, primarily due to small numbers of mice that were still alive and available for analysis at this age.

Figure 5.2.2.2 Changes in proteinuria score over time MRL-*lpr/lpr* autoimmune mice.

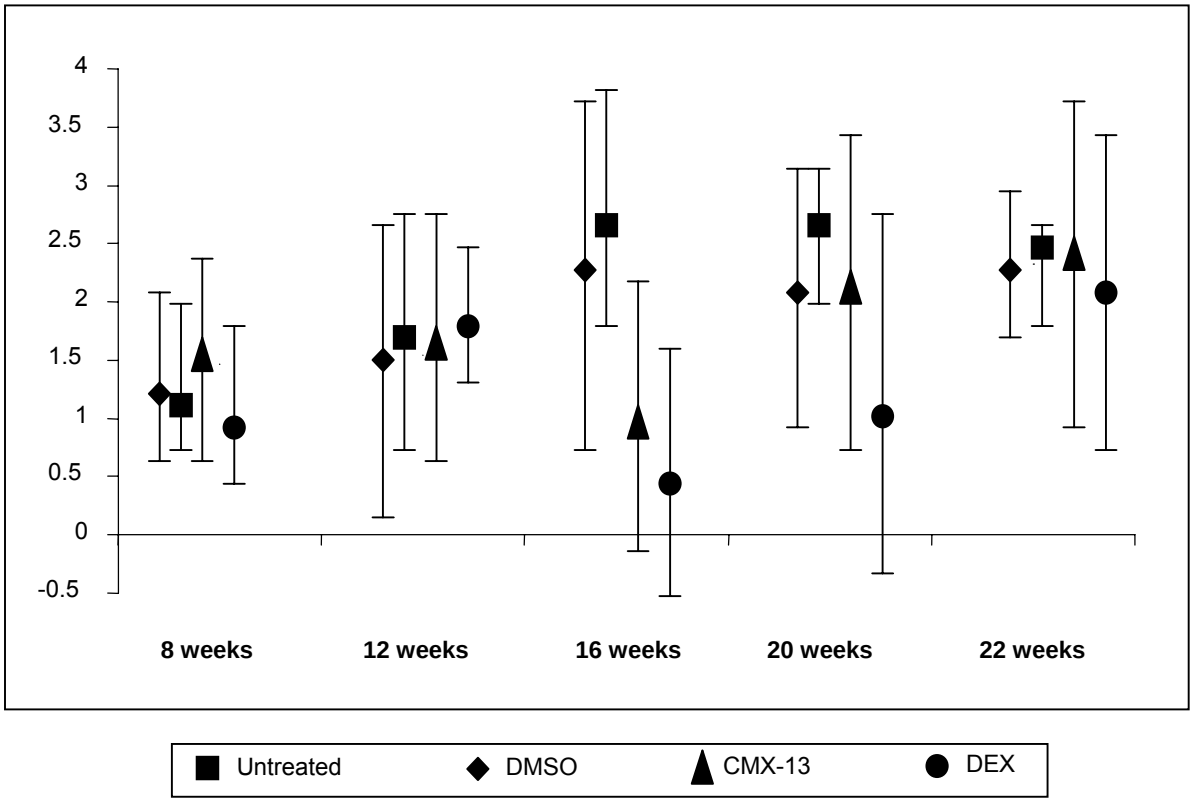

5.2.3 Effect of CMX-13 on Anti-dsDNA Antibodies

Lupus-specific anti-dsDNA autoantibodies appear in the MRL-*lpr/lpr* mice at the age of 6-8 weeks [Andrews et al, 1978; Putterman and Naparstek, 1994]. Sera were collected from the untreated controls, DMSO controls, CMX-13-treated and DMSO-treated mice at the ages of 8, 12 and 16 weeks for analysis of IgG-specific anti-dsDNA autoantibody levels (Appendix 5.2). It was not possible to analyse the differences in the anti-dsDNA antibody levels after 16 weeks, due to a progressive increase in the number of mice dying, especially in the negative control groups.

As shown in Table 5.2.3.1, at 8 weeks of age the anti-dsDNA antibody levels in all the groups were not significantly different, and ranged from 0.10-1.40 ηg/ml. At 12 weeks of age, the anti-dsDNA antibody levels increased over the baseline in all the groups. Following treatment with either CMX-13 or DEX in two groups, the rise in anti-dsDNA antibody levels with time was decreased compared to the control group and the group treated with the solvent DMSO ($p<0.05$) (Figure 5.2.3.1).

Table 5.2.3.1 Serum anti-dsDNA antibody levels in MRL-*lpr/lpr* mice at age 8, 12 and 16 weeks.

Groups	Age of mice		
	8 weeks	**12 weeks**	**16 weeks**
Untreated	0.39±0.26	0.73±0.09	1.48±0.46[a,b]
DMSO control	0.36±0.35	0.53±0.31	1.58±0.50[a,b]
CMX-13	0.22±0.06	0.57±0.20	1.03±0.43[a]
DEX	0.23±0.04	0.38±0.19	0.88±0.40[b]

[a]p<0.05, comparing CMX-13 with disease control and DMSO control.
[b]p<0.03, comparing DEX with disease control and DMSO control.

Figure 5.2.3.1 Serial serum anti-DNA antibody levels in MRL-*lpr/lpr* mice at age 8, 12 and 16 weeks. CMX-13 and DEX treated mice had a lower elevation of anti-dsDNA antibody levels than untreated or DMSO-treated mice. [a]Comparing CMX-13 with disease control and DMSO control, p<0.05. [b]Comparing DEX with disease control and DMSO control, p<0.03.

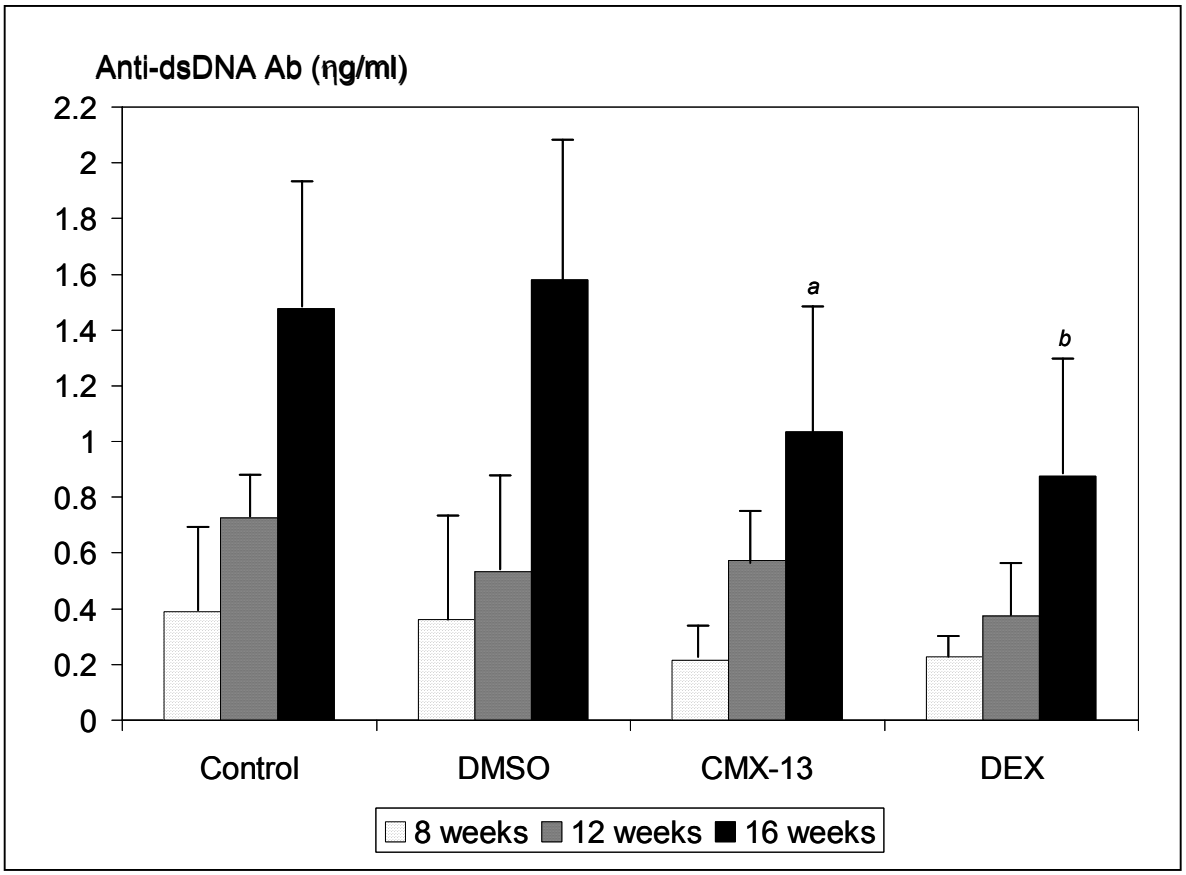

5.2.4 Effect of CMX-13 on Serum Creatine level

The creatinine levels in the sera of the Untreated group was lower (0.551±0.074 mg/ml) when compared to the DMSO (0.84±0.041 mg/ml) or the DEX (0.82±0.062 mg/ml) treated group. Higher creatinine levels in the samples Untreated mice were expected. The creatinine levels did not differ significantly in the Untreated group when compared to the DMSO and DEX group. The creatinine levels in the CMX-13 treated group also was not significantly different from the Untreated group (0.68±0.111 mg/ml). These results are shown in Figure 5.2.4.1 and in Table 5.2.4.1.

Figure 5.2.4.1. Serum creatine in CMX-13 treated mice. Serum creatine levels did not significantly decreased in CMX-13 mice when compared to Untreated or DMSO treated mice.

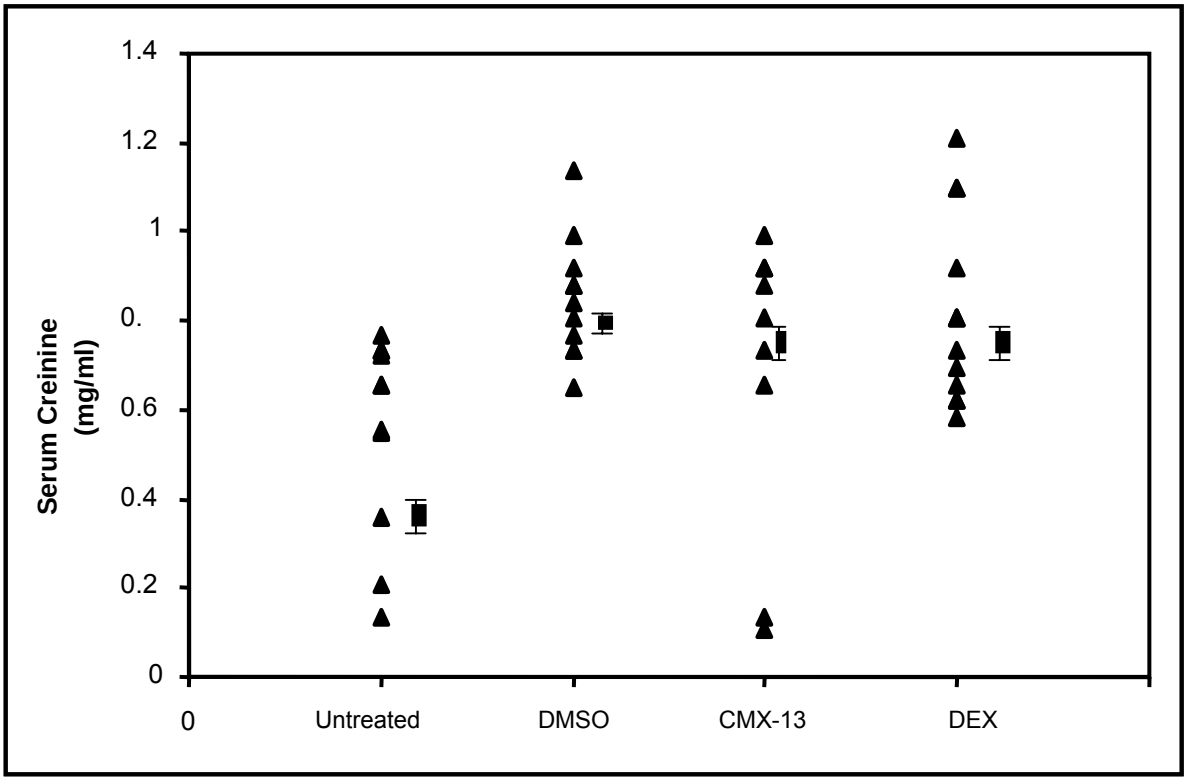

Table 5.2.4.1 . Serum Creatine levels in the MRL-*lpr/lpr* mice after treatment with CMX-13 (mean±SD).

Untreated (n = 11)	DMSO (n = 11)	CMX-13 (n =9)	DEX (n = 12)
0.356	0.651	0.879	0.658
0.731	0.805	0.916	0.916
0.768	0.842	0.104	1.1
0.658	0.879	0.99	0.805
0.209	0.916	0.731	0.731
0.725	1.137	0.805	0.621
0.135	0.879	0.916	0.584
0.658	0.99	0.135	1.1
0.547	0.768	0.658	0.621
0.731	0.731		0.805
0.5518	0.731		0.694
			1.211
0.5518±0.074	0.84± 0.041	0.68± 0.111	0.82± 0.062

5.2.5 Histological Scoring of Lupus Nephritis in MRL-*lpr/lpr* Mice

To define the effects of CMX-13 treatment on the development of glomeurlonephritis in *MRL-lpr/lpr* mice, we evaluated kidneys at the age of 23 weeks of two mice in each group and those mice, which became moribund earlier according to the WHO morphologic classification of lupus nephritis (Peutz-Kootstra *et al*, 2001). The following histological characteristics were graded from 0 to 3+ according to severity for: 1) glomerular cell proliferation; 2) leucocyte exudation; 3) karyorrhexis and fibrinoid necrosis; 4) cellular crescents; 5) hyaline deposits; 6) interstitial inflammation as described in section 2.3.6, with a maximum score of 24. These histological characteristics are demonstrated in Figures 5.2.5.1 to 5.2.5.3, and varied from mild mesangial proliferation to full-blown proliferative and crescentic glomerulonephritis.

Figure 5.2.5.1 Light microscopic examination of kidney specimen in control MRL-*lpr/lpr* mouse with diffuse proliferative lupus nephritis showing fibrinoid necrosis, interstitial inflammation, cellular crescents and leucocyte exudation (X100).

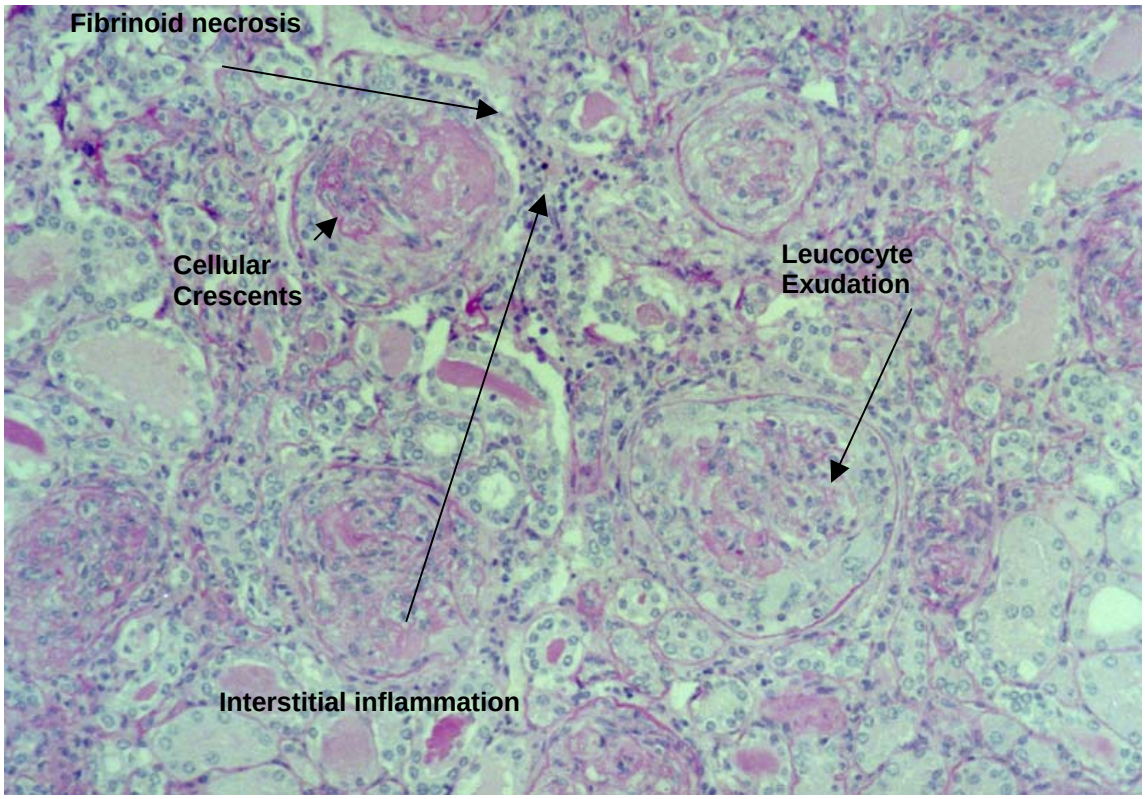

Figure 5.2.5.2 Light microscopic examination of kidney specimen in control MRL-*lpr/lpr* mouse with diffuse proliferative lupus nephritis showing mesangial proliferation (x400).

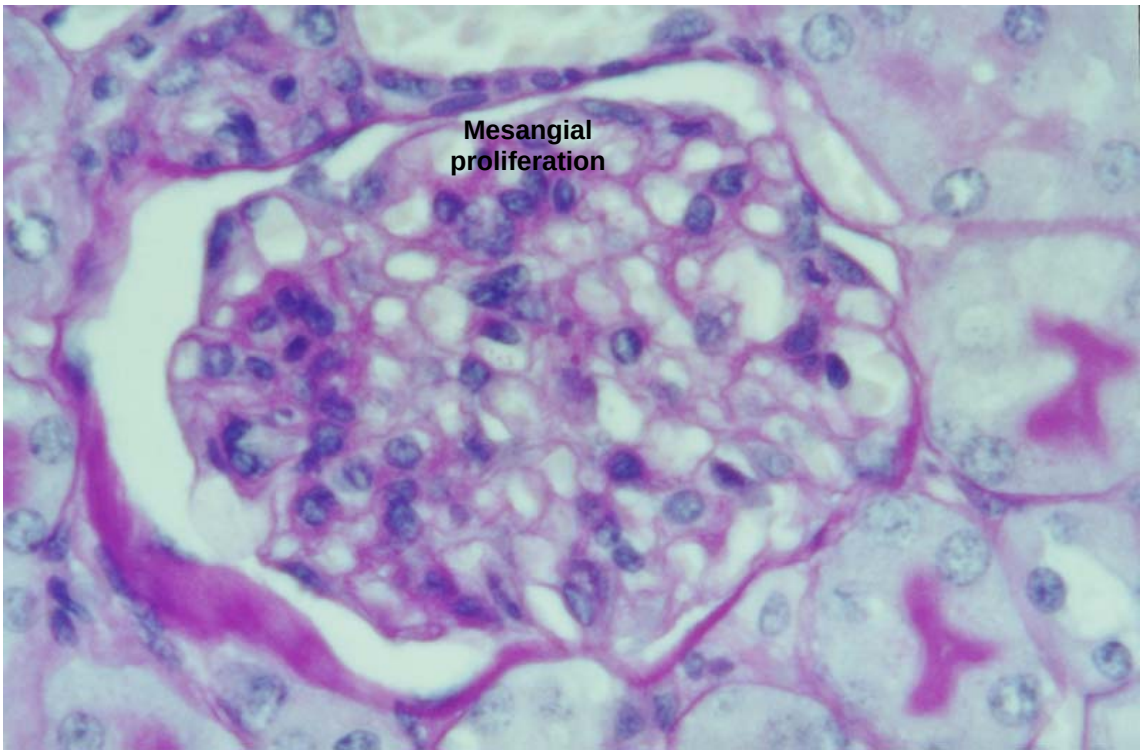

Figure 5.2.5.3 Light microscopic examination of kidney specimen in control MRL-*lpr/lpr* mouse with diffuse proliferative lupus nephritis showing karyorrhexis and hyaline deposits (x200).

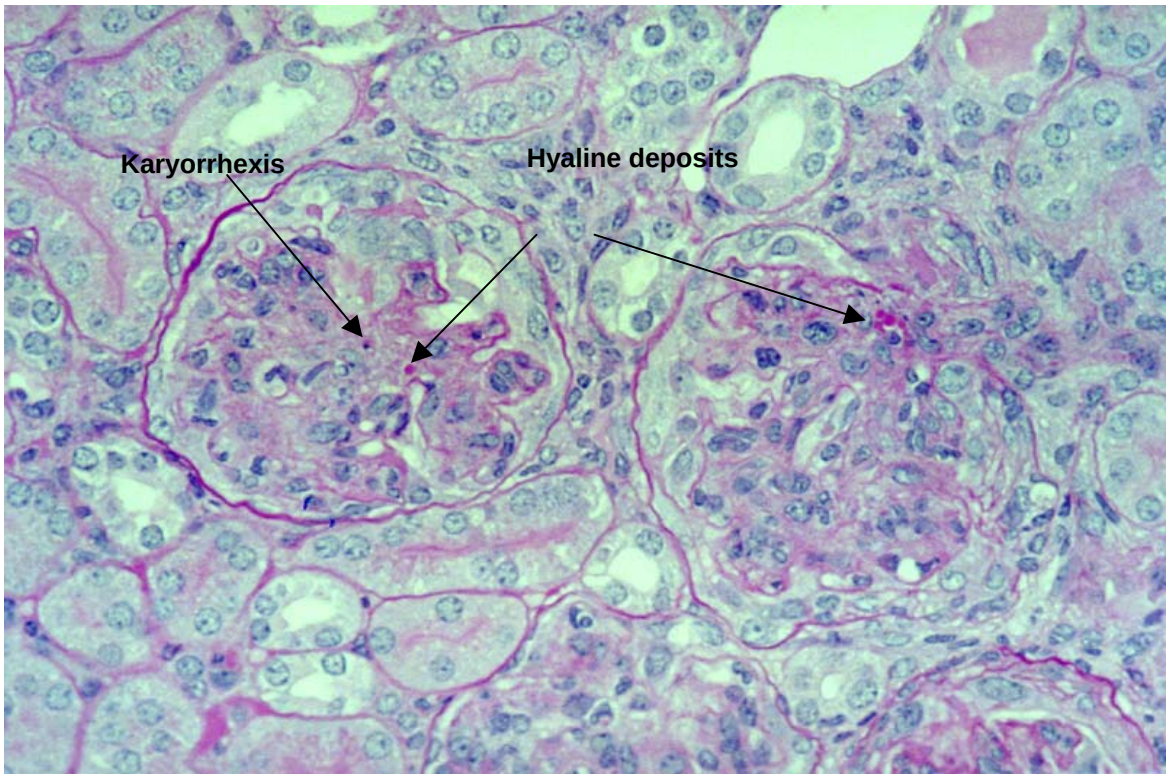

An overall histological index for each kidney was obtained by a score/age ratio to compensate for the effect of age on the progression of disease, summarized in Table 5.2.5.2. Both the CMX-13 treated (0.52±0.18) and Dex-treated groups (0.40±0.11) had lower histological indices than the untreated controls (0.66±0.18) and DMSO controls (0.62±0.20) (Figure 5.2.5.4). However, only the DEX-treated group had significantly different histological index than untreated controls ($p<0.005$) and DMSO-treated group ($p<0.03$).

Table 5.2.5.2. Individual histological scores of the Untreated, DMSO, CMX-13 and DEX treated animals. An overall histological index for each kidney was obtained by a score/age ratio.

Untreated

Age in weeks (n = 7)	score	Histological index (score/age)
23	14	0.608
23	16	0.695
19	14	0.736
17	9	0.529
16	9	0.562
18	9	0.5
22	22	1
Mean ±SD		0.66±0.18

DMSO

Age in weeks (n = 11)	Score	Histological index (score/age)
23	9	0.391
22	11	0.5
23	14	0.608
25	12	0.48
17	16	0.941
22	15	0.681
18	11	0.611
23	9	0.391
21	16	0.761
21	10	0.476
19	20	1.052
Mean ±SD		0.62±0.20

CMX-13 treated mice

Age in weeks (n = 8)	Histological score	Histological index (score/age)
23	15	0.652
25	20	0.8
23	16	0.695
22	12	0.545
24	10	0.416
26	9	0.346
23	10	0.434
25	9	0.36
Mean ±SD		0.52±0.18

DEX treated mice

Age in weeks (n =9)	Histological score	Histological index (score/age)
17	7	0.411
23	7	0.304
18	9	0.5
23	7	0.304
26	10	0.384
26	8	0.307
26	17	0.653
19	8	0.421
26	9	0.346
Mean ±SD		0.40±0.11

Figure 5.2.5.4 Histological indices expressed as a ratio of histological score/age in untreated controls, DMSO controls, CMX-treated and DEX-treated groups. [a]Comparing DEX-treated group with controls, p<0.005. [b]Comparing DEX-treated group with DMSO controls, p<0.03.

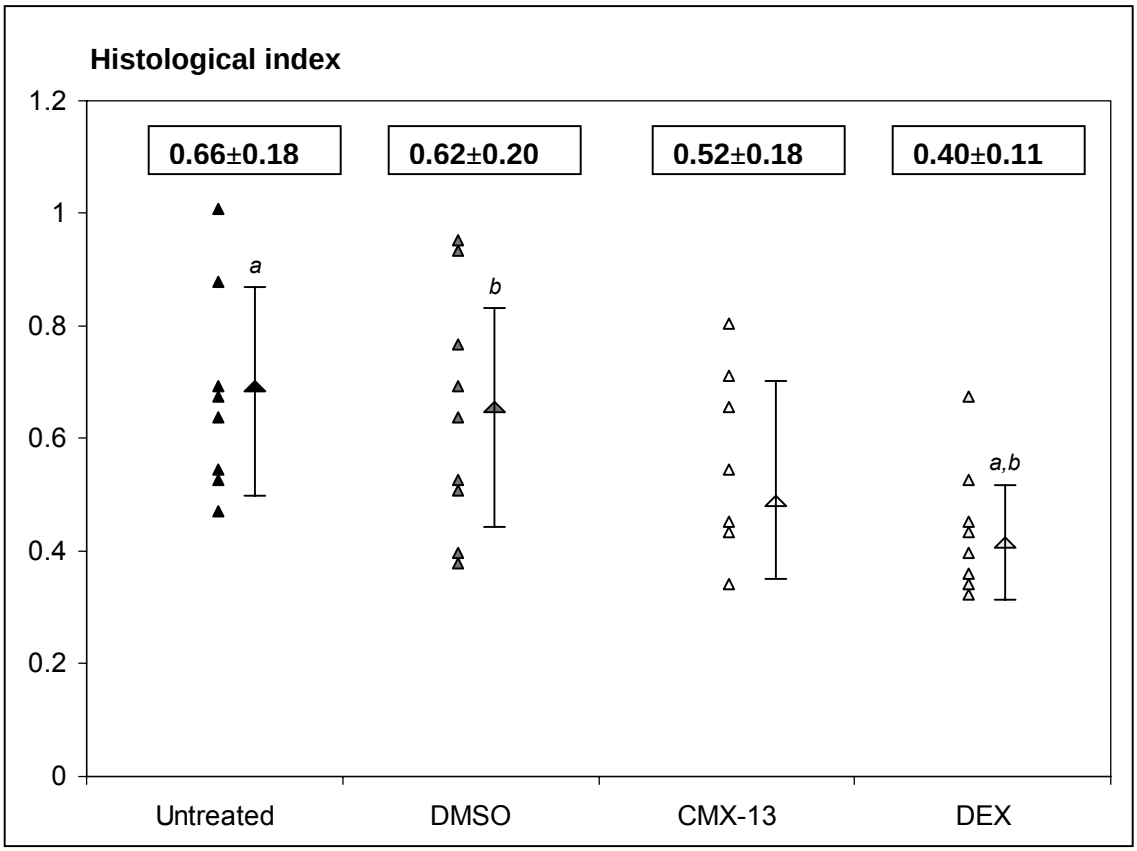

5.2.6 Effect of CMX-13 on Life Span of MRL-*lpr/lpr* Mice

In the autoimmune MRL-*lpr/lpr* mice, the severity of the disease increases with age of the mice, with the majority dying of renal failure at 16-24 weeks of age [Putterman and Naparstek, 1994]. At the beginning of this study, 8-week old female MRL-*lpr/lpr* mice were divided randomly into 4 groups of 13 animals. Each group received by intra-peritoneal injection either 100μl PBS, 16% v/v of DMSO, 25 mg/kg of CMX-13, or 1 μg/kg of DEX, on alternate days, and was observed daily. A Kaplan-Meier survival analysis was done on the MRL-*lpr/lpr* mice where death before the age of 22 weeks was defined as the outcome parameter. Appendix 5.3 shows the life-table calculations for the different groups.

As shown in Figure 5.2.6.1, only 2 mice of the untreated controls and 3 of the DMSO controls survived at 22 weeks of age. The survival of each group is summarized in Table 5.2.6.1 On the other hand 9 of the mice treated with CMX-13 and 7 of DEX-treated mice were alive at 22 weeks. Kaplan-Meier analysis showed that only the CMX-13-treated group had significantly increased survival when compared with control ($p=0.005$) and DMSO-treated ($p=0.049$) groups. DEX treatment did improve survival, as 7 animals were alive when the experiment was terminated at week 22, however it was not statistically significant when compared to the Untreated and DMSO treated animals.

Table 5.2.6.1 (I): Cumulative survival of individual mice in the Untreated group

Case	Time in weeks	Status	# mouse entered	Prop. Dead q_i = = dead / = entered	Prop. Surv. P_1= 1- q_i	Cum. Surv. P_1 = P_{i-1} x P_i
1	8	Surv	13	0/13 = 0	1	1 x 1 = 1
2	12	Dead	12	1/12 = 0.08	0.92	1 x 0.92 = 0.92
3	13	Surv	12	0	1	0.92 x 1= 0.92
4	14	Dead	11	1/11 =0.09	0.90	0.92 x 0.9 = 0.83
5	15	Surv	11	0	1	0.83 x 1 = 0.83
6	16	Dead	10	1/10 = 0.1	0.90	0.83 x 0.9 = 0.75
7	17	Dead	7	3/7 = 0.4	0.6	0.75 x 0.6 = 0.45
8	18	Dead	5	2/5 = 0.4	0.6	0.45 x 0.6 = 0.27
9	19	Dead	3	2/3 = 0.67	0.33	0.27 x 0.33 = 0.09
10	20	Dead	3	0/3 = 0	1	0.09 x 1 = 0.09
11	21	Surv	3	0	1	0.09 x 1 = 0.09
12	22	Dead	2	½ = 0.5	0.5	0.09 x 0.5 0.045

Table 5.2.6.1 (II): Cumulative survival of individual mice in the DMSO treated group.

Case	Time in weeks	Status	# mouse entered	Prop. Dead q_i = = dead / = entered	Prop. Surv. P_1= 1- q_i	Cum. Surv. P_1 = P_{i-1} x P_i
1	8	Surv	13	0/13 = 0	1	1
2	12	Surv	13	0	1	1
3	13	Surv	13	0	1	1
4	14	Surv	13	0	1	1
5	15	Surv	13	0	1	1
6	16	Surv	13	0	1	1
7	17	Dead	12	1/12 = 0.08	0.92	0.92
8	18	Dead	10	2/10 = 0.2	0.8	0.92 x 0.8 = 0.74
9	19	Dead	9	1/9 = 0.1	0.9	0.74 x 0.9 = 0.67
10	20	Surv	9	0	1	0.67
11	21	Dead	6	3/9 = 0.30	0.7	0.67 x 0.7 = 0.47
12	22	Dead	3	3/6= 0.5	0.5	0.47 x 0.5 = 0.24

Table 5.2.6.1 (III): Cumulative survival of individual mice in the CMX-13 treated group.

Case	Time in weeks	Status	# mouse entered	Prop. Dead q_i = = dead / = entered	Prop. Surv. P_1= 1- q_i	Cum. Surv. P_1 = P_{i-1} x P_i
1	8	Surv	13	0/13 = 0	1	1
2	12	Surv	13	0	1	1
3	13	Surv	13	0	1	1
4	14	Dead	12	1/12 = 0.08	0.92	0.92
5	15	Surv	12	0	1	0.92
6	16	Dead	11	1/11 = 0.09	0.91	0.92 x 0.91 =
7	17	Dead	10	1/10 = 0.1	0.9	0.83
8	18	Surv	10	0	1	0.83
9	19	Surv	10	0	0.9	0.83 x 0.9 = 0.75
10	20	Surv	10	0	1	0.75
11	21	Surv	10		0.7	0.75 x 0.7 = 0.53
12	22	Surv	9	1/9= 0.1	0.9	0.53 x 0.9 = 0.48

Table 5.2.6.1 (IV): Cumulative survival of individual mice in the DEX treated group.

Case	Time in weeks	Status	# mouse entered	Prop. Dead q_i = = dead / = entered	Prop. Surv. P_1= 1- q_i	Cum. Surv. P_1 = P_{i-1} x P_i
1	8	Surv	13	0/13 = 0	1	1
2	12	Surv	13	0	1	1
3	13	Surv	12	1/12 = 0.08	0.92	0.92
4	14	Dead	12	0	0.92	0.92 x 0.92 = 0.85
5	15	Surv	12	0	1	0.85
6	16	Surv	12	0	0.91	0.85 x 0.91 = 0.77
7	17	Dead	9	3/9 = 0.3	0.7	0.77 x 0.7 = 0.54
8	18	Surv	8	1/8 = 0.12	0.88	0.88 x 0.54 = 0.48
9	19	Surv	7	1/7 = 0.14	0.86	0.48 x 0.86 = 0.41
10	20	Surv	7	0	1	0.41 x 1= 0.41
11	21	Surv	7	0	1	0.41
12	22	Surv	7	0	1	0.41

Figure 5.2.6.1 Kaplan-Meier survival analysis in MRL-lpr/lpr mice following CMX-13 or DEX treatment compared with Untreated controls and solvent (DMSO) controls. [a]Comparison between CMX-13 treatment group and untreated controls, p<0.005. [b]Comparison between CMX-13 treatment group and DMSO controls, p<0.05).

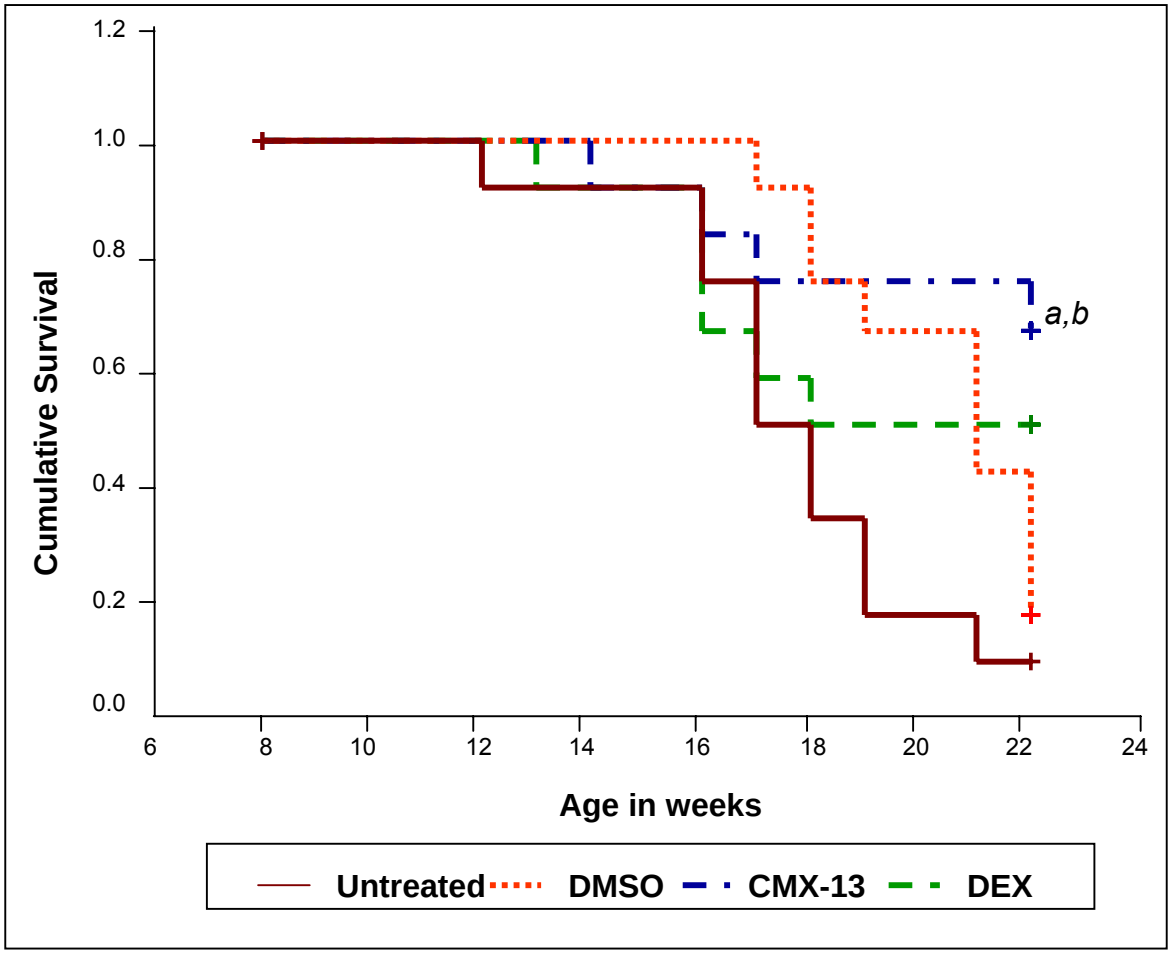

5.3 DISCUSSION

MRL-*lpr/lpr* mice represent an excellent model to study the pathogenesis of lupus nephritis [Theofilopoulos et al., 1985]. These mice spontaneously develop a generalized autoimmune disease, including vasculitis, generalized lymphadenopathy, arthritis and a severe immune complex glomerulonephrititis, dying of renal failure between 5 to 8 months of age [Andrews et al., 1978]. These mice also produce autoantibodies such as anti-double-stranded DNA antibodies and anti-IgG (rheumatoid factor). Defective transcription of the apoptosis gene encoding Fas (CD95) causes lymphoproliferation of double-negative ($TCR\alpha\beta CD3^{+}CD4^{-}CD8^{-}B220^{+}$) T cells and autoantibody-producing B cells [Watanabe et al., 1992; Adachi et al., 1993]. This leads to massive lymphadenopathy, elevated serum anti-dsDNA antibody levels, and progressive lupus nephritis, as seen in the untreated control mice and the control group treated with the solvent DMSO in our experiment.

In the untreated and DMSO control mice, lymphadenopathy started to become visible from the age of 12-13 weeks (Figure 5.2.1.4), whereas development of significant lymphadenopathy in the CMX-13 and DEX treatment groups was delayed until at least 18 weeks, and was less severe than the control groups. In previous studies, Morton and co-workers reported that 3% DMSO supplemented in the drinking water of C3H/*lpr* SLE mouse model decreased the severity of lymphadenopathy [Morton and Siegel, 1986]. On the other hand, intraperitoneal

injections of 50% DMSO over a period of 20 weeks, was not shown to reduce lymphadenopathy [Morton et al., 1983]. In our experiment, where CMX-13 and DEX were dissolved in 16% DMSO, it was unlikely that DMSO was responsible for the reduction of lymphadenopathy in these treatment groups, as the DMSO control group given 16% DMSO intraperitoneally, developed marked lymphadenopathy early, similar to the untreated controls. The *lpr* $CD4^+$ T-cells have been shown to be the source of the $TCR\alpha\beta CD3^+CD4^-CD8^-B220$ T-cells responsible for the massive lymphadenopathy in MRL-*lpr/lpr* mice [Laouar and Ezine, 1994], and these cells are resistant to apoptosis [Bossu et al., 1993]. As we have shown in chapter 4 that CMX-13 was able to induce apoptosis, studies on apoptosis of these cells in the lymph nodes of CMX-13 treated mice may provide further insight into its immunosuppressive mechanism.

MRL-*lpr/lpr* mice typically develop skin lesions of back, neck and ears by the age of 20-24 weeks [Reininger et al., 1990; Chan et al., 2001]. As the surviving mice in our experiment were sacrificed after 22 weeks of age, development of skin lesions and arthritis was not universally seen in our experimental mice, with only some of the DMSO controls developing these lesions. However, all our mice developed anti-dsDNA antibodies from the age of 8 weeks. The untreated and DMSO control mice had the highest level of rise in antibody concentrations by 16 weeks of age, whereas both the CMX-13 and DEX-treated groups had significantly lower anti-dsDNA antibody levels (Figure 5.2.3.1). Serum creatine levels were also measured at the age of 16 weeks. However, the changes in the

serum creatine levels were not significant (Figure 5.4.2.1). The solvent DMSO had no effect on anti-dsDNA antibody levels in our studies, similar to the work by Milner and co-workers who showed that DMSO given intraperitoneally as a 75% solution did not affect the development of autoantibodies in NZB/W F_1 lupus mice [Milner et al., 1987].

Mice homozygous for the mutation in the *lpr* gene develop lupus-like autoimmunity characterized not only by the accumulation of double negative T cells, but also non-malignant autoantibody-producing B cells. Anti-dsDNA antibodies were first described 40 years ago, and it is well-known that the production of these autoantibodies is driven by hyperreactive B-cells [Kotzin, 1996]. However, little is known about their role in the pathogenesis of tissue and organ injury [Eilat and Naparstek, 1999]. Anti-dsDNA antibodies have often been implicated in the development of glomerulonephritis [Koffler et al., 1967; Lambert and Dixon, 1968]. Earlier studies suggested that entrapment of anti-dsDNA antibodies in the glomerulus could be the cause of the proliferative lesion seen in lupus nephritis [Yamada et al, 1982]. Recent studies on the autoantibody specificities from kidney eluates in lupus mice have shown that cross-reactive anti-dsDNA antibodies predominate, and these antibodies also bound to glomerular substrate and laminin [Xie et al., 2003]. Hence development of glomerulonephritis and vasculitis could be due to *in-situ* immune complex formation in the glomerular and vascular sites [Vlahakos et al, 1992]. The *in-situ* formation of these immune complexes was also thought to be due to the binding

of anti-DNA antibodies to structural proteins found in mesangial cells and glomerular podocytes, such as α-actinin [Mostoslavsky et al, 2001]. Moreover, prevention of binding of anti-DNA antibodies to the glomeruli by low-dose heparin was found to inhibit the progression of glomerulonephritis in MRL-*lpr/lpr* mice [Naparstek et al., 1990].

The increased mortality seen in the MRL-*lpr/lpr* mice is attributed in a large part to the development of progressive severe proliferative lupus nephritis, with the majority of mice dying of renal failure at 16-24 weeks of age. In this chapter, we have shown that CMX-13 was able to improve survival of the MRL-*lpr/lpr* mice compared to the untreated or DMSO controls (Figure 5.2.6.1). At 22 weeks of age, 9 of the mice treated with CMX-13 were still alive, whereas only 2 of the untreated controls and 3 of the DMSO controls survived.

In the MRL-*lpr/lpr* mice, the severity of kidney disease increases with age and manifests as mesangial and endothelial cell proliferation, occasional crescent formation, thickening of the glomerular capillary walls and tubulointerstitial nephritis with vasculitis [Austin et al, 1984: Moyer et al, 1987; Appel and Valeri, 1994; Putterman and Naparstek, 1994]. The acute glomerular inflammation results in proteinuria, which is usually apparent by the age of 8-12 weeks in the MRL-*lpr/lpr* mice [Eilat and Naparstek, 1999; Appel and Valeri, 1994]. In our experiment, CMX-13 treatment of MRL-*lpr/lpr* mice with progressive lupus

nephritis resulted in decrease in the degree of proteinuria and improvement in renal histological indices (Figure 5.2.5.4).

In conclusion, this chapter shows that CMX-13 appeared to be effective in attenuating clinical and histological disease activity in the MRL-*lpr/lpr* mouse model of SLE. The exact mechanism of the immunosuppressive action of CMX-13 remains to be elucidated, and the next chapter will be addressing some of the possible pathways that CMX-13 may be exerting its effect.

CHAPTER 6 EFFECT OF CMX-13 ON CYTOKINE GENE EXPRESSION IN THE MRL-*lpr/lpr* SLE MOUSE MODEL

6.1 INTRODUCTION

SLE is an autoimmune disease that involves increased production of IgG autoantibodies and immune complex deposition in the microvasculature of organs such as the kidney, resulting in complement activation, leucocyte infiltration and tissue damage. Affinity maturation of B cells with isotype switching are T-cell dependent processes, hence the similarity of the anti-dsDNA response in murine and human SLE strongly supports the hypothesis that T helper cells are involved in the pathogenesis. $CD4^+$ T-cells act as the driving force for the hyperreactive B-cells through the production of cytokines [Kotzin, 1996;Theofilopoulos et al., 1989]. The role of cytokines in providing the non-specific help, as well as in mediating tissue injury is currently being investigated.

In patients with active disease as well as in experimental murine models of SLE, both the serum cytokine levels and gene expression in PBMCs have been found to be abnormal [Prud'homme, 1995]. In fact, there have been reports of a relationship between abnormal cytokine mRNA levels and disease activity [Linker-Israeli et al., 1991]. For example, increased IL-10 and IFN-γ gene expressions have been described in SLE patients, and this correlated with disease activity [Csiszar et al., 2000]. Moreover, several studies have described

an imbalance of Th1 (IL-2 and IFN-γ) and Th2 (IL-6 and IL-10) cytokines in patients with SLE. mRNA expression of IFN-γ has been shown to be elevated in MRL-lpr/lpr autoimmune mice [Murray and Martens, 199o; Prud'Homme et al., 1995], suggesting that IFN-γmay play a role in the genesis of SLE. In contrast, IL-2 mRNA expression in the MRL-*lpr/lpr* mice was downregulated.

IFN-γ is a key cytokine that controls Th1-dependent Ab production and is crucial for functional immune responses. IFN-γ is secreted by activated T-cells and natural killer (NK) cells and promotes inflammation. High levels of IFN-γ mRNA have been found in PBMCs from SLE patients [Csiszar et al., 2000]. IFN-γ has also been demonstrated in the renal tissue of SLE patients with severe lupus nephritis, compared to individuals with milder renal disease [Akahoshi et al., 1999; Masutani et al., 2001]. The predominant role of IFN-γ in disease pathogenesis has been demonstrated in murine lupus [Takahashi et al., 1996], where disease activity in the MRL-*lpr/lpr* mice was linked to the presence of IFN-γ [Peng et al., 1997; Haas et al., 1997]. Interestingly, transgenic expression of IFN-γ in the epidermis of non-autoimmune mice resulted in the development of inflammatory skin disease resembling lupus erythematosus [Seery et al., 1997]. Following treatment with IFN-γ the onset of disease was aggravated in NZB X NZWF1 mice [Jacob et al., 1987]. Blocking or inhibition of IFN-γ had a positive affect on disease symptoms, and deletion of either the IFN-γ gene or IFN-γ receptor gene in lupus mice reduced the severity of glomerulonephritis [Haas et

al., 1998]. Decreasing IFN-γ production by approximately 50% decreased both autoantibody production and onset of glomerulonephritis [Lawson et al., 2000; Ozmen et al., 1995]

IL-2 mRNA expression has been shown to be downregulated in PBMCs from SLE patients [Crispin and Alcocer-Varela, 1998]. Moreover, *in-vitro* IL-2 production by PBMCs was impaired following stimulation with antigens [Alcocer-Varela and Alarcon-Segovia, 1982]. Other studies have shown that the defective production of IL-2 occurred in both $CD4^+$ and $CD8^+$ T-cells [Murakawa et al., 1985]. Additionally, there was impaired IL-2-stimulated T-cell proliferation in SLE patients [Miyasaka et al., 1984]. This decrease in PBMC IL-2 secretion was not due to an intrinsic T-cell defect, as production of IL-2 returned to normal when the cells were isolated and allowed to rest *in-vitro* for a few days before antigen stimulation [Huang et al., 1986]. However, in the MRL-*lpr/lpr* murine lupus model, no difference was observed in the IL-2 mRNA expression when compared to the MRL-*wt* mice. There was also no detectable increase in IL-2 gene expression in the $TCR\alpha\beta CD3^+CD4^-CD8^-B220^+$ T-cells of these mice [Murray et al, 1990]. IL-2 is an important cytokine that determines the balance between cell proliferation and apoptosis [Lenardo, 1991]. IL-2 induces apoptosis in $CD4^+$ and $CD8^+$ T-cells [Lenardo, 1991] and this is mediated by the Fas-FasL-pathway [Refaeli et al., 1998]. As discussed in chapter 4, the Fas-FasL apoptotic pathway is defective in the murine MRL-*lpr/lpr* autoimmune model. Hence administration of IL-2 could result in improvement in the disease. Guitierrez-Ramos and co-

workers were able to prevent autoimmune disease in MRL-*lpr/lpr* mice by transfecting them with IL -2/vaccinia recombinant virus [Gutierrez-Ramos, 1991].

The levels of Th2 cytokines IL-6 and IL-10 were found to be elevated in the serum of SLE patients [Grondal et al., 2000; Jones et al., 1999]. IL-6 is a multifunctional cytokine and is involved in the growth and differentiation of B and T-cells. IL-6 is produced by a variety of different cell types upon induction by viral infections [Cayphas et al., 1987; van Snick, 1990] and stimulation by other pro-inflammatory cytokines such as IL-1 and TNF-α [Akira et al., 1993]. IL-6 has B-cell stimulatory activity and induces the secretion of other cytokines. Together with IFN-γ it plays a significant role in inflammation and may be linked to the development of inflammatory lesions [Prud'homme, 1993], including proliferative glomerulonephritis [Horii et al, 1993]. IL-6 has been reported to be upregulated in the sera [Swaak et al., 1989] and renal biopsy specimens of SLE patients [Horii et al., 1993]. This finding was supported by studies which showed that treatment of lupus-prone NZB/NZW F1 mice with anti-IL-6 antibody abrogated the disease [Finck et al., 1994b]. Several studies have reported elevation of IL-6 concentrations in the urine of patients with lupus nephritis, and this was a reliable indicator of the progression of lupus nephritis [Iwano et al., 1993]. IL-6 has been shown to stimulate glomerular mesangial cell proliferation [Horii et al, 1993].

B-cell hyperactivity in SLE patients is thought to be induced by IL-6 [Linker-Isreali et al., 1991]. The increased IL-6 levels were shown to be related to increased stability of IL-6 mRNA expression levels in these patients [Linker-Israeli et al., 1999]. The stability of the IL-6 gene transcripts implies that there would be no correlation between the increased levels of IL-6 protein and mRNA expression during periods of active disease [Cross and Benton et al., 1999].

IL-10 is a regulatory cytokine that inhibits Th1 cytokine production and proliferation of $CD4^+$ T cells [Moore et al., 2001]. This anti-inflammatory cytokine promotes Th2 immune responses by their effect on antigen-presenting cells as well as a direct effect on T-cells [Moore et al., 1993]. Patients with SLE have been shown to have increased serum levels of IL-10 [Llorente et al., 1995], with enhanced gene expression in the PBMC [Csiszar et al., 2000]. The serum IL-10 levels correlated with disease activity [Park et al., 1998; Hagiwara et al., 1996]. The precise role of IL-10 in the pathogenesis of SLE is not well understood. Continuous administration of IL-10 to the NZB/NZW F1 SLE mouse accelerated the onset of renal disease, while treatment with anti-IL-10 monoclonal antibodies (mAb) delayed onset of the disease [Ishida et al., 1994]. In another study, significant improvement of SLE symptoms and SLEDAI scores was achieved when 6 patients with active SLE were treated with murine IgG1 anti-IL-10 mAb for 21 days [Llorente et al., 2000]. This beneficial effect was seen up to 6 months following cessation of treatment.

Studies on the MRL-*lpr/lpr* mice have identified various cytokine abnormalities [Lemay et al., 1996; Prud'Homme et al., 1995]. The following cytokine genes were found to be upregulated in the MRL-*lpr/lpr* mice with autoimmune disease: IFN-γ in lymph nodes, spleen and kidney, TNF-α in the spleen and kidney, IL-1β in lymph nodes, spleen, kidney, and liver, and IL-10 in lymph nodes of diseased mice (Table 6.1.1). IL-2, IL-4, and IL-6 mRNA were not detected in these organs.

Table 6.1.1 Cytokine mRNA expression in MRL-*lpr/lpr* (d) and MRL-*wt* (n) mouse organs by RNase protection assay. LN = lymph nodes; SP =Spleen; KID = Kidney; LIV = Liver. - = no expression, +/- = Normal level, + = Detectable, ++ = heightened level [Lemay et al., 1996; Prud'Homme et al., 1995].

Cytokine	LN/n	LN/d	SP/n	SP/d	KID/n	KID/d	LIV/n	LIV/d
IL-1β	-	++	+/-	++	+/-	++	-	++
IL-2	-	-	-	-	-	-	-	-
IL-4	-	-	-	-	-	-	-	-
IL-6	-	-	-	-	-	-	-	-
IFN-γ	-	+	-	+	-	+	-	-
TNF-α	+	+	-	+	-	+	-	-
IL-10	+	++						

Hence this chapter examined the effect of CMX-13 on cytokine gene expression particular $CD4^+$ and $CD8^+$ T-cells, liver and glomeruli of the autoimmune MRL-*lpr/lpr* mouse. The mice were treated with either, DMSO (solvent control), CMX-13 or DEX as described in chapter 2.3.2, from the age of 12 weeks. Real-time RT-PCR was employed to examine IL-2, IL-6, IL-10 and IFN-γ mRNA expression

in tissues and lymphocyte subsets from each of the groups of MRL-*lpr/lpr* mice that were moribund during the experiment and up to the age of 23 weeks. As a control for these experiments, the mRNA cytokine expression in the corresponding tissues of MRL-*wild type* (MRL-*wt*) mice was examined.

6.2 RESULTS

6.2.1 IL-2 mRNA Expression in and Splenic $CD4^+$ and $CD8^+$ T-cells from MRL-*lpr/lpr* Mice

The IL-2 mRNA expression levels in splenic $CD4^+$ cells of MRL-*lpr/lpr* mice and MRL-*wt* mice at age 23 weeks prior to sacrifice of the surviving mice in all groups, are shown in Table 6.2.1.1. IL-2 mRNA expression was lower in both untreated (0.006±0.003) and DMSO control MRL-*lpr/lpr* mice (0.010±0.003) as compared to MRL-*wt* mice (0.048±0.027) ($p<0.04$). Treatment of the MRL-*lpr/lpr* mice with CMX-13 resulted in a significant increase in IL-2 mRNA expression in $CD4^+$ cells (0.030±0.017), as compared to untreated controls ($p<0.05$) (Figure 6.2.1.1). However, when compared to DMSO controls, this did not reach statistical significance. On the other hand, DEX treatment did not result in a significant increase in $CD4^+$ IL-2 mRNA expression in the MRL-*lpr/lpr* mice (0.021±0.007).

Table 6.2.1.1 IL-2 mRNA expression in $CD4^+$ T-cells from MRL-*lpr/lpr* and MRL-*wt* mice at 23 weeks (mean ± SEM).

Treatment	Untreated (n=6)	DMSO (n=6)	CMX-13 (n=6)	DEX (n=6)	MRL-wt (n=3)
IL-2/ Cyclo-α ratio	0.016	0.022	0.1332	0.014	0.0234
	0.007	0.016	0.0906	0.028	0.0194
	0	0.0009	0.104	0.0031	0.102
	0.0002	0.008	0.1	0.035	
	0.003	0.0008	0.036	0.005	
	0.002	0.014	0.274	0.002	
Mean ± SEM	0.006.±0.003[b,c]	0.010±0.003[a]	0.030±0.017[c]	0.021±0.007	0.048±0.027[a, b]

[a]p<0.02, comparing with MRL-wt mice
[b]p<0.04, comparing with MRL-wt mice
[c]p<0.05, comparing with untreated MRL-*lpr/lpr* mice

Figure 6.2.1.1 Quantitative analysis of IL-2 mRNA expression in splenic $CD4^+$ T-cells isolated from MRL-*lpr/lpr* mice and MRL-*wt* mice at 23 weeks. IL-2 mRNA transcription level was significantly lower in untreated and DMSO-control MRL-*lpr/lpr* mice, as compared to MRL-*wt* mice[a,b]. Treatment with CMX-13 resulted in an increase in $CD4^+$ IL-2 mRNA expression, compared with DMSO control MRL-*lpr/lpr* mice[c]. Bars represent mean ± SEM. (Note: [a]p<0.02; [b]p<0.04; [c]p<0.05)

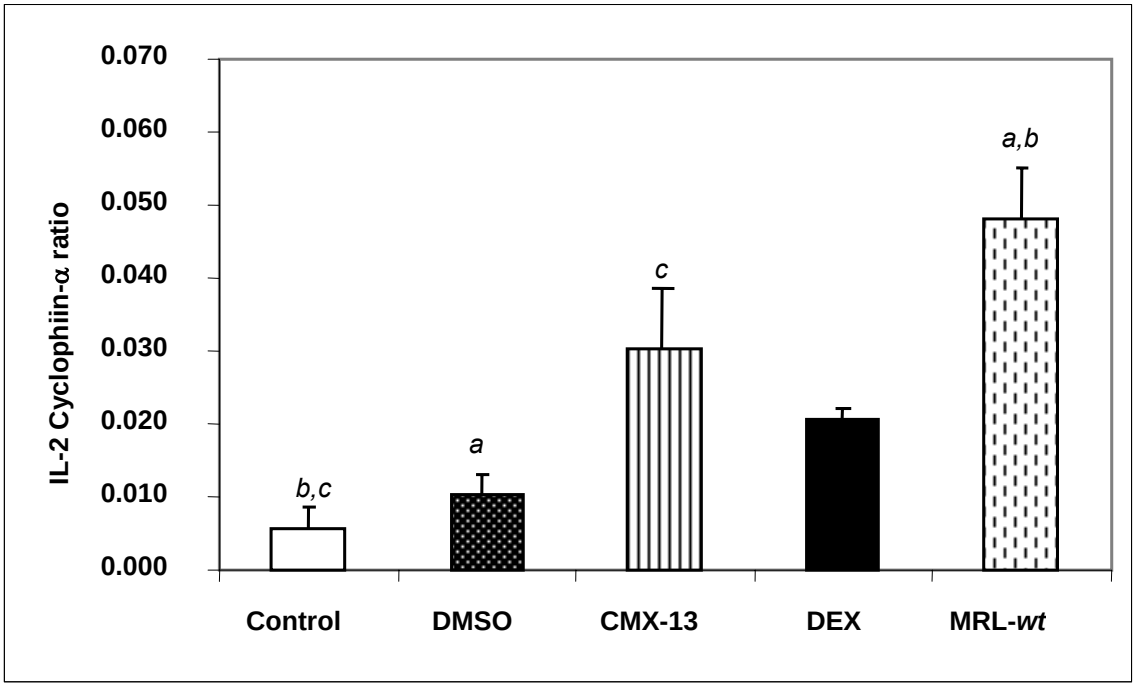

The IL-2 mRNA expression levels in splenic $CD8^+$ T-cells were significantly lower in untreated MRL-lpr/lpr mice (0.005±0.002) compared to MRL-*wt* mice (0.058±0.036) ($p<0.04$). Although DMSO control MRL-*lpr/lpr* mice also had lower $CD8^+$ IL-2 mRNA expression levels (0.010.±0.003) than MRL-*wt* mice, however this did not reach statistical significance probably because of the small numbers. Treatment of MRL-*lpr/lpr* mice with CMX-13 (0.123±0.033) resulted in a significant increase in $CD8^+$ IL-2 mRNA expression compared to untreated and DMSO control animals ($p<0.005$) (Figure 6.2.1.2).

Table 6.2.1.2 IL-2 mRNA expression in $CD8^+$ T-cells from MRL-*lpr/lpr* and MRL-*wt* mice at 23 weeks (mean ± SEM).

Treatment	Untreated (n=6)	DMSO (n=6)	CMX-13 (n=6)	DEX (n=6)	MRL-wt (n=3)
IL-2/ Cyclo-α ratio	0.0062	0.0143	0.1332	0.0048	0.129
	0.004	0.0071	0.0906	0.014	0.0089
	0.0003	0.0087	0.104	0.009	0.037
	0.002	0.011	0.1	0.0067	
	0.003	0.0008	0.036	0.038	
	0.018	0.02	0.274	0.109	
Mean ± SEM	0.005±0.002[a,b]	0.010.±0.003[c]	0.123±0.033[b,c]	0.015±0.006	0.058±0.036[a]

[a]p<0.04, comparing with MRL-*wt* mice
[b]p<0.005, comparing with untreated MRL-*lpr/lpr* mice
[c]p<0.005, comparing with DMSO control MRL-*lpr/lpr* mice

Figure 6.2.1.2 Quantitative analysis of IL-2 mRNA expression in splenic $CD8^+$ T-cells isolated from MRL-*lpr/lpr* mice and MRL-*wt* mice at 23 weeks. IL-2 mRNA transcription level was significantly lower in untreated MRL-*lpr/lpr* mice, as compared to MRL-*wt* mice[a]. Treatment with CMX-13 resulted in an increase in $CD8^+$ IL-2 mRNA expression, compared with Untreated[b] and DMSO control[c] MRL-*lpr/lpr* mice. Bars represent mean ± SEM. (Note: [a]p<0.04; [b]p<0.005; [c]p<0.005)

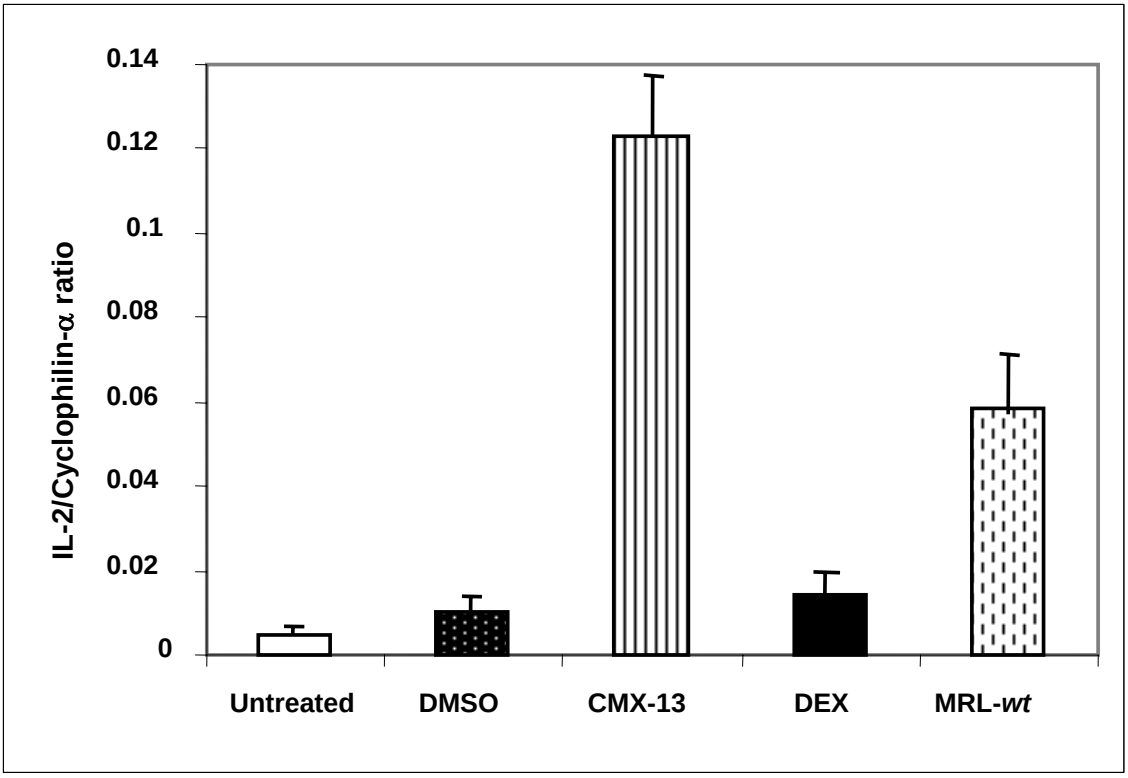

6.2.2 IFN-γ mRNA Expression in Splenic $CD4^+$ and $CD8^+$ T-cells, Liver and Glomeruli from MRL-*lpr/lpr* Mice

The IFN-γ mRNA expression levels in splenic $CD4^+$ cells at age of 23 weeks prior to sacrifice of the surviving mice in all groups, are shown in Table 6.2.2.1. All the groups of MRL-*lpr/lpr* mice had higher IFN-γ mRNA expression than MRL-*wt* mice, although this did not reach statistical significance probably because of the small numbers. Moreover, the IL-2/IFN-γ mRNA ratio was significantly lower in the untreated (0.0095±0.005) and DMSO control (0.011±0.003) MRL-*lpr/lpr* mice, compared to the MRL-*wt* mice (0.73±0.34) ($p<0.03$). Treatment with either CMX-13 or DEX did not reduce the IFN-γ mRNA expression levels (Figure 6.2.2.1). However, CMX-13 treatment of the MRL-*lpr/lpr* mice resulted in an increase in the IL-2/IFN-γ mRNA ratio (0.027±0.010), compared to either the untreated or DMSO control mice, although this did not reach statistical significance because of the small numbers (Table 6.2.2.1).

Table 6.2.2.1 IFN-γ mRNA expression and IL-2/IFN-γ mRNA ratio in splenic $CD4^+$ T-cells from MRL-*lpr/lpr* and MRL-*wt* mice at age 23 weeks (mean ± SEM).

Treatment	Utreated (n= 6)	DMSO (n= 6)	CMX-13 (n= 6)	DEX (n= 6)	MRL-wt (n= 3)
IFN-g/Cyclo ratio	6.798	0.925	0.204	0.322	0.0205
	0.185	1.01	0.211	3.256	0.0196
	0.16	2.398	1.74	0.554	1.925
	0.357	0.521	1.556	0.308	
	0.795	0.341	0.796	2.139	
	1.403	1.19	8.012	1.138	
Mean ± SEM	1.62±1.05	1.06±0.30	2.09±1.21	1.29±0.49	0.66±0.64
IL-2/IFN-γ ratio	0.0095±0.005[a]	0.011±0.003[a]	0.027±0.010	0.017±0.004	0.73±0.34

[a] $p<0.03$; comparing with MRL-*wt* mice

Figure 6.2.2.1 Quantitative analysis of IFN-γ mRNA expression in splenic $CD4^+$ T-cells of MRL-*lpr/lpr* mice and MRL-*wt* mice at age 23 weeks. The IFN-γ mRNA transcripts were higher in all the groups of MRL-*lpr/lpr* mice compared to the MRL-*wt* mice. Bars represent mean ± SEM.

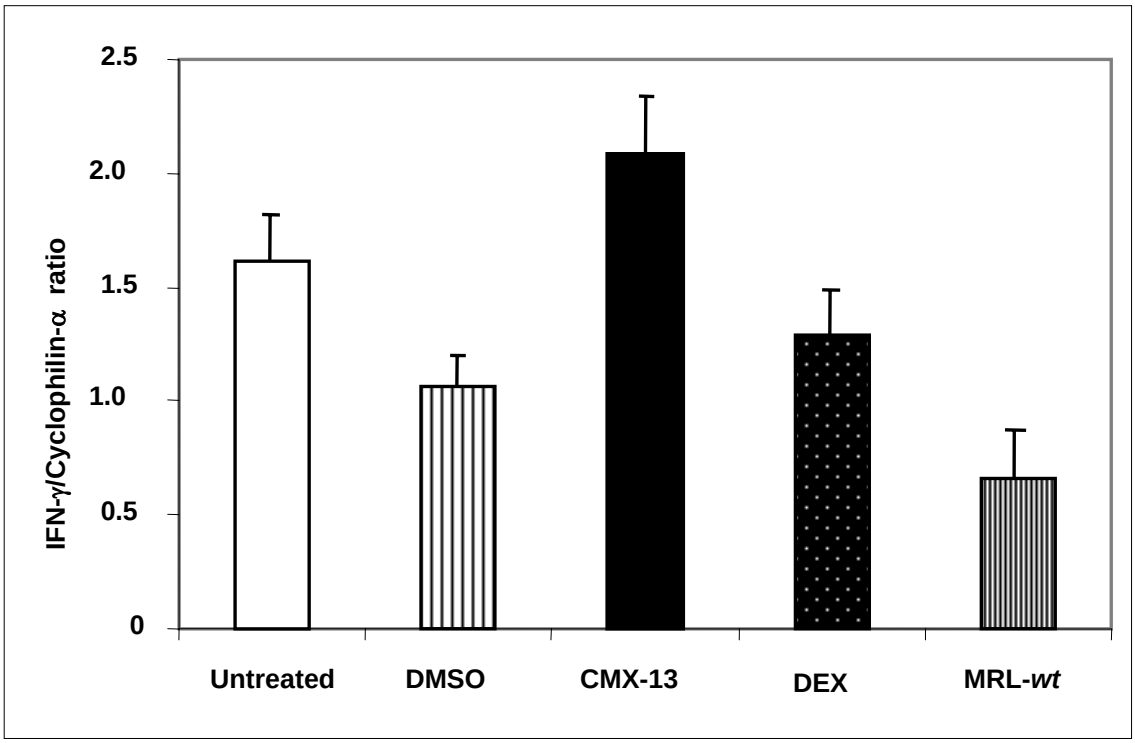

The IFN-γ mRNA expression levels in splenic $CD8^+$ cells at age of 23 weeks prior to sacrifice of the surviving mice in all groups, are shown in Table 6.2.2.2. There was no significant difference between the IFN-γ mRNA levels in the untreated, DMSO control, CMX-13 and DEX-treated MRL-*lpr/lpr* mice, as well as the MRL-*wt* mice (Figure 6.2.2.2). However, the IL-2/IFN-γ mRNA ratio was significantly lower in the untreated MRL-*lpr/lpr* mice (0.0041±0.0011) compared to the MRL-*wt* mice (0.086±0.050) ($p<0.03$) (Table 6.2.2.2). Treatment with CMX-13 resulted in an increase in the IL-2/IFN-γ mRNA ratio (0.42±0.25) compared to the untreated ($p<0.005$) and the DMSO control MRL-*lpr/lpr* mice (0.018±0.005).

Table 6.2.2.2 IFN-γ mRNA expression in splenic $CD8^+$ T-cells from MRL-*lpr/lpr* and MRL-*wt* mice at 23 weeks (mean ± SEM).

Treatment	Utreated (n= 6)	DMSO (n= 6)	CMX-13 (n= 6)	DEX (n= 6)	MRL-wt (n= 3)
IFN-γ/Cyclo ratio	1.998	0.627	0.132	0.54	2.026
	1.251	0.917	0.065	2.015	0.049
	0.151	0.065	4.643	0.015	3.262
	0.04	1.778	3.76	0.046	
	0.967	0.028	2.502	3.087	
	0.648	1.963	6.608	0.431	
Mean ± SEM	0.84±0.30	0.90±0.34	2.95±1.06	1.02±0.51	1.78±0.94
IL-2/IFN-γ ratio	0.0041±0.0011[a]	0.018±0.005[c]	0.42±0.25[b]	0.17±0.12	0.086±0.050

[a] $p<0.03$; comparing with MRL-*wt* mice
[b] $p<0.005$; comparing with untreated MRL-*lpr/lpr* mice
[c] $p<0.03$; comparing with untreated MRL-*lpr/lpr* mice

Figure 6.2.2.2 Quantitative analysis of IFN-γ mRNA expression in the splenic $CD8^+$ T-cells of MRL-*lpr/lpr* and the MRL-*wt* mice. CMX-13 treatment of the MRL-*lpr/lpr* mice resulted in an increase in the IFN-γ mRNA transcripts. Bars represent mean ± SEM.

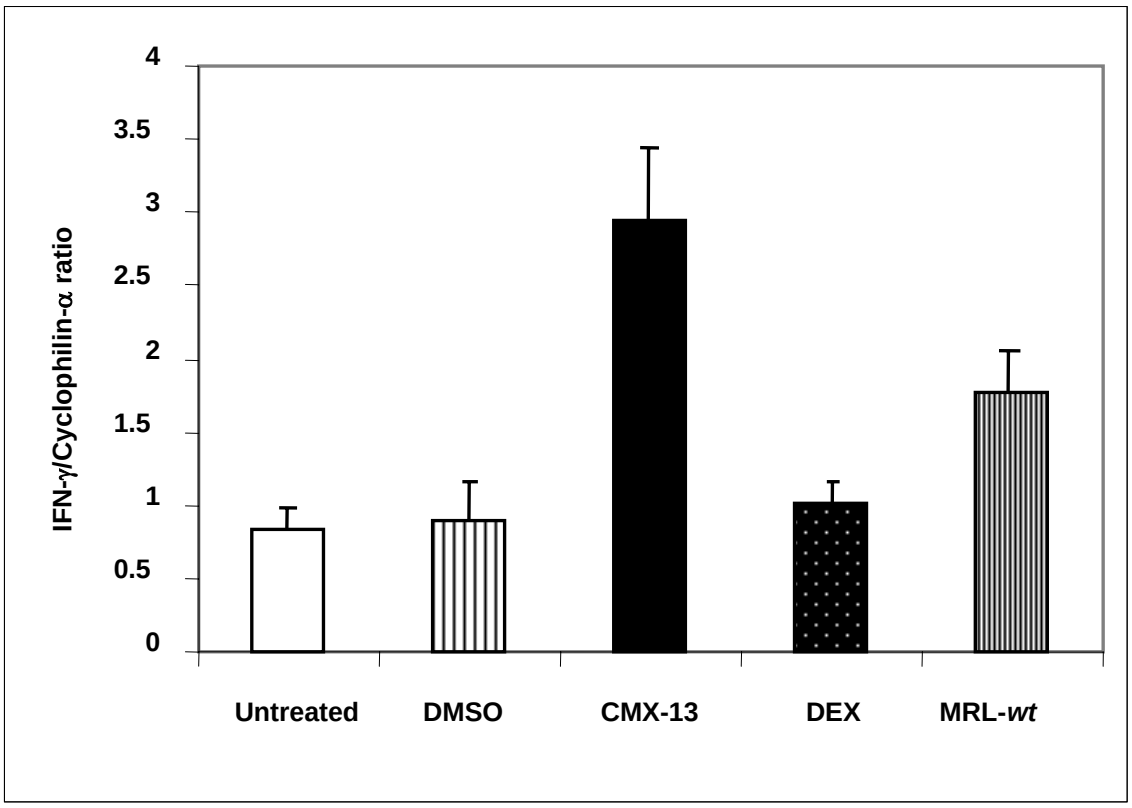

The IFN-γ mRNA expression levels in the glomeruli isolated from the different treatment groups of MRL-*lpr/lpr* and MRL-*wt* mice are illustrated in Table 6.2.2.3. The glomerular expression of IFN-γ mRNA was significantly higher in the DMSO control MRL-*lpr/lpr* mice (0.022±0.004) compared to the MRL-*wt* mice (0.005±0.001) ($p<0.02$) (Figure 6.2.2.3). Although the IFN-γ mRNA levels were also higher in the untreated, CMX-13 treated and DEX treated MRL-*lpr/lpr* mice, as compared to the MRL-*wt* mice, but because of their small numbers, no statistical significance was observed.

Table 6.2.2.3 IFN-γ mRNA expression in glomeruli isolated from kidneys of MRL-*lpr/lpr* and MRL-*wt* mice at 23 weeks (mean ± SEM).

Treatment	Utreated (n=6)	DMSO (n=6)	CMX-13 (n=6)	DEX (n=6)	MRL-wt (n=3)
IFN-γ/Cyclo ratio	0.198	0.012	0.027	0.021	0.005
	0.043	0.03	0.002	0.003	0.003
	0.007	0.012	0.004	0.002	0.006
	0.002	0.03	0.004	0.011	
	0.034	0.012	0.056	0.042	
	0.018	0.035	0.129	0.035	
Mean ± SEM	0.050±0.030	0.022±0.004[a]	0.037±0.02	0.019±0.07	0.005±0.001

[a] $p<0.03$; compared to MRL-*wt* mice

Figure 6.2.2.3 Quantitative analysis of IFN-γ mRNA expression in glomeruli isolated from the kidneys of MRL-*lpr/lpr* and MRL-*wt* mice. The MRL-*lpr/lpr* mice had higher expression of IFN-γ mRNA transcripts in the glomeruli as compared to the MRL-*wt* mice, however only the DMSO control group reached statistical significance ($p<0.02$)[a]. Bars represent mean ± SEM.

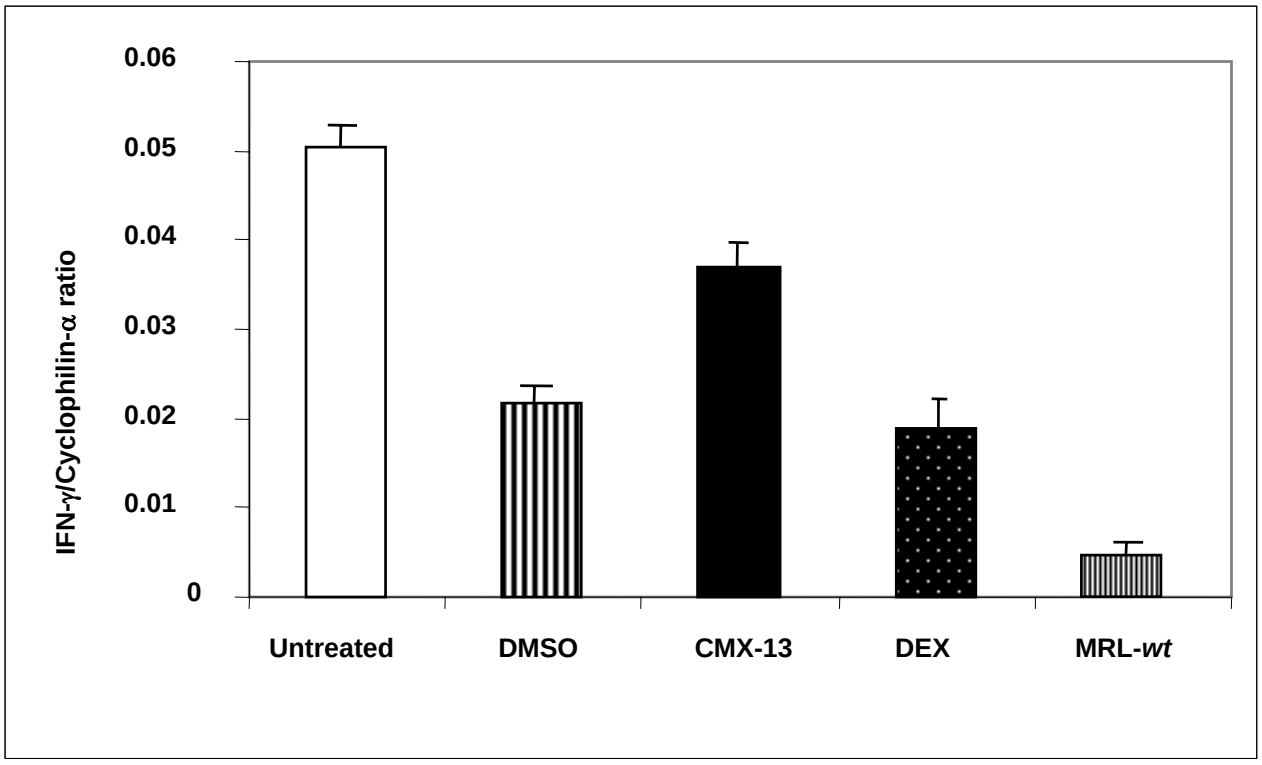

Table 6.2.2.4 outlines the IFN-γ mRNA expression in the liver of MRL-*lpr/lpr* and MRL-*wt* mice. The CMX-13 treated mice had higher IFN-γ mRNA expression than the other groups of MRL-*lpr/lpr* mice, and the MRL-*wt* mice, but this did not reach statistical significance (Figure 6.2.2.4).

Treatment	Untreated (n=6)	DMSO (n=6)	CMX-13 (n=6)	DEX (n=6)	MRL-wt (n=3)
IFN-γ/Cyclo ratio	0.285	0.4	0.003	0.312	0.127
	0.218	0.348	0.009	0.178	0.121
	0.003	0.005	0.997	0.002	0.122
	0.003	0.149	0.495	0.005	
	0.105	0.005	0.262	0.047	
	0.129	0.13	0.395	0.131	
Mean ± SEM	0.12±0.046	0.17±0.069	0.36±0.15	0.11±0.049	0.12±0.002

Figure 6.2.2.4 Quantitative analysis of IFN-γ mRNA expression in the liver of MRL-*lpr/lpr* and MRL-*wt* mice. The highest number of IFN-γ mRNA transcripts was found in the liver of CMX-13 treated MRL-*lpr/lpr* mice. Bars represent mean ± SEM.

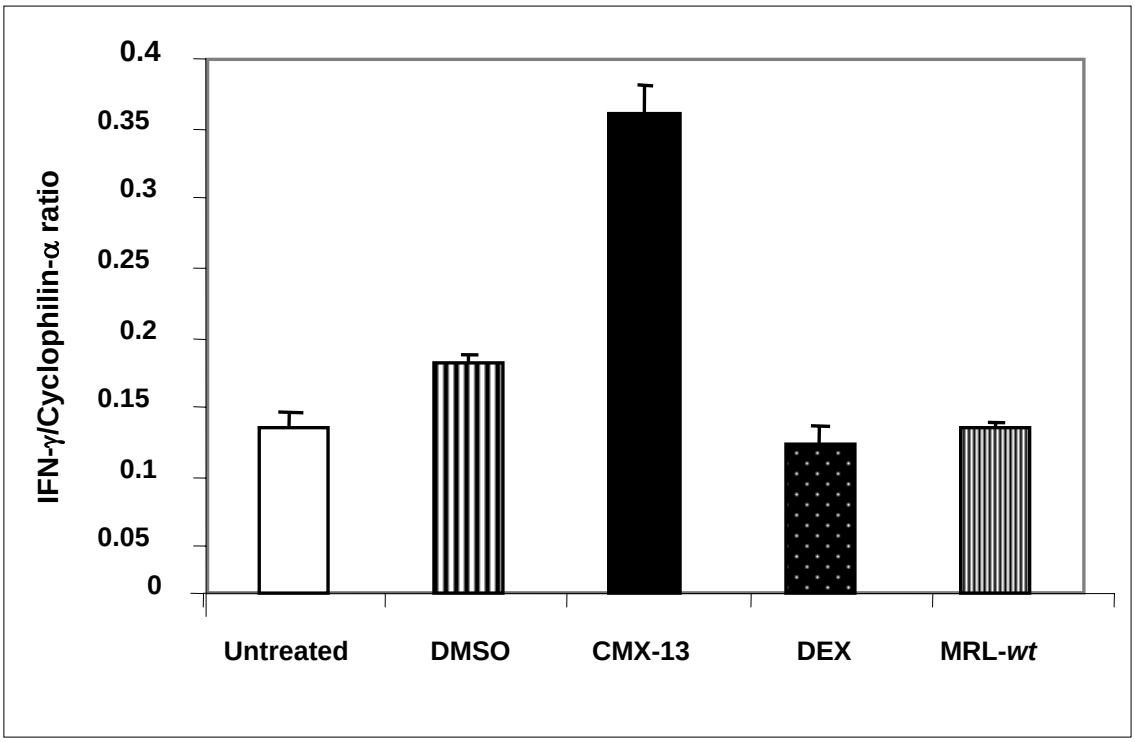

6.2.3 IL-6 mRNA Expression in Splenic $CD4^+$ and $CD8^+$ T-cells and Glomeruli from MRL-*lpr/lpr* Mice

Table 6.2.3.1 outlines the IL-6 mRNA expression levels in splenic $CD4^+$ cells of MRL-*lpr/lpr* and MRL-*wt* mice at the age of 23 weeks. The untreated MRL-*lpr/lpr* mice had higher $CD4^+$ IL-6 mRNA expression compared to MRL-*wt* mice, although this was not statistically significant, probably because of the small numbers in each group. Treatment with CMX-13 and DEX both resulted in lower IL-6 mRNA expression, however, a solvent effect could not be excluded as the DMSO controls had the lowest IL-6 mRNA expression levels (Figure 6.2.3.1).

Table 6.2.3.1 IL-6 mRNA expression in splenic $CD4^+$ T-cells from MRL-*lpr/lpr* and MRL-*wt* mice at age 23 weeks (mean ± SEM).

Treatment	Untreated (n=6)	DMSO (n=6)	CMX-13 (n=6)	DEX (n=6)	MRL-wt (n=3)
IL-6/Cyclo ratio	0.052	0.002	0.0009	0.002	0.0057
	0.005	0.001	0.0009	0.001	0.0055
	0.002	0.009	0.002	0.024	0.0012
	0.001	0.001	0.001	0.0009	
	0.2	0.0005	0.004	0.018	
	0.005	0.005	0.123	0.023	
Mean ± SEM	0.044.±0.032	0.003±0.001	0.022±0.02	0.011±0.005	0.004±0.001

Figure 6.2.3.1 Quantitative analysis of IL-6 mRNA expression in splenic $CD4^+$ T-cells of MRL-*lpr/lpr* mice and MRL-*wt* mice at age 23 weeks. The IL-6 mRNA transcripts were highest in the $CD4^+$ T-cells of the untreated MRL-*lpr/lpr* mice, compared to the MRL-*wt* mice. Treatment with CMX-13 and DEX resulted in a decrease in IL-6 mRNA transcripts, similar to that seen in the DMSO control MRL-*lpr/lpr* mice. Bars represent mean ± SEM.

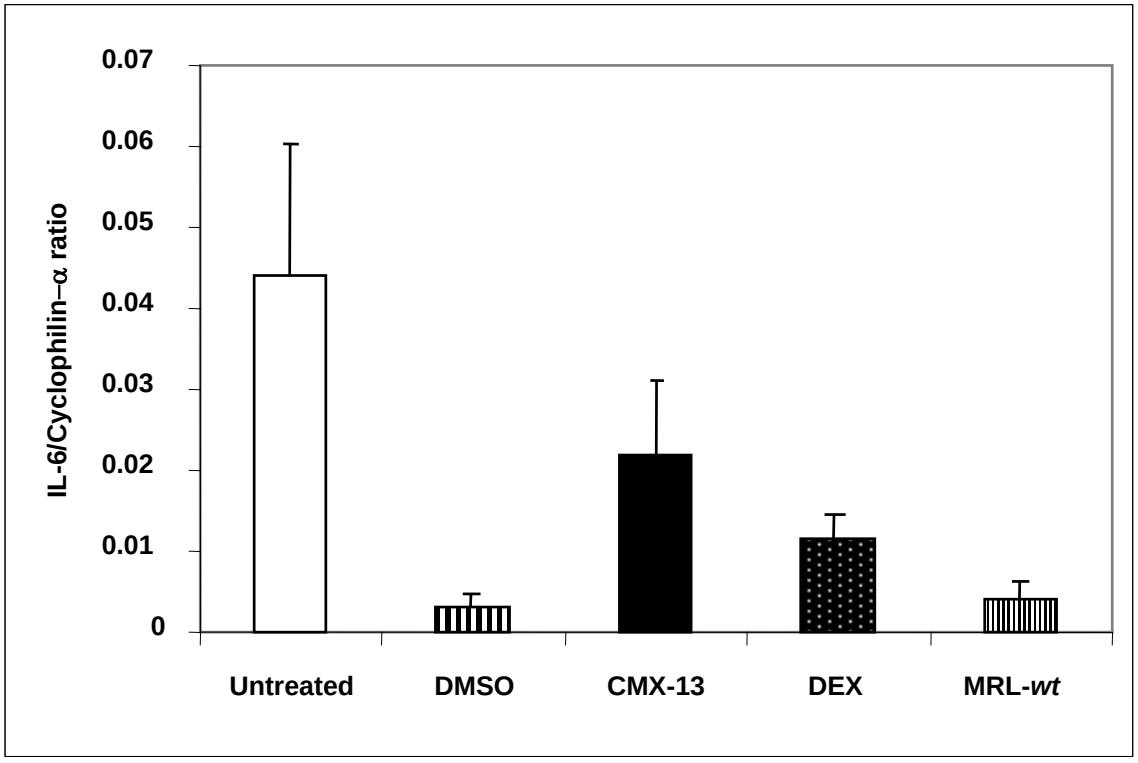

Table 6.2.3.2 shows the IL-6 mRNA expression levels in the splenic $CD8^+$ cells isolated from the different groups of MRL-*lpr/lpr* and MRL-*wt* type mice at age 23 weeks. The untreated (0.020±0.014) and DMSO control (0.014±0.004) MRL-*lpr/lpr* mice had low CD8+ IL-6 mRNA expression, similar to the MRL-*wt* mice (0.043±0.020). Treatment with CMX-13 resulted in a significant increase in the IL-6 mRNA levels (0.121±0.039) when compared to the DMSO control MRL-*lpr/lpr* mice ($p<0.005$) (Figure 6.2.3.2).

Table 6.2.3.2 IL-6 mRNA expression in splenic CD8$^+$ T-cells from MRL-*lpr/lpr* and MRL-*wt* mice at age 23 weeks (mean ± SEM).

Treatment	Untreated (n= 6)	DMSO (n= 6)	CMX-13 (n= 6)	DEX (n= 6)	MRL-wt (n= 3)
IL-6/Cyclo ratio	0.0048	0.0017	0.185	0.006	0.082
	0.0018	0.0015	0.035	0.0036	0.02
	0.025	0.013	0.167	0.031	0.027
	0.0013	0.017	0.033	0.038	
	0.085	0.022	0.05	0.08	
	0.002	0.029	0.258	0.021	
Mean ± SEM	0.020±0.014	0.014±0.004	0.121±0.039[a,b,c]	0.030±0.011	0.043±0.020

[a]p<0.02; compared to untreated MRL-lpr/lpr mice
[b]p<0.005; compared to DMSO controls
[c]p<0.04; compared to DEX-treated mice

Figure 6.2.3.2 Quantitative analysis of IL-6 mRNA expression in splenic CD8$^+$ T-cells of MRL-*lpr/lpr* mice and MRL-*wt* mice at age 23 weeks. Treatment with CMX-13 resulted in a significant increase in the IL-6 mRNA transcripts. Note: [a]p<0.02, compared to untreated MRL-lpr/lpr mice; [b]p<0.005, compared to DMSO controls; [c]p<0.04, compared to DEX-treated mice. Bars represent mean ± SEM.

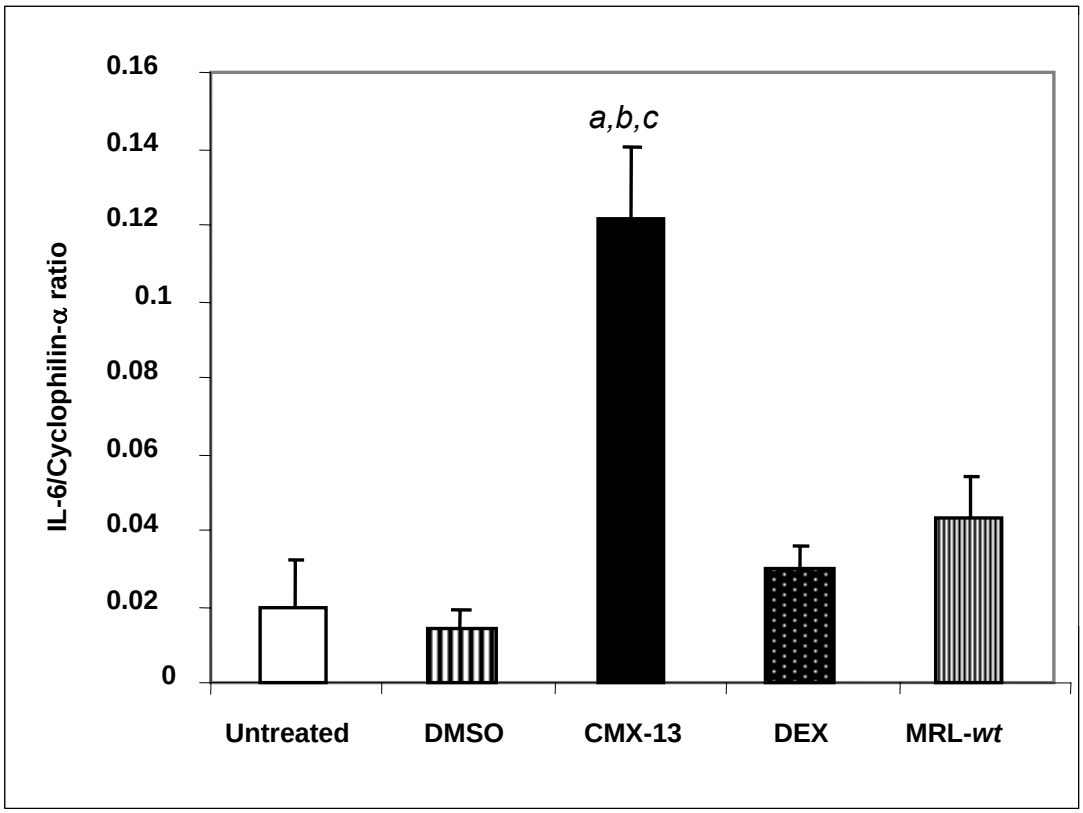

Table 6.2.3.3 summarizes the IL-6 mRNA expression in the glomeruli isolated from kidneys of MRL-*lpr/lpr* and MRL-wt mice at age 23 weeks. The IL-6 mRNA expression was very low in the glomeruli of MRL-*wt* mice (0.067±0.062). On the other hand, the untreated (0.579±0.309) and DMSO control (0.716±0.407) MRL-*lpr/lpr* mice had higher IL-6 mRNA expression in their glomeruli (0.656±0.369). CMX-13 treatment did not reduced the IL-mRNA expression in the glomeruli of these mice, however, DEX treatment resulted in lower IL-6 mRNA glomerular expression (0.281±0.118), although this did not reach statistical significance (Figure 6.2.3.3).

Table 6.2.3.3 IL-6 mRNA expression in glomeruli isolated from kidneys of MRL-*lpr/lpr* and MRL-*wt* mice at 23 weeks (mean ± SEM).

Treatment	Untreated (n=6)	DMSO (n=6)	CMX-13 (n=6)	DEX (n=6)	MRL-wt (n=3)
IL-6/Cyclo ratio	0.081	0.006	0.523	0.838	0.007
	0.002	0.046	0.175	0.037	0.004
	0.758	0.309	0.036	0.152	0.190
	0.169	5.071	0.054	0.152	
	2.017	0.141	2.412	0.183	
	0.445	1.294	0.736	0.325	
Mean ± SEM	0.58±0.31	0.72±0.41	0.66±0.37	0.28±0.12	0.067±0.062

Figure 6.2.3.3 Quantitative analysis of IL-6 mRNA expression in glomeruli isolated from the kidneys of MRL-*lpr/lpr* and MRL-*wt* mice. The untreated and DMSO control MRL-*lpr/lpr* mice had higher IL-6 mRNA transcripts in the glomeruli as compared to the MRL-*wt* mice. Treatment with DEX resulted in lower IL-6 mRNA glomerular expression. Bars represent mean ± SEM.

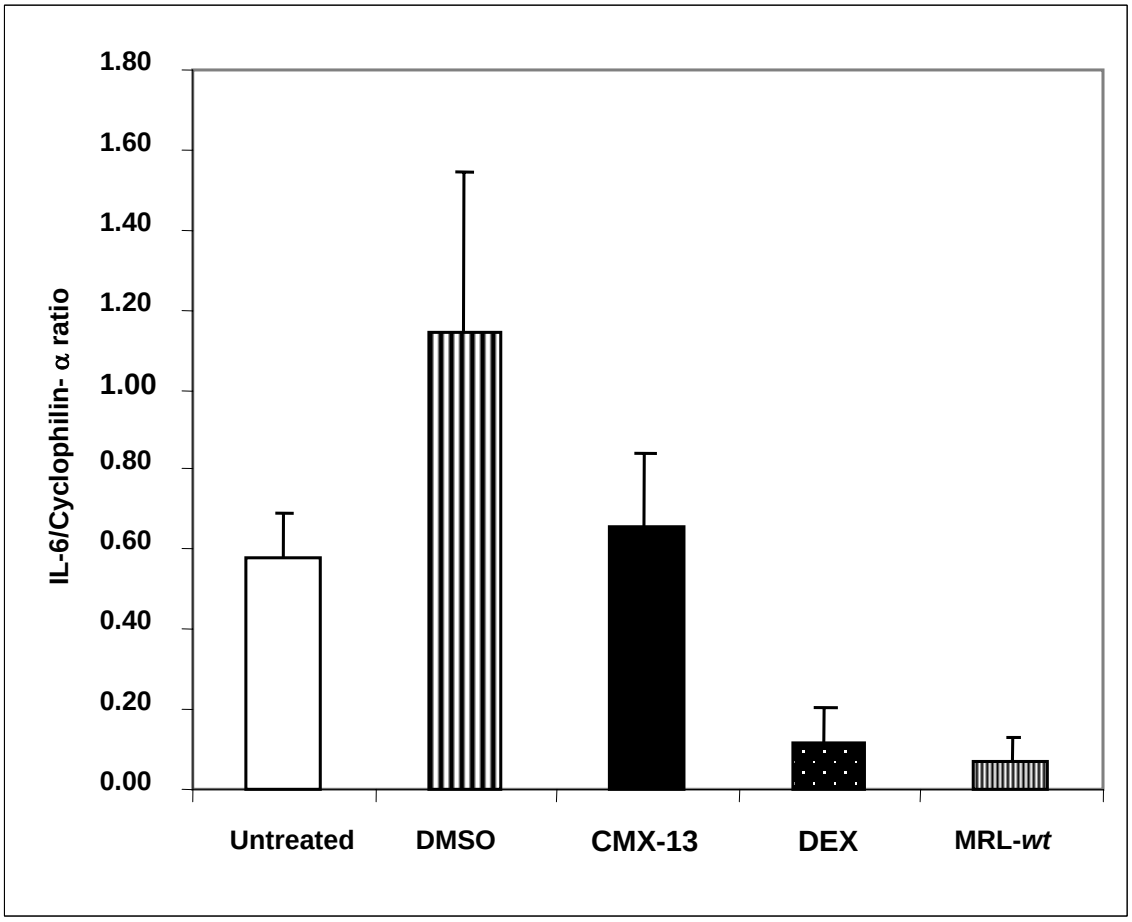

6.2.4 IL-10 mRNA Expression in Splenic $CD4^+$ and $CD8^+$ T-cells and Glomeruli from MRL-*lpr/lpr* Mice

Table 6.2.4.1 outlines the IL-10 mRNA expression in $CD4^+$ T cells isolated from the spleens of the different groups of MRL-*lpr/lpr* mice and MRL-*wt* mice. The DMSO control MRL-*lpr/lpr* mice had significantly higher IL-10 mRNA expression (0.78±0.11) compared to the MRL-*wt* mice (0.080±0.005) ($p<0.04$). Treatment with CMX-13 resulted in a significant decrease in the IL-10 mRNA expression level in MRL-*lpr/lpr* mice (0.28±0.029), compared to the DMSO controls ($p<0.02$) (Figure 6.2.4.1). DEX treatment did not influence the IL-10 mRNA levels (0.86±0.32) in the MRL-*lpr/lpr* mice.

Table 6.2.4.1 IL-10 mRNA expression in splenic $CD4^+$ T-cells from MRL-*lpr/lpr* and MRL-*wt* mice at age 23 weeks (mean ± SEM).

Treatment	Untreated (n=4)	DMSO (n=4)	CMX-13 (n=4)	DEX (n=4)	MRL-wt (n=3)
IL-10/Cyclo ratio	0.408	0.742	0.368	0.841	0.0787
	0.188	0.658	0.242	1.61	0.0756
	0.188	0.631	0.226	0.0613	0.085
	0.919	1.1	0.325	0.943	
Mean ± SEM	0.43±0.17	0.78±0.11	0.28±0.029[a]	0.86±0.32	0.080±0.005[b]

[a] $p<0.02$; compared with DMSO controls
[b] $p<0.04$; compared with DMSO controls

Figure 6.2.4.1 Quantitative analysis of IL-10 mRNA expression in splenic $CD4^+$ T-cells of MRL-*lpr/lpr* mice and MRL-*wt* mice at age 23 weeks. The IL-10 mRNA transcripts were higher in the DMSO control MRL-*lpr/lpr* mice compared to the MLR-*wt* mice ($p<0.04$)[a]. Treatment with CMX-13 resulted in a significant decrease in IL-10 mRNA transcripts compared to the DMSO control MRL-*lpr/lpr* mice ($p<0.02$)[b]. Bars represent mean ± SEM.

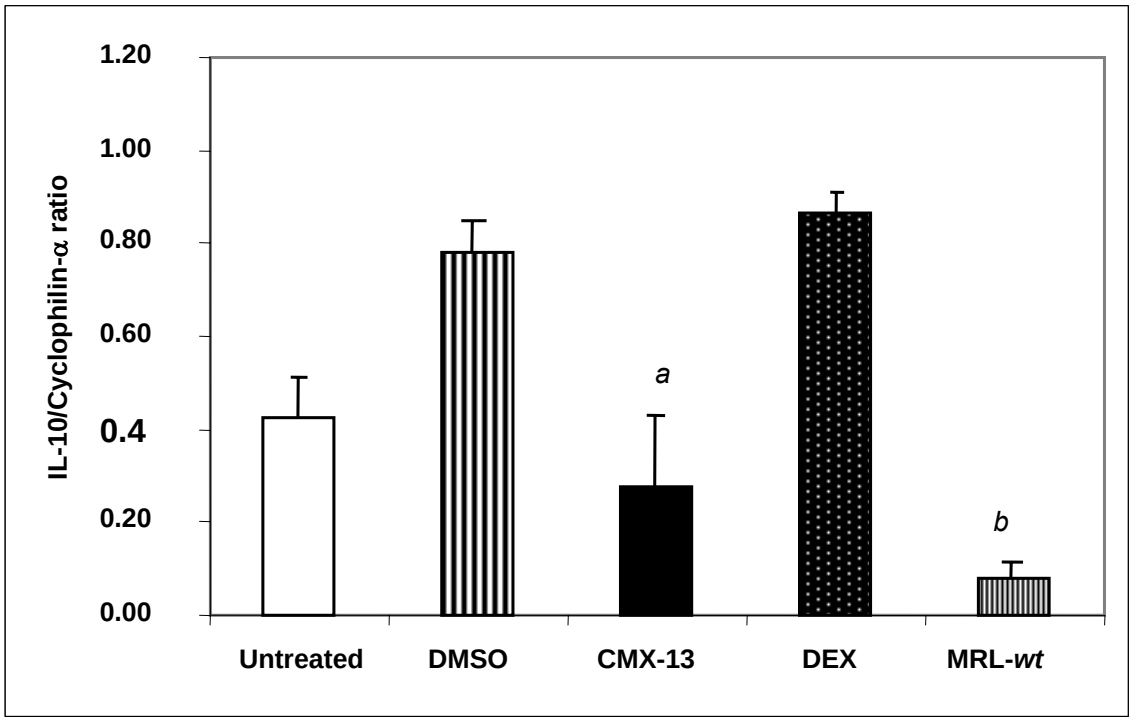

As shown in Table 6.2.4.2, the glomerular IL-10 mRNA expression was low, especially in the MRL-*wt* mice (0.003±0.000). The IL-10 mRNA expression was only slightly higher in the untreated (0.046±0.023) and DMSO control (0.045±0.021) MRL-*lpr/lpr* mice, and treatment with either CMX-13 (0.072±0.036) or DEX (0.037±0.016) did not significantly upregulate its expression (Figure 6.2.4.2).

Table 6.2.4.2 IL-10 mRNA expression in glomeruli isolated from kidneys of MRL-*lpr/lpr* and MRL-*wt* mice at 23 weeks (mean ± SEM).

Treatment	Untreated (n=4)	DMSO (n=4)	CMX-13 (n=4)	DEX (n=4)	MRL-wt (n=3)
IL-10/Cyclo Ratio	0.030	0.030	0.027	0.007	0.003
	0.008	0.008	0.027	0.014	0.003
	0.114	0.114	0.056	0.076	0.003
	0.030	0.030	0.180	0.052	
Mean ± SEM	0.046±0.023	0.045±0.021	0.072±0.036	0.037±0.016	0.003±0.000

Figure 6.2.4.2 Quantitative analysis of IL-10 mRNA expression in glomeruli isolated from the kidneys of MRL-*lpr/lpr* and MRL-*wt* mice. The IL-10 mRNA transcripts in the glomeruli were very low in MRL-*wt* mice compared to the MRL-*lpr/lpr* mice. Bars represent mean ± SEM.

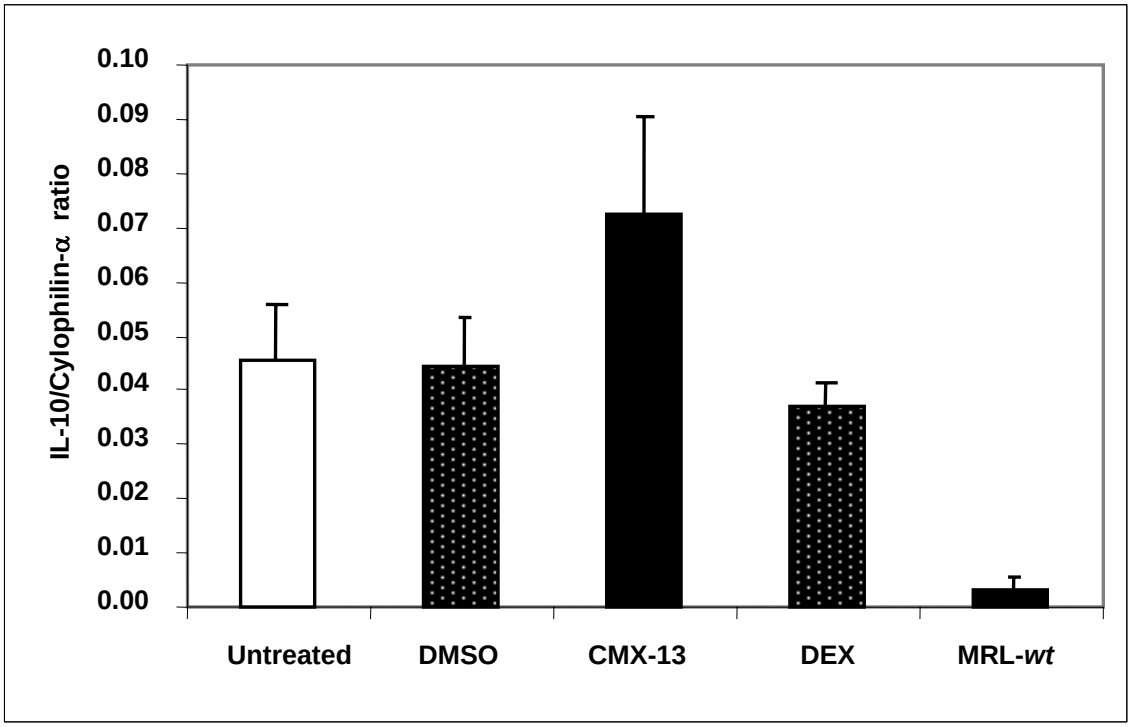

6.3 DISCUSSION

Studies on the MRL-*lpr/lpr* autoimmune mice have identified various cytokine abnormalities [Lemay et al., 1996; Prud'Homme et al., 1995]. Data from such studies in the literature are conflicting, due to the different methodologies utilized (mRNA expression versus cytokine excretion), different sources (cells *vs* serum) and different experimental approaches (*in-vitro* versus *in-vivo* with or without various stimuli). In our study, quantitative real-time RT-PCR was utilized to study the changes in the number of mRNA cytokine transcripts upon treatment of MRL-*lpr/lpr* mice with CMX-13 and DEX, as compared to the untreated or DMSO control MRL-*lpr/lpr* mice, and MRL-*wt* mice. The abnormalities in cytokine mRNA expression in MRL-*lpr/lpr* mice as compared to MRL-*wt* mice in our study, and the effect of CMX-13 on these abnormalities are outlined in Table 6.3.1.

Table 6.3.1 Effect of CMX-13 on cytokine mRNA expression in MRL-*lpr/lpr* mice. N=no difference from MRL-*wt* mice; D=decreased; I=increased; ND=not done. *Changes in MRL-*lpr/lpr* mice following CMX-13 treatment, NC=no change; D=decreased; I=increased.

Cytokine	$CD4^+$	$CD8^+$	Glomeruli	Liver
IFN-γ	N	N	I	N
*CMX-13	NC	NC	NC	NC
IL-2	D	D	ND	ND
*CMX-13	I	I	ND	ND
IL-6	N	N	I	ND
*CMX-13	NC	I	NC	ND
IL-10	I	ND	I	ND
*CMX-13	NC	ND	NC	ND

We used the quantitative real-time RT-PCR to study the changes in the number of mRNA cytokine transcripts following treatment of MRL-*lpr/lpr* mice with CMX-13 and DEX, as compared to DMSO controls or untreated MRL-*lpr/lpr* mice. In order to define the cytokine gene expression abnormalities in MRL-*lpr/lpr* mice, MRL-*wt* mice were used as controls. As the numbers in this section of the study were small, due to the fact that the diseased mice tended to die early limiting the numbers available for cytokine gene studies after 23 weeks of treatment. Nevertheless, there was a trend showing that in the $CD4^+$ and $CD8^+$ cells, IL-2 mRNA transcripts at 23 weeks of age were decreased, whereas IL-6 mRNA expression was increased in CD8+ cells from MRL-*lpr/lpr* mice compared to MRL-*wt* mice. Treatment with CMX-13 resulted in a significant correction of these abnormalities in the MRL-*lpr/lpr* mice. On the other hand, there was an increase in the glomerular mRNA expression of IFN-γ, IL-6 and IL-10 in MRL-*lpr/lpr* mice, but treatment with CMX-13 did not show any changes in cytokine gene expression. Treatment with CMX-13 also increased IFN-γ mRNA expression in the liver of MRL-*lpr/lpr* mice.

Our data showing a decrease in IL-2 mRNA transcripts in $CD4^+$ and $CD8^+$ cells were consistent with the studies on PBMCs in human SLE, where IL-2 mRNA expression has been shown to be downregulated [Crispin and Alcocer-Varela, 1998]. Moreover, *in-vitro* IL-2 production by PBMCs was impaired following stimulation with antigens [Alcocer-Varela and Alarcon-Segovia, 1982]. Other studies have shown that the defective production of IL-2 occurred in both $CD4^+$

and $CD8^+$ T-cells [Murakawa et al., 1985]. Moreover, these studies demonstrated that IL-2 production was not defective *in vivo*, but suppressed [Alcocer-Varela and Alarcon-Segovia, 1982; Murakawa et al., 1985; Huang et al., 1986], and induction of IL-2 production by an IL-2/vaccinia recombinant virus was effective in correcting the immunological abnormalities in the MRL-*lpr/lpr* mice [Gutierrez-Ramos, 1991]. The authors speculated that the dramatic reduction in the abnormally expanded $CD3^+CD4^-CD8^-$ (double negative) T-cell population following IL-2 therapy might be directly related to the amelioration and/or prevention of autoimmune disease in these mice. Our studies also showed that treatment of MRL-*lpr/lpr* mice with CMX-13 was associated with an increase in IL-2 mRNA expression as compared to the untreated mice, and this finding could have therapeutic significance, as we have previously shown in chapter 5 that CMX-13 appeared to be effective in attenuating the clinical and histological disease activity in the MRL-*lpr/lpr* mouse.

A possible causal relationship has been shown between the development of SLE and IFN-γ up-regulation in human and mice [Haas et al, 1997; Prud'Homme et al., 1995]. Increased levels of IFN-γ mRNA transcipts have been demonstrated in PBMCs, kidney, lymph nodes, and spleen of diseased MRL-*lpr/lpr* mice [Prud'Homme et al., 1995]. Additionally, suppression of IFN-γ has been shown to improve disease activity. Treatment of autoimmune prone NZB/NZW F1 mice with exogenous IFN-γ treatment accelerated the autoimmune response and renal disease, while blocking of IFN-γ with anti-IFN-γ monoclonal antibodies or soluble

IFN-γ receptor inhibitor inhibited the onset of glomerulonephritis [Ozmen et al., 1995]. Moreover, MRL-*lpr/lpr* mice lacking the IFN-γ receptor did not develop glomerulonephritis.

In our study, we could only demonstrate an increase in the IFN-γ mRNA expression in the glomeruli of untreated and DMSO control MRL-*lpr/lpr* mice, similar to the results from other groups [Lemay et al., 1996]. CMX-13 did not affect the IFN-γ gene expression in the glomeruli, but it resulted in an increase in the number of IFN-γ mRNA transcripts in the liver, although this did not reach statistical significance due to the small numbers studied. However, as shown in Table 6.2.2.2 and 6.2.2.3, the IL-2/IFN-γ mRNA ratio in $CD4^+$ and $CD8^+$ T-cells was significantly lower in untreated MRL-*lpr/lpr* mice. Treatment with CMX-13 resulted in improvement in the IL-2/IFN-γ mRNA ratio in $CD4^+$ and $CD8^+$ T-cells from MRL-*lpr/lpr* mice.

IL-6 has been shown to promote B-cell hyperactivity in SLE patients [Linker-Isreali et al., 1991] and lupus in NZB/NZW F1 mice. Additionally, IL-6 was found to be upregulated in the sera [Swaak et al., 1989] and renal biopsy tissue of SLE patients [Horii et al., 1993]. Treatment of lupus-prone mice with anti-IL-6 antibody abrogated the disease [Finck et al., 1994b]. Our study also demonstrated an increase in IL-6 mRNA expression in the glomeruli of MRL-*lpr/lpr* mice compared to MRL-*wt* mice. Unfortunately, CMX-13 had no effect on glomerular IL-6 gene expression. Only treatment with DEX down-regulated IL-6

gene expression. On the other hand, treatment with CMX-13 resulted in upregulation of $CD8^+$ IL-6 gene expression. As auto-aggressive $CD4^+CD8^-$ $\alpha\beta$T-cells have been postulated to be the driving force for autoreactive B-cells in the development of SLE, upregulation of suppressor $CD8^+$ cells which secrete the Th2 cytokine IL-6, may be important in modulating B-cell hyperreactivity, suppressing the disease.

IL-10 is produced by several cell types and is also a potent stimulator of B-cells. Hence it may play an important role in B lymphocyte hyperreactivity associated with SLE [Mosmann, 1994; Cross and Benton, 1999]. In fact, IL-10 induced the secretion of IgG1 and IgG3 [Briere et al., 1994]. PBMCs from SLE patients spontaneously expressed higher levels of the IL-10 gene and released large amounts of the IL-10 protein. Several studies have attempted to define the role of IL-10 in autoantibody production by hyperactive B-cells. Inhibition of IL-10 with anti-IL-10 monoclonal antibodies in lupus-prone mice significantly reduced autoantibody production [Llorente et al., 1995], and delayed onset of the disease [Ishida et al., 1994].

Previous studies employing the RNase protection assay technique have shown that IL-10 was only detectable in the lymph nodes of MRL-*wt* mice, but was significantly upregulated in diseased MRL-*lpr/lpr* mice [Prud'homme et al., 1995].

In our study, we showed that IL-10 mRNA expression was increased in splenic CD4+ cells, as well as glomeruli of untreated MRL-*lpr/lpr* mice. Unfortunately, we could not demonstrate any downregulation of IL-10 gene expression following treatment with CMX-13 or DEX, although these mice had better clinical and histopathological outcomes than the untreated or DMSO-control MRL-*lpr/lpr* mice.

In conclusion, our studies showed that diseased MRL-lpr/lpr mice which did not receive any treatment had decreased $CD4^+$ and $CD8^+$ IL-2/IFN-γ mRNA ratio at the age of 23 weeks, as well as upregulation of $CD4^+$ IL-10 mRNA expression, similar to other reports in the literature. In addition, glomerular mRNA expression of IFN-γ, IL-6 and IL-10 were also upregulated. On the other hand, the CMX-13 treated group showed significantly higher $CD4^+$ and $CD8^+$ IL-2/IFN-γ mRNA ratio, and this was associated with improved clinical, serological and histopathological parameters, including survival. However, CMX-13 treatment did not improve the abnormality in glomerular IFN-γ, IL-6 and IL-10 gene expression.

CHAPTER 7 CONCLUSION

Our research group's interest in the "Ming Decoction of 21 Tonics for Kidney" arose from treatment in a patient with lupus nephritis and chronic nephritic syndrome, in whom clinical remission started after ingestion of this Chinese herbal decoction (CM). Preliminary studies have demonstrated the immunosuppressive potency of both the crude decoction CM, as well as the active fraction CMX-13, a derivative of the herb *RC*, on *in-vitro* T-lymphocyte proliferation, as well as B-cell secretion of immunoglobulins in both normal individuals as well as patients with SLE. In addition, we have shown the efficacy of CMX-13 on preventing acute rejection in a rat lung transplant model of hyperacute allograft rejection. This thesis utilizes the MRL-*lpr/lpr* murine model of lupus nephritis to study the mechanism of the immunosuppressive action of CMX-13 and its derivatives.

7.1 CHARACTERIZATION OF CMX-13

In the first part of this thesis, work was performed to characterize CMX-13, which is the fraction which contains the active component(s) of the herb *RC,* following separation by liquid chromatography using spectroscopic and chemical methods. RP-HPLC revealed that CMX-13 contained a mixture of possibly 8 or more compounds. Two RP-HPLC fractions of CMX-13, namely CMX-13-1 and CMX-13-5 had 100% immunosuppressive properties. The RP-HPLC fraction CMX-13-5 contained fewer impurities than CMX-13-1 as shown in the RP-HPLC profiles of CMX-13-1 and CMX-13-5 (Figures 3.2.5.2 and 3.2.5.7 respectively). Therefore we attempted to elucidate the structure of CMX-13-5 by ^{1}H-NMR and LC-Mass spectrometry. The LC chromatogram of CMX-13-5 showed a single peak, suggesting either a single molecule with a weight of 807.5 or two molecules with a weight of 270 and 537.5. ^{1}H-NMR spectrum of CMX-13-5 was shown to resemble the ^{1}H-NMR spectra of a bicyclic hexapeptide isolated by the group of Itokawa and co-workers [Itokawa et al., 1992; Itokawa et al., 1993]. Subsequent to our work, our collaborators were able to analyze the structure of the purified bioactive compound in CMX-13' (using material from the same source) and showed that the bioactive compound in CMX-13' was identical to a compound previously identified by Itokawa and co-workers, namely, RA-VII (Figure 3.3.1).

7.2 MOLECULAR BASIS FOR IMMUNOSUPPRESSIVE EFFECTS OF CMX-13

We have previously shown that CMX-13 was able to suppress mitogen-stimulated lymphoproliferative responses and PBMC immunoglobulin production, as well as inhibit T-cell colony formation. In our earlier studies on the possible mechanisms of action, CMX-13 did not show any inhibitory effects on IL-2 and IFN-γ mRNA expression, suggesting that its mechanism of action was different from that of CsA [Zuo et al., 2000]. As there is strong evidence that dysregulation of apoptosis in the immune regulatory cells could have a role in the genesis of SLE, the second part of the thesis examined the effect of CMX-13 on:

1) Cell cycle progression in PBMCs isolated from normal controls and patients with SLE, as well as Jurkat cells, a human T-cell line
2) Apoptotic events.

In addition to its effect on PBMC, CMX-13 was also shown to significantly inhibit spontaneous Jurkat cell proliferation by >99% even at low concentrations of 1 μg/ml. The inhibitory effect of CMX-13 on Jurkat cell proliferation was not due to inhibition of cell-cycle progression, but rather by the induction of spontaneous apoptosis in cells in the G_0/G_1 phase. This effect of CMX-13 on apoptosis in Jurkat cells was confirmed by DNA fragmentation analysis and Annexin-V staining. Apoptosis was induced at a very early phase, as was demonstrated by the “sub-G1” or apoptotic peaks appearing in the cell-cycle analysis. This

mechanism of action was different from drugs such as cyclohexmide, which induces apoptosis related to a G_0/G_1 cell-cycle arrest.

Defective apoptosis has been suggested to be an important mechanism in the pathogenesis of various autoimmune diseases [Mountz et al., 1994; Carrichio et al., 1999; Papo et al., 1998]. Apoptosis is important for the immune system to regulate cell growth and terminate immune responses in order to ensure that overall the rate of division is balanced by cell death [Lorenz et al., 2001]. In SLE, one of the hypothesis is that dysregulation of apoptosis might be responsible for the induction of anti-nuclear antibodies, pathognomonic of the disease. In some patients, decreased apoptosis in SLE appears to be associated with increased production sFas molecule that is capable of inhibiting apoptosis after a stimulus to proliferate [Cheng et al., 1994], whereas other studies reported accelerated apoptosis of lymphocytes in SLE patients [Emlen et al., 1994; Lorenz et al., 1998]. Similarly, in our SLE patients, the percentage of apoptotic cells was increased with increasing activity of the disease as measured by the SLICC score.

Hence the immunosuppressive mechanism of CMX-13 could be partly related to its effect on apoptosis, especially in the context of suppression of SLE activity, where increased apoptosis has been demonstrated. Two distinct pathways of apoptosis have been described that induce the activation of caspases and other pro-apoptotic activities. One of the pathways leading to apoptosis is activation of

caspase 8 upon binding of a death ligand on the cell membrane [Hakem et al., 1998], whereas the second pathway is related to cellular stress, whereby mitochondria release cytochrome *c* which binds to an apoptotic protease activating factor (Apaf-1), activating caspase-9 [Zheng et al., 1999; Cecconi, 1999]. Therefore further studies are required to determine if induction of apoptosis by CMX-13 is related to the caspase-8 or caspase-9 pathway.

7.3 EFFECT OF CMX-13 ON MRL-*lpr/lpr* AUTOIMMUNE MOUSE MODEL

MRL-*lpr/lpr* mice spontaneously develop an autoimmune disorder with pathological features similar to human SLE, including vasculitis, generalized lymphadenopathy, arthritis and a severe immune complex glomerulonephritis, [Andrews et al., 1978]. These clinical features, accompanied by elevation of serum anti-dsDNA antibody levels, were seen in the untreated control mice and the control group treated with the solvent DMSO in our experiments. The severity of the autoimmune disease increased with the age of the mice, with the majority dying of renal failure at 16-24 weeks of age.

Treatment of the MRL-*lpr/lpr* mice with CMX-13 and DEX resulted in delay by at least 4 weeks in the development of lymphadenopathy, which was also less severe than in the control groups. All of the mice developed anti-dsDNA antibodies from the age of 8 weeks, with the untreated and DMSO control mice having the highest level of rise in antibody concentrations by 16 weeks of age, whereas both the CMX-13 and DEX-treated groups had significantly lower anti-dsDNA antibody levels.

Anti-dsDNA antibodies have often been implicated in the development of glomerulonephritis [Koffler et al., 1967; Lambert and Dixon, 1968], where deposition of anti-dsDNA antibodies in the glomerulus resulted in a proliferative

glomerulonephritis [Yamada et al, 1982]. Recent studies on the autoantibody specificities from kidney eluates in lupus mice have shown that cross-reactive anti-dsDNA antibodies predominate, and these antibodies also bound to glomerular substrate and laminin [Xie et al., 2003]. Hence development of glomerulonephritis and vasculitis could be due to *in-situ* immune complex formation in the glomerular and vascular sites [Vlahakos et al, 1992]. The increased mortality seen in the MRL-*lpr/lpr* mice is attributed in a large part to the development of progressive severe proliferative lupus nephritis, with the majority of mice dying of renal failure at 16-24 weeks of age.

This thesis has shown that CMX-13 was able to improve survival of the MRL-*lpr/lpr* mice compared to the untreated or DMSO controls, where 9 of the mice treated with CMX-13 were still alive at 22 weeks of age, whereas only 2 of the untreated controls and 3 of the DMSO controls survived. This was despite the fact that in the MRL-*lpr/lpr* mice, the severity of kidney disease increases with age due to progressive mesangial and endothelial cell proliferation, crescent formation, thickening of the glomerular capillary walls and tubulointerstitial nephritis with vasculitis [Austin et al, 1984: Moyer et al, 1987; Appel and Valeri, 1994; Putterman and Naparstek, 1994]. In our experiment, CMX-13 treatment of MRL-*lpr/lpr* mice with progressive lupus nephritis resulted in decrease in the degree of proteinuria and improvement in renal histological indices. Hence CMX-13 appeared to be effective in attenuating the clinical and histological disease activity in the MRL-*lpr/lpr* mouse model of SLE.

In patients with active disease as well as in experimental murine models of SLE, both the serum cytokine levels and gene expression in PBMCs have been found to be abnormal [Prud'homme, 1993]. In fact, there have been reports of a relationship between abnormal cytokine mRNA levels and disease activity [Linker-Israeli et al., 1996]. Hence we examined the effect of CMX-13 on cytokine gene expression in particular $CD4^+$ and $CD8^+$ T-cells, liver and glomeruli of the autoimmune MRL-*lpr/lpr* mouse. The mice were treated with either DMSO (solvent control), CMX-13 or DEX as described in chapter 2.3.2, from the age of 12 weeks, and real-time RT-PCR was employed to examine IL-2, IL-6, IL-10 and IFN-γ mRNA expression levels in tissues and lymphocyte subsets from each of the groups of MRL-*lpr/lpr* mice that were sacrificed at 23 weeks. Our studies showed that diseased MRL-*lpr/lpr* mice which did not receive any treatment had decreased $CD4^+$ and $CD8^+$ IL-2/IFN-γ mRNA ratio at the age of 23 weeks, as well as upregulation of $CD4^+$ IL-10 mRNA expression, similar to other reports in the literature. In addition, glomerular mRNA expression of IFN-γ, IL-6 and IL-10 were also increased. On the other hand, the CMX-13 treated group showed significantly higher $CD4^+$ and $CD8^+$ IL-2/IFN-γ mRNA ratio, and this was associated with improved clinical, serological and histopathological parameters, including survival. However, CMX-13 treatment did not improve the abnormality in glomerular IFN-γ, IL-6 and IL-10 gene expression.

Our data showing a decrease in IL-2 mRNA transcripts in $CD4^+$ and $CD8^+$ cells were consistent with the studies on PBMCs in human SLE, where IL-2 mRNA

expression has been shown to be downregulated [Crispin and Alcocer-Varela, 1998]. Other studies have shown that induction of IL-2 production by an IL-2/vaccinia recombinant virus was effective in correcting the immunological abnormalities in the MRL-*lpr/lpr* mice [Gutierrez-Ramos, 1991]. A possible causal relationship has been shown between the development of SLE and IFN-γ up-regulation in human and mice [Haas et al, 1997; Prud'Homme et al., 1995]. Additionally, suppression of IFN-γ has been shown to improve disease activity. In our study, we could only demonstrate an increase in the IFN-γ mRNA expression in the glomeruli of untreated and DMSO control MRL-*lpr/lpr* mice, similar to the results from other groups [Lemay et al., 1996]. CMX-13 did not affect the IFN-γ gene expression in the glomeruli, but it resulted in an increase in the number of IFN-γ mRNA transcripts in the liver, although this did not reach statistical significance due to the small numbers studied. However, the IL-2/IFN-γ mRNA ratio in $CD4^+$ and $CD8^+$ T-cells was significantly lower in untreated MRL-*lpr/lpr* mice. Treatment with CMX-13 resulted in improvement in the IL-2/IFN-γ mRNA ratio in $CD4^+$ and $CD8^+$ T-cells from MRL-*lpr/lpr* mice.

IL-6 has been shown to promote B-cell hyperactivity in SLE patients [Linker-Isreali et al., 1991] and lupus in NZB/NZW F1 mice. Treatment of lupus-prone mice with anti-IL-6 antibody abrogated the disease [Finck et al., 1994b]. Our study also demonstrated an increase in IL-6 mRNA expression in the glomeruli of MRL-*lpr/lpr* mice compared to MRL-*wt* mice. Unfortunately, CMX-13 had no effect on glomerular IL-6 gene expression. Treatment with CMX-13 resulted in

upregulation of $CD8^+$ IL-6 gene expression. As auto-aggressive $CD4^+CD8^-$ $\alpha\beta$T-cells have been postulated to be the driving force for autoreactive B-cells in the development of SLE, upregulation of suppressor $CD8^+$ cells which secrete the Th2 cytokine IL-6, may be important in modulating B-cell hyperreactivity, suppressing the disease.

IL-10 has been postulated to play an important role in B lymphocyte hyperreactivity associated with SLE [Mosmann, 1994; Cross and Benton, 1999]. Inhibition of IL-10 with anti-IL-10 monoclonal antibodies in lupus-prone mice significantly reduced autoantibody production [Llorente et al., 1995], and delayed onset of the disease [Ishida et al., 1994]. Previous studies have also shown that IL-10 was was significantly upregulated in diseased MRL-*lpr/lpr* mice [Prud'homme et al., 1995]. In our study, we showed that IL-10 mRNA expression was increased in splenic CD4+ cells, as well as glomeruli of untreated MRL-*lpr/lpr* mice, however, CMX-13 did not appear to have any effect on its expression.

In conclusion, one possible mechanism by which CMX-13 acts an immunosuppressive agent in the treatment of lupus nephritis in the autoimmune MRL-*lpr/lpr* mouse model is through the induction of apoptosis of autoreactive lymphocytes, as illustrated in Figure 7.1. Auto-aggressive $CD4^+CD8^-$ $\alpha\beta$T-cells have been postulated to be the driving force for autoreactive B-cells in SLE resulting in abnormalities in cytokine production, and suppression of these

autoreactive lymphocytes could result in inhibition of autoantibody production, thus retarding the progression of lupus nephritis.

Further investigations into the apoptotic mechanisms are required to examine the transcription of apoptotic and cell-cycle genes, so that the exact molecular targets of CMX-13 or its purified molecule, RA-VII can be identified.

Figure 7.1 Hypothetical model for the therapeutic effect of CMX-13 on Human and Mouse SLE. CMX-13 induces apoptosis in $CD4^+$ T-cells and autoreactive B-cells. Consequently no production of autoantibodies occurs and no autoantibody mediated disease.

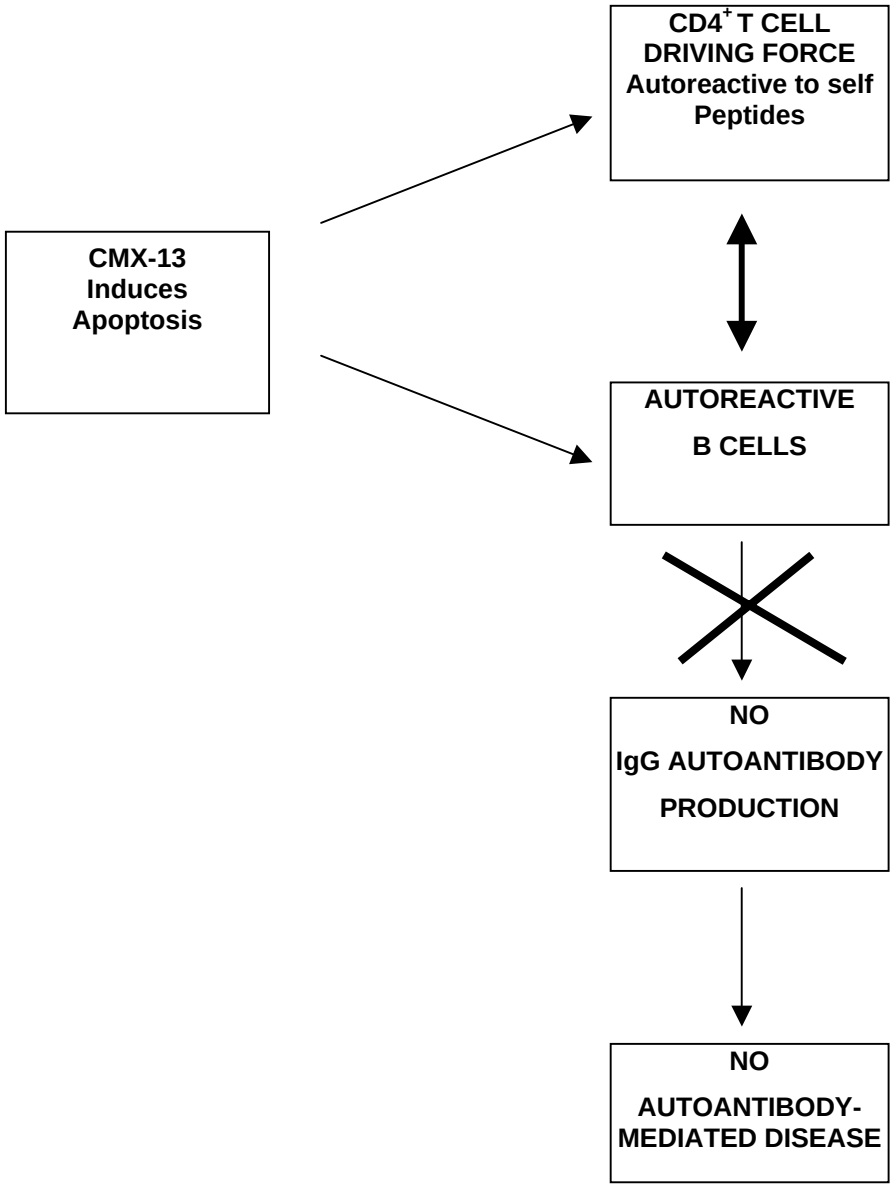

REFERENCES

1 Adachi M, Watanabe-Fukunaga R and Nagata S. 1993. Abberrant transcription caused by the insertion of an early transposable element in an intron of the Fas antigen gene of lpr mice. Proceedings of the National Academy of Sciences of the United States of America. 90:1756-60.

2 Aihara M, Aihara Y, Takahashi Y and Nakajima H. 1997. Effects of lipostreoid on skin lesions in autoimmune MRL *lpr/lpr* mice. Journal of Dermatological Science. 16: 45-51.

3 Akahoshi M, Nakashima H, Tanaka Y, Kohsaka T, Nagano S, Ohgami E, Arinobu Y, Yamaoka K, Niiro H, Shinozaki M, Hirakata H, Horiuchi T, Otsuka T, Niho Y. 1999. Th1/Th2 balance of peripheral T helper cells in systemic lupus erythematosus. Arthritis Rheumatism. 42:1644-8.

4 Akira S, Taga T, Kishimoto T. 1993. Interleukin-6 in biology and medicine. Advances in Immunology.54:1-78.

5 Alcocer-Varela J and Alarcon-Segovia D. 1982. Decreased production of and response to interleukin-2 by cultured lymphocytes from patients

with systemic lupus erythematosus. Journal of Clinical Investigations. 69:1388-1392.

6 Alnemri ES, Livingston DJ, Nicholson DW, Salvesen G, Thornberry NA, Wong WW and Yuan J. 1996. Human ICE/CED-3 protease nomenclature. Cell. 87:171.

7 Altman A, Theofilopoulos AN, Weiner R, Katz DH and Dixon FJ. 1981. Analysis of T cell function in autoimmune murine strains. Defects in production and responsiveness to interleukin 2. Journal of Experimental Medicine. 154:791-808.

8 Amano H, Morimoto S, Kaneko H, Tokano Y, Takasaki Y and Hashimoto H. 2000. Effect of intravenous cyclophosphamide in systemic lupus erythematosus: relation to lymphocyte subsets and activation markers. Lupus. 9:26-32.

9 Anderson CC, Panoskaltsis A and Sinclair NR. 1993. Immunoregulatory characteristics of the in vitro anti-ssDNA response. Immunology Research.12:349-57.

10 Anderson CC, Mukherjee R, Sinclair NR and Jevnikar AM. 1997. Hypogammaglobulinaemia occurs in Fas-deficient MRL-lpr mice

following deletion of MHC class II molecules. Clinical Experimental Immunology.109:473-9.

11 Andrews BS, Eisenberg RA, Theofilopoulos AN, Izui S, Wilson CB, McConahey PJ, Murphy ED, Roths JB and Dixon FJ. 1978 Spontaneous murine lupus-like syndromes. Clinical and immunopathological manifestations in several strains. Journal of Experimental Medicine. 148:1198-1215.

12 Appel GB and Valeri A. 1994.The course and treatment of lupus nephritis. Annual Revue Medicine. 45:525-37.

13 Arends MJ, Morris RG and Wyllie AH. 1990. Apoptosis. The role of endonuclease. American Journal of Pathology.136:593-608.

14 Aringer M, Wintersberger W, Steiner CW, Kiener H, Presterl E, Jaeger U, Smolen S and Granninger WB. 1994. High levels of bcl-2 protein in circulating T lymphocytes, but not B lymphocytes, of patients with Systemic Lupus Erythematosus. Arthritis and Rheumatism. 37:1423-30.

15 Arnett FC, Edworthy SM, Bloch DA, McShane DJ, Fries JF, Cooper NS, Healey LA, Kaplan SR, Liang MH, Luthra HS, et al.1988. The

American Rheumatism Association 1987 revised criteria for the classification of rheumatoid arthritis. Arthritis Rheumatism. 31:315-24.

16 Ashwell JD, Lu FW and Vacchio MS. 2000. Glucocorticoids in T cell development and function. Annual Revue of Immunology.18:309-45.

17 Austin HA 3rd, Muenz LR, Joyce KM, Antonovych TT and Balow JE. 1984. Diffuse proliferative lupus nephritis: identification of specific pathologic features affecting renal outcome. Kidney International. 25:689-95.

18 Baumann I, Kolowos W, Voll RE, Manger B, Gaipl U, Neuhuber WL, Kirchner T, Kalden JR and Herrmann M. 2002. Impaired uptake of apoptotic cells into tingible body macrophages in germinal centers of patients with systemic lupus erythematosus. Arthritis and Rheumatism. 46:191-201.

19 Bancroft JD, Stevens A and Turner DR. Theory and ractices of histological techniques. Churhill Livingstone 3rd edition 1990. Pg 188-89.

20 Bedner E, Li X, Gorczyca W, Melamed MR and Darzynkiewicz Z. 1999. Analysis of apoptosis by laser scanning cytometry. Cytometry. 35:181-195.

21 Bennett WM. The nephrotoxicity of immunosuppressive drugs. 1995. Clinical Nephrology. 43:S3-7.

22 Bennett WM, DeMattos A, Meyer MM, Andoh T and Barry JM. 1996. Chronic cyclosporine nephropathy: the Achilles' heel of immunosuppressive therapy. Kidney International. 50:1089-100.

23 Bernstein KA, Valerio RD and Lefkowith JB. 1995. Glomerular binding activity in MRL/lpr serum consists of antibodies that bind to a DNA/histone/type IV collagen complex. Journal of Immunology. 154:2424-2433.

24 Bigazzi PE and Rose NR. 1996. In Weir's Handbook of experimental immunology. Volume III. The lymphoid system. Edited by Herzenberg EA, Weir DM, Herzenberg LA, Blackwell C. 5th edition Blackwell Science. pg 96.1-21.

25 Blaschke V, Reich K, Blaschke S, Zipprich S, Neumann C. Rapid quantitation of proinflammatory and chemoattractant cytokine

expression in small tissue samples and monocyte-derived dendritic cells: validation of a new real-time RT-PCR technology. 2000. Journal of Immunological Methods. 246:79-90.

26 Briere F, Servet-Delprat C, Bridon JM, Saint-Remy JM and Banchereau J. 1994. Human interleukin 10 induces naive surface immunoglobulin D+ (sIgD+) B cells to secrete IgG1 and IgG3. J Exp Med Feb.179:757-762.

27 Bombardier C, Gladman DD, Urowitz MB, Caron D and Chang CH. 1992. Derivation of the SLEDAI: a disease activity index for lupus patients. Arthritis and Rheumatism. 35:630-640.

28 Bossu P, Singer GG, Andres P, Ettinger R, Marshak-Rothstein A and Abbas AK. 1993. Mature $CD4^+$ T lymphocytes from MRL*/lpr* mice are resistant to receptor-mediated tolerance and apoptosis. Journal of Immunology.151:7233-7239.

29 Boswell JM, Yui M, Endres S, Burt DW and Kelley VE. 1988a. Increased tumor necrosis factor and IL-1 beta gene expression in the kidneys of mice with lupus nephritis. Journal of Immunology.141:3050-4.

30 Boswell JM, Yui MA, Endres S, Burt DW and Kelley VE. 1988b. Novel and enhanced IL-1 gene expression in autoimmune mice with lupus. Journal of Immunology. 141:118-24.

31 Budd RC, MacDonald HR, Lowenthal JW, Davignon JL, Izui S and Cerottini JC. 1985. Growth and differentiation in vitro of the accumulating Lyt-2-/L3T4- subset in *lpr* mice. J Immunol.135:3704-3711.

32 Carrichio R and Cohen PL. 1999. Spontaneous and induced apoptosis in Systemic Lupus Erythematous: Multiple assays fail to reveal consistent abnormalities. Cellular Immunology. 198:54-60.

33 Cayphas S, Van Damme J, Vink A, Simpson RJ, Billiau A, Van Snick J. 1987. Identification of an interleukin HP1-like plasmacytoma growth factor produced by L cells in response to viral infection. Journal of Immunology. 139: 2965-9.

34 Cecconi F. 1999. Apaf-1 and the apoptotic machinery. Cell Death and Differentiation. 6:1087-98

35 Chan OT, Paliwal V, McNiff JM, Park SH, Bendelac A and Shlomchik MJ.2001. Deficiency in beta (2)-microglobulin, but not CD1,

accelerates spontaneous lupus skin disease while inhibiting nephritis in MRL-Fas(lpr) nice: an example of disease regulation at the organ level. Journal of Immunology.167:2985-90.

36 Chen JK and Chen K. 1989. Achievements in clinical research of treating internal disease with traditional Chinese medicine in recent years. Chinese Medical Journal. 102:735-9.

37 Chen X, Yu L and Lu Y. 1995. Image analysis for intercellular adhesion molecule-1 expression in MRI/lpr mice: effects of Chinese herb medicine. Zhonghua Yi Xue Za Zhi. 75:204-206.

38 Cheng J, Zhou T, Liu C, Shapiro JP, Brauer MJ and Kiefer MC. 1996. Protection from Fas-mediated apoptosis by a soluble form of the Fas molecule. Science. 263:1759-62.

39 Cheng J, Zhou T, Liu C, Shapiro JP, Brauer MJ, Kiefer MC, Barr PJ and Mountz JD. 1994. Protection from Fas-mediated apoptosis by a soluble form of the Fas molecule. Science. 263:1759-1762.

40 Chu JL, Drappa J, Parnassa A and Elkon KB. 1993. The defect in Fas mRNA expression in MRL/lpr mice is associated with insertion of the retrotransposon, ETn. Journal of Experimental Medicine.178:723-730.

41 Cohen PL and Eisenberg RA. 1991. Lpr and gld: single gene models of systemic autoimmunity and lymphoproliferative disease. Annual Revue Immunology. 9:243-69.

42 Cohen JJ.1993. Apoptosis. Immunology Today. 14:126-30.

43 Cohen JJ, Duke RC, Fadok VA, and KS Sellins. 1992. Apoptosis and programmed cell death in immunity. Annual Revue Immunology. 10:267-293.

44 Colombel M, Olsson CA, Ng PY and Buttyan R. 1992. Hormone-regulated apoptosis results from reentry of differentiated prostate cells onto a defective cell cycle. Cancer Research. 413-9.

45 Courtney PA, Crockard AD, Williamson K, McConnell J, Kennedy RJ and Bell AJ. 1998. Lymphocyte apoptosis in systemic lupus erythematosus: relationship with Fas expression, serum soluble fas and disease activity. Lupus.8:508-13.

46 Covas MI, Esquerda A, Arner M, Sanz F and Mahy N. 1996.Differential effects of 2'-deoxyguanosine on peripheral blood mononuclear cell

proliferation in healthy donors and Hashimoto's thyroiditis patients. Cell Proliferation. 29:513-21.

47 Crispin JC and Alcocer-Varela J. 1998. Interleukin-2 and systemic lupus erythematosus fifteen years later. 7:214-22.

48 Cross JT, Benton HP. 1999. The roles of interleukin-6 and interleukin-10 in B cell hyperactivity in systemic lupus erythematosus. Inflammation Research. 48: 255-61.

49 Csiszar A, Nagy G, Gergely P, Pozsonyi T, Pocsik E. 2000. Increased interferon-gamma (IFN-gamma), IL-10 and decreased IL-4 mRNA expression in peripheral blood mononuclear cells (PBMC) from patients with systemic lupus erythematosus (SLE). Clinical Experimental Immunology. 122:464-70.

50 Davidoff AN and Mendelow BV. 1992. Unexpected cytokinetic effects induced by puromycin include a G2-arrest, a metaphase-mitotic-arrest, and apoptosis. Leukocyte Research. 16:1077-85.

51 Dhein J, Walczak H, Baumler C, Debatin KM and Krammer PH.1995. Autocrine T-cell suicide mediated by APO-1/. Nature. 373:438-41.

52 Drake CG, Rozzo SJ, Vyse TJ, Palmer E and Kotzin BL. 1995. Genetic contributions to lupus-like disease in (NZB x NZW)F1 mice. Immunological Revue.144:51-74.

53 Donadio JV and Galssock RJ. 1993. Immunosuppressive drug therapy in lupus nephritis. American Journal of Kidney Diseases. 21: 239-50.

54 Dooley MA and Falk RJ. 1998. Immunosuppressive therapy for lupus nephritis. Lupus.7:630-634.

55 Dumoulin FL, Nischalke HD, Leifeld L, von dem Bussche A, Rockstroh JK, Sauerbruch T, Spengler U. Semi-quantification of human C-C chemokine mRNAs with reverse transcription/real-time PCR using multi-specific standards.2000. Journal of Immunological Methods. 2411:109-19.

56 Eilat D and Naparstek Y. 1999. Anti-DNA autoantibodies: a puzzle of autoimmune phenomena. Immunology Today. 20:339-42.

57 Emlen W, Niebur J and Kadera R. 1994. Accelerated in vitro apoptosis of lymphycotes from patients with systemic lupus erythematosus. Journal of Immunology.152:3685-692.

58 van Engeland M, Nieland LJ, Ramaekers FC, Schutte B and Reutelingsperger CP. 1998. Annexin V-affinity assay: a review on an apoptosis detection system based on phosphatidylserine exposure. Cytometry. 31:1-9.

59 Evan GI, Wyllie AH, Gilbert CS, Littlewood TD, Land H, Brooks M, Waters CM, Penn LZ and Hancock DC. 1992. Induction of apoptosis in fibroblasts by c-myc protein. Cell. 69:119-28.

60 Fadok VA, Voelker DR, Campbell PA, Cohen JJ, Bratton DL and Henson PM. 1992. Exposure of phosphatidylserine on the surface of apoptotic lymphocytes triggers specific recognition and removal by macrophages. Journal of Immunology. 148:2207-16.

61 Fan X, Oertli B and Wuthrich RP. 1997. Up-regulation of tubular epithelial interleukin-12 in autoimmune MRL-Fas^{lpr} mice with renal injury. Kidney International. 51:79-86.

62 Farnsworth N. R. 1990.The role of ethnopharmcology in drug development, D. J. Chadwick and J. Marsh (Eds) Bioactive Compounds from Plants. John Wiley & sons Ltd, Chinchester.pg 2-22.

63 Finck BK, Linsley PS and Wofsy D. 1994a Treatment of murine lupus with CTLA4Ig. Science. 265:1225-1227.

64 Finck BK, Chan B and Wofsy D. 1994b. Interleukin 6 promotes murine lupus in NZB/NZW F1 mice. J Clin Invest. 94:585-591.

65 Fisher GH, Rosenberg FJ, Straus SE, Dale JK, Middleton LA and Lin AY. 1995. Dominant interfering Fas gene mutations impair apoptosis in a human autoimmune lymphoproliferative syndrome. Cell. 81:935-46.

66 Gaffney PM, Kearns GM, Shark KB, Ortmann WA, Selby SA, Malmgren ML, Rohlf KE, Ockenden TC, Messner RP, King RA, Rich SS and Behrens TW. 1998. A genome-wide search for susceptibility genes in human systemic lupus erythematosus sib-pair families. Proceedings of the National Academy of Sciences of the United States of America. 95:14875-9.

67 Gladman D, Ginzler E, Goldsmith C, Fortin P, Liang M, Urowitz M, Bacon P, Bombardieri S, Hanly J, Hay E, Isenberg D, Jones J, Kalunian K, Maddison P, Nived O, Petri M, Richter M, Sanchez-Guerrero J, Snaith M, Sturfelt G, Symmons D and Zoma A. 1996. The development and initial validation of the Systemic Lupus International Collaborating Clinics/American College of Rheumatology damage

index for systemic lupus erythematosus. Arthritis and Rheumatism. 39:363-369.

68 Gmelig-Myeling F, Dawisha S and Steinberg AD. 1992. Assessment of in-vivo frequency of mutated T cells in patients with systemic lupus erythematosus. Journal of Experimental Medicine. 175:297-300.

69 Gong J, Li X and Darzynkiewicz Z. 1993. Different patterns of apoptosis of HL-60 cells induced by cycloheximide and camptothecin. Journal of Cellular Physiology. 157:263-70.

70 Graninger WB, Steiner CW, Graninger MT, Aringer M and Smolen JS. 2000. Cytokine regulation of apoptosis and Bcl-2 expression in lymphocytes of patients with systemic lupus erythematosus. Cell Death and Differentiation. 7:966-72.

71 Grondal G, Gunnarsson I, Ronnelid J, Rogberg S, Klareskog L and Lundberg I. 2000. Cytokine production, serum levels and disease activity in systemic lupus erythematosus. Clinical Experimental Rheumatology. 18:565-70.

72 Gu WZ, Banerjee S, Rauch J and Brandwein SR. 1992. Suppression of renal disease and arthritis, and prolongation of survival in MRL-lpr mice treated with an extract of Tripterygium wilfordii Hook f. Arthritis and Rheumatism. 35:1381-6.

73 Gutierrez-Ramos JC, Andreu JL, Marcos MA, Vegazo IR and Martinez C. 1991. Treatment with Il-2/caccinia recombinant virs leads to serologic, histologic and phenotypic normalization of autoimmune MRL-*lpr/lpr* mice. Autoimmunity. 10:5-25.

74 Guerder S and Flavell R. 1996. In Weir's Handbook of experimental immunology; Volume III, The lymphoid system. Edited by Herzenberg EA, Weir DM, Herzenberg LA, Blackwell C. 5th edition Blackwell Science. pg. 96.1-22.

75 Haas C, Ryffel B, Le Hir M. 1997. IFN-gamma is essential for the development of autoimmune glomerulonephritis in MRL/lpr mice. Journal of Immunology. 158:5484-91.

76 Haas C, Ryffel B, Le Hir M. 1998. IFN-gamma receptor deletion prevents autoantibody production and glomerulonephritis in lupus-prone (NZB x NZW)F1 mice. Journal of Immunology.160:3713-8.

77 Hagiwara E, Gourley MF, Lee S, Klinman DK.1996.Disease severity in patients with systemic lupus erythematosus correlates with an increased ratio of interleukin-10:interferon-gamma-secreting cells in the peripheral blood. Arthritis Rheumatism. 39: 379-85.

78 Hakem R, Hakem A, Duncan GS, Henderson JT, Woo M, Soengas MS, Elia A, de la Pompa JL, Kagi D, Khoo W, Potter J, Yoshida R, Kaufman SA, Lowe SW, Penninger JM and Mak TW. 1998. Differential requirement for caspase 9 in apoptotic pathways in vivo. Cell. 94:339-52.

79 Harper J. Traditional Chinese medicine for eczema. 1994. British Medical Journal. 308:489-490.

80 Heid CA, Stevens J, Livak KJ and Williams PM. 1996. Real time quantitative PCR. Genome Research. 6:986-94.

81 Herron LR, Eisenberg RA, Roper E, Kakkanaiah VN, Cohen PL and Kotzin BL. 1993. Selection of the T cell receptor repertoire in *lpr* mice. Journal of Immunology. 151:3450-3459.

82 Hochberg MC. 1997. Updating the American College of Rheumatology revised criteria for the classification of systemic lupus erythematosus. Arthritis Rheumatism. 40:1725.

83 van Houten N and Budd RC. 1994. Introduction: lessons from the lpr mouse--T lymphocyte development. Seminars in Immunology. 6:1-2.

84 Horii Y, Iwano M, Hirata E, Shiiki M, Fujii Y, Dohi K and Ishikawa H. 1993. Role of interleukin-6 in the progression of mesangial proliferative glomerulonephritis. Kidney Int Suppl. 39:S71-S75.

85 Huang YP, Miescher PA and Zubler RH. 1986. The interleukin 2 secretion defect in vitro in systemic lupus erythematosus is reversible in rested cultured T cells. Journal of Immunology.137:3515-3520.

86 Ibnou-Zekri N, Iwamoto M, Fossati L, McConahey PJ, Izui S. 1997. Role of the major histocompatibility complex class II Ea gene in lupus susceptibility in mice. Proceedings of the National Academy of Sciences of the United States of America. 94:14654-9.

87 Ishida H, Muchamuel T, Sakaguchi S, Andrade S, Menon S and Howard M. 1994. Continuous administration of anti-interleukin 10

antibodies delays onset of autoimmunity in NZB/W F1 mice. Journal of Experimental Medicine.179:305-310.

88 Iwano M, Dohi K, Hirata E, Kurumatani N, Horii Y, Shiiki H, Fukatsu A, Matsuda T, Hirano T and Kishimoto T.1993. Urinary levels of IL-6 in patients with active lupus nephritis. Clinical Nephrology. 40:16-21.

89 Itokawa H, Takeya K, Mori N, Kidokoro and Yamamoto H. 1984. Studies on antitumor cyclic hexapeptides from Rubiae Radix, Rubiaceae (IV): Quantative determination of RA-VII and RA-V in commercial Rubiae Radix and collected plants. Planta Medica. 50:313-6.

90 Itokawa H, Morita H and Takeya K. 1992. Solution forms of an antitumor cyclic hexapeptides, RA-VII in dimethyl sulfoxide-de6 from Nuclear Magnetic Studies Chemical Pharmaceutical Bulletin. 40:1050-52.

91 Itokawa H, Kondo K, Hitotsuyanagi, Nakamura A, Morita H and Takeya K. 1993. Preparation and cytotoxicity of cyclic hexapeptides, RA Derivatives. Chemical Pharmaceutical Bulletin. 41:1266-69

92 Jacob CO, van der Meide PH, McDevitt HO.1987. In vivo treatment of (NZB X NZW)F1 lupus-like nephritis with monoclonal antibody to gamma interferon. Journal of Experimental Medicine.166: 798-803.

93 Jevnikar AM, Grusby MJ and Glimcher LH. 1994. Prevention of nephritis in major histocompatibility complex class II-deficient MRL-*lpr* mice. Journal of Experimental Medicine. 179:1137-43.

94 Jones BM, Liu T and Wong RW. 1999. Reduced in vitro production of interferon-gamma, interleukin-4 and interleukin-12 and increased production of interleukin-6, interleukin-10 and tumour necrosis factor-alpha in systemic lupus erythematosus. Weak correlations of cytokine production with disease activity. Autoimmunity. 31:117-24.

95 Jonsson R, Tarkowski A, Backman K, Holmdahl R and Klareskog L. 1987. Sialadenitis in the MRL-l mouse: morphological and immunohistochemical characterization of resident and infiltrating cells. Immunology. 60:611-6.

96 Kao NI, Richmond GW and Moy JM. 1993. Resolution of severe lupus nephrtis associated with *Tripterium wilfordii* Hook f ingestion. Arthritis and Rheumatism. 36:1751-56.

97 Kerr JF, Wyllie AH and Currie AR. 1972. Apoptosis: a basic biological phenomenon with wide-ranging implications in tissue kinetics. British Journal of Cancer. 26:239-57.

98 Koh DR, Ho A, Rahemtulla A, Fung-Leung WP, Griesser H and Mak TW. 1995. Murine lupus in MRL/lpr mice lacking CD4 or CD8 T cells. European Journal of Immunology. 25:2558-62.

99 Koffler D, Schur PH and Kunkel HG. 1967. Immunological studies concerning the nephritis of systemic lupus erythematosus. Journal of Experimental Medicine. 126:607-24.

100 Kondo T, Marchevsky A, Jordan SC, Koerner SK, Matloff JM and Waters PF. 1991. Vascular rejection and graft eosinophilia in rat lung allografts. Journal of Surgical Research. 51:310-5.

101 Kotzin BL. 1996. Systemic Lupus Erythematosus. Cell. 85:303-306.

102 Kotzin BL and O'Dell JR. 1995. Systemic lupus erythematosus. In Samter's Immunologic Diseases, 5th Edition, Frank MM, Austen KF, Claman HN, Unanue ER, eds. Boston: Little, Brown & Co. pp 667-697.

103 Kuo YC, Sun CM, Tsai WJ, Ou JC, Chen WP and Lin CY. 1998. Chinese herbs as modulators of human mesangial cell proliferation: preliminary studies. Journal of Laboratory and Clinical Medicine. 132:76-85.

104 Kreisberg JI, Hoover RL and Karnovsky MJ. 1978. Isolation and characterization of rat glomerular epithelial cells in vitro. Kidney International 14:21-30.

105 Kroemer G. 1997. The proto-oncogene Bcl-2 and its role in regulating apoptosis. Nat Med. 3:614-20.

106 Lambert PH and Dixon FJ. 1968. Pathogenesis of the glomerulonephritis of NZB/W mice. Journal of Experimental Medicine. 127:507-22.

107 Lane DP. Cancer. 1992. p53, guardian of the genome. Nature. 358:15-16.

108 Laouar Y and Ezine S. 1994. In vivo CD4+ lymph node T cells from lpr mice generate CD4-CD8-B220+TCR-beta low cells. Journal of Immunology. 153:3948-3955.

109 Latiff A. 1991. Plant resorces for natural products: an ethnobotanical perspective. K. Shaari, A. A. Kadir, A. R. M. Ali (Eds) Medicinal Products from Tropical Rain Forest. May 13-15.

110 Lawson BR, Prud'homme GJ, Chang Y, Gardner HA, Kuan J, Kono DH, Theofilopoulos AN. 2000. Treatment of murine lupus with cDNA encoding IFN-gammaR/Fc. Journal of Clinical Investigations.106: 207-15.

111 Lemay S, Mao C and Singh AK. 1996. Cytokine gene expression in the MRL/lpr model of lupus nephritis. Kidney Int. 50:85-93.

112 Lenardo MJ. 1991. Interleukin-2 programs mouse alpha beta T lymphocytes for apoptosis. Nature. 353: 858-61.

113 Lewis DE, Giorgi JV and Warner NL. 1981.Flow cytometry analysis of T cells and continuous T-cell lines from autoimmune MRL/l mice. Nature. 289:298-300.

114 Li SY, Ling LH, Teh BS, Seow WK and Thong YH. 1989. Anti-inflammatory and immunosuppressive properties of the bis-benzylisoquinolines: in vitro comparisons of tetrandrine and

berbamine. International Journal of Immunopharmacology. 11:395-401.

115 Li XW and Weir MR. 1990. Radix *Tripterygium wilfordii*--a Chinese herbal medicine with potent immunosuppressive properties. Transplantation. 50:82-86.

116 van der Linden MW, van Lopik T, Aarden LA, Westendorp RG and Huizinga TW. 2001. Soluble CD95 concentrations are increased in patients with severe systemic lupus erythematosus, but not in their first degree relatives. Annals Rheumatic Disease. 60:237-41.

117 Lindqvist AKB and Alarcon-Riquelme ME. 1999. The genetic of Systemic Lupus Erythematosus. Scandinavian Journal of Immunology. 50:562-571.

118 Linker-Israeli M, Deans RJ, Wallace DJ, Prehn J, Ozeri-Chen T, Klinenberg JR. 1991. Elevated levels of endogenous IL-6 in systemic lupus erythematosus. A putative role in pathogenesis. Journal of Immunology. 147:117-123.

119 Linker-Israeli M, Wallace DJ, Prehn J, Michael D, Honda M, Taylor KD, Paul-Labrador M, Fischel-Ghodsian N, Fraser PA, Klinenberg JR. 1999.

Association of IL-6 gene alleles with systemic lupus erythematosus (SLE) and with elevated IL-6 expression. Genes Immunology.1:45-52.

120 Llorente L, Zou W, Levy Y, Richaud-Patin Y, Wijdenes J, Alcocer-Varela J, Morel-Fourrier B, Brouet JC, Alarcon-Segovia D and Galanaud P. 1995. Role of interleukin 10 in the B lymphocyte hyperactivity and autoantibody production of human systemic lupus erythematosus. Journal of Experimental Medicine. 181:839-844.

121 Lorenz HM, Grunke M, Hieronymus T, Herrman M, Kuhnel A and Manger B. 1997. In vitro apoptosis and expression of apoptosis-related molecules in lymphocytes from patients with systemic lupus erythematosus and other autoimmune diseases. Arthritis and Rheumatism. 40:306-17.

122 Lorenz HM, Herrmann M and Kalden JR. 2001. The pathogenesis of autoimmune diseases. Scandinavian Journal Clininical Laboratory Investigations. 61 (Suppl 235) 16-26.

123 Los M, Wesselborg S and Schulze-Osthoff K. 1999. The role of caspases in development, immunity, and apoptotic signal transduction: lessons from knockout mice. Immunity. 10:629-639.

124 Los M, Stroh C, Janicke RU, Engels IH and Schulze-Osthoff K. 2001. Caspases: more than just killers? Trends in Immunology. 22:31-34.

125 Luo CN, Lin X and Wang LW. 1995. Study on immunosuppressive effects of berbamnine and its mechanism. Chinese Journal of integrated Traditional Western Medicine.15:217-9.

126 Luo CN, Lin X, Li WK, Pu F, Wang LW, Xie SS and Xiao PG. 1998. Effect of berbamine on T-cell mediated immunity and the prevention of rejection on skin transplants in mice. Journal of Ethnopharmacology. 59:211-215.

127 Mazel S, Burtrum D and Petrie HT. 1996. Regulation of cell division cycle progression by bcl-2 expression: a potential mechanism for inhibition of programmed cell death. Journal of Experimental Medicine. 183:2219-2226.

128 Masutani K, Akahoshi M, Tsuruya K, Tokumoto M, Ninomiya T, Kohsaka T, Fukuda K, Kanai H, Nakashima H, Otsuka T, Hirakata H. 2001. Predominance of Th1 immune response in diffuse proliferative lupus nephritis. Arthritis and Rheumatism. 44:2097-106.

129 McNally J, Yoo DH, Drappa J, Chu JL, Yagita H and Friedman SM. 1997. Fas ligand Expression and Function in Systemic Lupus Erythematosus. Journal of Immunology.159:4628-36.

130 Mihara M, Takagi N, Urakawa K, Moriya Y and Takeda Y. 1997. A novel antifolate, MX-68, inhibits the devlopemnt of autoimmune disease in MRL/lpr mice. International Arhcives of Allergy and Immunology. 113: 454-459.

131 Mehrian R, Quismorio FP Jr, Strassmann G, Stimmler MM, Horwitz DA, Kitridou RC, Gauderman WJ, Morrison J, Brautbar C and Jacob CO. 1998. Synergistic effect between IL-10 and bcl-2 genotypes in determining susceptibility to systemic lupus erythematosus. Arthritis and Rheumatism. 41:596-602.

132 Milner LS, de Chadarevian JP, Goodyer PR, Mills M and Kaplan BS. 1987. Amelioration of murine lupus nephritis by dimethylsulfoxide. Clinical Immunology and Immunopathology. 45:259-67.

133 Miyasaka N, Nakamura T, Russell IJ, Talal N. 1984. Interleukin 2 deficiencies in rheumatoid arthritis and systemic lupus erythematosus. Clinical Immunology Immunopathology. 31:109-117.

134 Mohan C, Adams S, Stanik V and Datta SK. 1993. Nucleosome: a major immunogen for pathogenic autoantibody-inducing T cells of lupus. Journal of Experimental Medicine. 177:1367-1381.

135 Mohan C and Datta SK. 1995. Lupus: key pathogenic mechanisms and contributing factors. Clinical Immunology Immunopathology. 77:209-20.

136 Moore KW, de Waal Malefyt R, Coffman RL, O'Garra A. 2001. Interleukin-10 and the interleukin-10 receptor Annual Review of Immunology. 19: 683-765.

137 Moore KW, O'Garra A, de Waal Malefyt R, Vieira P, Mosmann TR. 1993. Interleukin-10. Annual Review of Immunology. 11: 165-90.

138 Morse HC 3rd, Davidson WF, Yetter RA, Murphy ED, Roths JB and Coffman RL. 1982. Abnormalities induced by the mutant gene lpr: expansion of a unique lymphocyte subset. Journal of Immunology. 129:2612-2615.

139 Morton JI, Siegel BV, Weaver WJ, Bristol T and Jacob SW. 1983. The effects of chronic DMSO administration on the spontaneous

development of autoimmune disease in NZB, BXSB, and MRL/lpr strain mice. Annual New York Academic Science.411:344-6.

140 Morton JI and Siegel BV. 1986. Effects of oral dimethyl sulfoxide and dimethyl sulfone on murine autoimmune lymphoproliferative disease. Proceedings of Soc Experimental Biological Medicine.183:227-30.

141 Mosmann TR. Properties and functions of interleukin-10. 1994. Advances in Immunology. 56:1-26.

142 Mostoslavsky G, Fischel R, Yachimovich N, Yarkoni Y, Rosenmann E, Monestier M, Baniyash M and Eilat D. 2001. Lupus anti-DNA autoantibodies cross-react with a glomerular structural protein: a case for tissue injury by molecular mimicry. European Journal of Immunology. 31:1221-7.

143 Mountz JD, Jiangguo Wu, Jianhua C and Tong Z. 1994. Autoimmune diseases: A problem of defective Apoptosis. Arthritis and Rheumatism. 37:1415-20.

144 Moyer CF, Strandberg JD and Reinisch CL. 1987. Systemic mononuclear-cell vasculitis in MRL/Mp-lpr/lpr mice. A histologic and

immunocytochemical analysis. American Journal of Pathology. 127:229-42.

145 Murakawa Y, Takada S, Ueda Y, Suzuki N, Hoshino T and Sakane T. 1985. Characterization of T lymphocyte subpopulations responsible for deficient interleukin 2 activity in patients with systemic lupus erythematosus. J Immunol. 134:187-195.

146 Murray L and Martens C. 1990. Abnormal T cells from lpr mice down-regulate transcription of interferon-γ and tumor necrosis factor-α in vitro. Cellular Immunology.126:367-76.

147 Murray LJ, Lee R and Martens C. 1990. In vivo cytokine gene expression in T cell subsets of the autoimmune MRL/Mp-lpr/lpr mouse. European Journal of Immunology. 20:163-170.

148 Mustelin T and Altman A. 1993. Signal transduction pathways in T lymphocytes and their relevance to autoimmunity. The Molecular Pathology of Autoimmune diseases. Edited by Bona C, Siminovitch KA, Zanetti M, Theofilopoulos. Harwood academic publishers. Pg 137-147.

149 Mysler E, Bini P, Drappa J, Ramos P, Friedman SM, Krammer PH and Elkon KB. 1994. The apoptosis-1/Fas protein in human systemic lupus erythematosus. Journal of Clinical Investigations. 151:621-27.

150 Nagata S and Suda T. 1995. Fas and Fas ligand*: lpr* and *gld* mutations. Immunology Today.16:39-43.

151 Naparstek Y, Ben-Yehuda A, Madaio MP, Bar-Tana R, Schuger L, Pizov G, Neeman ZV and Cohen IR. 1990. Binding of anti-DNA antibodies and inhibition of glomerulonephritis in MRL-lpr/lpr mice by heparin. Arthritis Rheum. 33:1554-9.

152 Nicoletti I, Migliorati G, Pagliacci MC, Grignani F and Riccardi C. 1991. A rapid and simple method for measuring thymocyte apoptosis by propidium iodide staining and flow cytometry. J Immunol Methods. 139:271-9.

153 Nikolic-Zugic J, 1991. Phenotypic and functional stages in the intrathymic development of $\alpha\beta$T cells. Immunology Today. 12:65-70.

154 Nozawa K, Kayagaki N, Tokano Y, Yagita H, Okumura K and Hashimoto H. 1997. Soluble Fas (APO-1, CD95) and soluble Fas

ligand in Rheumatic diseases. Arthritis and Rheumatism. 40:1126-1129.

155 Ozmen L, Roman D, Fountoulakis M, Schmid G, Ryffel B, Garotta G. 1995. Experimental therapy of systemic lupus erythematosus: the treatment of NZB/W mice with mouse soluble interferon-gamma receptor inhibits the onset of glomerulonephritis. Eur J Immunol. 25:6-12.

156 Papo T, Parizot C, Ortova M, Piette JC, Frances C and Debre P. 1998. Apoptosis and expression of soluble Fas mRNA in systemic lupus erythematosus. Lupus. 7: 455-61.

157 van Parijs L and Abbas AK. 1998. Homeostasiss and Self-Tolerance in the immune system: Turning lymphocytes off. Science. 280:243-48.

158 Park YB, Lee SK, Kim DS, Lee J, Lee CH, Song CH. 1998. Elevated interleukin-10 levels correlated with disease activity in systemic lupus erythematosus. Clinical Experimental Rheumatology. 16: 283-8

159 Peng SL, Madaio MP, Hayday AC and Craft J. 1996. Propagation and regulation of systemic autoimmunity by gammadelta T cells. Journal of Immunology. 157:5689-98.

160 Peng SL, Moslehi J and Craft J. 1997. Roles of interferon-gamma and interleukin-4 in murine lupus. Journal of Clinical Invesigtions. 99:1936-46.

161 Peng SL, Cappadona J, McNiff JM, Madaio MP, Owen MJ, Hayday AC and Craft J. 1998. Pathogenesis of autoimmunity in alphabeta T cell-deficient lupus-prone mice. Clinical Experimental Immunology. 111:107-16.

162 Perniok A, Wedekind F, Herrmann M, Specker C, Schneider M. 1998. High levels of circulating early apoptic peripheral blood mononuclear cells in systemic lupus erythematosus. Lupus.72:113-8.

163 Peutz-Kootstra CJ, de Heer E, Hoedemaeker PJ, Abrass CK and Bruijn JA. 2001. Lupus nephritis: lessons from experimental animal models. Journal of Labotory Clinical Medicine.137:244-60.

164 Piacentini M, Fesus L and Melino G. 1993. Multiple cell cycle access to the apoptotic death programme in human neuroblastoma cells. FEBS Letters. 320:150-4.

165 Pircher H, Burki K, Lang R, Hengartner H and Zinkernagel RM. 1989. Tolerance induction in double specific T-cell receptor transgenic mice varies with antigen. Nature. 342:559-561.

166 Planey SL and Litwack G Glucocorticoid-induced apoptosis in lymphocytes. 2000. Biochemical Biophysical Research Communications. 279:307-12.

167 Potter A, Kim C, Gollahon KA and Rabinovitch PS. 1999. Apoptotic human lymphocytes have diminished CD4 and CD8 receptor expression. Cellular Immunology. 193:36-47.

168 Prud'homme GJ, Kono DH and Theofilopoulos AN. 1995. Quantitative polymerase chain reaction analysis reveals marked overexpression of interleukin-1 beta, interleukin-1 and interferon-gamma mRNA in the lymph nodes of lupus-prone mice. Molecular Immunology. 32:495-503.

169 Putterman C and Naparstek Y. 1994. Murine models of spontaneous Systemic Lupus Erythematosus. Autoimmune disease models: a guidebook. Edited by Irun R. Cohen and Ariel Miller. San Diego: Academic Press.

170 Qin WZ, Liu Ch and Yang SM. 1981. *Tripterium wilfordii* Hook F in Systemic Lupus Erythematosus. Chinese Medical Journal.94:827-31.

171 Radic MZ, Mackle J, Erikson J, Mol C, Anderson WF and Weigert M. 1993. Residues that mediate DNA binding of autoimmune antibodies. Journal of Immunology. 150: 4966-77.

172 Refaeli Y, Van Parijs L, London CA, Tschopp J, Abbas AK Biochemical mechanisms of IL-2-regulated Fas-mediated T cell apoptosis. 1998. Immunity.8:615-23.

173 Raff MC. 1992. Social controls on cell survival and cell death. Nature. 356:397-400.

174 Rathmell JC and Goodnow CC. 1994. Effects of the lpr mutation on elimination and inactivation of self-reactive B cells. Journal of Immunology. 153:2831-2842.

175 Reap EA, Felix NJ, Wolthusen PA, Kotzin BL, Cohen PL and Eisenberg RA. 1995. bcl-2 transgenic Lpr mice show profound enhancement of lymphadenopathy. Journal of Immunology. 155:5455-62.

176 Reed JC, Tanaka S and Cuddy M.1992. Cell cycle analysis of p26-BCL-2 protein levels in proliferating lymphoma and leukemia cell lines. Cancer Research. 52:2802-5.

177 Reininger L, Berney T, Shibata T, Spertini F, Merino R and Izui S. 1990. Cryoglobulinemia induced by a murine IgG3 rheumatoid factor: skin vasculitis and glomerulonephritis arise from distinct pathogenic mechanisms. Proceedings of the National Academy of Sciences of the United States of America. 87:10038-10042.

178 Renno T, Hahne M, Tschopp J and MacDonald HR.1996. Peripheral T cells undergoing superantigen-induced apoptosis in vivo express B220 and upregulate Fas and Fas ligand. Journal of Experimental Medicine. 183:431-7.

179 Rieux-Laucat F, Le Deist F, Hivroz C, Roberts IA, Debatin KM and Fischer A. 1995. Mutations in Fas associated with human lymphoproliferative syndrome and autoimmunity. Science. 268:1347-9.

180 Rose LM, Latchman DS and Isenberg DA. 1997. Elevated soluble fas production in SLE correlates with HLA status not with disease activity. Lupus. 6:717-22.

181 Rothenberg EV. 1990. Death and transfiguration of Cortical thymocytes a Reconsideration. Immunology Today.11:116-19.

182 Ruan J and Ye RG. 1994 Lupus nephritis treated with impact therapy of cyclophossphomaide and traditional Chinese medicines. Chung Hsi I Chieh Ho Tsa Chih.14:276-8.

183 Santoro TJ, Lehmann KR, Batt RA and Kotzin BL. 1987. The role of L3T4+ cells in the pathogenesis of lupus in lpr-bearing mice. I. Defects in the production of interleukins 2 and 3. European Journal of Immunology. 17:1131-6.

184 Sakata K, Sakata A, Kong L, Dang H and Talal N. 1998a. Role of Fas/FasL interaction in physiology and pathology: the good and the bad. Clinical Immunology and Immunopathology. 87:1-7.

185 Sakata K, Sakata A, Vela-Roch N, Espinosa R, Escalante A, Kong L, Nakabayashi T, Cheng J, Talal N and Dang H. 1998b. Fas (CD95)-transduced signal preferentially stimulates lupus peripheral T lymphocytes. European Journal of Immunology. 28:2648-60.

186 Salvesen GS and Dixit VM. 1997. Caspases: intracellular signaling by proteolysis. Cell. 91:443-6.

187 Sato M, Konuma T, Yanagisawa N, Haizuka H, Asakura H and Nakashima Y. 2000. Fas-Fas ligand system in the peripheral blood of patients with renal diseases. Nephron. 85:107-13.

188 Savill J, Fadok V, Henson P and Haslett C. 1993. Phagocyte recognition of cells undergoing apoptosis. Immunology Today.14:131-36.

189 Schultes RE. 1972. The future of plants as sources of new biodynamic compounds. T. Swain (Ed.) Plants in the Development of Modern Medicine.

190 Schwartz LM, Smith SW, Jones ME and Osborne BA.1993. Do all programmed cell deaths occur via apoptosis? Proceedings National Academy Sciences of the USA.90:980-4.

191 Sha WC, Nelson CA, Newberry RD, Kranz DM, Russell JH and Loh DY. 1988. Positive and negative selection of an antigen receptor on T cells in transgenic mice. Nature. 336:73-76.

192 Shi YF, Bissonette RP, Parfrey N, Szalay M, Kubo RT, and Green DR. 1989. In vivo administration of monoclonal antibodies to the CD3 T cell

receptor complex induces cell death (apoptosis) in immature thymocytes. Journal of Immunology, 146: 3340-46.

193 Searle J, Kerr JF and Bishop CJ. 1982. Necrosis and apoptosis: distinct modes of cell death with fundamentally different significance. Pathology Annual. 2:229-59.

194 Seki M, Ushiyama C, Seta N, Abe K, Fukazawa T and Asakawa J. 1998. Apoptosis of lymphocytes induced by glucocorticoids and relationship to therapeutic efficacy in patients with systemic lupus erythematosus. Arthritis and Rheumatism. 41:823-30.

195 Sewing K Fr, Christians U, Kohlhaw K, Radeke H, Strohmeyer S, Kownatzki R, Budniak J, Schottmann R, Bleck JS and Almeida VM. 1990. Biologic activity of cyclosporine metabolites. Transplantation Proceedings. 22:1129-34.

196 Seery JP, Wang EC, Cattell V, Carroll JM, Owen MJ and Watt FM. 1999. A central role for alpha beta T cells in the pathogenesis of murine lupus. Journal of Immunology. 162:7241-8.

197 Seery JP, Carroll JM, Cattell V, Watt FM. 1997. Antinuclear autoantibodies and lupus nephritis in transgenic mice expressing

interferon gamma in the epidermis. Journal of Experimental Medicine.186:1451-9.

198 Sheehan MP, Rustin MH, Atherton DJ, Buckley C, Harris DW, Brostoff J, Ostlere L, Dawson A and Harris DJ. 1992. Efficacy of traditional Chinese herbal therapy in adult atopic dermatitis. Lancet. 340:13-17.

199 Sheehan MP and Atherton DJ. 1992. A controlled trial of traditional Chinese medicinal plants in widespread non-exudative atopic eczema. British Journal of Dermatology. 126:179-184.

200 Singer GG and Abbas AK. 1994. The Fas Antigen is involved in Peripheral but not Thymic Deletion of T Lymphocytes in T Cell Receptor transgenic Mice. Immunity.1:365-71.

201 Singer GG, Carrera AC, Marshak-Rothstein A, Martinez C and Abbas AK. 1994. Apoptosis, Fas and systemic autoimmunity: the MRL-lpr/lpr model. Current Opinion in Immunology.6:913-920.

202 van Snick J. 1990. Interleukin-6: an overview. Annu Rev Immunol. 8:253-278.

203 Sperandio S, de Belle I and Bredesen DE. 2000. An alternative, nonapoptotic form of programmed cell death. Proceedings National Academy of Science U S A. 97:14376-14381.

204 Sobel ES, Kakkanaiah VN, Rapoport RG, Eisenberg RA and Cohen PL. 1995. The abnormal lpr double-negative T cell fails to proliferate in vivo. Clin Immunol Immunopathol. 74:177-184.

205 Steinberg AD. 1994. Systemic Lupus Erythematosus: Theories of Pathogenesis and Approach to Therapy. Clinical Immunology and Immunopathology. 72:171-76.

206 Steinberg AD, Klassen LW, Raveche ES, Gerber NL, Reinertsen JL, Krakauer RS, Ranney DF, Gershwin ME, Williams GW, Kovacs K and Reeves JP.1978. Study of the multiple factors in the pathogenesis of autoimmunity in New Zealand mice. Arthritis and Rheumatism 21:S190-201.

207 Stoll T, Seifert B and Isenberg DA. 1996. SLICC/ACR Damage Index is valid, and renal and pulmonary organ scores are predictors of severe outcome in patients with systemic lupus erythematosus. British Journal of Rheumatology. 35:248-54.

208 Strasser A, Whittingham S, Vaux DL, Bath ML, Adams JM, Cory S and Harris AW. 1991. Enforced *Bcl-2* expression in B-lymphoid cells prolongs antibody responses and elicits autoimmune diseases. Proceedings of National Academy Sciences of the U S A;88:8661-65.

209 Strasser A. Apoptosis. Death of a T cell. 1995. Nature.373:385-6.

210 Suda T, Hashimoto H, Tanaka M, Ochi T and Nagata S. 1997. Membrane Fas ligand kills human peripheral blood T lymphocytes, and soluble Fas ligand blocks the killing. Journal of Experimental Medicine.186:2045-50.

211 Suda T and Nagata S. 1997. Why do defects in the Fas-Fas system cause autoimmunity? Journal of Allergy and Clinical Immunology.100; S97-101.

212 Swaak AJ, van Rooyen A and Aarden LA. 1989. Interleukin-6 (IL-6) and acute phase proteins in the disease course of patients with systemic lupus erythematosus. Rheumatol Int. 8:263-268.

213 Takahashi S, Fossati L, Iwamoto M, Merino R, Motta R, Kobayakawa T, Izui S.1996. Imbalance towards Th1 predominance is associated with

acceleration of lupus-like autoimmune syndrome in MRL mice. Journal of Clinical Investigations.97:1597-604.

214 Talal N. 1994. Oncogenes, autogenes, and rheumatic diseases. Arthritis and Rheumatism. 37:1421-2.

215 Tamaki T, Kawamura A, Komatsu Y, Kawamura H, Maruyama H and Morota T. 1996. Phenolic nortriterpene demethylzeylasteral: a new immunosuppressive component of *Tripterygium Wilfordii* Hook f. Transplant Proceedings. 28:1379-1380.

216 Tan EM, Cohen AS, Fries JF, Masi AT, McShane DJ, Rothfield NF, Schaller JG, Talal N and Winchester RJ. 1982. The 1982 revised criteria for the classification of systemic lupus erythematosus. Arthritis and Rheumatism 25:1271-7.

217 Tan EM. 1989. Antinuclear antibodies: diagnositic markers for autoimmune diseases and probes for cell biology. Advances in Immunology. 44:93-151.

218 Thornberry NA and Lazebnik Y. 1998. Caspases: enemies within. Science. 281:1312-1316

219 Terui Y, Furukawa Y, Kikuchi J and Saito M. 1995. Apoptosis during HL-60 cell differentiation is closely related to a G0/G1 cell cycle arrest. Journal of Cellular Physiology. 164:74- 84.

220 Tezcan H, Zimmer W, Fenstermaker R, Herzig GP and Schriber J. 1998. Severe cerebellar swelling and trombotic thrombocytopenic purpura associated with FK506. Bone Marrow Transplantation. 22:105-09.

221 Theofilopoulos AN and Dixon FJ. 1985. Murine models of systemic lupus erythematosus. Advances in Immunology. 37:269-390.

222 Theofilopoulos AN, Eisenberg RA, Bourdon M, Crowell JS Jr and Dixon FJ.1979. Distribution of lymphocytes identified by surface markers in murine strains with systemic lupus erythematosus-like syndromes. Journal of Experimental Medicine.149:516-34.

223 Theofilopoulos AN, Kofler R, Singer PA and Dixon FJ. 1989. Molecular genetics of murine lupus models. Advances in Immunology. 46:61-109.

224 Theofilopoulos AN. 1993. Immunologic genes in mouse lupus models, in The Molecular Pathology of Autoimmune Diseases, edited by Bona

CA, Siminovitch KA, Zanettie, Theofilopoulos AN, Chur, Switserland, Harwood Academic Publishers,pg. 281-316.

225 Vaishnaw AK, Toubi E, Ohsako S, Drappa J, Buys S, Estrada J, Sitarz A, Zemel L, Chu JL and Elkon KB. 1999a. The spectrum of apoptotic defects and clinical manifestations, including systemic lupus erythematosus, in humans with CD95 (Fas/APO-1) mutations. Arthritis and Rheumatism. 42:1833-42.

226 Vaishnaw AK, Orlinick JR, Chu JL, Krammer PH, Chao MV and Elkon KB. 1999b. The molecular basis for apoptotic defects in patients with CD95 (Fas/Apo-1) mutations. Journal of Clinical Investigations.103:355-63.

227 Vermes I, Haanen C, Steffens-Nakken H and Reutelingsperger C. 1995. A novel assay for apoptosis. Flow cytometric detection of phosphatidylserine expression on early apoptotic cells using fluorescein labelled Annexin V. Journal of Immunological Methods.184:39-51.

228 Vlahakos DV, Foster MH, Adams S, Katz M, Ucci AA, Barrett KJ, Datta SK and Madaio MP. 1992. Anti-DNA antibodies form immune deposits

at distinct glomerular and vascular sites. Kidney International. 41:1690-700.

229 Vyse TJ and Kotzin BL. 1998. Genetic susceptibility to systemic lupus erythematosus. Annual Review of Immunology.16:261-92.

230 Wang ZY. 1989. Clinical and laboratory studies of the effect of an antilupus pill on Sytemis Lupus Erythematosus. Chung his I Chieh Ho Tsa Chih.9:465-8.

231 Wang BX and Yuan ZZ. 1989. A tablet of Tripterygium wilfordii in treating lupus erythematosus. Zhong Xi Yi Jie He Za Zhi. 9:407-8.

232 Watanabe-Fukunaga R, Brannan CI, Copeland NG, Jenkins NA, Nagata S. 1992. Lymphoproliferation disorder in mice explained by defects in Fas antigen that mediates apoptosis. Nature. 356:314-7.

233 Watson ML, Rao JK, Gilkeson GS, Ruiz P, Eicher EM, Pisetsky DS, Matsuzawa A, Rochelle JM and Seldin MF. 1992. Genetic analysis of MRL-lpr mice: relationship of the Fas apoptosis gene to disease manifestations and renal disease-modifying loci. Journal of Experimental Medicine. 176:1645-1656.

234 Wigfall DR, Sakai RS, Wallace DJ and Jordan SC.1988. Interleukin-2 receptor expression in peripheral blood lymphocytes from systemic lupus erythematosus patients: relationship to clinical activity. Clinical Immunology and Immunopathology. 47:354-62.

235 Wofsy D, Hardy RR and Seaman WE. 1984 The proliferating cells in autoimmune MRL/lpr mice lack L3T4, an antigen on "helper" T cells that is involved in the response to class II major histocompatibility antigens. Journal of Immunology.132:2686-2689.

236 Wofsy D, Murphy ED, Roths JB, Dauphinee MJ, Kipper SB and Talal N. 1981. Deficient interleukin 2 activity in MRL/Mp and C57BL/6J mice bearing the lpr gene. Journal of Experimental Medicine .54:1671-1680.

237 Wu J, Wilson J, He J, Xiang L, Schur PH, Mountz JD. 1996. Fas ligand mutation in a patient with systemic lupus erythematosus and lymphoproliferative disease. Journal of Clinical Investigations. 98:1107-13.

238 Wu J, Zhou T, He J and Mountz JD. 1993. Autoimmune disease in mice due to integration of an endogenous retrovirus in an apoptosis gene. Journal of Experimental Medicine.178:461-468.

239 Wu J, Zhou T, Zhang J, He J, Gause WC and Mountz JD. 1994. Correction of accelerated autoimmune disease by early replacement of the mutated lpr gene with the normal Fas apoptosis gene in the T cells of transgenic MRL-lpr/lpr mice. Proceedings of National Academy of Sciences of the U S A. 91:2344-2348.

240 Wyllie AH. 1986. What is apoptosis? Histopathology. 10:995-8.

241 Wyllie AH. 1993. Apoptosis (the 1992 Frank Rose Memorial Lecture). British Journal of Cancer. 67:205-8.

242 Wyllie AH, Kerr JF and Currie AR. 1980. Cell death: the significance of apoptosis. International Revue of Cytology. 68:251-306.

243 Wyllie AH and Morris RG. 1982. Hormone-induced cell death. Purification ad properties of thymocytes undergoing apoptosis after glucocorticoid treatment. American Journal of Pathology. 109:78-87.

244 Xie C, Liang Z, Chang S, Mohan C. 2003. Use of a novel elution regimen reveals the dominance of polyreactive antinuclear autoantibodies in lupus kidneys. Arthritis and Rheumatism.48:2343-52.

245 Yamada A, Miyakawa Y and Kosaka K. 1982. Entrapment of anti-DNA antibodies in the kidney of patients with systemic lupus erythematosus. Kidney International. 22:671-6.

246 Yamamoto KA, Mori T, Nakahama T, Ito M, Okudaira H, Miyamoto T. 1990. Experimental treatment of autoimmune MRL-*lpr/lpr* mice with immunosuppressive compound FK506. Immunology. 69:222-7.

247 Yang LY, Chen A, Kuo YC and Lin CY. 1999. Efficacy of a pure compound H1-A extracted from *Corycepsis sinensis* on autoimmune disease of MRL-lpr/lpr mice. The Journal of laboratory and Clinical medicine.

248 Yap HK, Zuo XJ, Toyoda M, Okada Y, Ang SG, Lai YH, Matloff JM, Marchevsky A, Ramgolam VS and Jordan SC. 1998.Immunosuppressive effect of the hydrophobic extract of a Chinese herb on rat lung allograft rejection. Transplant Proceedings. 30:980-1.

249 Yap HK, Ang SG, Lai YH, Ramgolam V and Jordan SC. 1999. Improvement in lupus nephritis following treatment with a Chinese herbal preparation. Archives of Pediatric and Adolescent Medicine.153:850-2.

250 Yap HK, Ng SC, Lee BW, Seah CC, Tan MA, Choy MY, Jordan SC. 1993. Modulation of MHC expression on human endothelial cells by sera from patients with systemic lupus erythematosus. Clinical Immunology and Immunopathology. 68:321-6.

251 Yoshida H, Kong YY, Yoshida R, Alia AJ, Hakem A and Hakem R. 1998. Apaf1 is required for mitochondrial pathways of apoptosis and brain development. Cell. 94:739-50.

252 Yu C, Yap N, Chen D and Cheng S. 1997. Modulation of hormone-dependent transcriptional activity of the glucocorticoid receptor by the tumor suppressor p53. Cancer Letters. 116:191-6.

253 Yu D. 1983. Clinical observations of 144 cases of Rheumatoid Arthritis treated with glycosides of *Tripterium wilfordii*. Journal of Traditional Medicine Clinical Medicine.3:125-9.

254 Yuan ZZ and Feng JC. 1989. Observation on the treatment of systemic lupus erythematosus with a Gentiana macrophylla complex tablet and a minimal dose of prednisolone. Chung his I Chieh Ho Tsa Chih.9:156-7.

255 Zhang XY, Tsuchiya N, Dohi M, Yamamoto K, Ishihara K, Okudaira H, Ito K, Miyamoto T. 1992. Prolonged survival of MRL-*lpr/lpr* mice treated with *Tripterygium wilfordii* Hook-F. Clinical Immunology and Immunopathology. 62:66-71.

256 Zheng TS, Hunot S, Kuida K, Flavell RA. 1999. Caspase knockouts:matters of life and death. Cell death and differentiation. 6:1043-53

257 Zuo XJ, Okada Y, Toyoda M, Yap HK, Marchevsky A, Matloff JM, Jordan SC. 2000. Hydrophobic extracts of a Chinese herb (CMX-13) exhibit potent immunosuppressive properties and prevent acute rejection in a highly histoincompatible model of rat lung transplantation. Transplantation. 70:1094-8.

APPENDICES

Appendix 4.1 The individual SLEDAI and SLICC scores of the SLE patients.

No	SLEDAI	SLICC	SEX	APOPTOTIC Cells after CMX-13 treatment
1	0	1	F	12
2	6	0	F	33
3	0	1	F	45
4	0	3	M	42
5	4	0	F	46
6	1	1	M	51
7	0	2	F	38
8	14	4	F	36
9	0	0	F	71
10	2	2	M	45
11	4	2	F	50
12	20	3	F	47
13	0	3	F	68
14	18	2	M	73
15	0	1	F	24
16	0	0	M	40
17	2	1	F	32
18	12	1	F	58
19	0	2	M	24
20	10	4	F	50

Appendix 4.2 .1 SLICC Score Of SLE Patients (I)

Patient No.	Ocular	Neuropsychiatry	Renal	Pulmonary	Cardiovascular	Peripheral Vascular
1	0	0	0	0	0	0
2	0	0	0	0	0	0
3	0	0	0	0	0	0
4	0	0	3	0	0	0
5	1	0	2	0	0	0
6	0	0	0	0	0	0
7	0	0	0	1	0	0
8	0	0	0	0	0	0
9	1	0	0	1	0	0
10	1	0	0	0	0	0
11	0	0	1	0	2	0
12	0	0	0	0	0	0
13	0	0	1	0	1	0
14	1	0	0	0	0	0
15	0	0	0	0	1	0
16	0	0	1	0	0	0
17	0	1	0	0	0	0
18	0	0	0	0	0	0
19	0	0	0	0	0	0
20	0	0	0	0	0	0

Appendix 4.2.2 SLICC Score Of SLE Patients (II)

Patient No.	Gastro-intestinal	Musculo-skeletal	Skin	Premature Gonadal Failure	Dia-betes mellitus	Malig-nancy
1	0	0	1	0	0	0
2	0	0	0	0	0	0
3	0	0	0	0	0	0
4	0	0	0	0	0	0
5	0	0	0	0	0	0
6	0	0	0	0	0	0
7	0	0	1	0	0	0
8	0	0	0	0	0	0
9	0	0	0	0	0	0
10	0	0	0	0	0	0
11	0	0	0	0	0	0
12	0	0	0	0	0	0
13	0	0	0	0	1	0
14	0	0	0	0	0	0
15	0	0	0	0	0	0
16	0	0	0	0	0	0
17	0	0	0	0	1	0
18	0	0	0	0	0	0
19	0	0	0	0	0	0
20	0	0	0	0	0	0

APPENDIX 4.3.1. SLEDAI Score Of SLE Patients (I)

Patient No.	Seizure	Psychosis	Organic brain syn-drome	Visual distur-bance	Cranial nerve disorder
1	0	0	0	0	0
2	0	0	0	0	0
3	0	0	0	0	0
4	0	0	0	0	0
5	0	0	0	0	0
6	0	0	0	0	0
7	0	0	0	0	0
8	0	0	0	0	0
9	0	0	0	0	0
10	0	0	0	0	0
11	0	0	0	0	0
12	0	0	0	0	0
13	0	0	0	0	0
14	0	0	0	0	0
15	0	0	0	0	0
16	0	0	0	0	0
17	0	8	8	0	0
18	0	0	0	0	0
19	0	0	0	0	0
20	0	0	0	0	0

APPENDIX 4.3.2 SLEDAI Score Of SLE Patients (II)

Patient No.	Lupus headache	CVA	Vasculitis	Arthritis	Myositis
1	0	0	0	0	0
2	0	0	0	0	0
3	0	0	0	0	0
4	0	0	0	0	0
5	0	0	0	0	0
6	0	0	0	0	0
7	0	0	0	0	0
8	0	0	0	0	0
9	0	0	0	0	0
10	0	0	0	0	0
11	0	0	0	0	0
12	0	0	0	0	0
13	0	0	0	0	0
14	0	0	0	0	0
15	0	0	0	0	0
16	0	0	0	0	0
17	0	0	0	0	0
18	0	0	0	0	0
19	0	0	0	0	0
20	0	0	0	0	0

APPENDIX 4.3.3 SLEDAI Score Of SLE Patients (III)

Patient No.	Urinary casts	Hematuria	Proteinuria	Pyuria	New rash
1	0	0	0	0	0
2	0	4	0	0	0
3	0	0	0	0	0
4	0	0	0	0	0
5	0	0	0	0	0
6	0	0	0	0	0
7	0	0	0	0	0
8	0	0	0	0	2
9	0	0	0	0	0
10	0	0	0	0	0
11	0	4	4	4	0
12	0	0	0	0	0
13	0	4	4	4	0
14	0	0	0	0	0
15	0	0	0	0	0
16	0	0	0	0	0
17	0	0	0	0	0
18	0	0	0	0	0
19	0	0	0	0	0
20	0	0	0	0	0

APPENDIX 4.3.4 SLEDAI Score Of SLE Patients (IV)

Patient No.	Alopecia	Mucosal ulcers	Pleurisy	Pericarditis	Low complement
1	0	0	0	0	0
2	0	0	0	0	0
3	0	0	0	0	2
4	0	0	0	0	0
5	0	0	0	0	0
6	0	0	0	0	0
7	0	0	0	0	0
8	0	0	0	0	0
9	0	0	0	0	0
10	0	0	0	0	0
11	0	0	0	0	2
12	0	0	0	0	0
13	0	0	2	2	2
14	0	0	0	0	0
15	0	0	0	0	0
16	0	0	0	0	0
17	0	0	0	0	0
18	0	0	0	0	0
19	0	0	0	0	0
20	0	0	0	0	0

APPENDIX 4.3.5 SLEDAI Score Of SLE Patients (V)

Patient No.	Increased DNA binding	Fever	Thrombocytopenia	Leukopenia
1	0	0	0	0
2	2	0	0	0
3	2	0	0	0
4	0	0	0	0
5	0	0	0	0
6	0	0	0	0
7	0	0	0	0
8	2	0	0	0
9	2	0	0	0
10	0	0	0	0
11	2	0	0	0
12	0	0	0	0
13	2	0	0	0
14	0	0	1	0
15	0	0	0	0
16	2	0	0	0
17	2	0	0	0
18	0	0	0	0
19	0	0	0	0
20	0	0	0	0

APPENDIX 5.1 Urine proteinuria score. Urine protein levels were assessed using Urine reagent strips (TECO Diagnostics URS-2P) and graded the semiquantitatively : 0 = Negative; 1 = Trace; 2 = 0-30 mg/dl (+); 3 = 30-100 mg/dl (++); 4 = 100-300 mg/dl (+++) ;5 = > 300 mg/dl (++++)

WK 8	0 Negative	1 Trace	2 0-30 mg/dl	3 30-100 mg/dl	4 100-300 mg/dl	5 > 300 mg/dl
CONTROL	1	6	6			
DMSO		8	4	1		
CMX-13	1	5	5	2		
DEX	1	9	3			

WK 12	0	1	2	3	4	5
CONTROL		3	8	2		
DMSO	2	5	3	2		
CMX-13	1	4	7	1		
DEX		2	10	1		

WK16	0	1	2	3	4	5
CONTROL			7	4		1
DMSO	2		5	5		1
CMX-13	4	2	4	1		
DEX	7	3	1	1		

WK18	0	1	2	3	4	5
CONTROL				4	1	
DMSO		2	3	2	3	
CMX-13	1	3	4	1	1	
DEX	3	2	1	2		

WK19	0	1	2	3	4	5
CONTROL			1	2	1	
DMSO			4	3	2	
CMX-13	1	3	3	1	2	
DEX	2	3	2			

WK 20	0	1	2	3	4	5
CONTROL			1	2		
DMSO		3	3	2	1	
CMX-13	3	1	1	2		
DEX	3	1	1	2		

APPENDIX 5.2 IgG-specific anti-ds DNA autoanitbody levels. Anti-dsDNA antibody in serum of MRL-lpr/lpr mice at 8, 12 and 16 weeks of age.

8 weeks old mice

Control	DMSO	CMX-13	DEX
0.17	0.17	0.27	0.21
0.18	0.24	0.10	0.24
0.21	0.16	0.20	0.25
0.27	0.20	0.32	0.24
0.24	0.22	0.29	0.28
0.41	0.25	0.17	0.18
0.96	0.47	0.19	0.27
0.45	0.21	0.16	0.22
0.24	1.40	0.17	0.20
0.17	0.17	0.23	0.28
0.70	0.59	0.28	0.20
0.66	0.26	0.21	0.16

12 weeks old mice

Control	DMSO	CMX-13	DEX
0.82	0.47	0.80	0.30
0.63	0.26	0.49	0.73
0.78	0.42	0.24	0.26
0.68	0.98	0.80	0.27
		0.52	0.24
		0.67	0.45
		0.50	

16 weeks old mice

Control	DMSO	CMX-13	DEX
1.02	1.33	1.15	0.23
1.35	2.00	0.57	1.17
1.39	0.79	0.74	1.29
1.25	1.14	1.32	0.51
1.27	1.81	0.74	0.65
1.60	1.78	0.76	0.54
2.45	2.21	1.12	1.06
		1.88	1.04
			1.39

APPENDIX 5.3 Life-table of MRL-*lpr/lpr* mice in the different treatment groups

Untreated group

Time in weeks	Dead	Cause of Dead	Total of living animals
8	0		13
12	1	Found dead	12
13	0		12
14	1	Found dead	11
15	0		11
16	1	Found dead	10
17	3	3 Moribund	7
18	2	2 Moribund	5
19	2	1 Moribund 1 Found dead	3
20	0		3
21	0		3
22	1	1 Found dead	2
23	2	2 Moribund	0

DMSO Controls

Time in weeks	Dead	Cause of Dead	Total of living animals
8	0		
12	0		
13	0		
14	0		
15	0		
16	0		
17	1	1 Moribund	12
18	2	2 Moribund	10
19	1	1 Moribund	9
20	0		9
21	3	3 Moribund	6
22	3	3 Moribund	3
23	3	3 Sacrificed	0

CMX-13-treated

Time in weeks	Dead	Cause of Dead	Total of living animals
8	0		13
12	0		13
13	0		13
14	1	1 Found dead	12
15	0		12
16	1	1 Found dead	11
17	1	1 Found dead	10
18	0		10
19	0		10
20	0		10
21	0		10
22	1	1 Found dead	9
23-26	9	9 Sacrificed	0

DEX treated group

Time in weeks	Dead	Cause of Dead	Total of living animals
8	0		13
12	0		13
13	1	1 Found dead	12
14	0		12
15	0		12
16	0		12
17	3	1 Found dead 2 Moribund	9
18	1	1 Moribund	8
19	1	1 Moribund	7
20	0		7
21	0		7
22	0		
23	7	7 Sacrificed	0